

**SEDIMENTOLOGY AND GEOCHEMISTRY OF THE CAMPANO-  
MAASTRICHTIAN MUDSTONES OF THE MAMU FORMATION, BENIN  
FLANK, SW ANAMBRA BASIN, NIGERIA**

**Dissertation**

*zur Erlangung des Doktorgrades  
der Mathematisch-Naturwissenschaftlichen Fakultät  
der Christian-Albrechts-Universität zu Kiel*

vorgelegt von  
Aitalokhai Joel EDEGBAI

Kiel, 2019

Erster Gutachter: Prof. Dr. Lorenz Schwark

Zeiter Gutachter: Prof. Dr. Wolfgang Kuhnt

Tag der mündlichen Prüfung: 22/10/2019



## **Acknowledgement**

*It takes a community to raise a child (African proverb)*

Firstly, I wish to thank my supervisor – Prof. Dr. Lorenz Schwark for inviting me to his workgroup, creating an enabling atmosphere and pushing me out of my comfort zone. This research have benefitted immensely from his broad knowledge base and excellent supervision. Special thanks goes to Dr. Wolfgang Rübsam who assisted with the German translation of my thesis abstract, and made valuable suggestions that greatly improved my first paper. In addition, I also wish to acknowledge the guidance, instruction and support received from Drs. Thorsten Bauersachs, Martin Stockhausen, as well as Nicole Häuser, Ann-Sophie Jonas, Florian Panitz, Jan Weber, Petra Fiedler, Eyke Kirchhoff, Vanessa Grote, Marieke Sieverding all of whom were senior colleagues, colleagues and technical staff at Organic Geochemistry Work group, Kiel University. Janina Fischer-Garbrecht: the secretary of the Organic Geochemistry Work group is appreciated for taking care of all my administrative issues. Linda Piálek and Katrin Gerle of the Forschungsförderung EU und International (Central administration) were very helpful in taking care of all my funding issues.

This study has received support from the German Academic Exchange Service (DAAD), Fulbright commission, US, the Niger Delta Development Commission, Nigeria, and the University of Benin, Benin City, Nigeria.

Members of the Redeemed Christian Church of GOD (Solution Arena) who have been my family in Kiel provided lots of support in many ways, which I cannot mention.

My time in US while I was on a Fulbright fellowship at the Missouri University of Science and Technology (Missouri S&T) was very rewarding due to the warm atmosphere created by my research collaborator - Prof. Franca Oboh-Ikuenobe. Whilst there, I was able to undertake sedimentological, palynofacies, XRD, and some geochemical analyses on my outcrop materials. Worth mentioning is the support I received from the under mentioned people while I was at the Missouri S&T. Drs. David Wronkiewicz, Jonathan Obrist Farner, Marek Locmelis and Eric Bohannan provided valuable guidance and instruction. Patty Robertson and Wendy Albers took care of all my administrative issues. In addition, I will not fail to mention the warm hand of fellowship extended to me by members of the Micropaleontology Work group at Missouri S&T (Robert Haselwander, Onema Adojoh, Feyi Ilesanmi, Walaa Awad, and Marissa Spencer), as well as members of the First Assembly of GOD church who supported me in many ways.

The Management of the University of Benin, Benin City Nigeria is acknowledged for granting me Training Leave throughout the duration of this study. I sincerely appreciate all my colleagues at the Department of Geology, University of Benin, Benin City as well as members of the New Covenant Gospel church Benin City (my home church) for the love and support showered on me, and for checking up on my family throughout this training period.

The assistance rendered by Julius Imarhiagbe who provided great assistance during my fieldwork as well as Reuben Okoliko who assisted with sample collection at the Nigerian Geological Survey Agency Core shed, Kaduna respectively is greatly appreciated.

Heartfelt thanks goes to Prof. W.O. Emofurieta who took special interest in me and sparked up my interest on the Anambra Basin. My training has benefitted greatly from the mentorship of senior colleagues in Nigeria - Mr. Sam Coker and Dr. Kehinde Ladipo whose pieces of advice have been very valuable during the course of this study. Special thanks goes to all my lecturers and teachers who invested time and effort in nurturing me and contributing to my academic development.

It is impossible to quantify the love, care and support showered on wife, my kids, and me by members of my extended family throughout this journey of obtaining a PhD. Of particular note is the immense sacrifice offered by my Mother –in-law and my Father. You deserve some accolades. All I can say is thanks! GOD bless you.

Esther, Ikhuemoise, Ohihoinme, Ohikhokhai, and Ohiremen: my beloved wife and kids, you have endured a lot during this time. I have missed sharing joyful moments with you, and being there for you when you needed me. This has been the hardest time of my life yet. I am happy I am coming home to you! I cannot fix everything but I commit to do all I can to make you see that your sacrifice for me was worth it. All shall be well!

To GOD be all the Glory!



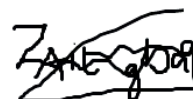
## **Declaration**

I certify that the conceptualization and execution of this research titled *Sedimentology and Geochemistry of the Campano-Maastrichtian mudstones of the Mamu Formation, Benin flank, SW Anambra Basin, Nigeria* was carried out by me under the supervision of Prof. L. Schwark. In addition, I affirm that no part of this thesis has been submitted in fulfillment of the award of Doctoral degree at any university, neither was it published nor submitted for publication. Furthermore, I wish to state that I adhered to the Rules of Good Scientific Practice of the German Research Foundation while embarking on this research and preparing this thesis. I so state that none of my previous academic degrees has been withdrawn at any time.

05/09/2019

-----

**(Ort, Datum)**



-----

**(Unterschrift Doktorand)**





## **Abstract**

The late Campanian-middle Maastrichtian (upper Cretaceous) Mamu Formation is very important in the geological development of the Nigerian sector of the West African Rift System (WARS), as it provides supporting evidence for the Maastrichtian re-establishment of the Trans-Saharan Seaway (Tethys-South Atlantic Ocean connection). In addition to providing useful insight into the prevailing paleoceanographic condition of the Trans-Saharan Seaway, as well as identifying source regions that contributed detritus into the Anambra Basin (southern Trans-Saharan Seaway), a strong impetus for this study is its economic potential. The Mamu Formation holds the largest coal reserves in Nigeria. In addition, it is prospective for secondary enrichment of Pb, Zn, Sn and W (as observed in this study), and a potential hydrocarbon source rock in southern Nigeria. Furthermore, an integration of interdisciplinary tools involving sedimentology, geochemistry (bulk and stable isotope), mineralogy as well as palynofacies, which was employed in this study, affords us an opportunity to understand the scales of variability in the dark mudstone lithofacies.

In the western segment of the Anambra Basin, seven lithofacies were identified and grouped into central basin, marsh, bay, barrier, beach, and washover fan facies association as well as meandering fluvial-tidal channel facies association. The facies associations suggest a tidally influenced wave dominated estuarine paleoenvironment. In addition, mineralogical and palynofacies characterization, as well as microfabric analysis reveal the heterogeneous nature of the dark mudstone lithofacies, which vary from a proximal lower salinity and quartz rich marsh and bay subenvironments with terrestrial organic matter (organic facies C and CD) to a more distal higher salinity and clay rich central basin subenvironment with mixed terrestrial – marine organic matter (organic facies BC and C).

Bottom water paleo-oxygenation condition was predominantly oxic. However, palynofacies and microfabric evidences as well as inferences from Fe-S-TOC relationship suggests pyrite formation occurred in at least two phases. The first phase of syngenetic to early diagenetic pyrite formation, was due to bacterial sulphate reduction, whereas secondary (late diagenetic) pyrite growth which formed the bulk of pyrite preserved occurred at a later phase. In addition, the Campano-Maastrichtian units show a high degree of chemical alteration, textural and mineralogical maturity attributable to prevailing warm humid tropical condition as well as detrital contribution from reworked pre-Santonian units and silica rich igneous and metamorphic rocks.

Furthermore, outcrop and well data show spatial geochemical variability of the Mamu Formation, which is a consequence of detrital contributions from three source regions with clear evidence of mixing. These regions comprise of: a Pb, Zn, W rich and Nb, Ta, Sn poor eastern provenance with Zn enriched over Pb ( $Pb/Zn \ll 1$ ); a Nb, Ta, Sn rich and W poor western region with Pb enrichment over Zn ( $Pb/Zn > 1$ ); and a northern provenance region enriched in Nb, Ta, Sn, and W with Zn enriched over Pb ( $Pb/Zn < 1$ ).

## **Zusammenfassung (German Abstract)**

Die Mamu Formation (spätes Campanium bis mittleres Maastrichtium; Obere Kreide) bildet zentrale Prozesse in der geologischen Entwicklung Nigerias ab, insbesondere in dem Bereich des westlichen Afrikanischen Rift Systems. Unter anderem dokumentiert sie die Öffnung der Trans-Sahara Meeresstraße, welche eine Verbindung zwischen Tethys und Süd-Atlantik etablierte. Die Sedimente der Mamu Formation gewähren somit dezidierte Einblicke in die paläogeographische Entwicklung dieses marinen Korridors. Zudem ermöglichen sie die Identifizierung der Liefergebiete der klastischen Sedimentkompartimente des Anambra Beckens, welches den südlichen Teil der Trans-Sahara Meeresstraße representiert. Die Untersuchung der Mamu Formation erlaubt zudem eine Bewertung des ökonomischen Potentials ihrer Sedimente. So beinhaltet die Mamu Formation Nigerias größte Kohlevorkommen und ist zudem Prospektionsziel für Elemente wie Pb, Zn, Sn und W (wie in dieser Arbeit dokumentiert). Im südlichen Teil Nigerias stellen die Sedimente der Mamu Formation ein wichtiges Muttergestein für die Exploration von Kohlenwasserstoff dar. Die vorliegende Arbeit basiert auf einem interdisziplinären Arbeitsansatz, der Sedimentologie, Geochemie, Mineralogie als auch Palynofazies mit dem Ziel kombiniert Entstehung, Entwicklung und Variabilität der vorwiegend dunklen tonigen Lithologien der Mamu Formation verstehen.

Im westlichen Teil des Anambra Beckens konnten sieben Lithofaziestypen differenziert und in zentrale Becken-, Marsch/Küstensumpf-, Bucht-, Strandwall/Schwellen-, Strand-, randmarine Schwemmfächer-, und mäandrierende Fluß-Tidenkanal- Fazies gruppiert werden. Diese Faziestypen können als ein wellen-dominiertes Ästuar interpretiert werden. Mineralogische und palynologische Charakteristika in Verbindung mit Analysen des sedimentären Mikrogefüges unterstreichen die heterogene Natur der dunklen Tonsteine. Diese dokumentieren proximale frischwasser-beeinflusste, quarz-reiche Marsh und Bucht Bereiche

mit Landpflanzenmaterial (Organofazies C und CD), als auch distale Bereiche, in denen tonigere Lithologien unter höherer Salinität abgelagert wurden. In diesem Faziesbereich ist zudem eine Mixtur aquatisch-stämmigen und Landpflanzen-stämmigen organischen Materials zu dokumentieren (Organofazies BC und C).

Der Ablagerungsraum war vorwiegend gut durchlüftet. Allerdings belegen Palynofazies, sedimentäre Mikrotextrur und Fe-S-TOC Daten eine verstärkte Pyritbildung die in zwei Phasen erfolgte. Eine erste syngenetische Pyritisierung erfolgte durch dissimilatorische Sulfatreduktion, wobei eine zweite Phase auf spät-diagenetische Prozesse zurückzuführen ist. Letztere kann als die Hauptphase der Pyritbildung angesehen werden. Zudem zeigen die Lithologien Campano-Maastrichtian Altes einen hohen Grad an chemischer Alteration, was auf ein vorwiegend warmes und humides Klima schließen lässt. Detritische Sediment-Kompartimente stammen von prä-Santonischen Lithologien, als auch von silizium-reichen Magmatiten und Metamorphiten.

Daten aus Aufschlüssen und Kernbohrungen dokumentieren eine hohe räumliche Variabilität der Mamu Formation, welche im Eintrag klastischen Materials und derer Mischung aus drei unterschiedlichen Liefergebieten begründet ist. Diese können anhand ihrer chemischen Signatur wie folgt differenziert werden: eine Pb, Zn, W reiche und Nb, Ta, Sn arme östliche Provinz, mit einer Dominanz von Zn über Pb ( $Pb/Zn \ll 1$ ); eine Nb, Ta, Sn reiche und W arme westliche Provinz, mit einer Dominanz von Pb über Zn ( $Pb/Zn > 1$ ); und eine nördliche Provinz, die eine Anreicherung von Nb, Ta, Sn, und W zeigt und zudem eine Dominanz von Zn über Pb ( $Pb/Zn < 1$ ) aufweist.

## TABLE OF CONTENTS

Acknowledgment .....	iii
Declaration .....	v
Abstract .....	viii
Table of Contents .....	xii

<b>INTRODUCTION</b> .....	1
---------------------------	---

## CHAPTER ONE

A regional synthesis of mid to late Cretaceous tectonostratigraphic evolution of Nigeria

Abstract .....	6
1.0 Introduction .....	7
1.1 Geological Overview .....	9
1.1.1 Pre-Santonian geological evolution .....	9
1.1.2 Santonian (to Maastrichtian) inversion .....	12
1.1.3 Post-Santonian geological evolution .....	12
1.2 Latest Cenomanian to Maastrichtian stratigraphy .....	13
1.2.1 Sokoto (Iullemeden) Basin .....	13
1.2.1.1 Taloka Formation .....	14
1.2.1.2 Dukamaje Formation .....	14
1.2.1.3 Wurno Formation .....	15
1.2.2 Bornu (Chad) Basin .....	15
1.2.2.1 Gongila Formation .....	15
1.2.2.2 Fika Formation .....	16
1.2.2.3 Gombe Formation .....	16

1.2.3 Bida Basin .....	17
1.2.3.1 Bida Formation .....	17
1.2.3.2 Sakpe Formation .....	18
1.2.3.3 Enagi Formation .....	18
1.2.3.4 Batati Formation .....	18
1.2.3.5 Lokoja Formation .....	20
1.2.3.6 Patti Formation .....	20
1.2.3.7 Agbaja Formation .....	20
1.2.4 Benue Trough .....	21
1.2.4.1 Dukul Formation .....	22
1.2.4.2 Jessu Formation .....	23
1.2.4.3 Numanha Formation .....	23
1.2.4.4 Sukuliye Formation .....	23
1.2.4.5 Lamja Formation .....	23
1.2.4.6 Eze-Aku Group .....	23
1.2.4.6.1 Keana Formation .....	24
1.2.4.6.2 Eze-Aku Formation .....	24
1.2.4.6.3 Makurdi Formation .....	24
1.2.4.6.4 Wukari Formation .....	24
1.2.4.6.5 Amaseri Formation .....	25
1.2.4.7 Awgu Group .....	25
1.2.4.7.1 Awgu Formation .....	25
1.2.4.7.2 Agbani Formation .....	25
1.2.4.7.3 Ogugu Formation .....	26
1.2.4.8 Lafia Formation .....	26

1.2.5 Anambra Basin .....	26
1.2.5.1 Nkporo Group .....	27
1.2.5.1.1 Afikpo Formation .....	27
1.2.5.1.2 Owelli Formation .....	27
1.2.5.1.3 Enugu Formation .....	27
1.2.5.1.4 Nkporo Formation .....	28
1.2.5.2 Mamu Formation .....	28
1.2.5.3 Ajali Formation .....	28
1.2.5.4 Nsukka Formation .....	29
1.2.6 Benin Basin .....	29
1.2.6.1 Afowo Formation .....	29
1.2.6.2 Araromi Formation .....	30
1.3 Discussion .....	30
1.3.1 Implication for source rock development .....	36
1.3.1.1 Latest Cenomanian to Coniacian .....	36
1.3.1.2 Campanian-Maastrichtian source rocks.....	38
1.3.2 Implication for solid mineral and groundwater development .....	39
1.3.2.1 Limestone .....	39
1.3.2.2 Ironstone .....	39
1.3.2.3 Clay .....	40
1.3.2.4 Groundwater resources .....	40
1.4 Conclusion .....	41

## CHAPTER TWO

Campano-Maastrichtian paleoenvironment, paleotectonics and sediment provenance of western Anambra Basin, Nigeria: Multi-proxy evidences from the Mamu Formation

Abstract .....	43
2.0 Introduction.....	44
2.1 Geologic overview .....	45
2.1.1 Tectonics and Stratigraphy of the Anambra Basin .....	45
2.1.2 Lithostratigraphy of the Mamu Formation .....	48
2.2 Methodology.....	50
2.2.1 Sedimentological analysis.....	50
2.2.2 Palynofacies analysis .....	51
2.2.3 Mineralogical analysis .....	51
2.2.4 Geochemical analysis.....	52
2.3 Results.....	52
2.3.1 Particle size distribution.....	52
2.3.2 Palynofacies characterization.....	53
2.3.3 Mineralogical characterization.....	53
2.3.4 Geochemistry .....	55
2.4 Discussion.....	56
2.4.1 Lithofacies characterization .....	56
2.4.1.1 Lithofacies 1 (L1): Dark mudstone.....	57
2.4.1.1.1 Dark coloured planar to wavy laminated microfacies (M1) .....	57
2.4.1.1.2 Dark coloured planar to wavy laminated microfacies (M2) .....	57
2.4.1.1.3 Dark coloured wavy to curved microfacies (M3).....	73



2.4.1.2 Lithofacies 2 (L2): Thin bedded poorly-moderately sorted, moderately cemented sheet-like sMs-Ss .....	75
2.4.1.3 Lithofacies 3 (L3): light coloured moderately sorted weakly cemented, weakly to mildly bioturbated sheet-like sMs-mSs .....	75
2.4.1.4 Lithofacies 4 (L4): MgO – poor oolitic ironstone .....	75
2.4.1.5 Lithofacies 5 (L5): Poorly sorted cross-bedded, very coarse- to medium-grained mSs to Ss.....	76
2.4.1.6 Lithofacies 6 (L6): Light coloured sMs to mSs .....	77
2.4.1.7 Lithofacies 7 (L7): Heterolithics.....	77
2.4.1.8 Lithofacies Associations (LFA) .....	78
2.4.1.8.1 Marsh/bay/central basin-beach-barrier/washover fan lithofacies association (L1-L2-L3-L4 LFA).....	78
2.4.1.8.2 Fluvial-tidal channel lithofacies association (L5-L6- L7 LFA).....	79
2.4.1.9 Facies Succession.....	79
2.4.2 Geochemical characterization .....	82
2.4.2.1 Source and distribution of elements.....	82
2.4.2.2 Paleoclimate, provenance and tectonic setting .....	83
2.4.2.2.1 Paleoclimate .....	85
2.4.2.2.2 Provenance and Paleotectonics .....	85
2.5 Conclusion .....	89

### **CHAPTER THREE**

Organic facies characterization and paleoredox conditions of the Campano-Maastrichtian dark mudstone unit, Benin flank, western Anambra Basin: implications for Maastrichtian Trans-Saharan seaway paleoceanographic conditions

Abstract .....	98
3.0 Introduction.....	99
3.1 Geologic overview .....	101
3.1.1 Tectonics and Stratigraphy of the Anambra Basin .....	101
3.1.2 Lithostratigraphy of the Mamu Formation in the western section.....	102
3.2 Materials and Methods.....	102
3.2.1 Kerogen analysis .....	102
3.2.2 Geochemical analyses .....	105
3.2.2.1 Major and trace element measurements.....	105
3.2.2.2 Carbon, Nitrogen, Sulphur content and stable organic carbon isotope measurements .....	106
3.2.2.2.1 UF analytical techniques .....	107
3.2.2.2.2 CAU analytical techniques .....	109
3.2.3 Microfabric analysis.....	109
3.3 Results.....	110
3.3.1 Palynofacies analysis .....	110
3.3.2 TOC, TN, and TS analyses .....	110
3.3.3 Stable carbon isotope geochemistry.....	115
3.3.4 Major and trace element geochemistry .....	115
3.4 Discussion.....	116
3.4.1 Organic matter characterization.....	116
3.4.2 Paleoredox evaluation.....	119
3.5 Conclusion .....	124

## CHAPTER FOUR

Differentiation of sediment source regions in the Southern Benue Trough and Anambra Basin:  
insights from major and trace element geochemistry

Abstract .....	126
4.0 Introduction.....	127
4.1 Geologic overview .....	128
4.2 Materials and Methods.....	130
4.2.1 Elemental analysis .....	130
4.2.2 Total organic carbon (TOC) analysis.....	132
4.3 Results.....	133
4.3.1 Major elements (Ca, Fe, K, Mg, Mn, Na, Ti and Al) .....	133
4.3.1.1 Outcropping Mamu Formation .....	133
4.3.1.2 Well data .....	134
4.3.1.2.1 Mamu Formation .....	134
4.3.1.2.2 Pre-Santonian Units .....	136
4.3.2 High Field strength elements (HFSE: Th, U, Ta, Nb, Zr, Y, Hf) .....	137
4.3.2.1 Outcropping Mamu Formation .....	137
4.3.2.2 Well data .....	139
4.3.2.2.1 Mamu Formation .....	139
4.3.2.2.2 Pre-Santonian units .....	140
4.3.3 Transition trace elements [(TTE) Ni, Co, V, Cr and Sc].....	141
4.3.3.1 Outcropping Mamu Formation .....	141
4.3.3.2 Well data .....	142
4.3.3.2.1 Mamu Formation .....	142
4.3.2.2.2 Pre-Santonian units .....	142

4.3.4 Pb, Sn, W, Zn, Mo and Cu bivalent metals.....	143
4.3.4.1 Outcropping Mamu Formation .....	143
4.3.4.2 Well data .....	143
4.3.4.2.1 Mamu Formation .....	143
4.3.4.2.2 Pre-Santonian units .....	144
4.4 Discussion .....	145
4.4.1 Degree of chemical alteration .....	145
4.4.2 Source rock composition.....	148
4.4.2.1 Pre-Santonian Units .....	149
4.4.2.2 Mamu Formation .....	150
4.4.3 Provenance.....	152
4.4.3.1 Mamu Formation .....	152
4.4.3.2 Awgu Group.....	154
4.4.3.3 Eze-Aku Group .....	155
4.4.4 Differentiation of provenance regions .....	156
4.4.4.1 Pre-Santonian Units .....	156
4.4.4.2 Mamu Formation .....	157
4.4.4.2.1 Western provenance region.....	158
4.4.4.2.2 Eastern provenance region .....	159
4.4.4.2.3 Northern provenance region .....	159
4.4.4.3 Mixing of provenance regions .....	160
4.5 Conclusion .....	162

## **CHAPTER FIVE**

### 5.0 Conclusion and Outlook

5.1 Conclusion .....182

5.2 Outlook .....184

**REFERENCES**.....186



## **Introduction**

The multi-cycle Benue Trough is part of the West African Rift System whose initiation is cogenetic with the early Cretaceous break-up phase of the South Atlantic Ocean. Its tectonostratigraphic evolution comprises of a rift phase (Neocomian to Coniacian), an inversion phase (Santonian), a sag phase (Campanian to Danian) and a passive margin phase (Thanetian to Recent). The post-Santonian Anambra Basin belongs to the sag phase of the Benue Trough evolution, and its basin fill comprises of the Nkporo Group, the Mamu Formation and the Nsukka Formation in stratigraphic order.

The Mamu Formation, which is the subject of this study, was deposited in the late Campanian to middle Maastrichtian age. Apart from hosting vast coal resources, and holding potential for hydrocarbon generation, this time is an important phase in Nigeria's geologic record as it provides ample evidence in support of the re-establishment of the Tethys-South Atlantic Ocean connection: the Trans-Saharan seaway.

A large proportion of previous works focused on material from the eastern section of the Anambra Basin. These studies mostly carried out by palynological investigation, characterization of coal resources as well as evaluation of the hydrocarbon potential of the coal and dark mudstone units. This study was conceived out of recommendations arising from a preliminary investigation of the hydrocarbon potential of the dark mudstone in the Benin flank (western segment) that was carried out in 2015. The primary objective of this study is to undertake a high-resolution description and characterization of the lithofacies units in the western margin for the first time and linking this to the central part of the basin as well as the eastern flank. The outcome of this study has far-reaching implications on regional studies and mineral resource exploration as it provides important information on the lithofacies and organic facies variability, sediment provenance, as well as paleoceanographic information of the

Maastrichtian Trans-Saharan Seaway. Furthermore, the integrated approach employed in this study provides insight on the scales of heterogeneity in mudstones as well as the driving mechanisms. To guide this study, seven research questions were raised:

- What are the lithofacies types deposited in the western section of the Anambra Basin during the Campano-Maastrichtian age?
- What kind of paleoenvironment prevailed in the western section of the Anambra Basin during the Campano-Maastrichtian age?
- What is the nature of organic facies preserved in the dark mudstone facies?
- What is the nature of the paleoxygenation and paleosalinity conditions that prevailed in the western section of the Anambra Basin at this time?
- Was there any spatial variability in the organic facies, paleo-oxygenation and paleosalinity conditions?
- What were the dominant detrital source regions during the Campano-Maastrichtian age?
- What is the nature of these source areas?

Materials used for this study include 166 samples from four outcrops on the western margin of the Anambra Basin. The outcrop sites (Fig. 2.4) are the Okpekpe and Imiegba locations, which represents the basal – mid section of the Mamu Formation; Uzebba location, which represents the mid – upper section of the Mamu Formation, and Auchi location, which represents the upper section of the Mamu Formation. In addition, 90 ditch cutting/ cores were collected from 5-wells, two of which penetrated pre-Santonian strata (rift sediments). The wells include Owan-1 (located on the western segment); Idah-1 and Nzam-1 (centrally located); Amansiodo-1 and Akukwa-II wells (located on the eastern segment) (Fig. 4.2). All the wells



drilled through the entire section of the Mamu Formation, whereas only the Akukwa-II well drilled through the entire section of the pre-Santonian Awgu Group.

To achieve our objective, a methodology was formulated based on guidelines on study of mudstones as detailed by O'Brien and Slatt (1990), Potter et al. (2005) and Lazar et al. (2015). This methodology comprises of three core aspects, which include:

- Sedimentological and mineralogical characterization
  - Particle size analysis (laser diffraction)
  - X-ray diffraction and acid test
  - microfabric analysis (thin section and hand specimen)
- Palynofacies characterization
  - Palynofacies analysis
- Geochemical characterization
  - Major and trace element analysis (XRF and ICP-MS)
  - Carbon (TC, TOC and TIC), Nitrogen, Sulphur analysis
  - Isotope geochemistry (  $^{13}\text{C}_{\text{org}}$  )

Furthermore, the study was carried out in two phases: phase one involves high-resolution description of outcrops as well as sedimentological, mineralogical, palynofacies and geochemical characterization of outcrop samples, while phase two entails geochemical characterization of well samples as well as data integration with data from phase one for a broader outlook.

The results of this study is presented in five chapters. **In chapter One**, a regional synthesis of mid to late Cretaceous tectonostratigraphic evolution of Nigeria is presented. This synthesis helps to situate the subject matter within a regional context as well as identify gaps in literature, some of which this study sought to fill. This chapter is titled: *A review of the latest*

*Cenomanian to Maastrichtian geological evolution of Nigeria and its stratigraphic and paleogeographic implications.*

**Chapter Two** details the results of a high-resolution description and characterization of the lithofacies units in the western section, which was carried by integrating sedimentological, mineralogical, geochemical and palynofacies techniques. Results show that these units were a product of a tidally influenced, wave dominated, estuarine depositional setting. In addition, we could infer that the Campano-Maastrichtian sediments were sourced from felsic rocks under an extensional tectonic regime, and had undergone a high degree of chemical alteration. This Chapter is titled: *Campano-Maastrichtian paleoenvironment, paleotectonics and sediment provenance of western Anambra Basin, Nigeria: Multi-proxy evidences from the Mamu Formation.*

**In Chapter Three**, it was sought to investigate the nature of organic matter preserved in the Mamu Formation as well as the paleo-oxygenation prevailing at this time. This study, which focused on the dark mudstone lithofacies identified two palynofacies groups: group A (organic facies C and CD) dominated by terrestrial organic matter preserved in the marsh and bay subenvironments and group B (organic facies BC and C) with a mixture of marine and terrestrial organic matter were preserved in these sediments under prevailing oxic bottom water condition. This chapter is titled: *Nature of dispersed organic matter and paleoxygenation of the Campano-Maastrichtian dark mudstone unit, Benin flank, western Anambra Basin: implications for Maastrichtian Trans-Saharan seaway paleoceanographic conditions*

At the tail end of this study, the scope was expanded a bit further by investigating the spatial and temporal variability of source regions in pre- and post-Santonian time. This was achieved by integrating results of geochemical assessment of ditch cuttings from wells in the western, central, and eastern parts of the Anambra Basin with our previously generated outcrop

data on the western margin. The results of this last phase is presented **in Chapter Four**. We observed a clear distinction in the geochemical characteristics of the Mamu Formation in comparison to the pre-Santonian Awgu and Eze-Aku groups, which is attributable to detrital contribution for different source regions. There is also evidence for mixing of detritus from source regions during the pre- and post-Santonian as well as secondary enrichment of Pb, Sn and W in the Mamu Formation. Chapter four is titled: *Differentiation of sediment source regions in the Southern Benue Trough and Anambra Basin: insights from major and trace element geochemistry*.

In **Chapter Five**, we present a summary of the findings from this study as well as future outlook/recommendations for more research

## Chapter One

A regional synthesis of mid to late Cretaceous tectonostratigraphic evolution of Nigeria

Published as:

*Edegbai, A.J., Schwark, L., Oboh-Ikuenobe, F.E., 2019. A review of the latest Cenomanian to Maastrichtian geological evolution of Nigeria and its stratigraphic and paleogeographic implications. J. Afr. Earth Sci. 150, 823–837. <https://doi.org/10.1016/j.jafrearsci.2018.10.007>.*

### A B S T R A C T

This contribution presents a comprehensive review of the Upper Cretaceous geological evolution of Nigeria focusing on the Benue Trough and adjacent basins. It addresses the controversies regarding potential pathways of ingression during transgressive episodes that led to the establishment of the Trans-Saharan seaway. An improved understanding of the paleogeographic evolution is essential for assessing the economic potential of the region, including the Upper Cretaceous petroleum system and coal deposits, as well as groundwater and mineral resources. Two transgressive episodes connected much of Nigeria's sedimentary terrain in the Upper Cretaceous. The first transgression, which followed the opening of the Equatorial Atlantic Ocean in mid-Albian times, established the Trans-Saharan seaway that connected the Tethys and the South Atlantic oceans through an eastward route via the Benue Trough in the Turonian. This resulted in widespread deposition of commercially exploited marine limestone and clay deposits, and subordinate coal, with sediments possessing very limited groundwater resource potential. This marine connection ceased with the continent-wide Santonian inversion tectonics that led to folding, faulting, uplift, and intrusion of older strata. A second transgression, commencing in the Campanian, reestablished the Trans-Saharan seaway through a westward Bida Basin route in the Maastrichtian, culminating in widespread, mostly marginally marine conditions in the Sokoto, Bida, Anambra, and Benin basins as

confirmed in this review. The influx of marine waters from the Tethys Ocean, limited in extent by the uplifted region of the southern Benue Trough brought about marginally marine conditions in the Chad Basin and the northern and central Benue Trough. Widespread deposition of coal, clay, ironstone, and good to prolific aquiferous units occurred during this time.

## **1.0 Introduction**

Nigeria is located between Latitude 4° and 14°N and Longitudes 3° and 15°E (Fig. 1.1) in West Africa. An (almost) even proportion of basement and sedimentary rocks underlies its landmass. The sedimentary rocks are contained within seven major sedimentary basins, most of them initiated by the evolution of the West African Rift System (WARS) (Fairhead and Binks, 1991; Binks and Fairhead, 1992). The sedimentary succession ranges from the Lower Cretaceous (Neocomian?) epoch (in the Benue Trough, the Benin, the Sokoto and the Bida basins) to Recent (Niger Delta and Benin basins). The Cretaceous rocks that underlie 25% of Nigeria's land area is subdivided into two broad coeval groups: the pre-Santonian (Neocomian to Coniacian), and the post-Santonian (Campanian to Maastrichtian) (Adeleye, 1975). These subgroups are separated by a hiatus caused by the continent-wide inversion, which was characterized by folding, faulting, intrusion, uplift and erosion during the Santonian (Guiraud and Bosworth, 1997; El Hassan et al., 2017).

For over 50 years, there have been multiple reviews of the Upper Cretaceous paleogeography of Nigeria. These studies began in the 1960's and 1970's (notably Reyment, 1965; Murat, 1972; Kogbe, 1976; Adeleye, 1975; Petters, 1978), and peaked in the 1980's (e.g., Reyment, 1980; Kogbe, 1980, 1981; Petters, 1982; Petters and Ekweozor, 1982; Zaborski, 1983; Popoff et al., 1986; Adetunji and Kogbe, 1986; Reyment and Dingle, 1987; Ladipo, 1988; Benkhelil, 1989). There has been a decline in the publication of similar studies since the

1990's, and Gebhardt (1998), Courville et al. (1998), Zaborski, and Morris (1999) published the most recent studies.

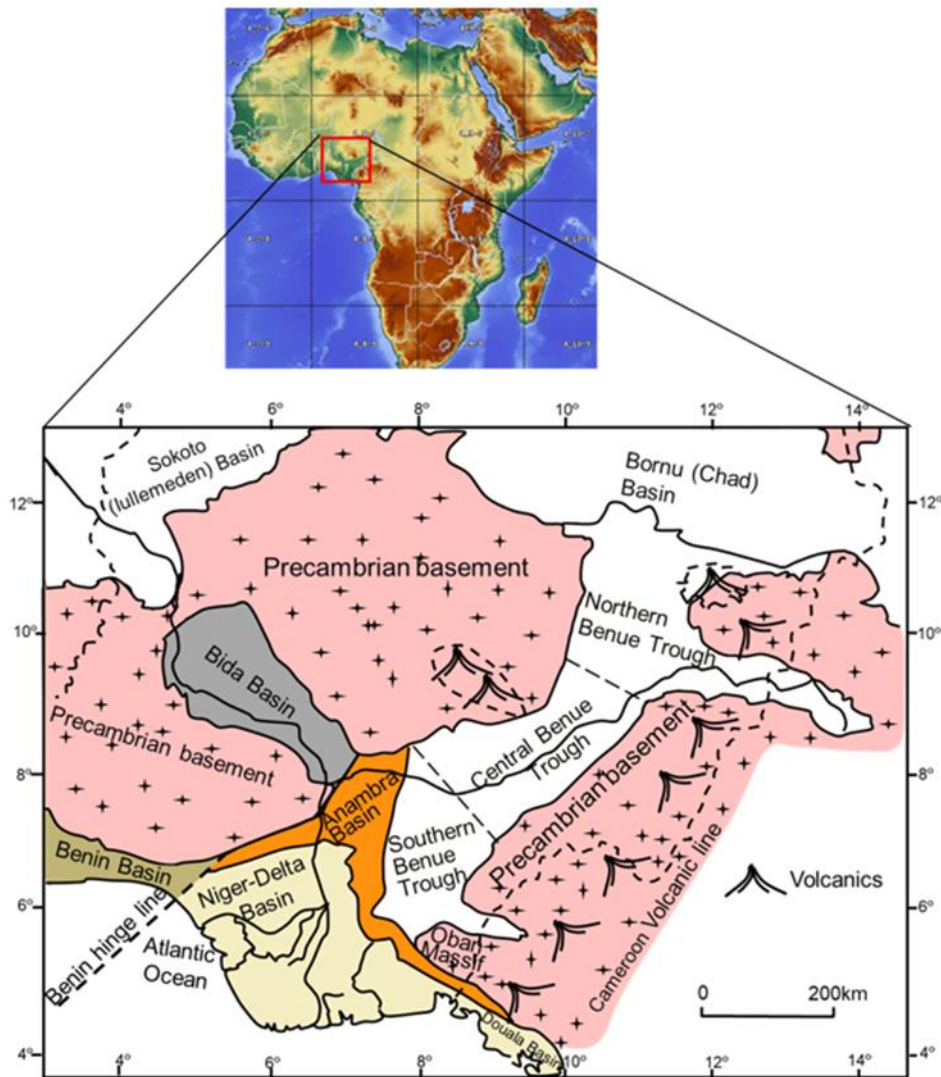


Fig. 1.1: Map of Nigeria showing areas underlain by sedimentary and basement rocks (redrawn and modified from Benkhelil, 1989).

Palaeogeographical reconstructions of the African continent by Scotese (2014) illustrate the need for a comprehensive review of the latest Cenomanian to Maastrichtian stratigraphic development of Nigeria's sedimentary basins. The objective of this paper, therefore, is to bridge the almost 20-year review hiatus noted above by revisiting all existing ideas on the Upper Cretaceous stratigraphy and paleogeography of Nigeria, and address the controversies surrounding the pathways of the transgressive episodes that led to the

establishment of the Trans-Saharan seaway. Furthermore, we envisage that an improved understanding of the paleogeography will allow for better assessment of Cretaceous petroleum systems, and evaluation of groundwater and mineral resource potentials of Nigeria.

## **1.1 Geological Overview**

This section briefly reviews the latest Cenomanian to Maastrichtian geological evolution of Nigeria.

### *1.1.1 Pre-Santonian geological evolution*

Numerous lines of evidence indicate that the North, South, and Central Atlantic did not open coevally (Fairhead and Binks, 1991; Moulin et al., 2010). Thus, it is imperative to view the pre-Santonian stratigraphic evolution of Nigerian sedimentary basins in terms of the pre- and post-Equatorial (South) Atlantic Ocean formation. The Neocomian to early Albian successions (“continental intercalaire”, Kogbe, 1981) mark sedimentation upon inception of rifting in the WARS, which is contemporaneous with the initial “break up phase” of the South Atlantic (Fairhead, 1988; Fairhead and Binks, 1991; Binks and Fairhead, 1992; Moulin et al., 2010). Reactivation of pre-existing faults and initiation of abundant narrow but isolated faults induced alluvial depositional conditions characterized by conglomerates and coarse grit arkosic sandstones (Fairhead and Binks, 1991; Binks and Fairhead, 1992; Withjack et al., 2002). With time, the individual faults enlarged and merged, ultimately resulting in increased subsidence and accommodation creation outpacing sediment supply; these led to the deposition of limnic and fluvio-deltaic rocks (Fig. 1.2). The un-named pre-mid Albian strata in the Southeast (central and southern Benue Trough), and the Bima, Gundumi, Illo and Ise formations in the Northeast (northern Benue Trough and Bornu Basin), Northwest (Sokoto Basin) and Southwest (Benin Basin) comprise this group (Kogbe, 1981; Benkhelil, 1986; Coker and Ejedawe, 1987;

Zaborski et al. 1997; Kaki et al. 2013; Sarki Yandoka et al., 2014; Dim et al., 2016; Shettima et al., 2018).

Edegbai’s unpublished data (Fig. 1.3a, b) on the Benin Flank, less than 200km from the southern Bida sub-basin, has revealed the presence of a highly indurated, poorly sorted cross-bedded arkosic sandstone outlier which is interpreted to be pre-Santonian based on its similarity in mineralogy and texture to the Bima Formation. Olawoki et al (2018) also reported the occurrence of medium to coarse-grained sandstone believed to be pre-Santonian at Filele – northwest of Lokoja. These findings suggest that the southern Bida Basin, which has similar rocks as the Benin flank, was probably not emergent as previously thought and fluvio-deltaic conditions persisted at this time.

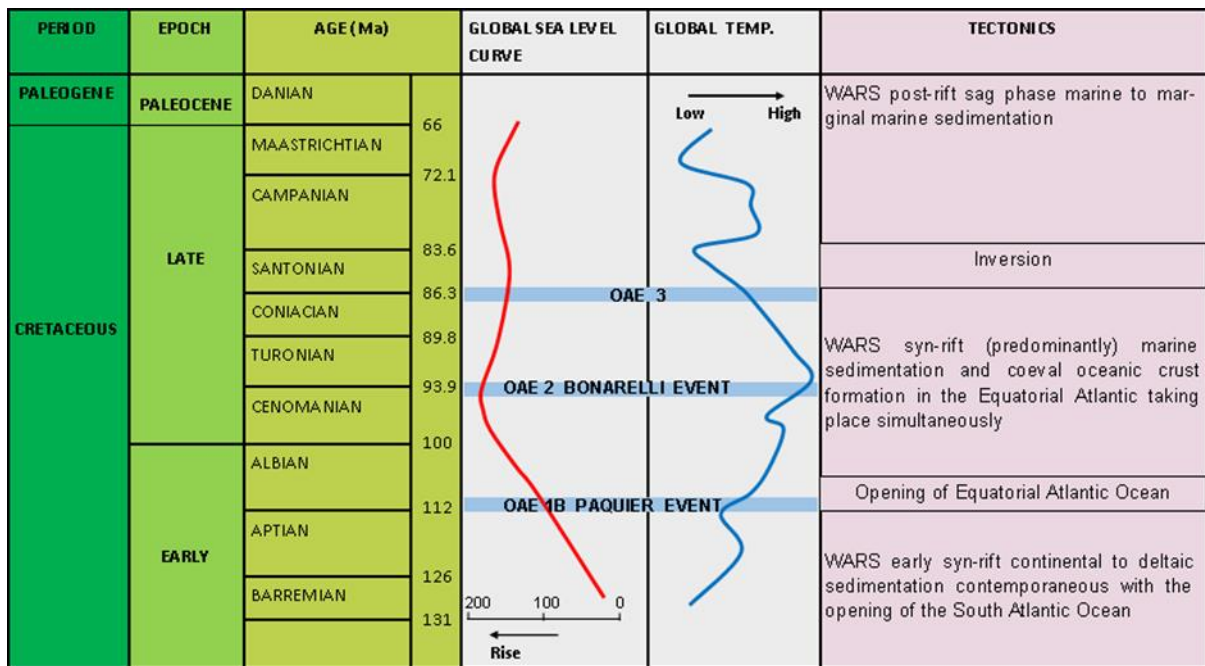
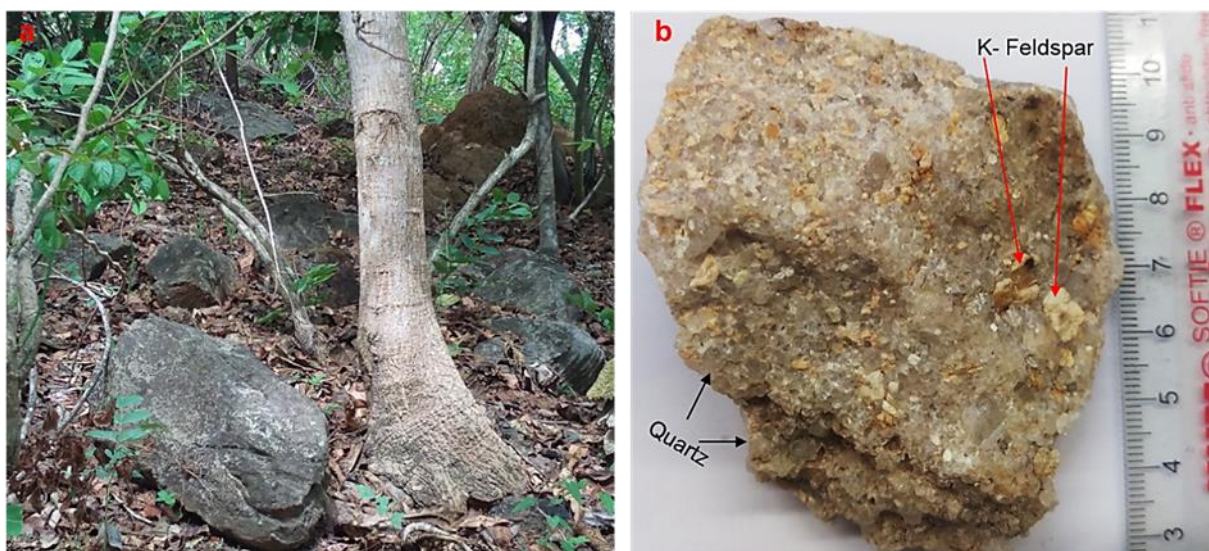


Fig. 1.2: Cretaceous –Paleogene tectonic evolution (adapted from Fairhead and Binks, 1991; Binks and Fairhead, 1992; Skelton et al., 2003; Jenkyns, 2010; Bodin, et al., 2015). WARS = West African Rift System; black arrow indicates sea level and temperature rise

Following the opening of the Equatorial Atlantic Ocean (Moulin et al., 2010), increased basin subsidence and global sea level rise in the mid- to late Albian (Fig. 1.2), marine sedimentation commenced with the deposition of -sandstone, limestone and thick mudrock



units of the Asu-River Group- inclusive of the Awe, Awi and Mfamosing formations in the Southeast (Uzuakpunwa *in* Adeleye, 1975; Offodile, 1984; Benkhelil, 1989; Nwajide, 2013, Dim et al., 2016). In the Southwest, the “Albian Sandstone” marks the onset of marine deposition (Kaki et al., 2013). This transgressive episode continued until the Coniacian age and was marked by short spells of regression. Copiously fossiliferous limestone, mudrock and sandstone units of the Eze-Aku Group and the Awgu Group were deposited in the Southeast (Benkhelil, 1989; Nwajide, 2013; Dim et al., 2016), and the Afowo (“Turonian Sandstone”) and Awgu formations in the Southwest (Kaki et al., 2013; d’Almeida et al., 2016) (Fig. 1.4).



*Fig. 1.3. a,b. Outcrop and hand specimen of pre-Santonian cross bedded arkosic sandstone (coeval with the Bima, Gundumi and Illo formations) discovered in the Benin Flank, Anambra basin*

However, in the Northeast, marine sedimentation did not commence until the Cenomanian (Fig. 1.2) when the marine shale, limestone, and sandstone units of the Yolde and lower Gongila formations were deposited (Fig. 1.4) (Popoff et al., 1986; Nwajide, 2013; Sarki Yandoka et al., 2017). As noted earlier for the Southeast and Southwest, marine deposition persisted until the Turonian-Coniacian when the amply fossiliferous facies of the Gongila, Dukul, Numanha, Sekuliye, Jessu, Fika and Lamja formations were deposited (Fig. 1.4) (Adeleye, 1975; Benkhelil, 1989; Obaje, 2009). The vast amounts of fossils preserved

(especially the Cenomanian-Turonian interval) correspond to a time of global sea level rise, contemporaneous with the development of oceanic anoxia — the Bonarelli Oceanic Anoxic Event 2 (OAE-2, Fig. 1.2; Petters and Ekweozor, 1982; Jenkyns, 2010). It is likely that the Bida Basin was emergent at this time since there is apparently no record of pre-Santonian rocks (Nwajide, 2013; Ojo et al., 2016; Obaje, 2009). There is also no record of Cenomanian-Coniacian strata in the Northwest. Further research is needed to determine if this absence is due to erosion/non-deposition or non-discovery.

### *1.1.2 Santonian (to Maastrichtian) inversion*

Differential spreading rates of the Central and South Atlantic Oceans during the Santonian resulted in the reactivation of the mid-Atlantic transform faults that extend into the WARS. This led to a change from sinistral to dextral strike-slip motion along the reactivated oceanic faults (Fairhead and Green, 1989), and consequently, continent-wide inversion tectonics characterized by folding, faulting, intrusion, uplift and erosion of pre-Santonian rocks (Benkhelil and Robineau, 1983; Benkhelil, 1989; Guiraud and Bosworth, 1997; Suleiman et al., 2017). The southern Benue Trough (Abakaliki area) experienced the most severe deformation, and some studies (Guiraud and Bosworth, 1997; Nwajide, 2013) have proposed that the inversion tectonics probably lasted until the Maastrichtian in the Northeast.

### *1.1.3 Post-Santonian geological evolution*

Slow basin subsidence due to thermal relaxation (sag) resulted in the deposition of sediments (Fairhead and Binks, 1991; Binks and Fairhead, 1992), which unconformably overlie pre-Santonian sedimentary rocks. In the Sokoto Basin, the sandstone, mudrock and limestone facies of the Rima Group (Fig. 1.4) were deposited under marginal marine (tidal flat) to shallow marine depositional conditions (Kogbe, 1981; Adetunji and Kogbe, 1986; Zaborski and Morris, 1999). The Northeast (Gongola sub-basin) experienced estuarine conditions, which

deposited sand, mudrock, and thin ironstone and coal strata of the Gombe Formation (Suleiman et al., 2017; Nwajide, 2013; Obaje, 2009). Prevailing marginal marine to marine conditions in the Anambra and Bida basins (which were active depocenters at this time), central Benue Trough and the Benin Basin led to the deposition of sand, mudrock, ironstone, coal and limestone units of the Nkporo Group, as well as the Mamu, the Ajali and the Nsukka formations (in the Anambra Basin) the Lokoja, Bida, Patti, Sakpe, Patti, Enagi, Agbaja and Batati formations (in the Bida Basin), the Araromi Formation (in the Benin Basin), as well as the Lafia Formation in the central Benue Trough (Fig. 1.4).

## **1.2 Latest Cenomanian to Maastrichtian stratigraphy**

This section reviews the latest Cenomanian to Maastrichtian lithostratigraphic units of the six Cretaceous sedimentary basins in Nigeria (Fig. 1.1, 1.4), beginning with the basins in the northern part of the country (Fig. 1.4). While the review focuses on the rock types comprising the formations, it should be noted that the original definition of these units noted and was partially based on the types of fossils preserved (where present). An overview of the pre-latest Cenomanian geologic and stratigraphic evolution has been provided (see section 1.1) and will not be discussed in detail here.

### *1.2.1 Sokoto (Iullemeden) Basin*

The Sokoto Basin represents the Nigerian portion of the more extensive Iullemeden Basin (Fig. 1.1), which covers an area of about 800,000 km<sup>2</sup> from Algeria to the North to Niger in the East, and from Nigeria and the Republic of Benin in the South to Mali in the West (Kogbe, 1981; Zaborski and Morris, 1999). This large interior sag basin (Kogbe, 1981; Zaborski and Morris, 1999; and Nwajide, 2013) has an older interior fracture or rift component in its axial zones (Busby and Ingersoll, 1995; Klein, 1995). The Basin's initiation is believed to have occurred in the late Jurassic, though this is not well constrained yet (Wright et al.,

1985). The Rima Group (Taloka, Dukamaje, Wurno formations) is Campano-Maastrichtian in age (Figs. 1.4, 1.5a).

#### *1.2.1.1 Taloka Formation*

The Taloka Formation unconformably overlies the pre-Santonian Gundumi and Illo formations (see section 1.1.1). Strata consist of weakly cemented fine-grained sand and silt interbedded with dark mudrock bearing lignite seams in some intervals (Kogbe, 1981). The sand and silt are often thinly bedded, variegated, bioturbated (*Ophiomorpha*, *Skolithos*, and *Thalassinoides*), and commonly display flaser, wavy and lenticular bedding. Kogbe (1981) has reported fossilized remains of marine reptile parts also. The observed ichnofabric as well as the remains of extinct marine reptiles and tidal structures have been used to interpret a lower coastal plain /tidal flat depositional setting for the formation (Kogbe, 1981; Zaborski and Morris, 1999). Whereas this review favors a tidal influenced shallow marine depositional setting based on the lithological, paleontological and ichnological characteristics.

#### *1.2.1.2 Dukamaje Formation*

This formation is mainly shaly (which may be gypsiferous or carbonaceous), and contains some shelly limestone beds rich in agglutinated foraminifera, bivalves, corals, echinoderms, ammonites (*Libyoceras* sp.), and gastropods. In addition, bone beds of fish and reptilian remains occur around its base (Kogbe, 1981; Zaborski and Morris, 1999). The Dukamaje Formation has been interpreted as nearshore/shallow marine (Kogbe, 1981; Adetunji and Kogbe, 1986; Zaborski and Morris, 1999).

#### *1.2.1.3 Wurno Formation*

The lithofacies of the Wurno Formation is similar to that of the Taloka Formation, described in section 1.2.1.1 (Kogbe, 1981; Adetunji and Kogbe, 1986). A tidal influenced shallow marine depositional setting has been inferred for the formation.

### *1.2.2. Bornu (Chad) Basin*

The Bornu Basin represents the Nigerian sector of the much larger Chad Basin (Fig. 1.1) with an area of approximately 2,335,000 km<sup>2</sup> covering northeastern Nigeria, Chad, Cameroon, Central African Republic, and Niger. It is a multi-cycle sedimentary basin, whose current structure is an intracratonic sag basin (Genik, 1992). It is a component of the West and Central Atlantic Rift System (from which the Benue Trough persists) initiated when the African and South American plates separated (Benkhelil, 1989; Fairhead, 1988; Fairhead and Binks, 1991; Binks and Fairhead, 1992; Genik, 1992). The Gongila and Fika formations which are equivalent to the Pindiga Formation of Wozny and Kogbe (1983) represent the latest Cenomanian to Coniacian succession, while the Gombe Formation represents the basin's post-Santonian Cretaceous strata (Figs. 1.4, 1.5b).

#### *1.2.2.1 Gongila Formation*

The Gongila Formation is characterized by alternating copiously fossiliferous limestone-mudrock lithofacies (which may change to massive fossiliferous limestone lithofacies in some areas) at the base, and interbedded mudrock and-planar and hummocky cross-bedded, bioturbated sandstone (Ophiomorpha ichnofacies) at the top. These sediments have been interpreted as deposits of a shallow marine environment (Obi, 1998; Akande et al., 1998; Obaje, 2009; Adepoju and Ojo, 2013; Nwajide, 2013).

#### *1.2.2.2 Fika Formation*

The Fika Formation is dominantly fossiliferous, occasionally gypsiferous mudrock unit with subordinate limestone and fine sandstone interbeds (Obaje, 2009; Hamza et al., 2011; Adegoke et al., 2014). It is uncertain if the gypsum is of primary origin or due to the weathering of pyrite. A normal marine to brackish depositional setting has been inferred based on its lithofacies and fossil contents (Gebhardt, 1997; Akande et al., 1998; Hamza et al., 2011).

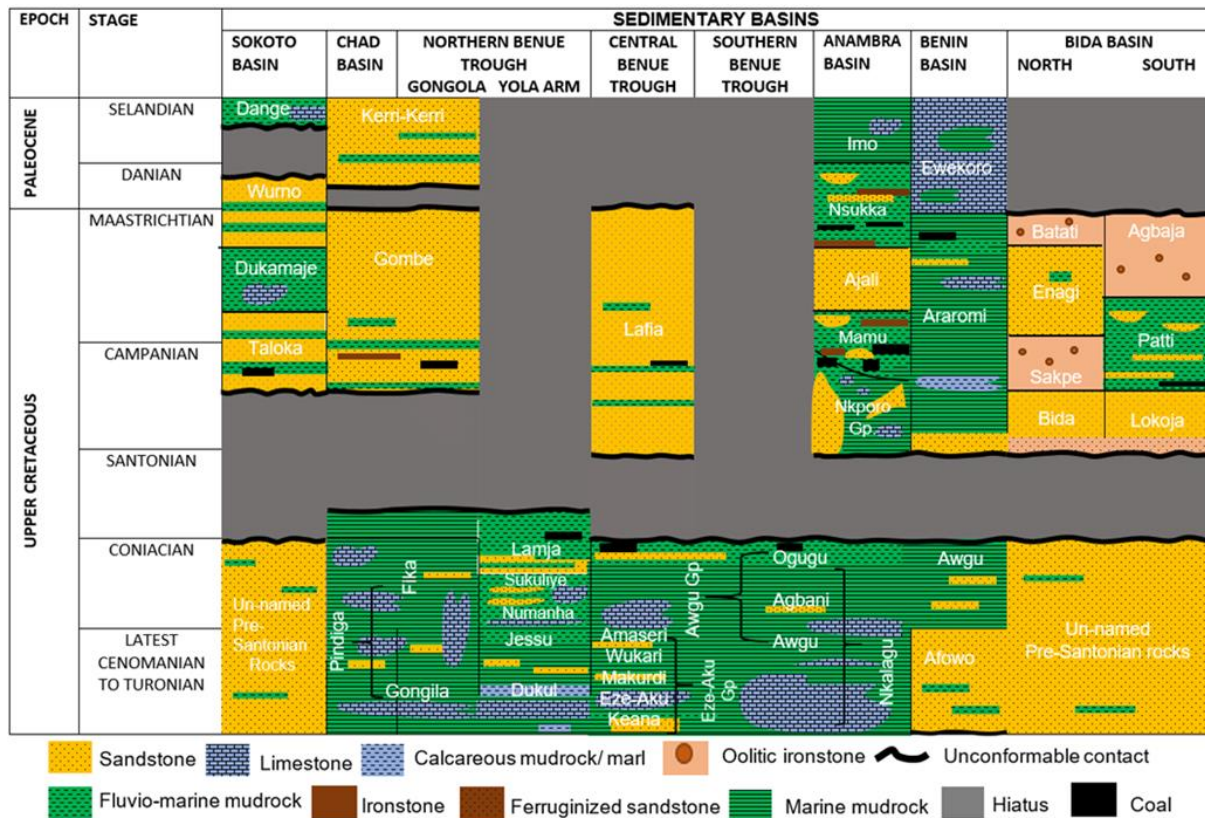


Fig. 1.4: Latest Cenomanian to Paleocene stratigraphic chart of Nigeria depicting the stratigraphic groups and important formations in the sedimentary basins discussed, with schematic differentiation of lithology.

### 1.2.2.3 Gombe Formation

The Gombe Formation (Fig. 1.4) unconformably overlies the pre-Santonian rocks. Although not ubiquitous in the Bornu Basin, it is better developed in the southern end of the basin and the northern Benue Trough (see section 1.2.4). Its absence in other areas may be due to erosion or non-deposition (Suleiman et al., 2017; Nwajide, 2013; Obaje, 2009). Three main lithofacies characterize this formation: (i) a basal heterolithic unit comprising phytoclast-rich, thinly bedded mudrock with interbeds of fine- to medium-grained sand and thin beds of ironstone; (ii) a middle well bedded fine- to medium-grained sand (mainly arenites) with interbeds of mudrock; and (iii) a top unit characterized by tabular to planar cross-bedded, fine- to coarse-grained reddish sand (Zaborski et al., 1997). These sediments have been interpreted

as deposits of a lower delta plain to estuarine environment (Zaborski et al., 1997; Akande et al., 1998; Ojo and Akande, 2004; Carter, *in* Suleiman et al., 2017).

### 1.2.3. Bida Basin

The Bida Basin also known as the Nupe Basin or Middle Niger Basin is a NW-SE trending rift basin (King, 1950; Kogbe et al., 1983) infilled with post-Santonian Cretaceous sediments covering an area of approximately 60,000 km<sup>2</sup> (Fig. 1.1; Adeleye *in* Nwajide, 2013). Its sedimentary infill exhibits widespread facies variability, resulting in its subdivision into a northern Bida sub-basin and southern Bida sub-basin (Jones *in* Ojo and Akande, 2009). In the northern Bida sub-basin, the Bida, Sakpe, Enagi and Batati formations represent the post-Santonian sediments, while the Lokoja, Patti and Agbaja formations comprise the lithic infill in the southern sub-basin (Figs. 1.3, 1.5c).

#### 1.2.3.1 Bida Formation

The Bida Formation unconformably overlies Precambrian basement rocks in the flanks of the northern Bida sub-basin. It is mainly a sand unit, which is ferruginized in places with mudrock and indurated breccia units occurring at some stratigraphic horizons. The sand unit is subdivided into three sub-facies: (i) poorly to moderately sorted basal conglomeratic sandstone; (ii) poorly sorted coarse-grained, massive arkosic sandstone; (iii) loose, poorly to moderately sorted sand; and (iv) moderately sorted, fine-grained sand (Olaniyan and Olobaniyi, 1996). The lithofacies is interpreted to represent fluvial (braided river channels) to alluvial fan depositional environment (Adeleye, 1974; Obaje, 2009; Braide, *in* Nwajide, 2013).

#### 1.2.3.2 Sakpe Formation

The Sakpe Formation is an ironstone unit consisting of thinly bedded oolitic ironstone, which grades into pisolitic ironstone, ferruginized sandstone, and claystone containing fossil wood. Ferruginized *Skolithos* burrows and poorly preserved gastropod and bivalve shells have

been reported (Adeleye, *in* Nwajide, 2013). A shallow marine (near shore) depositional environment has been inferred for the formation.

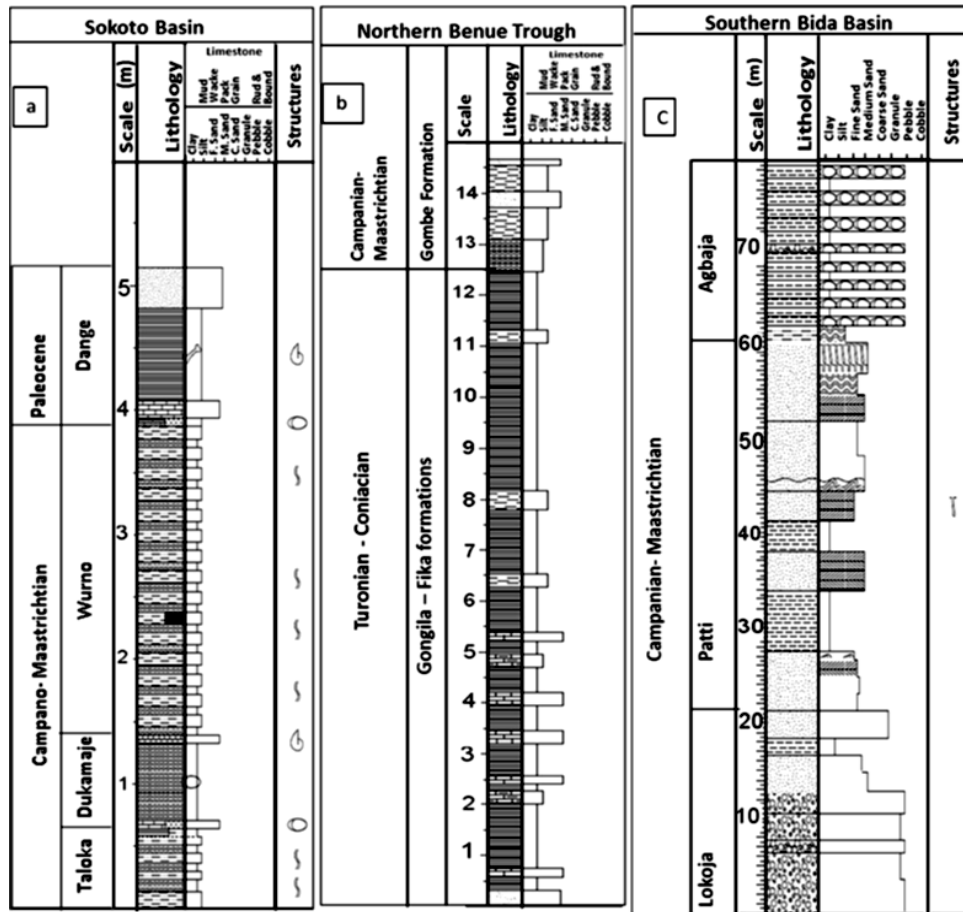
#### *1.2.3.3 Enagi Formation*

Ojo and Akande (2012) identified and interpreted four distinct lithofacies in the Enagi Formation: (i) conglomeratic lithofacies formed as tidal channel lags; (ii) tidal channel and shoreface sand; (iii) braided river sand; and (iv) overbank/floodplain claystone. These lithofacies depict shallow marine depositional conditions, influenced by fluvial processes at relative sea-level fall.

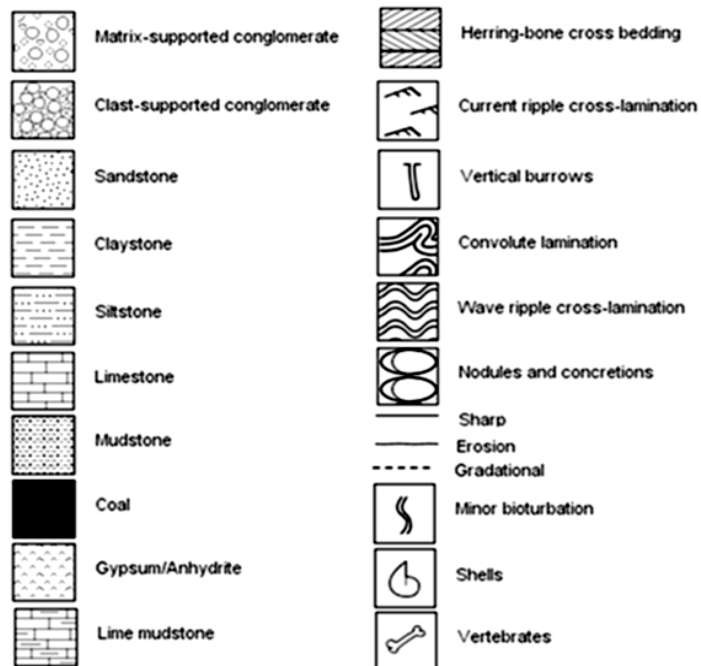
#### *1.2.3.4 Batati Formation*

The Batati Formation is dominantly an oolitic and goethitic ironstone unit with subordinate ferruginous mudrock intercalations (Obaje, 2009; Nwajide, 2013). A marginal marine depositional condition has been inferred for the formation based on the lithofacies and fossil fauna recovered by Adeleye *in* Nwajide (2013).





**Legend**



*Figs. 1.5. Upper Cretaceous to Paleocene stratigraphy. 5a, Campanian-Maastrichtian–Paleocene lithostratigraphy of the Sokoto Basin (modified from Kogbe, 1981). 5b, Turonian – Maastrichtian lithostratigraphy of the northern Benue Trough (modified from Akande et al., 1998). 5c, Campanian-Maastrichtian lithostratigraphy of the southern Bida Basin (modified from Ojo and Akande, 2009).*

#### *1.2.3.5 Lokoja Formation*

The Lokoja Formation unconformably overlies Precambrian basement rocks in the flanks of the southern Bida sub-basin and the Benin flank (western flank of the Anambra Basin) where it occurs as a lateral facies equivalent of the Nkporo Group (see section 1.2.5.1. below; Nwajide, 2013) and coeval with the Bida Formation (Osokpor and Okiti, 2013). It is mainly a sand unit, which is feruginized in places. Osokpor and Okiti (2013) described the formation as comprising poorly sorted massive pebbly sands in a fine sand/mudstone matrix, poorly to moderately sorted cross-bedded coarse-grained sand and thin oolitic ironstone unit. The sediments have been interpreted as depicting alluvial to fluvial depositional conditions.

#### *1.2.3.6 Patti Formation*

The Patti Formation is characterized by grey to white, fine- to medium-grained sandstone, siltstone, claystone and organic-rich mudrock interbedded with bioturbated ironstone (Abimbola, 1997; Akande et al., 2005; Ojo and Akande, 2009; Nwajide 2013). The siltstone beds are commonly bioturbated and may display occasional soft sediment deformation structures. Based on the palynology and the lithofacies succession of the formation, Ojo and Akande (2009) concluded that the deposits were formed by an interplay of marine tidal versus fluvial processes. This interpretation is supported by micropaleontological data (Agyingi, 1993; Petters, *in* Obaje, 2009).

#### *1.2.3.7 Agbaja Formation*

This ironstone unit caps the Patti Formation. It comprises three lithofacies (Abimbola, 1997) as follow: (i) Poorly sorted yellowish brown oolitic ironstone unit; (ii) Well sorted reddish brown pisolitic ironstone unit; and (iii) muddy concretionary ironstone unit. Adeleye (1973) attributed the deposits to marine processes, whereas Umeorah (1987), Abimbola (1997),

and Mücke et.al (1999) inferred the prevalence of marginal marine conditions for their deposition.

#### *1.2.4 Benue Trough*

The Benue Trough is a linear NE-SW trending depression with dimensions of 1000 km in length and approximately 50-100 km in width (Fig. 1.1) (Benkhelil, 1989). It is a component of the WARS initiated in the Barremian during the early phase of the separation of the South American Plate from the African Plate (Fairhead, 1988; Fairhead and Green, 1989; Benkhelil, 1989; Fairhead and Binks, 1991; Binks and Fairhead, 1992; Genik, 1992, Fairhead et al., 2013). Two schools of thought exist regarding its basin type. The first group proposed a simple rift structure, i.e., the failed arm of a Ridge-Ridge-Ridge (R-R-R) or Ridge-Ridge-Fault (R-R-F) rift system (King, 1950; Cratchley and Jones, 1965; Stoneley, 1966; Burke et al., 1970; Burke and Dewey, 1974; and Olade, 1975). The second group, which has a wider acceptance, favors a more complex pull-apart structure with mini-basins forming along a zone of pre-existing transcurrent faults (Benkhelil, 1982, 1986, 1989; Guiraud, 1990; Allix and Popoff, 1983, Popoff et al., 1986). The current structure of the Benue Trough, which was slightly modified by extensional tectonics in the early Cenozoic, is considered a product of the plate-wide Santonian compressional tectonics driven by the reactivation of mid-Atlantic transform faults caused by differential spreading rates of the Central versus South Atlantic Ocean (Burke and Whiteman, 1973, Guiraud and Bosworth, 1997). Consequently, the pre-Santonian strata were folded, faulted, intruded, and eroded (Benkhelil and Robineau, 1983; Benkhelil, 1989; Guiraud and Bosworth, 1997; Suleiman et al., 2017).

Based on its tectonostratigraphy and geography, the Benue Trough is subdivided into three segments (Fig. 1.1), namely, the northern (upper Benue Trough), central (middle Benue Trough) and southern (lower Benue Trough/Abakaliki Basin) (Benkhelil, 1989, Nwajide,

2013). For the northern Benue Trough two sub-basins are differentiated: the Gongola sub-basin and the Yola sub-basin or arm (also known as the Garoua Basin in Cameroon). The pre-Santonian (latest Cenomanian to Coniacian) succession is represented by the Gongila and Fika formations in the Gongola sub-basin. In the Yola sub-basin, this interval comprises the Dukul, Jessu, Numanha, Sukuliye and Lamja formations. During the post-Santonian, the Yola sub-basin was emergent, and only the Gongola sub-basin acted as a depocenter at that time. The Gombe Formation in the Gongola sub-basin (Fig. 1.5b) represents the Campanian–Maastrichtian succession. Refer to sections 1.2.2.1, 1.2.2.2, and 1.2.2.3 for descriptions of the Gongila, Fika and Gombe formations in the Chad Basin.

In the central and southern Benue Trough, the Eze-Aku Group (Keana, Eze-Aku, Makurdi, Wukari and Amaseri formations), and Awgu Group (Awgu, Agbani, and Ogugu formations) represent the latest Cenomanian to Coniacian stratigraphy. The southern Benue Trough was emergent during the post-Santonian, and consequently became a source for clastic sediments. Only the Lafia Formation was deposited in the central Benue Trough at this time (Benkhelil, 1989; Nwajide, 2013).

It is important to note here that based on sedimentological and micropaleontological data, Petters and Ekweozor (1982) and Gebhardt (1997, 1999, 2001) considered the latest Cenomanian to Coniacian succession in the southern Benue Trough as one continuous depositional sequence characterized by deep marine anoxic (turbidite) to shallow marine dysoxic to oxic conditions. They considered the subdivision of the rocks as the Eze-Aku and Awgu Groups as unnecessary and proposed the Nkalagu Formation.

#### *1.2.4.1 Dukul Formation*

The Dukul Formation comprises of fossiliferous, bioturbated (*Cruziana* ichnofacies) interbeds of mudrock, limestone and marl deposited in a shallow marine setting (Akande et al., 1998; Nwajide, 2013).

#### *1.2.4.2 Jessu Formation*

Interbedded sandstone and mudrock beds characterize the Jessu Formation. The mudrock beds are subordinate at the base but progressively increase upwards (Sarki Yandoka et al., 2016). A shallow marine depositional setting has been interpreted for this stratigraphy (Ojo and Akande *in* Nwajide, 2013).

#### *1.2.4.3 Numanha Formation*

Blue-black mudrock interbedded occasionally with thin calcareous sandstone and limestone characterize this formation, which has been interpreted as shallow marine (Nwajide, 2013; Sarki Yandoka et al., 2016).

#### *1.2.4.4 Sukuliye Formation*

This formation consists of interbeds of mudrock and limestone. The mudrock beds are commonly thicker than the limestone beds, which contain abundant shelly fauna. The sediments have been interpreted as shallow marine deposits (Nwajide, 2013; Sarki Yandoka et al., 2016).

#### *1.2.4.5 Lamja Formation*

The Lamja Formation, the youngest unit in the Yola sub-basin, consists of massive sandstone with interbedded fossiliferous, organic-rich mudrock and limestone, as well as thin coal interbeds deposited under shallow marine to brackish depositional conditions (Opeloye, *in* Nwajide, 2013).

#### *1.2.4.6 Eze-Aku Group*

The Eze-Aku Group comprises the Keana, Eze-Aku, Makurdi, Wukari and Amaseri formations in stratigraphic order from bottom to top, which represent latest Cenomanian–Turonian succession in the central and southern Benue Trough.

#### *1.2.4.6.1 Keana Formation*

Arkosic planar cross-bedded, poorly sorted, strongly cemented, micaceous sandstone unit, interbedded occasionally with mudrock characterizes this formation, which has been interpreted as fluvial in origin (Offodile, 1984; Nwajide, 2013).

#### *1.2.4.6.2 Eze-Aku Formation*

Note that this formation forms a part of the homonymous Eze-Aku Group, which may lead to confusion, depending on literature source. It consists of dark grey to black, micaceous, calcareous and gypsiferous organic-rich mudrock alternating with limestone. This lithofacies association contains a copious amount of shelly fauna and has been interpreted as marine (Nwajide, 2013; Igwe and Okoro, 2016; Dim et al., 2016).

#### *1.2.4.6.3 Markurdi Formation*

The Makurdi Formation is a lateral equivalent of the Eze-Aku Formation. This dominant sandstone unit is arkosic, planar to trough cross-bedded, medium- to coarse-grained and micaceous. A sharp irregular base with pebbly lags, grading into finer grained particle sizes, characterizes a typical depositional cycle. A fluvial channel depositional setting has been interpreted for this formation (Nwajide, 1988, 2013). Nwajide (2013) also described the Wadatta Limestone Member within this formation, which comprises bioclastic limestone interbedded with sandstone and marl, suggesting a short marine transgression in a fluvial-dominated setting.

#### *1.2.4.6.4 Wukari Formation*

The Wukari Formation is a little-known unit that overlies the Markurdi Formation. It comprises intercalations of mudrock, limestone and sandstone interpreted to represent marginal marine-brackish depositional setting (Nwajide, 2013).

#### *1.2.4.6.5 Amaseri Formation*

This predominantly sandy formation (especially towards the top of the succession) consists of intercalated sandstone, conglomerate, and mudrock (Igwe and Okoro, 2016; Dim et al., 2016). The sandstone beds are bioturbated (*skolithos* and *Glossifungites* ichnofacies), moderately to poorly sorted, and vary from wavy laminated fine-grained calcareous sandstone to arenaceous cross-bedded medium- to coarse-grained sandstone. The mudrock beds are dark grey to black coloured. The conglomerate beds often show a sharp irregular base and contain reworked pebble to cobble-sized intraformational / extraformational limestone and mudrock clasts in a sandy matrix. This facies association is interpreted as deposited under shallow marine to marginal marine (Igwe and Okoro, 2016; Dim et al., 2016).

#### *1.2.4.7 Awgu Group*

The Awgu Group comprises the Awgu, Agbani, and Ogugu formations in stratigraphic order from bottom to top, which represent late Turonian-Coniacian strata in the central and southern Benue Trough.

##### *1.2.4.7.1 Awgu Formation*

Note that this formation forms a part of the homonymous Awgu Group, which may lead to confusion, depending on literature source. The Awgu Formation consists of grey to black, organic-rich mudrock, marl, bioclastic limestone, medium- to fine-grained calcareous sandstone and coal, which occur at the top of the unit (Obaje et al., 1994; Nwajide, 2013). A marine environment has been inferred based on lithofacies and biostratigraphic information (Petters and Ekweozor, 1982; Agagu *in* Nwajide, 2013; Kaki et al., 2013).

##### *1.2.4.7.2 Agbani Formation*

The Agbani Formation is a lateral facies equivalent of the Awgu Formation that consists of predominantly poorly sorted planar cross-bedded medium- to coarse-grained sandstone beds

interbedded with organic-rich mudrock beds, interpreted as upper delta plain in origin (Nwajide, 2013).

#### *1.2.4.7.3 Ogugu Formation*

This formation is laterally equivalent to the upper part of the Awgu Formation, and consists of dark grey organic-rich calcareous mudrock interbedded occasionally with thin beds of sandstone. The depositional environment has been interpreted as fluvio-deltaic (Agumanu and Enu, 1990).

#### *1.2.4.8 Lafia Formation*

The Lafia Formation represents post-Santonian (Maastrichtian) deposition in the Middle Benue Trough. It unconformably overlies the Awgu Formation and is coeval with the Nkporo Group (see section 1.2.5.1 below; Benkhelil, 1989; Nwajide, 2013). The formation consists of cross-bedded, poorly sorted, fine- to coarse-grained arkosic sand beds (which are occasionally strongly iron-cemented), mudrock beds and coal units interpreted as fluvial to marginal deposits (Obaje, 2009; Nwajide, 2013).

#### *1.2.5 Anambra Basin*

The Anambra Basin (Fig. 1.1) represents the post-rift phase (Fig. 1.2) of the Benue Trough. It formed because of slow basin subsidence caused by thermal relaxation (sag) in the aftermath of the westward shift in depocentre location following the Santonian inversion that affected the pre-Santonian strata of the southern Benue Trough (Fairhead and Binks, 1991; Binks and Fairhead, 1992). The basin covers an area of approximately 55,000 km<sup>2</sup> in size, and is bordered to the West, East, and South by the Benin Hinge Line (also known as the Okitipupa structure), the southern Benue Trough and the Niger Delta Basin, respectively (Fig. 1.1).



#### *1.2.5.1 Nkporo Group*

The Nkporo Group marks the onset of sedimentation in the Anambra Basin, and rests unconformably on basement rocks in the Benin flank (western section), and pre-Santonian rocks in the central and eastern parts of the basin. It is coeval with the Lafia Formation (Nwajide, 2013), and consists of the Afikpo, Nkporo, Lokoja (described in section 1.2.3.5) and Owelli, Enugu formations in stratigraphic order from bottom to top.

##### *1.2.5.1.1 Afikpo Formation*

The Afikpo Formation consists of a basal organic-rich mudrock unit, which grades into planar and herringbone cross-bedded sandstone to moderately bioturbated, hummocky cross-bedded sandstone at the midsection, and then passes into heterolith and organic-rich mudrock interbedded with coal at the top of the section. Nwajide (2013) interpreted this formation as paralic to marine.

##### *1.2.5.1.2 Owelli Formation*

The Owelli Formation is a lateral facies equivalent of the Nkporo Formation. It consists of well sorted, wave ripple laminated, fossiliferous siltstone-sandstone intercalated lithofacies at the bottom of the section, which is overlain by planar and hummocky cross-bedded, micaceous, reverse graded, fine-grained sandstone. Impressions of molluscs and *Ophiomorpha* burrows are also present (Odunze et al., 2013; Nwajide, 2013). A fluvial-tidal channel depositional setting has been inferred for this succession (Odunze et al., 2013; and Nwajide, 2013).

##### *1.2.5.1.3 Enugu Formation*

The Enugu Formation is a lateral facies equivalent of the Nkporo Formation and is characterized by mainly carbonaceous mudstone (with disseminated pyrite), interbedded with

lenticular to wavy laminated siltstone, and planar to herringbone cross-stratified sand interbeds. Shallow marine to estuarine conditions has been inferred for the formation based on the lithofacies association and fossil contents (Odunze et al., 2013; and Nwajide, 2013).

#### *1.2.5.1.4 Nkporo Formation*

The Nkporo Formation consists of mainly carbonaceous mudrock interbedded with fine-grained sand, marl or limestone. This formation is amply fossiliferous, with preserved ammonites, echinoids, crinoids, crabs, fish teeth, bryozoans, abundant benthic foraminifera, palynomorphs, etc. (Zaborski, 1983, 1999; Reyment *in* Nwajide, 2013). The lithofacies and fossils have been used to infer marine to marginal marine depositional conditions for this formation (Zaborski, 1983; Edet and Nyong, 1993; Odunze et al., 2013).

#### *1.2.5.2 Mamu Formation*

The Mamu Formation is characterized by a rhythmic succession of shale/sandy shale, sand, carbonaceous shale interbedded with coal, and is capped by sandy shale (Simpson, 1954, Nwajide, 2013). Also present are limestone and oolitic ironstone units (Akande and Mücke, 1993; Gebhardt, 1998; and Edegbai's unpublished data). Ladipo (1988) inferred a tidal flat to an estuarine depositional setting for this succession, whereas Reyment (1965), Murat (1972), Petters (1978), Petters and Ekweozor (1982), and Gebhardt (1998) interpreted the formation as deltaic.

#### *1.2.5.3 Ajali Formation*

The Ajali Formation is characterized by unconsolidated, medium-grained, poorly to moderately sorted, mineralogically and texturally mature cross-bedded sand beds. Nwajide (2013) noted the presence of liesegang rings, overturned cross-beddings, herringbone cross bedding, and water escape structures, as well as ichnofossils, including *Ophiomorpha*,

*Thalassinoides*, and *Rhizocorallium* at various stratigraphic levels. He inferred a tidally - influenced shallow marine to depositional setting

#### *1.2.5.4 Nsukka Formation*

The Nsukka Formation consists of carbonaceous shale interbedded with silt, coal, sand, ironstone and occasional limestone (Umeji and Nwajide, 2007). Marginal marine - to marine conditions, occasionally influenced by fluvial processes have been inferred for this lithofacies association (Umeji and Nwajide, 2007; Nwajide, 2013).

#### *1.2.6 Benin Basin*

The Benin Basin (Fig. 1.1) owes its origin to the opening of the South Atlantic Ocean as the African Plate separated from the South American Plate. It is a transform margin basin situated within the Gulf of Guinea shear zone (Okereke and Ofoegbu, 1990; Brownfield and Charpentier, 2006). The basin is about 500 km in length and up to 170 km onshore in width (close to the Nigeria-Benin Republic border). The basin extends from the Volta Delta in Ghana at its western limit through Togo and the Benin Republic into the Okitipupa Ridge in Southwest Nigeria at its eastern limit (Brownfield and Charpentier, 2006; Nwajide 2013; d'Almeida et al., 2016). The latest Cenomanian to Coniacian lithic infill comprises the Afowo and the Awgu (described in section 1.2.4.7.1) formations, while the Araromi Formation represents its post-Santonian sediment succession.

##### *1.2.6.1. Afowo Formation*

The Afowo Formation sits unconformably on the Lower Cretaceous Ise Formation, the 'Albian Sandstone' and basement rocks. It consists of moderately to well sorted, medium- to coarse-grained sandstone alternating with fossiliferous mudrock units that may contain pyrite (Kaki et al., 2013; Nwajide, 2013; d'Almeida et al., 2016). An estuarine to shallow marine depositional setting has been interpreted for this formation (Kaki et al., 2013; Nwajide, 2013).

#### *1.2.6.2. Araromi Formation*

The Araromi Formation unconformably overlies the Awgu Formation. It consists of fine- to medium-grained sandstone mostly at the base, and organic-rich fossiliferous, pyrite-rich mudrock with thin interbeds of marl, limestone, and lignite further up-section (Omatsola and Adegoke, 1981; d'Almeida et al., 2016). Based on its lithology, micropaleontology and the occurrence of pyrite, a shallow to deep marine environment has been inferred for the formation (Kaki et al., 2013; d'Almeida et al., 2016).

### **1.3 Discussion**

The opening of the Equatorial Atlantic in the mid-Albian marked the onset of marine deposition in present-day Nigeria (Fairhead and Binks, 1991). This transgressive episode caused by increased subsidence and rising global sea level (Fig. 1.2) was initially restricted in its extent to the Southeast and Southwest (Fig. 1.6), due to lower topography and proximity to the Equatorial Atlantic (Adeleye, 1975). With continued subsidence and rising global temperature and sea level (Fig. 1.2; Skelton et al., 2003; Bodin et al., 2015) in the Cenomanian-Turonian, and the linking of the South Atlantic with the Tethys Oceans which advanced southwards in the Cenomanian, marine deposition commenced in the Northeast (Fig. 1.7). In comparison to the Albian transgression, this episode was more far-reaching as topographic barriers that would have restricted its advance were overridden (Reyment, 1980; Reyment and Dingle, 1987). It marked the first time the Trans-Saharan seaway with the Benue Trough as an eastward connection route was established (Fig. 1.7) (Adeleye, 1975; Reyment, 1980; Benkhelil, 1986; Reyment and Dingle, 1987).

This hypothesis is supported by the presence of copiously fossiliferous marine sediments preserving fish, ammonite, gastropod and ostracod fauna that also occur in Niger (Adeleye, 1975; Benkhelil, 1989). Reyment (1980) and Petters and Ekweozor (1982) correlated

this episode to the Cenomanian-Turonian Bonarelli OAE 2 (Schlanger and Jenkyns, 1976; Jenkyns, 2010; Bodin et al., 2015). Edegbai's unpublished data on the Benin Flank (Figs. 1.3a, b), and a similar report of pre-Santonian rocks by Olawoki et al (2018) at Filele - northwest of Lokoja, Bida Basin, which is likely coeval with the pre-Santonian Bima, Ise, Gundumi and Illo formations, suggests that the Bida Basin and the Northwest was probably not emergent, and fluvio-deltaic conditions inferred to have existed in the Neocomian to early Albian probably continued to this time (Figs. 1.6 and 1.7). Paleogeographic reconstructions by Scotese (2014) (Figs. 1.8a, b) support this hypothesis, and the supposition that first opening of the Trans-Saharan seaway in the mid-Albian is untenable. As it is unlikely that the Bida Basin was already flooded in the early Turonian, no western arm of the Trans-Saharan prevailed, as depicted in the conceptual paleogeographic reconstructions of the late Albian (102 Ma) and early Turonian (92 Ma) provided in Figs. 1.6 and 1.7.

A change from sinistral to dextral strike-slip motion occurred along reactivated pre-existing oceanic faults formed by differential spreading rates of the South and Central Atlantic Oceans (Fairhead and Green, 1989). The resulting widespread inversion led to folding, faulting, intrusion, uplift and exhumation of pre-Santonian rocks in the Nigerian basins, and thus ultimately disrupted the Trans-Saharan connection and halted marine sedimentation in Nigerian basins (Benkhelil and Robineau, 1983; Benkhelil, 1989).

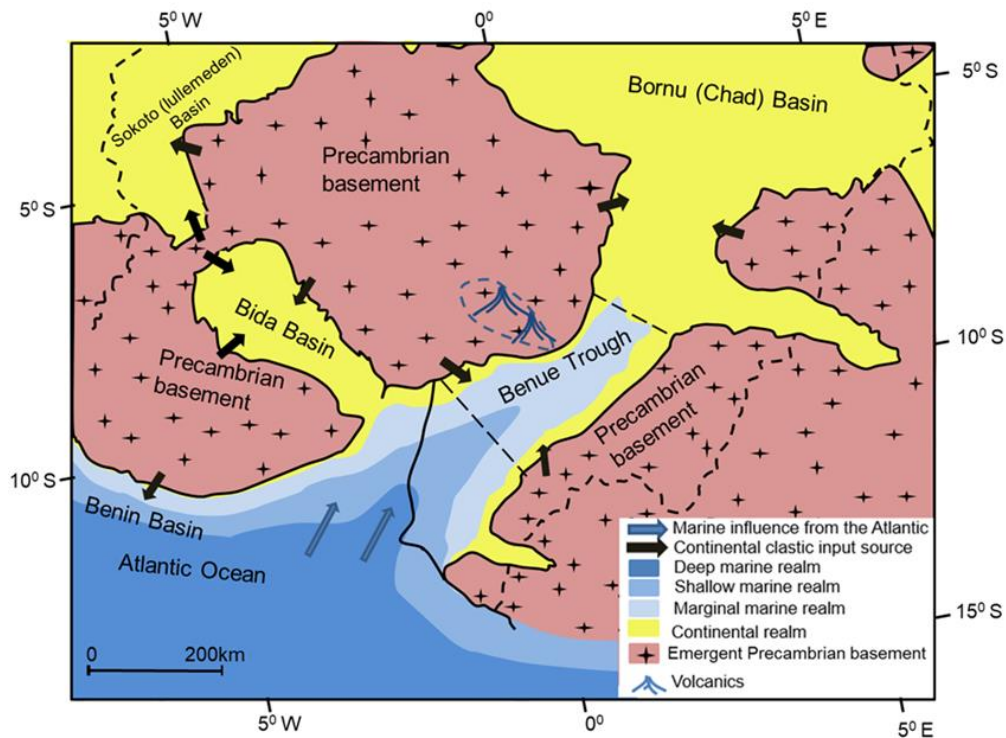


Fig. 1.6: Conceptual late Albian paleogeography of Nigeria (paleogeographic coordinates obtained from Scotese (2014)).

Renewed, slow subsidence in the Campanian-Maastrichtian in response to thermal relaxation (Fairhead and Binks, 1991; Binks and Fairhead, 1992) allowed for the accumulation of nearly flat-lying sediments in the Anambra and Bida basins, the central Benue Trough, as well as in the Southwest, Northwest, and Northeast. The lithostratigraphic similarity in these basins represented by widespread transgressive and predominantly marginal marine to shallow marine sediments records the global rise in sea level (Kogbe, 1981; Adetunji and Kogbe, 1986; Ojo and Akande, 2009). Ladipo (1988) noted that the paleogeographic implication of the post-Santonian Cretaceous succession in the Anambra Basin was indicative of one general widespread transgressive episode from the South Atlantic Ocean (marked by short spells regression in the latest Maastrichtian in some areas). This hypothesis contradicted the widespread regression identified in earlier studies (Murat, 1972; Petters, 1978).

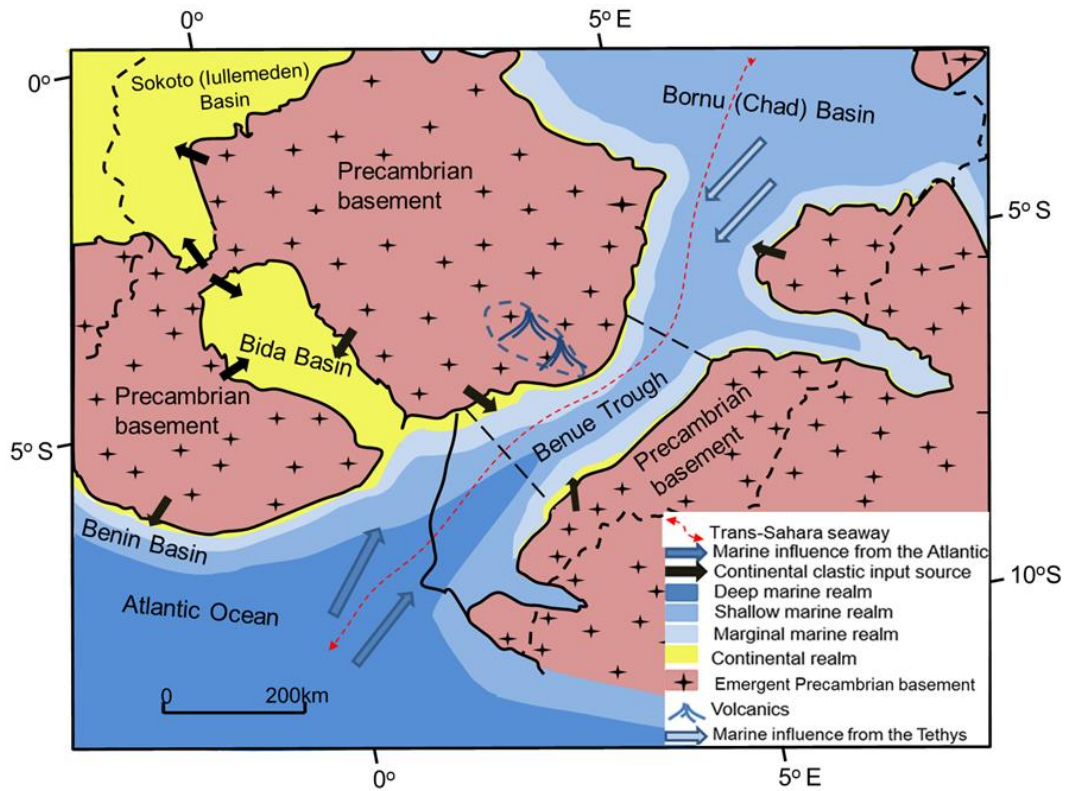


Fig. 1.7. Conceptual early Turonian paleogeography of Nigeria (paleogeographic coordinates obtained from Scotese (2014)).

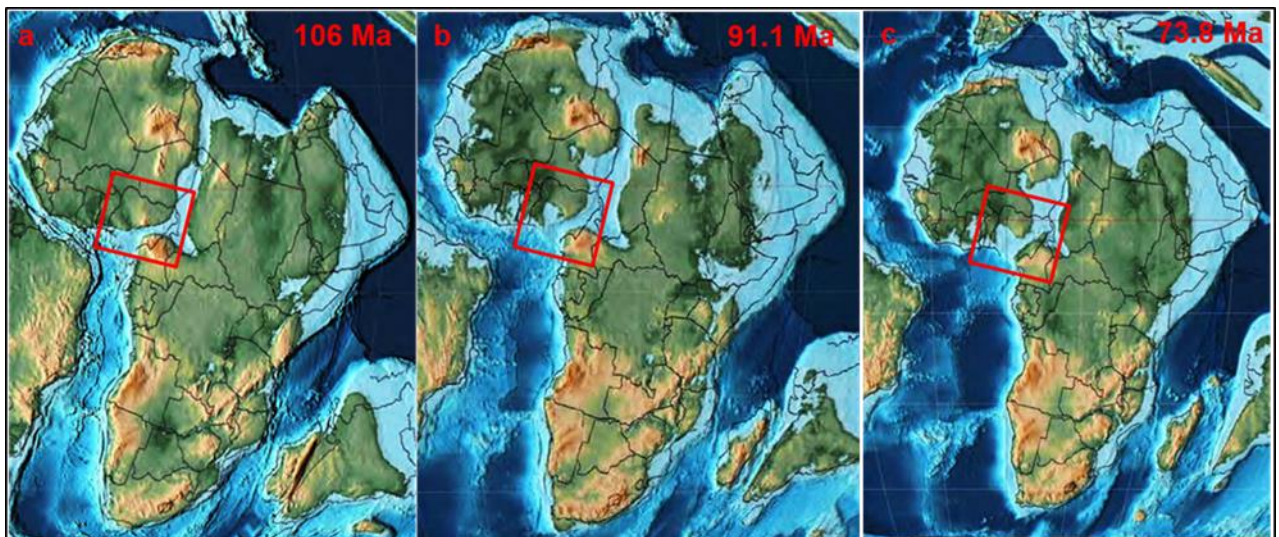


Fig. 1.8. Cretaceous paleogeographic reconstructions of Africa adapted from Scotese (2014) with boxes indicating the location of Nigeria; a, 106 Ma (mid Albian). b, 91.1 Ma (early Turonian). c, 73.8 Ma (late Campanian).

The similarity in depositional conditions, coupled with faunal similarity in parts of West and North Africa have been used as evidences of a second Trans-Saharan connection (Adeleye, 1975; Reyment, 1980; Kogbe, 1980, and 1981; Zaborski, 1983; Adetunji and Kogbe, 1986;

Moody and Sutcliffe, 1991; Gebhardt, 1998; Luger, 2003). An example is the occurrence of the ammonite fauna *Libyoceras* sp. believed to have originated in the Middle East and present in Campanian-Maastrichtian sediments in North Africa and Nigeria (Zaborski and Morris, 1999). In addition, widespread occurrences of several ostracod species, such as *Brachycythere ekpo* (common in Algeria and Nigeria), *Brachycythere oguni* (Tunisia, Algeria, Egypt, Mali, Niger, Nigeria and Togo), *Cytherella sylvesterbradleyi* (Libya, Mali, Nigeria and Ghana), and *Paracosta warriensis* (Algeria, Libya, Mali, Niger and Nigeria) were reported by Luger (2003) and Elewa (2017).

While it seems plausible that a second Tethyan-South Atlantic connection existed, there is no consensus about the connection pathway (Zaborski, 1983). Global Campanian-Maastrichtian paleogeographic reconstruction by Scotese (2014) prefer the same eastward Trans-Saharan connection route as for the Turonian (Figs. 1.8b and 1.8c), and shows flooding of the Bida Basin and Benue Trough, and an emergent Sokoto (Iullemeden) Basin. This scenario is unlikely because it contradicts local structural, stratigraphical and paleontological observations. The reconstruction does not account for the occurrence of marine to marginal marine conditions in the Sokoto Basin, and it favors flooding of the southern Benue Trough and the Yola sub-basin, which were emergent at this time. Any model proposed to explain widespread coeval marginal marine to marine sedimentation caused by the second Trans-Saharan linkage between the Tethys and Atlantic Oceans must take into account all local structural, stratigraphical and paleontological observations. Presently, the models that exist in the literature argue in favor of either a Benue Trough pathway, a Bida Basin pathway, or both.

The proposition of an eastward Trans-Saharan seaway via the Benue Trough pathway is based primarily on the premise that the Bida Basin is devoid of marine to marginal marine Campanian-Maastrichtian sediments and consequently, could not have been a seaway (Reyment, 1980; Braide, *in* Nwajide, 2013; Zaborski and Morris, 1999). Furthermore, the



discovery of poorly constrained ‘post-Santonian’ ammonite in the Benue Trough (Reyment *in* Reyment, 1980; Popoff et al., 1986) has been used as a supporting evidence. This interpretation was in spite of sedimentological, paleontological and geochemical evidence of marine to marginal marine conditions by Adeleye (1975), Umeorah (1987), Idowu and Enu (1992), Agyingi (1993), Abimbola (1997), Jan du Chêne et al., *in* Gebhardt (1998), and Mücke et.al (1999). More recently, Ojo and Akande (2009, 2012) published sedimentological, paleontological (dinoflagellate cysts, acritarchs, foraminifera, whole remains and cast of molluscs), and ichnological evidences of widespread marine to marginal marine conditions in the Bida Basin. In addition, they noted the sedimentological similarities between the Campanian-Maastrichtian strata in the Anambra and Bida basins, which Edegbai’s unpublished data has confirmed. As indicated earlier, the southern Benue Trough was emergent after the Santonian tectonics and likely inhibited any seaway via that route (Adeleye, 1975). Furthermore, the likelihood that *Libyoceras* preserved in the northern Benue Trough is pre-Santonian (Zaborski, 1983; Zaborski and Morris, 1999), and the difficulty in correlating it with Campanian-Maastrichtian sediments in the Anambra Basin (Reyment, 1980) strongly suggests the Bida Basin pathway as more likely than the Benue Trough connectivity.

A westward Trans-Saharan seaway hypothesis through the Bida Basin pathway is strengthened by: (i) the discovery of six hitherto endemic agglutinated foraminifera species, namely *Haplophragmoides haussa*, *Haplophragmoides nigeriense*, *Haplophragmoides sahariense*, *Textulariopsis gidankukaensis*, *Textulariopsis dukamajina*, *Trochammina* sp., and *Trochammina dutsuna* (Petters, 1982) in the Dukamaje and Mamu formations in the Sokoto and Anambra basins, respectively (Gebhardt, 1998); (ii) correlation of Campanian-Maastrichtian sediments in the Southeast and the Northwest using *Libyoceras* sp (Zaborski, 1983); and (iii) similar marine mosasaur species (*Pluridens walker*) in the Iullemeden Basin (Niger) and Anambra Basin (Lingham-Soliar, 1998).

Taking into consideration the Upper Cretaceous paleogeographic reconstructions by Scotese (2014), and information from Adeleye (1975), Kogbe (1980), Reyment and Dingle (1987), Ladipo (1988), Gebhardt (1998) and Zaborski and Morris (1999), we revise the paleogeography of the latest Campanian to middle Maastrichtian. This interpretation advocates a Trans-Saharan connection pathway via the Bida Basin, and flooding of the northern Benue Trough (Gongola sub-basin) and central Benue Trough by Tethys inflow via the Chad Basin (see Fig. 1.9). This is a more plausible explanation for the widespread marine to marginal marine conditions in Nigeria's sedimentary basin at this time, given that the lower Benue Basin experienced uplift, erosion, and non-deposition due to the Santonian tectonics. The emergent lower Benue Trough sourced the continental clastic sediments in the eastern Anambra Basin, as observed from paleocurrent analysis of the Ajali Formation (Amajor, 1987b) and geochemical data (M. E. Okiotor, pers. comm., 2015).

### *1.3.1 Implication for source rock development*

The opening of the Equatorial Atlantic led to widespread deposition of marine source rocks in the latest Cenomanian to Turonian, and subordinate coals in the Coniacian. However, widespread coal deposition occurred in the Campanian-Maastrichtian when marginal marine conditions prevailed.

#### *1.3.1.1 Latest Cenomanian to Coniacian*

In the Southeast, two source rock units exist in the Eze-Aku Group and Awgu Group: (i) lower to middle marine source unit; and (ii) subordinate upper coaly source unit. The source character of the lower to middle marine source unit is fair (mostly at its base?) to good organic richness, mature to post mature with gas prone Type III-IV kerogen (Petters and Ekweozor, 1982; Total, 1984; Unomah, 1991; Babatunde, 2010; Odigi and Amajor 2010; Akande et al., 2012). By contrast, the source character of the upper coaly source unit reveals organic richness

up to 66%, with Type III and subordinate Type II kerogen, and is early mature to post mature (Obaje et al., 2004; Ehinola et al., 2002; Obaje and Lingouis., 1996). In the Southwest, geochemical data from the Awgu Formation reveal early mature, oil and gas prone Type II-III source units, with fair to good organic richness (Kaki et al., 2013). In the Gongola sub basin, present day organic richness and source quality of the Gongila and Fika formations range from fair to good, gas prone Type III-IV kerogen, immature to late mature due to magmatic activity (Akande, et al., 1998; Obaje et al., 2004, 2006; Boboye and Abimbola, 2009; Adekoya et al., 2014; Alalade and Tyson, 2013). In the Yola sub-basin, the organic richness and source quality of the marine source unit range from poor to fair, gas prone Type III-IV kerogen, and early to post mature due to magmatic activity (Akande et al., 1998; Obaje et al., 2004, 2006; Abubakar, 2014; Sarki Yandoka et al., 2016). The Coniacian Lamja coals have organic richness up to 72%, early maturity with gas prone Type III and subordinate oil prone Type II kerogen (Jauro et al., 2007; Sarki Yandoka at al., 2015).

We note here that heavy oil within oil seeps and tar sand deposits in the Southeast (Eze-Aku and Awgu Groups), Southwest (Afowo Formation) and Northeast (Bima Formation) is sourced from these dominantly marine source units (Enu, 1985; Coker and Ejedawe, 1987; Brownfield and Charpentier, 2006; Babatunde, 2010; Reijers and Petters, *in* Nwajide, 2013; Bata et al., 2015).

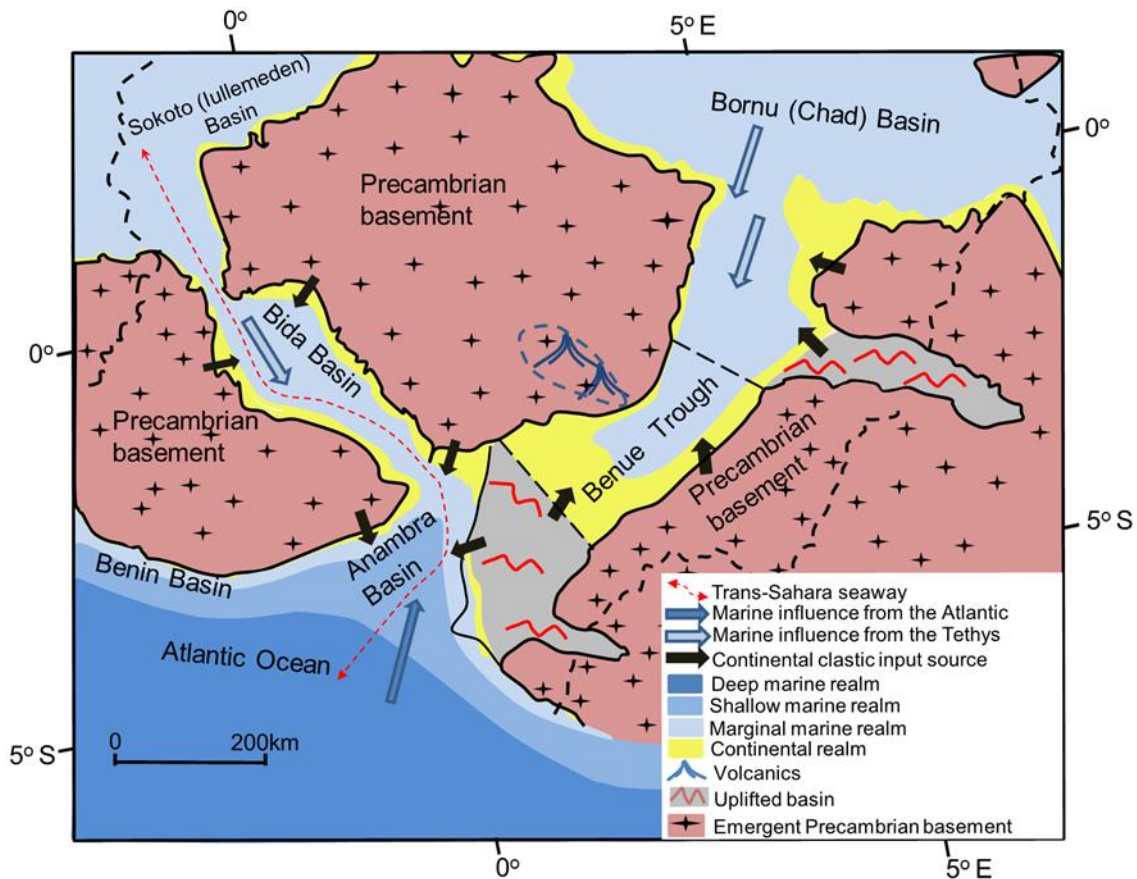


Fig. 1.9. Conceptual early Maastrichtian paleogeography of Nigeria (paleogeographic coordinates obtained from Scotese (2014)).

### 1.3.1.2 Campanian-Maastrichtian source rocks

Widespread post-Santonian (mostly) marginal marine conditions favored source rock development within the mudrock and coal units. This post-Santonian coal unit, which is best developed in the Anambra Basin, is more widespread than the pre-Santonian coal. In the Southwest, geochemical data from the Araromi Formation reveal oil prone Type II kerogen with good to excellent organic richness and early maturity (Kaki et al., 2013). In the Northeast, geochemical data from the mudrock facies in the Gombe Formation reveal thermally immature to early mature, gas prone Type III-IV kerogen, with fair to good present-day organic richness (Akande et al., 1998; Obaje et al., 2004; Abubakar, 2014; Ayinla et al., 2017). Furthermore, geochemical data from the Gombe Formation coal facies reveal thermally immature gas prone Type III kerogen, with up to 80% organic richness (Obaje et al., 2006; Abubakar, 2014, Ayinla

et al., 2017). Geochemical data from Bida Basin's Patti Formation indicate thermally immature gas prone Type III kerogen with fair to good organic richness (Idowu and Enu, 1992; Obaje et al., 2004, 2006; Akande, et al., 2005; Nton and Okunade, 2013). In the Anambra Basin, the source potential of the Nkporo Group and carbonaceous mudrocks of the Mamu Formation reveal thermally immature to early mature (at depth), dominantly Type III (with subordinate Type II) kerogen, with fair to good organic richness. The best source potential occurs at the top section of the Nkporo and Enugu formations, and the basal to mid sections of the Mamu Formation (Total 1984; Ehinola et al., 2005; Babatunde, 2010; Akande et al., 2012; Edegba and Emofurieta, 2015). Geochemical data from the Mamu Formation coal facies reveal thermally immature (early mature at depth) Type III-II kerogen with up to 77% organic richness (Akande et al., 2012).

### *1.3.2 Implication for solid mineral and groundwater resource development*

#### *1.3.2.1 Limestone*

Widespread flooding of Nigerian basins in the Cenomanian to Turonian led to the deposition of economically viable limestone units across the Benue Trough. The Nkalagu and Ashaka limestone deposits are good examples (Popoff et al., 1986; Gebhardt 1997, 1999, 2004; Aliyu et al., 2017). Limestone formation in the post-Santonian was limited due to widespread marginal marine conditions. These deposits are at best sub-economical.

#### *1.3.2.2 Ironstone*

Ironstone units exist in the post-Santonian rocks of the northern Benue Trough, Anambra, and Bida basins. Of prospect is Bida Basin's Agbaja Formation with approximately one billion tons of ironstone reserve (Alafara et al., 2005). The Agbaja ironstone possesses oolitic to pisolitic texture, and it is of the kaolinite type characterized by low magnesium oxide

(MgO) and an average iron content of 63.5% (Umeorah, 1987; Abimbola, 1997; Mücke et al., 1999).

#### *1.3.2.3 Clay*

Low energy conditions in marine to marginal marine depositional settings favored the formation of extensive clay deposits in the Upper Cretaceous. In general, kaolinite is the dominant clay mineral phase in these rocks which have subordinate illite and smectite. This is attributed to the warm humid paleoclimate, which favored intensive weathering and acidic leaching (Agumanu and Enu, 1990; Odoma et al., 2015; Ojo et al., 2016; Edegbai's unpublished data). Generally, there is a decline in kaolinite content from post-Santonian to pre-Santonian rocks attributed to a change from lower salinity marginal marine to higher salinity marine depositional conditions (Agumanu and Enu, 1990).

#### *1.3.2.4 Groundwater resources*

The best groundwater resources in Upper Cretaceous rocks occur within sandstone and siltstone units. The latest Cenomanian to Coniacian sediments are mostly aquicludes, except in areas where they are weathered or are sandstone units (Agbani, Ameseri, Lamja formations, etc.; Oteze, 1981). Better groundwater resource potential occurs in the post-Santonian rocks, which contain more sandstone and siltstone units. Among these units, the Ajali Formation is the most prolific; it holds the greatest Upper Cretaceous groundwater resource, which ranks it among the seven giant aquifers in Nigeria (Oteze, 1981, Akujieze et al., 2003). The Lokoja, Owelli, Enagi, Wurno, Taloka, Lafia and Gombe formations also hold vast amounts of groundwater resources that are currently exploited and are artesian in places (Oteze, 1981, Akujieze et al., 2003). Some potential exists in the aquicludes of the Nkporo, Enugu, Mamu, Araromi, and Nsukka formations due to the development of perched aquifers (Adelana et al., 2008) and occurrence of local sandstone units.

## 1.4 Conclusion

This comprehensive review of Upper Cretaceous rocks in Nigeria's sedimentary basins highlighted the following:

- (1) Consequent upon the opening of the Equatorial Atlantic during the Albian-early Cenomanian, marine flooding was restricted to the Southeast and Southwest, while continental-deltaic conditions prevailed in the Northeast, Bida, Sokoto, and Bornu basins
- (2) The initiation of the Bida Basin predates the Santonian, and is as old as the Benue Trough.
- (3) During the Turonian stage, the first Trans-Saharan seaway between the South Atlantic and the Tethys (which started flooding southwards from the Cenomanian) was established. The connection pathway was eastward via the Benue Trough.
- (4) The plate-wide Santonian inversion tectonics characterized by folding, faulting, uplift and intrusion halted sedimentation across Nigeria.
- (5) A second Trans-Saharan connection was re-established in the Maastrichtian. At this time, the connection pathway was westward via the Bida Basin. The Tethys flooded the northern Benue Trough (Gongola sub-basin) and central Benue Trough via the Chad Basin.
- (6) Widespread marine conditions in the pre-Santonian favored the deposition of economically exploited limestone and clay deposits, and marine source rocks with subordinate coal. These units are mostly aquicludes with potential for groundwater resource.

(7) Widespread mostly marginal marine conditions in the Campanian-Maastrichtian favoured the deposition of economically exploited coal, ironstone and clay deposits. The sandstone and siltstone units hold vast groundwater resources, which are currently being exploited.

### **Acknowledgement**

The first author thanks the University of Benin Research and Publications Committee, Tertiary Education Trust Fund, the Fulbright Commission (15160892), the Niger Delta Development Commission (NDDC/DEHSS/2015pgfs/EDS/011), the DAAD (ST32 - PKZ: 91559388) and the Nigerian Association of Petroleum Explorationists who have contributed to his educational development over the years. The Authors are grateful for the contributions of Drs. Kenny Ladipo, Sam Coker, Holger Gebhardt and Wolfgang Rübsam, which greatly improved the first draft of this paper.



## Chapter Two

Campano-Maastrichtian paleoenvironment, paleotectonics and sediment provenance of western Anambra Basin, Nigeria: Multi-proxy evidences from the Mamu Formation

Published as:

*Edegbai, A.J., Schwark, L., Oboh-Ikuenobe, F.E., 2019. Campano-Maastrichtian paleoenvironment, paleotectonics and sediment provenance of Western Anambra Basin, Nigeria: Multi-proxy evidences from the Mamu Formation. <https://doi.org/10.1016/j.jafrearsci.2019.04.001>*

### A B S T R A C T

This article presents the results of a high-resolution evaluation of the sedimentological, mineralogical, palynofacies, and geochemical aspects of the Mamu Formation aimed at deciphering the sediment provenance, as well as the prevailing paleoenvironmental, paleoclimatic and paleotectonic conditions that occurred during the late Campanian-middle Maastrichtian age in the less studied western section of the Anambra Basin, Nigeria. Four measured sections exposed in Uzebba (composite), Auchi, Okpekpe, and Imiegba were investigated using sedimentological (outcrop studies and laser diffraction particle size analysis), mineralogical (XRD), geochemical (ICP-MS and XRF) and palynofacies techniques. Seven lithofacies were identified and grouped into central basin, marsh, bay, barrier, beach, and washover fan facies association as well as meandering fluvial-tidal channel facies association interpreted as indicative of a tidally influenced wave dominated estuarine paleoenvironment. In addition, mineralogical and palynofacies characterization revealed the heterogeneous nature of the dark mudstone lithofacies, varying from a more proximal low salinity phytoclast and quartz dominated marsh and bay mudstones to a more distal higher salinity palynomorph and clay dominated central basin accumulating deepwater mudstones.

Consistent with recent Campano-Maastrichtian paleogeographic and paleoclimatic models we observed a dominance of kaolinite, a high chemical index of alteration above 90%, and a predominantly low index of compositional variability values ( $< 1\%$ ), which signifies mineralogical maturity of the sediments due to sediment recycling and intensive chemical weathering under humid tropical paleoclimate. Furthermore, trace and major element discriminant plots revealed a felsic-intermediate provenance for the sediments under passive margin paleotectonic regime, which is in agreement with the regional distribution, geology, and geochemistry of the pre-Santonian rocks and the Precambrian basement rocks in the area.

## **2.0. Introduction**

The late Campanian-early Maastrichtian stage of the Cretaceous period in Nigeria is characterized by the development of widespread marginal marine conditions due to eustatic sea level rise after the end of plate-wide (mostly) Santonian inversion tectonics (Obaje, 2009; Nwajide, 2013; Edegbai *et al.*, 2019). This development resulted in the deposition of kaolinite-rich mudstone, arenites, coal, ironstone and limestone units of the Patti and Sakpe formations (Bida Basin), Mamu Formation (Anambra Basin), Araromi Formation (Benin Basin), Taloka Formation (Sokoto Basin), and Gombe and Lafia formations (Benue Trough) (Edegbai *et al.*, 2019). The Mamu Formation holds the largest coal resource in Nigeria, which is estimated to be 1,374 million tonnes (Behre Dolbear and Company, 2006). In addition, its mudstone and coal units are regarded as important source units within the upper Cretaceous petroleum system in Southern Nigeria (Akande, *et al.*, 2007, 2012; Adedosu *et al.*, 2010; Abubakar, 2014).

In the last 10 years, studies of the Mamu Formation (mostly aimed at source rock characterization and palynology) have focused more on the eastern segment of the Anambra Basin (Akaegbobi *et al.*, 2000; Akande *et al.*, 2007, 2012; Aganbi and Emofurieta, 2010; Adedosu *et al.*, 2010, 2014; Nton and Awarun, 2011; Ogala, 2011; Chiaghanam *et al.*, 2013;

Uzoegbu *et al.*, 2014; Odoma *et al.*, 2015; Onuigbo *et al.*, 2015; Uzoegbu and Okon, 2017; Adebayo *et al.*, 2018; Dim *et al.*, 2019). However, in contrast few studies have been undertaken in the western part (Benin flank) of the basin (Odedede, 2013; Ola-Buraimo *et al.*, 2014; Edegbai *et al.*, 2015; Ejeh, 2016; Asadu and Ibe, 2017; Igbinigie *et al.*, 2017; Ogbamikhumi *et al.*, 2017). Recent road construction at Okpekpe and Imiegba revealed new exposures, which together with existing outcrop sections at Uzebba and Auchi localities (see Section 2.2) have afforded a unique opportunity to study the lithofacies units of the Mamu Formation in the western section of the Anambra Basin. This study, therefore, aims to unravel the provenance of the sediments, and to decipher the paleoenvironmental and paleotectonic conditions during the late Campanian-early Maastrichtian stage through a high-resolution evaluation of the mineralogy, palynofacies, sedimentology and geochemistry of the Mamu Formation exposed in this part of the basin. This investigation will provide valuable insight into the sediment provenance and paleoceanographic conditions of the Maastrichtian Trans-Saharan Seaway, as well as provide valuable information that will guide exploration of fossil fuel resources in the Anambra basin especially as there is renewed interest for fossil fuel exploration in Nigeria's onshore basins.

## **2.1 Geologic overview**

### *2.1.1 Tectonics and Stratigraphy of the Anambra Basin*

The Anambra Basin (Fig. 2.1) developed during the thermal sag phase of the Benue Trough, which formed following the plate-wide inversion tectonics that occurred in the Santonian and possibly continuing into the Maastrichtian in the Northern Benue Trough and Chad Basin (Nwajide, 2013; Edegbai *et al.*, 2019). The inversion was a consequence of stresses that had built up because of Africa-Europe plate interactions, resulting in different spreading rates of the Central and Southern Atlantic Oceans. This led to the rejuvenation of transform

faults that run into the West African Rift System (WARS) from the mid-Atlantic Ridge, resulting in a change from sinistral to dextral strike-slip movement (Fairhead and Green, 1989). The tectonic event, which was characterized by folding, faulting, volcanic extrusion, uplift and exhumation of pre-Santonian sedimentary fill, was more severe in the Southern Benue Trough (Guiraud and Bosworth, 1997) and sourced a large proportion of the Anambra Basin lithic fill (Benkhelil, 1982; Amajor, 1987b).

The Anambra Basin is about 55,000 km<sup>2</sup> in size, and is bordered to the West, East, and South by the Okitipupa Ridge, the Southern Benue Trough and the Oban Massif, and the Niger Delta Basin, respectively (Fig. 2.1). The river Niger separates the basin into east and west segments (Fig. 2.1). Its lithic fill is part of the post-Santonian Cretaceous coeval succession of Nigeria caused by rising eustatic sea level (Fig. 2.2) that led to the re-establishment of the Trans-Saharan Seaway, which connected the Tethys Ocean with the Atlantic Ocean through the Sokoto-Bida Basin route in the early Maastrichtian (Fig. 2.3) (Edegbai *et al.*, 2019). Using gravity measurements and well data, Agagu and Adighije (1983) noted that the Cretaceous basin fill was thicker in the eastern segment (up to 8000 m) particularly in the area around Nzam-1 well and thinned out to about 2000 m at the basin fringes in the western flank. This is illustrated in the W-E section line (Fig. 2.1) modified from Total (1988).

Sedimentation began with widespread deposition of the dominantly marine sediments of the Nkporo, Owelli, and Enugu formations in the eastern section and alluvial to fluvial sediments of the Lokoja Formation in the northern and western sections of the basin (Nwajide, 2013). This was followed by the largely estuarine to marine sediments of the Mamu Formation, which comprise of bay, marsh, central basin, fluvial-tidal channel, tidal flat, barrier-beach/washover fan deposits (Ladipo, 1988) as well as shoreface, offshore transition and open shelf deposits (Dim *et al.*, 2019). Thereafter, the subtidal/shallow marine Ajali Formation was deposited (Ladipo, 1986; Umeji, 2000; and Nwajide, 2013).

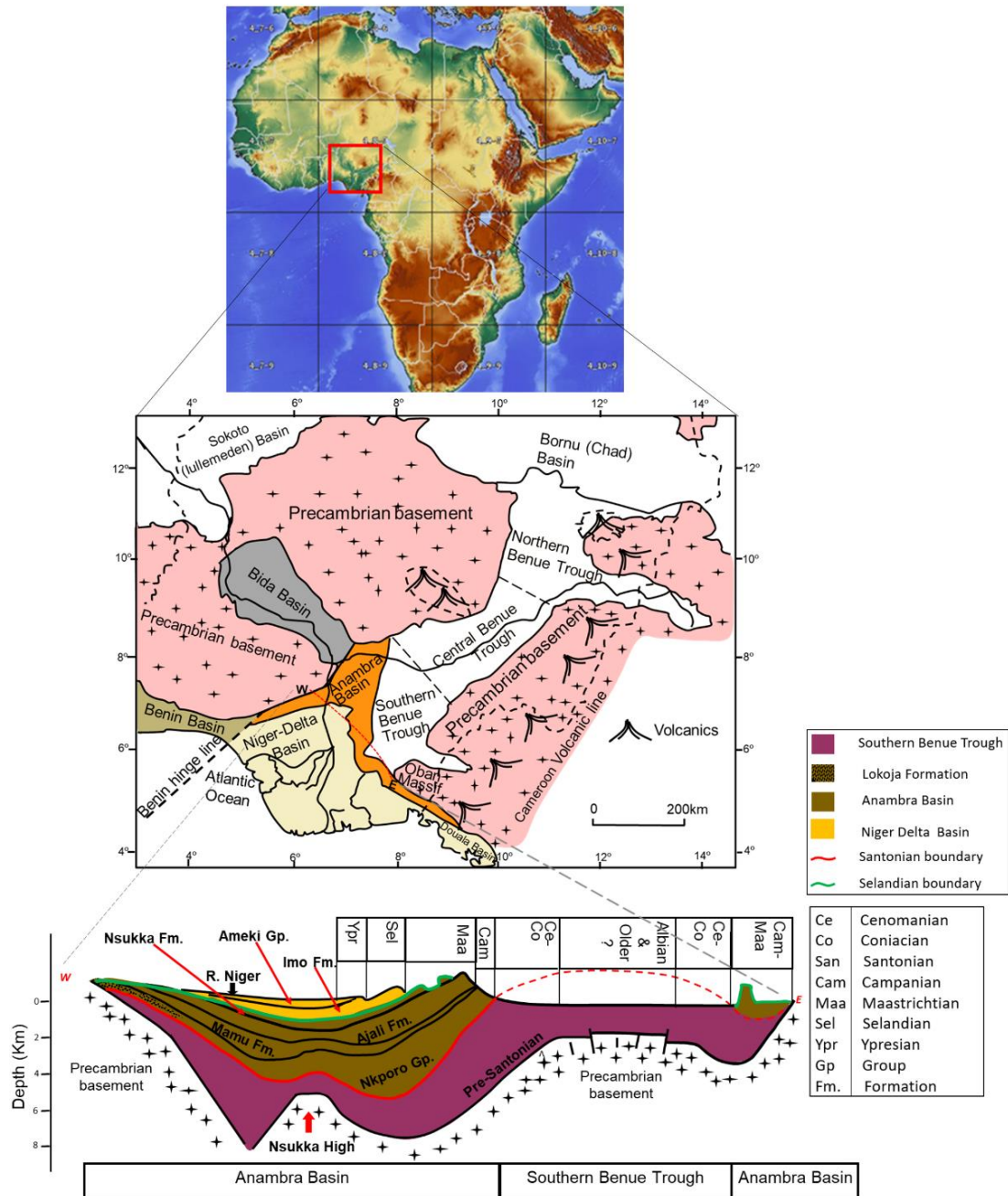


Fig. 2.1. Map of Nigeria showing areas underlain by sedimentary and basement rocks. Below a W-E cross section of the Anambra Basin showing lithostratigraphic packages (Modified from Total, 1988, and Edegbai et al., 2019a) is given.

Falling eustatic sea level from mid-Maastrichtian to Danian time (Fig. 2.2) led to the deposition of the regressive units of the Nsukka Formation, the youngest lithostratigraphic unit in the Anambra Basin (Nwajide, 2013). The Nsukka Formation, which has a lithostratigraphy similar to the Mamu Formation, is better developed in the eastern segment of the basin where complete sections exist (Nwajide, 2013), whereas only a thin ironstone unit capping the Ajali

Formation represents the Nsukka Formation in the western segment (S.J.L. Coker, pers. comm., 2016).

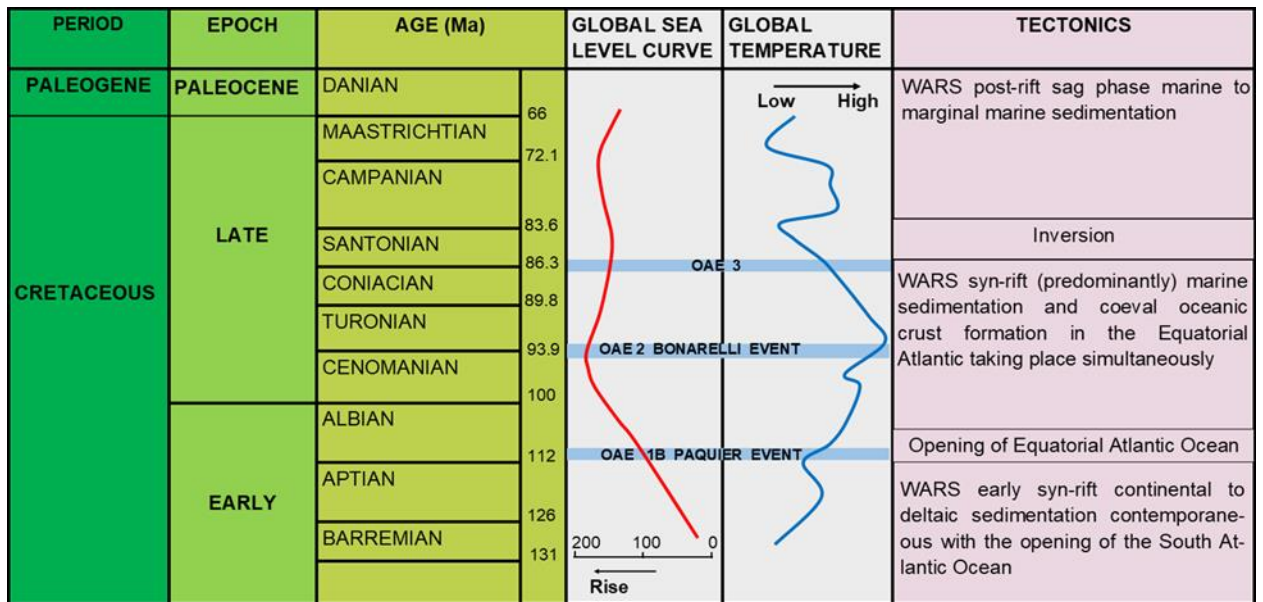


Fig. 2.2. Cretaceous-Paleogene tectonic evolution (adapted from Edegbai *et al.*, 2019a). WARS = West African Rift System; black arrows indicate sea level and temperature rise.

### 2.1.2. Lithostratigraphy of the Mamu Formation

The Mamu Formation has been previously described as a cyclothem with alternating marine and continental lithological units exhibiting basin-wide variability in thickness and facies (Ladipo, 1988; Gebhardt, 1998; Nwajide, 2013). This study, however, hypothesizes that estuarine depositional conditions are responsible for the widespread facies variability (Reinson, 1992; Boyd *et al.*, 2006). The age of the sediments varies from late Campanian to early Maastrichtian in the south to middle Maastrichtian in the north (Zaborski, 1983; Gebhardt, 1998). Simpson *in* Nwajide (2013) reported a thickness of up to 100 m in Enugu (in the eastern segment), while up to 20 m have been reported from outcrops in the western segment. However, subsurface data (Total, 1988) reveal thickness in excess of 600 m in the eastern segment of the basin (Fig. 2.4a).

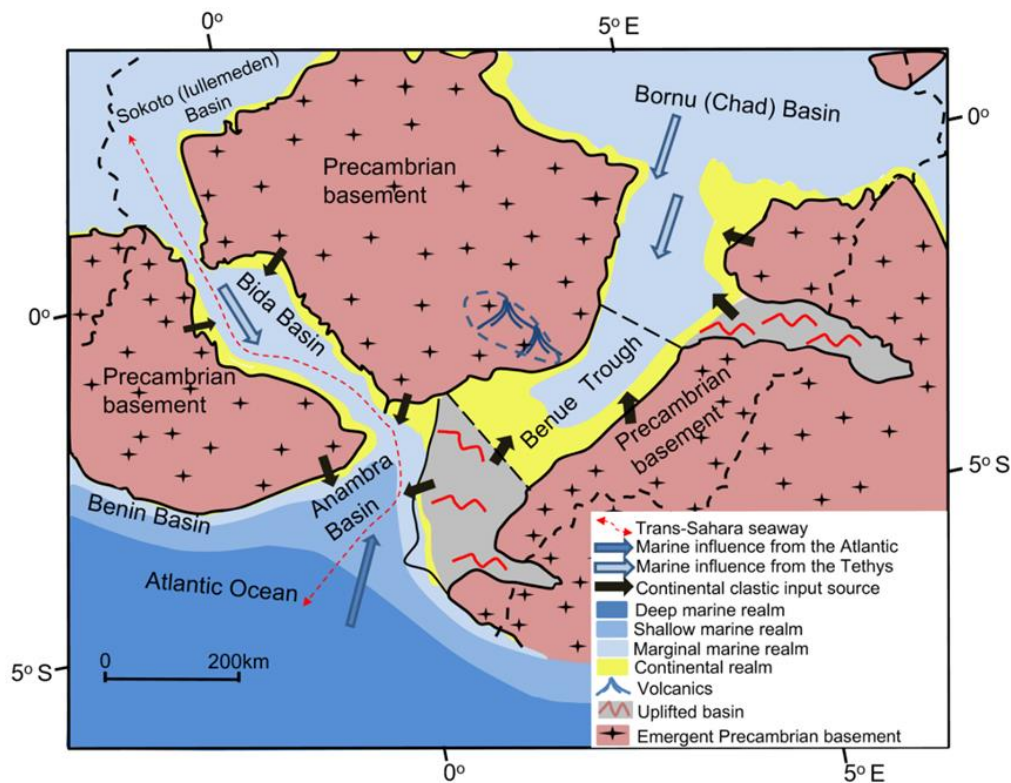


Fig. 2.3. Conceptual early Maastrichtian paleogeography of Nigeria (Edegbai et al., 2019a).

Five mudstone dominated sequences, each with the following units: basal shale/sandy shale unit overlain by sandstone, carbonaceous shale, coal, and sandy shale at the top were the initial units identified (Simpson *in* Nwajide, 2013). Limestone and ironstone units have also been described (Akande and Mücke, 1993; Gebhardt, 1998). Nwajide (2013) observed that coal beds were better developed at the base of the successions, interpreted to indicate gradual transitioning to open strand plain depositional condition. Based on facies analysis, Adeniran *in* Gebhardt (1998) and Ladipo (1988) suggested that the sediments were deposited in a tidal flat-estuarine setting. Simpson *in* Nwajide (2013) and Salami (1990) preferred shallow freshwater swamp/marsh conditions based on palynology, whereas deltaic depositional conditions were favored by Murat (1972), Petters (1978), Petters and Ekweozor (1982), Reyment *in* Salami (1990) and Gebhardt (1998) based on regional studies and micropaleontology. Recently, Dim *et al.* (2019) identified eleven lithofacies based on facies analysis from outcrops in the eastern

segment representing depositional environments varying from brackish water lagoons/swamp to open shelf.

## **2.2 Methodology**

Fieldwork was conducted on outcrop sections at Okpekpe, Imiegba, Uzebba and Auchi in the Benin Flank, western Anambra Basin (Figs. 2.4a, b). The Okpekpe, Imiegba and Uzebba sections (composite) approximate part of the basal to mid-section of the Mamu Formation, while the Auchi section approximates the top of the Formation. Several studies (Ajayi *et al.*, 1989; Teme, 1991; NGSA, 2006 (Fig. 2.4b); Imeokparia and Onyeobi, 2007; Ola-Buraimo *et al.*, 2014; Edegbai and Emofurieta, 2015; Ejeh, 2016) previously established the stratigraphic control of the outcrops chosen for this study. Detailed descriptions and logging of outcrops were carried out prior to selecting samples for particle size and petrographic studies, palynofacies, mineralogical and geochemical analyses. Characterization of lithofacies units subsequently was achieved after integrating data from outcrop descriptions with particle size, petrographic, palynofacies, mineralogical and geochemical analyses. Following these analyses paleoenvironmental, proximal-distal relationships, paleosalinity, provenance and paleotectonics were inferred.

### *2.2.1. Sedimentological analysis*

A few mudstone samples selected for microfacies analysis were cut into billets and made into thin sections at Precimat (precimat.com), Carrollton Texas 75006, USA. One hundred and sixty-six samples selected for grain size analysis were disaggregated by hand and soaked in deionized water. In addition, sodium hexametaphosphate (Calgon) was added as a dispersant to prevent flocculation of clay particles before subsequent particle size measurements were carried out using a Microtrac S3500 laser diffraction analyzer at the Missouri University of Science and Technology (Missouri S&T). The raw data were used to



plot cumulative frequency curves from which the percentages of clay, silt and sand fractions, as well as statistical data – including inclusive graphic standard deviation (sorting), graphic mean, skewness, kurtosis and median (Folk, 1974) – were determined. Textural analysis data were integrated with results from outcrop and microfacies studies, for a comprehensive sedimentological characterization.

### 2.2.2. *Palynofacies analysis*

Eighty-one samples (eight of which were composite samples) were selected for palynofacies analysis. Kerogen slides were prepared at Missouri S&T following standard palynological slide preparation technique detailed by Traverse (2007). Approximately 15 g from each sample was treated in HCl and HF to eliminate carbonates and silicates, respectively. The residue was washed several times, screened with a 10- $\mu$ m nylon sieve, and subsequently permanently mounted on slides sealed with Depex. Identification of the various groups was carried out using transmitted light microscopy, followed by point counting a minimum of 300 particulate organic matter (POM) and palynomorphs per sample (except in barren samples) and subsequent normalization to 100%. A simplified classification scheme for the palynomorph groups and POM was adapted for this study as follows: phytoclasts (woody and non-woody debris, cuticles, terrestrial amorphous organic matter), palynomorphs (marine palynomorphs [dinoflagellate cyst, acritarch and foraminiferal test linings], sporomorphs [pollen and spores] and fungal remains), and aquatic amorphous organic matter (Fig. 2.5).

### 2.2.3. *Mineralogical analysis*

An acid test (5% HCl) was carried out on all the samples before selecting ninety samples for further mineralogical analysis using X-ray diffraction (XRD). Selected samples were oven dried at 40°C for 48 hours and manually ground into powder using an agate mortar. XRD analysis was performed with a PANalytical X'Pert Pro multi-purpose Diffractometer at

Missouri S&T using CuK $\alpha$  radiation operated at 45 kV and 40 mA with no monochromator and a fixed 0.38 mm divergence slit. The samples were scanned from 5 to 80 two-theta degrees using 0.026 – degree steps and counted for 86.19 secs per step. Mineral concentrations were normalized to 100% after modelling the data using a Highscore controlling software with histogram-matching algorithm and Rietveld phase quantification method.

#### 2.2.4. *Geochemical analyses*

One hundred and thirty-three samples were analyzed for major and trace element concentrations at Bureau Veritas Mineral Laboratories (AcmeLabs), Vancouver, Canada, using X-ray fluorescence (XRF) and inductively coupled plasma mass spectrometry (ICP-MS). For the XRF analysis, approximately 5 g of powder sample was oven dried at 105°C and fused into a platinum mold with a commercial lithium tetraborate flux before subsequent analysis by a PANalytical Axios Max XRF. For the ICP-MS analysis, approximately 0.25 g of powder sample was (near totally) digested with a multi-acid solution comprising H<sub>2</sub>O-HF-HClO<sub>4</sub>-HNO<sub>3</sub> with 2:2:1:1 proportions, respectively. HCl (50%) was added to the residue before heating using a mixing hot block and allowed to cool. The cooled solution was analyzed by a PerkinElmer ELAN 9000 ICP-MS.

### 2.3. **Results**

The results of the particle size distribution, palynofacies characterization, mineralogical characterization, and geochemical characterization are presented in tables' 2.1a-c.

#### 2.3.1. *Particle size distribution*

Six sediment groups were identified from a ternary plot of clay %, silt % and sand % (Fig. 2.6a) (Lazar *et al.*, 2015): (a) sandstone (Ss) composed of  $\geq 75\%$  sand-sized particles; (b) muddy sandstone (mSs) composed of 50-74% sand-sized particles; (c) sandy mudstone (sMs) composed of 25-49% sand-sized particles; (d) coarse mudstone (cMs) composed of  $\geq 75\%$  fine

particles of which 67% are silt-sized; (e) medium mudstone (mMs) composed of  $\geq 75\%$  fine particles of which 33-66% are clay-sized; and (f) fine mudstone (fMs) composed of  $\geq 75\%$  fine particles of which 67% are clay-sized. The mMs and sMs sediment groups are the most dominant mudstone groups, whereas only a few were classified as fMs. A bivariate plot of skewness vs. sorting (Fig. 2.6b) reveals that majority of samples are poorly sorted.

### 2.3.2. *Palynofacies characterization*

Ternary plots of relative abundances of amorphous organic matter, phytoclasts and palynomorphs (APP, Fig. 2.6c), spores, microplankton and pollen (SMP, Fig. 2.6d), and phytoclast abundance, quartz and clay (PQC, Fig. 2.6e) of mudstone samples illustrates the relationship between palynofacies, mineralogy and proximity (Tyson, 1995; Potter *et al.*, 2005). The phytoclast group is the most dominant of the palynological organic matter in the mudstones, varying from 37.2% to 100 % of total organic constituents (Table 2.1a, Fig. 2.6c). The palynomorphs vary from 0% to 60.6% of total organic constituents, whereas the aquatic amorphous organic matter is the least abundant in the mudstone samples varying from 0% to 19.81% (Table 2.1a, Fig. 2.6c).

### 2.3.3. *Mineralogical characterization*

The HCl test showed that all samples were devoid of calcite. XRD results reveal quartz and kaolinite as the dominant minerals in the samples. Other minerals identified include illite, pyrite and goethite in accessory amounts (Appendix 1.1a-d; Table 2.1a). Following an amended guideline of mineralogical analysis of mudstones by Lazar *et al.* (2015), the samples were characterized into four classes (Fig. 2.6e): (a) Argillaceous (AR) consisting of  $\geq 75\%$  total clay; (b) Argillaceous-Siliceous (AR-SI) consisting of 50-74% total clay; (c) Siliceous-Argillaceous (SI-AR) consisting of 25-49% total clay; and (d) Siliceous (SI) comprising  $< 25\%$  total clay. The quartz vs. total clay bivariate plot show that the mudstone units are clay-rich with total

clay varying from AR to SI-AR, whereas the sand units are rich in quartz varying from SI-AR to SI (Fig. 2.6f).

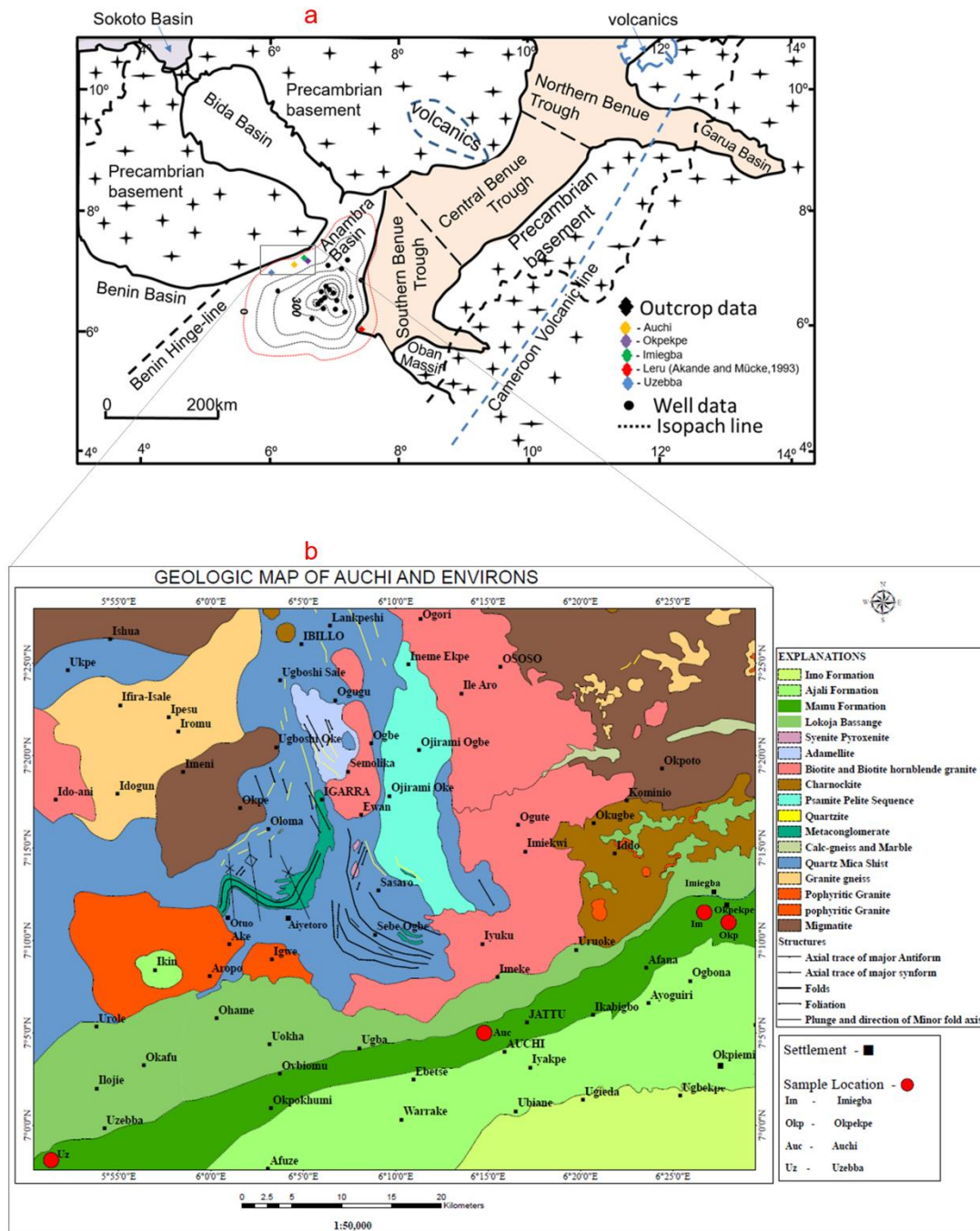
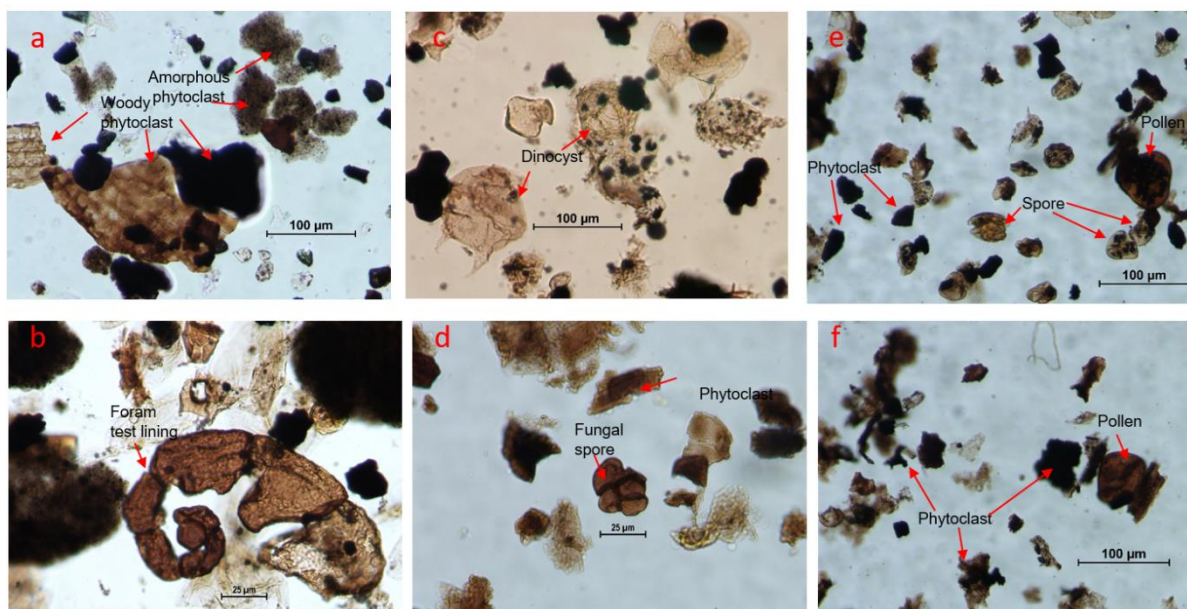


Fig. 2.4. a, Isopach map (in m) of the Mamu Formation adapted from well and outcrop data (Akande and Mücke, 1993; Total, 1988); b, Geological map of the area showing sample locations (modified from NGSa, 2006).



*Fig. 2.5. Photomicrographs showing various types of particulate organic matter components and palynomorphs.*

#### 2.3.4. Geochemistry

The results of the geochemical assay (Table 2.1b) show  $\text{SiO}_2$  and  $\text{Al}_2\text{O}_3$  as the most abundant major oxides in the samples analyzed, varying from 11.6 % to 95.2 % and 2.4 % to 33.6% respectively. 54.9 % and 39.8 % of the samples fall below the average upper continental crust (UCC, McLennan, 2001) for  $\text{SiO}_2$  (UCC = 65.9 %) and  $\text{Al}_2\text{O}_3$  (UCC = 15.2 %) respectively. In addition, the  $\text{Na}_2\text{O}$ ,  $\text{CaO}$ ,  $\text{MgO}$ , and  $\text{K}_2\text{O}$  concentration of the samples are low when compared with the average UCC (UCC = 6.18 %, 4.1 %, 2.2 %, and 3.37 % respectively). 80.5 % and 78.2 % of the samples are below the average UCC of  $\text{Fe}_2\text{O}_3$  (UCC = 5 %) and  $\text{MnO}$  (UCC = 0.0077 %) respectively, whereas 85 % of the samples exceed the average UCC for  $\text{TiO}_2$  (UCC = 0.68 %).

The majority of the samples have Zr, Hf and Y (i.e. 95.5 %, 97 %, and 63.9 % respectively) lower than the average for the UCC (i.e. 190 ppm, 5.8 ppm, and 22 ppm, respectively; Table 2.1b). In contrast Nb, Ta, Th, U and La (86.5 %, 84.2 %, 91.2 %, 91%, and 82.7 % respectively) of most of the samples (especially the mudstones) exceed the UCC value of 12 ppm, 1 ppm, 10.7 ppm, 2.8 ppm, and 30 ppm respectively. 53.4 % and 59.4 % of the

samples show a respective Cr and V content above the UCC (i.e. 83 ppm and 107 ppm respectively). Furthermore, 82.7 % and 81.2 % of the samples fall below the UCC for Ni (i.e. 44 ppm) and Co (i.e. 17 ppm), respectively.

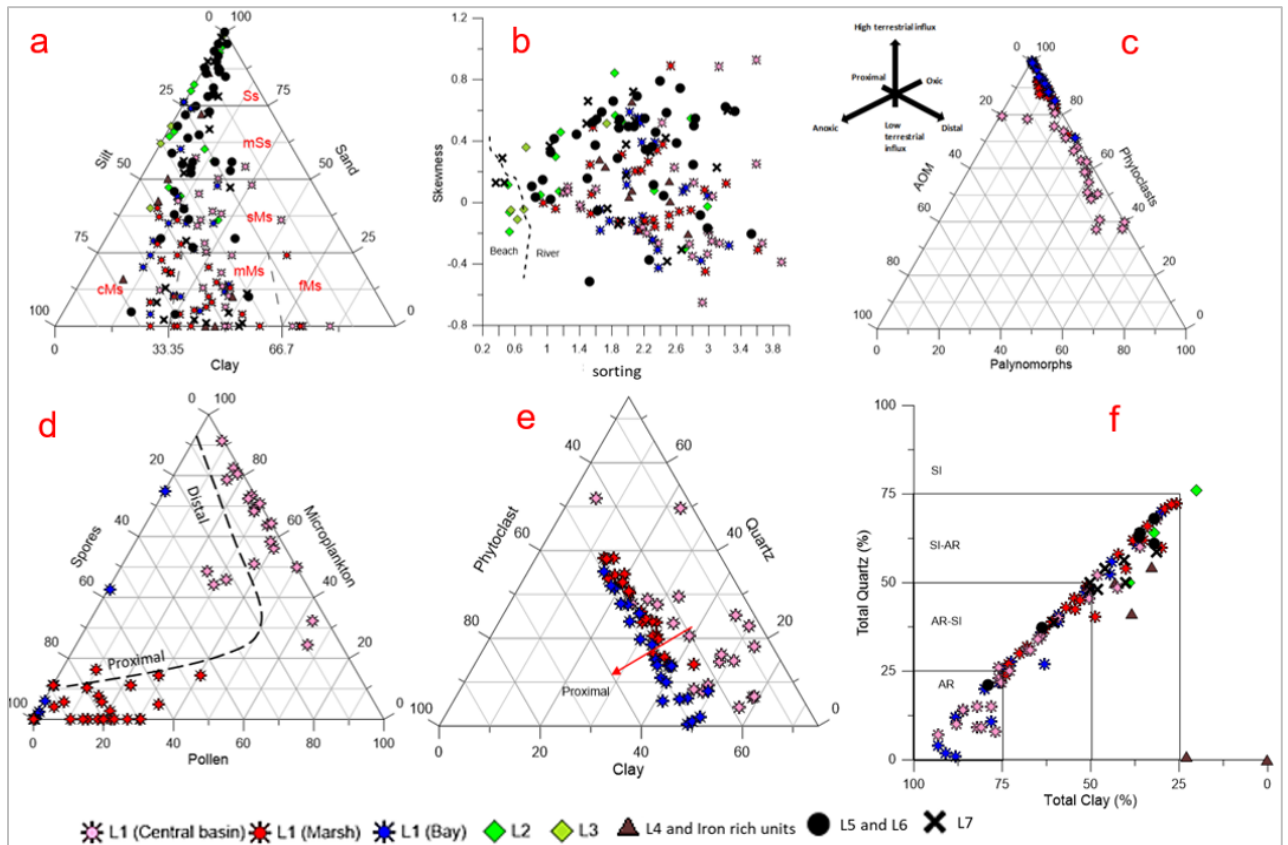


Fig. 6. a, Silt-Sand-Clay ternary plot (adapted from Lazar et al., 2015); b, skewness vs. sorting bivariate plot; c,d,e, APP, SMP (Tyson, 1995) and PQC ternary plots showing palynofacies distribution and proximal-distal relationships between the central basin, marsh and bay environments; f, Total quartz vs. total clay bivariate plot (modified from Lazar et al., 2015).

## 2.4. Discussion

### 2.4.1. Lithofacies characterization

Data integration from outcrop descriptions, sedimentological, mineralogical, and palynofacies analyses resulted in the identification of seven lithofacies. Graphic logs of the four measured sections are presented in Figs. 2.7a - d.

#### *2.4.1.1 Lithofacies 1 (L1): Dark mudstone*

This lithofacies comprises dark coloured and poorly sorted mudstone displaying planar, lenticular, wavy, and curved laminations, weak to moderate bioturbation (Figs. 2.7a-d, 2.8a, 2.8b), AR, AR-SI, SI-AR and SI compositions, and ranges texturally from fMs to mSs (Figs. 2.6f, 2.6a). Articulate brachiopod and gastropod molds, as well as iron concretions were observed in the Imiegba and Uzebba, and Okpekpe sections, respectively (Figs. 2.7a-c, 2.8c). In addition, L1 contains sand sized muscovite and phytoclasts concentrated on lamina planes, and often showed normal or reverse grading in grain size.

Three microfacies types (Figs. 2.8b1-b6) were identified based on observations from mudstone billets and thin sections. These microfacies provide insight on the varying proximal-distal settings and depositional conditions (O'Brien and Slatt, 1990 and Lazar *et al.*, 2015) of L1.

##### *2.4.1.1.1 Dark coloured planar to wavy laminated microfacies (M1)*

This microfacies is typically weakly bioturbated and is characteristically planar to wavy laminated (Figs. 2.8b1, 2.8b2), varying texturally from fMs to mMs. The fabric generally is AR, (Fig. 2.6f) and has the lowest frequency of occurrence among the three microfacies. M1 is interpreted as deposits of slow, continuous sediment accumulation in a single depositional event arising from low energy suspension settling (vertical accretion) in more distal deeper water condition (Lazar *et al.*, 2015).

##### *2.4.1.1.2 Dark coloured lenticular to wavy laminated microfacies (M2)*

This microfacies is typically weakly to mildly bioturbated and characteristically lenticular to wavy thickly laminated/thin bedded (Figs. 2.8b3, 2.8b4), varying texturally from mMs to sMs. The fabric is AR to AR-SI (Fig. 2.6f) and has the highest frequency of occurrence

among the three microfacies. M2 is interpreted as deposits that accumulated under intermediate condition between M1 and M3 (Lazar *et al.*, 2015).

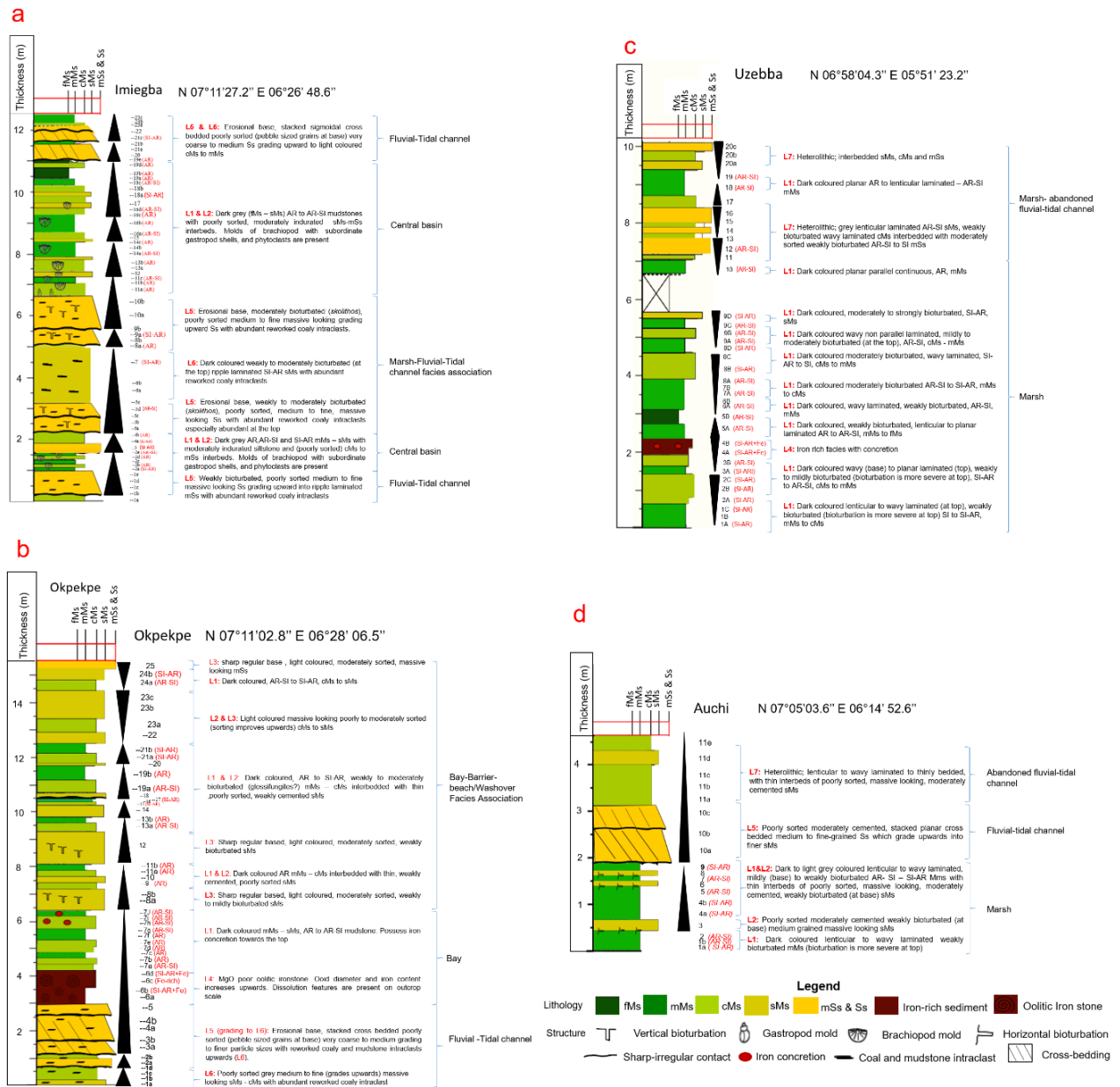


Fig. 7. a-d, Graphic logs of measured sections at Imiegba, Okpeke, Uzebba (composite), and Auchi. AR, AR-SI, SI-AR, and SI correspond to mineralogical class groups (see Section 4.2 and Fig. 5a).



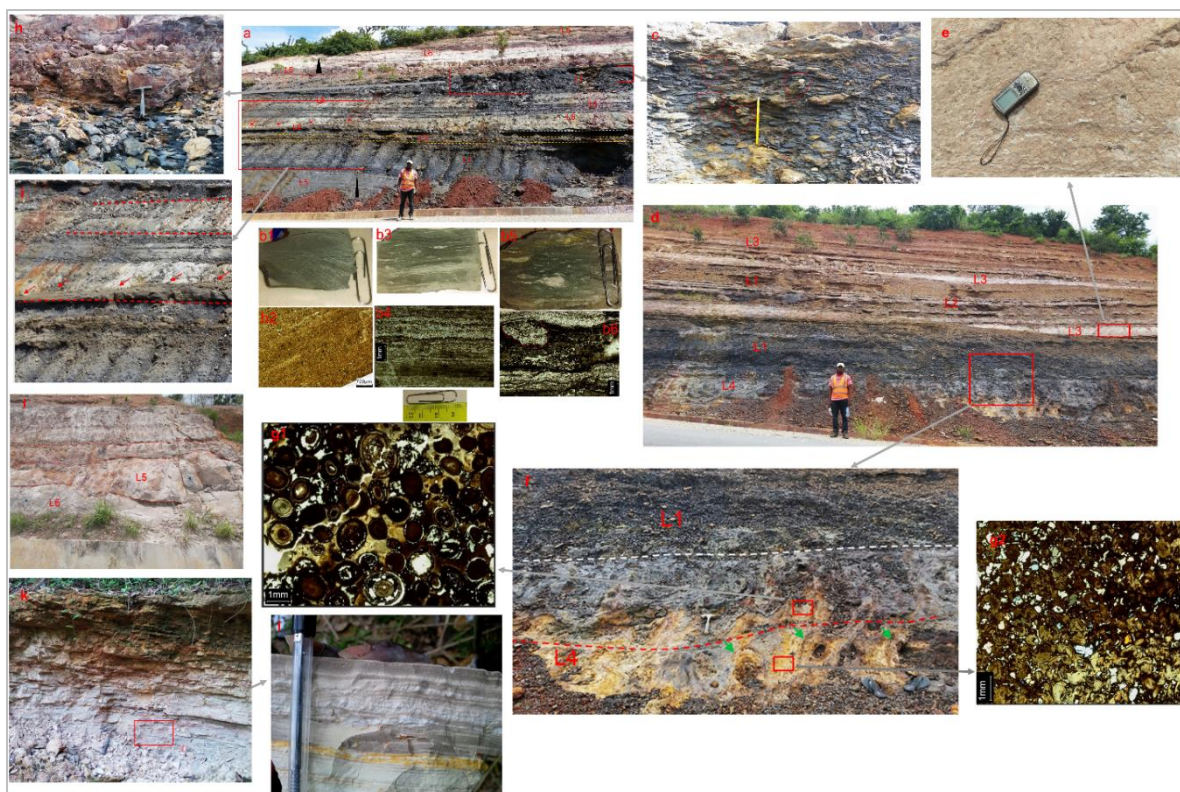


Fig. 2.8. a, Imiegba section showing the stratigraphic relationship between L1, L2, L5 and L6. Note the sheet-like geometry of L2 and channel geometry of L5. The black triangle indicates normal grading of L5 to L6. b1,b2, hand specimen and photomicrograph of dark coloured planar to wavy laminated microfacies (M1). Note the very thin to indistinct laminations. b3,b4, hand specimen and photomicrograph of dark coloured lenticular to wavy laminated microfacies. Notice the grading and mild bioturbation. b5,b6, hand specimen and photomicrograph of dark coloured, wavy to curve laminated microfacies (M3). Notice the moderate bioturbation and soft sediment deformation (ball structure typical of high rate of sedimentation). c, Close-up on L1 (Imiegba section) showing brachiopod molds indicated with red broken lines. d, Okpekpe section showing the stratigraphic position of L1, L2, L3 and L4. Notice the sheet-like geometry of L2 and L3. e, close up on L1 showing weak to mild bioturbation (Skolithos) of L3. f, Close-up on L1 and L4. Note the erosive contact in red broken lines separating the top of L4 from the bottom. Green arrows indicate solution cavities. g1, Top of L4 with more iron-oxide content, less compacted and larger ooid diameters. g2, Bottom of L4 with lower iron-oxide content, more compacted and smaller ooid diameters. h, close-up section showing the stratigraphic between L5 and L1. Note the erosive base of L5. i, close up of Imiegba section showing the stratigraphic contact between L5, L1 and L2. j, Amalgamated L5-units with sharp-erosive base and channel geometry. The red broken lines separate the individual L5 units. The blue arrow indicates reworked mudstone and intraclasts from underlying L1, which impart a grey colour on L6. k, Auchi section showing L7. l, Hand specimen of L6 at the Auchi section showing wavy to lenticular laminations/bedding.

Table 2.1. a, Table showing raw data from laser diffraction, XRD, and palynofacies counts used for particle size analysis, mineralogical characterization, and palynofacies characterization respectively. Composite samples used for palynofacies characterization are shaded in grey. b,c, Table showing raw data used for geochemical characterization (ICP-MS and XRF). Note average elemental values for Turonian sand, Turonian shale and Albian shale, Precambrian basement rocks and UCC obtained from Igwe (2017), Amajor (1987b), Imarhiagbe (2017), and McLennan (2001) respectively. \* = data obtained from ICP-MS;  $\lambda$  = Average elemental data for Turonian and Albian shale obtained from Amajor (1987b);  $\lambda$ =Average elemental data for Turonian sand obtained from Igwe (2017);  $\lambda\lambda$ =Average elemental data for Precambrian basement rocks obtained from Imarhiagbe (2017); UCC= average Upper continental crust (McLennan, 2001); Chemical index of alteration ( $CIA=(Al_2O_3/(Al_2O_3+CaO+Na_2O+K_2O)\times 100)$ ) (Nesbitt and Young, 1982); Index of compositional variability ( $ICV = (Fe_2O_3 + K_2O + Na_2O + CaO + MgO + MnO + TiO_2)/Al_2O_3$ ) (Cox et al., 1995).

Table 2.1a

S/N	Lithofacies		Particle size analysis					Palynofacies Characterization							Mineralogical Characterization					
			Sand %	Silt %	Clay %	Skewness	Inclusive graphic standard deviation	AOM %	% Palynomorph	% Phytoclast	% Spore Palynomorph	% Pollen Palynomorph	% Microplankton of Palynomorph	% Fungi of Palynomorph	Quartz %	Kaolinite %	Illite%	Calcite %	Total Clay %	Mineralogical group
U1 IA	L1	Marsh	8.0	68.0	24.0	2.10	0.20	1.99	5.71	92.31	47.83	17.39	0.0	34.78	66	29	5	0	34	SI-AR
U1 IB			22.5	57.5	20.0	2.64	-0.06	1.21	6.05	92.74	86.67	0.0	13.33	-	-	-	-	-	-	-
U1 1C			4.0	61.5	34.5	2.17	0.21	1.35	7.43	91.22	77.27	9.09	0.0	13.64	72.3	16.8	8.9	0	25.7	SI-AR
U1 2A			24.0	52.0	24.0	2.95	0.09	1.17	15.18	83.66	76.92	20.51	2.56	0.0	54	26	14	0	40	SI-AR
U1 2B			28.0	56.0	16.0	2.26	0.27	0.35	13.54	86.11	58.97	25.64	0.0	15.38	71	22	7	0	29	SI-AR
U1 2C			40.0	50.0	10.0	1.93	0.31	1.01	16.50	82.49	65.31	18.37	0.0	16.33	62	20	15	0	35	SI-AR
U1 3A			0.0	40.0	60.0	1.11	-0.04	0.65	10.42	88.93	62.50	18.75	0.0	18.75	58	29	13	0	42	SI-AR
U1 3B			0.0	72.0	28.0	1.53	0.25	0.66	11.15	88.20	70.59	2.94	2.94	23.53	49	37	14	0	51	AR-SI
U1 5A			18.0	57.0	25.0	2.78	-0.05	1.32	10.20	88.49	74.19	9.68	16.13	0.0	45.5	47.5	7	0	54.5	AR-SI
U1 5B			0.0	28.0	72.0	0.95	0.0	0.65	9.06	90.29	75.0	14.29	7.14	3.57	30	57	13	0	70	AR-SI
U1 6A			10.0	60.0	30.0	2.20	-0.12	0.48	15.87	83.62	71.21	9.09	9.09	10.61	43	45	12	0	57	AR-SI
U1 6B			19.0	58.0	23.0	2.52	-0.15	0.48	15.87	83.62	71.21	9.09	9.09	10.61	-	-	-	-	-	-
U1 7A			0.0	60.0	40.0	1.54	-0.07	2.63	9.54	87.83	62.07	20.69	10.34	6.9	42.6	27.7	26.7	0	54.4	AR-SI
U1 7B			0.0	65.0	35.0	1.55	0.06	2.63	9.54	87.83	62.07	20.69	10.34	6.9	-	-	-	-	-	-
U1 8A			6.5	52.5	41.0	2.22	-0.12	1.99	5.96	92.05	88.89	0.00	11.11	0.0	45.5	45.4	9.1	0	54.5	AR-SI
U1 8B			37.0	51.0	12.0	2.52	-0.08	0.65	8.74	90.61	81.48	14.81	0.0	3.7	62	26	12	0	38	SI-AR
U1 8C			28.0	49.0	23.0	3.22	0.13	0.65	8.74	90.61	81.48	14.81	0.0	3.7	72	18	9	0	27	SI-AR
U1 8D			10.0	50.0	40.0	2.34	-0.16	1.26	8.83	89.91	50.0	10.71	3.57	35.71	62	20	18	0	38	SI-AR
U1 9A			5.50	56.5	38.0	1.90	-0.12	1.26	8.83	89.91	50.0	10.71	3.57	35.71	39	45	16	0	61	AR-SI
U1 9B			36.0	46.0	18.0	2.37	0.34	1.60	11.82	86.58	83.78	5.41	5.41	5.41	45	39	14	0	53	AR-SI
U1 9C			0.0	64.0	36.0	1.57	0.49	1.95	7.82	90.23	66.67	29.17	0.0	4.17	39	44	17	0	61	AR-SI
U1 10			15.0	45.0	40.0	2.96	-0.45	2.17	25.47	72.36	81.71	13.41	0.0	4.88	24	61	13	0	74	AR-SI

U1 18			13.0	42.0	45.0	2.54	0.89	2.92	7.47	89.61	78.26	17.39	0.0	4.35	27	62	11	0	73	AR-SI	
U1 19			20.0	45.0	35.0	2.44	0.38	3.61	8.85	87.54	48.15	25.93	3.70	22.22	37	50	13	0	63	AR-SI	
AU-1a			8.0	50.0	42.0	2.32	-0.11	0.0	10.88	89.12	40.43	36.17	12.77	10.64	60	27	3	0	30	SI-AR	
AU-1b			24.0	20.0	56.0	3.62	-0.30	0.0	2.63	97.37	33.33	16.67	8.33	41.67	32	56	12	0	68	AR-SI	
AU 2			4.0	43.0	53.0	2.15	-0.18	0.0	1.30	98.70	66.67	16.67	0.0	16.67	40.4	45.5	3.1	0	48.6	SI-AR	
IM 2B	L1	Central Basin	39.0	34.0	27.0	-0.19	3.00	2.65	38.74	58.61	25.64	28.21	42.74	3.42	23	60	16	0	76	AR	
1M 2C			12.0	63.0	25.0	0.04	3.05	2.61	34.53	62.87	25.47	24.53	47.17	2.83	-	-	-	-	-	-	
1M 2D			38.0	32.0	30.0	-0.26	3.14	3.94	41.21	54.85	21.32	30.88	44.12	3.68	25	55	18	0	73	AR-SI	
1M 2E			6.50	46.5	47.0	-0.16	2.18	3.33	25.33	71.33	3.95	59.21	30.26	6.58	40	40	19	0	59	AR-SI	
IM 4A			36.0	39.0	25.0	-0.17	2.99	1.65	15.18	83.17	8.70	58.70	21.74	10.87	48.5	30.3	12.1	0	42.4	SI-AR	
IM 11A			42.5	42.5	15.0	0.23	2.58	1.31	31.05	67.65	1.05	25.26	72.63	1.05	15	67	11	0	78	AR	
IM 11B			34.0	41.0	25.0	-0.65	2.92	3.32	46.18	50.50	2.16	28.06	69.06	0.72	21.8	63.4	11.8	0	75.2	AR	
IM 11C			18.0	42.0	40.0	-0.35	2.79	2.89	23.47	73.63	1.37	34.25	63.01	1.37	47.5	33.7	16.8	0	50.5	AR-SI	
IM 13A			45.0	35.0	20.0	0.13	2.81	4.90	19.61	75.49	3.33	38.33	53.33	5.0	91	9	0	0	9	SI	
1M 13B			25.0	43.0	32.0	-0.34	2.98	2.29	17.32	80.39	11.32	35.85	49.06	3.77	15	64	18	0	82	AR	
IM 14A			13.0	50.0	37.0	-0.20	2.24	3.59	37.91	58.50	1.72	15.52	81.90	0.86	45.5	38.4	12.1	0	50.5	AR-SI	
IM 16A			50.0	27.0	23.0	0.89	3.12	0.00	60.24	39.76	2.61	24.84	71.90	0.65	35	49	15	0	64	AR-SI	
IM 16B			10.2	43.8	46.0	-0.27	2.38	6.48	45.06	48.46	5.48	15.75	78.08	0.68	9	71	11	0	82	AR	
1M 16C			0.0	49.0	51.0	0.09	1.60	7.57	51.74	40.69	3.05	28.66	68.29	0.0	25.9	56.8	19.2	0	76	AR	
1M 16D			36.0	15.5	48.5	-0.39	3.91	10.4	52.37	37.22	3.01	28.31	67.47	1.20	31	50	18	0	68	AR-SI	
IM 18a			57.0	30.0	13.0	0.52	2.42	19.8	0.65	79.55	0.0	50.0	50.0	0.0	52	31	17	0	48	SI-AR	
IM 18C			24.0	36.0	40.0	-0.27	3.66	3.27	30.39	66.34	3.23	37.63	56.99	2.15	34	51	14	0	65	AR-SI	
IM 19A			0.0	19.0	81.0	0.06	1.20	0.97	36.57	62.46	0.0	28.32	69.03	2.65	6.9	71.3	21.8	0	93.1	AR	
IM 19B			0.0	28.0	72.0	-0.03	1.42	1.95	60.59	37.46	0.54	8.06	91.40	0.00	13.1	67.7	18.2	0	85.9	AR	
IM 19D			54.0	17.0	29.0	0.93	3.59	6.60	42.57	50.83	1.55	17.83	79.84	0.78	10.1	70.7	17.2	0	87.9	AR	
IM 19E			0.0	30.0	70.0	-0.02	1.41	12.34	9.42	78.25	0.0	34.48	62.07	3.45	14	64	22	0	86	AR	
IM 2A			13.5	44.0	42.5	-0.27	2.76	-	-	-	-	-	-	-	60	29	7	0	36	SI-AR	
IM 4B			28.0	42.0	30.0	-0.25	3.04	-	-	-	-	-	-	-	31	51	16	0	67	AR-SI	
IM 14B			0.0	50.0	50.0	-0.25	3.04	-	-	-	-	-	-	-	-	-	-	-	-	-	
IM 14C			0.0	50.0	50.0	0.10	1.26	-	-	-	-	-	-	-	9	72	9	0	81	AR	
IM 18B			48.0	18.0	34.0	0.25	3.59	-	-	-	-	-	-	-	-	-	-	-	-	-	
IM 19C			0.00	27.0	73.0	0.07	1.25	-	-	-	-	-	-	-	8	60	17	0	77	AR	
OK 7A	L1	Bay	4.10	69.9	26.0	-0.04	1.66	0.0	9.28	90.72	80.0	0.04	10.0	6.0	26	59	15	0	74	AR-SI	
OK 7B			35.0	49.0	16.0	0.07	2.68	0.0	9.28	90.72	80.0	0.04	10.0	6.0	12	7	81	0	88	AR	
OK 7C			20.	64.0	16.0	-0.09	2.19	0.0	6.58	90.86	77.55	0.20	2.04	0.0	1	71	17	0	88	AR	
OK 7D			8.00	68.0	24.0	-0.12	1.77	0.0	6.58	90.86	77.55	0.20	2.04	0.0	2	74	17	0	91	AR	
OK 7E			29.0	56.5	14.5	-0.38	2.91	0.19	28.44	71.38	72.55	0.12	1.31	14.38	14	56	30	0	86	AR	
OK 7F			5.0	55.0	40.0	-0.18	1.66	0.0	14.89	85.11	71.60	0.15	0.0	13.58	4	55	38	0	93	AR	
OK 7G			24.0	60.0	16.0	0.20	1.99	0.0	11.66	88.34	67.50	0.23	0.0	10.0	48.5	34.7	15.8	0	50.5	AR-SI	
OK 7H			26.0	46.0	28.0	0.10	2.72	-	-	-	-	-	-	-	41	46	13	0	59	AR-SI	
OK 7I			35.0	36.0	29.0	-0.28	3.26	0.49	11.11	88.40	71.11	0.18	8.89	2.22	27	52	11	0	63	AR-SI	
OK 7J			11.5	44.5	44.0	-0.24	2.31	0.49	11.11	88.40	71.11	0.18	8.89	2.22	26	61	13	0	74	AR-SI	
OK 9			47.5	28.5	24.0	0.05	2.99	0.0	3.21	96.79	33.33	0.33	25.0	8.33	12	65	23	0	88	AR	

OK 11A			25.0	43.0	32.0	-0.31	2.38	0.0	0.61	99.39	0.0	0.0	0.0	100.0	22	58	18	0	76	AR	
OK 11B			14.0	42.0	44.0	-0.42	2.39	0.0	0.23	99.77	100.0	0.0	0.0	0.0	11	60	18	0	78	AR	
OK 13A			35.0	44.0	21.0	0.39	2.34	0.0	1.14	98.86	100.0	0.0	0.0	0.0	39	46	13	0	59	AR-SI	
OK 13B			10.0	58.0	32.0	-0.18	2.13	0.0	1.34	98.66	40.0	0.0	0.0	60.0	27.7	59.4	12.9	0	72.3	AR-SI	
OK 15			44.0	42.0	14.0	0.54	2.13	0.0	1.21	98.79	20.0	0.20	60.0	0.0	70	21	9	0	30	SI-AR	
OK 17			74.0	23.0	3.0	0.52	2.16	0.0	8.44	91.56	77.5	0.10	5.0	7.5	52.5	34.7	9.8	0	44.5	SI-AR	
OK 19A			44.0	42.0	14.0	0.12	1.99	0.0	0.64	99.36	0.0	0.0	0.0	100.0	47.5	43.4	8.1	0	51.5	AR-SI	
OK 19B			18.0	57.0	25.0	-0.12	2.06	0.0	0.0	100.0	0.0	0.0	0.0	0.0	20	54	26	0	80	AR	
OK 21A			60.0	33.0	7.0	0.55	2.13	0.0	6.21	93.79	45.45	0.09	0.0	45.45	61	24	13	0	37	SI-AR	
OK 21B			10.5	60.0	29.50	-0.24	2.31	0.0	0.0	100.0	0.0	0.0	0.0	0.0	56	37	7	0	44	SI-AR	
OK 24A			76.0	24.0	0.0	0.39	2.18	0.59	5.29	94.12	77.78	0.22	0.0	0.0	36	51	13	0	64	AR-SI	
OK 24B			40.0	42.0	18.0	0.59	2.02	0.0	0.65	99.35	50.0	0.0	0.0	50.0	64	29	7	0	36	SI-AR	
U1 9D	L2	Thin sheet-like coarse-sandy mudstone	60.0	26.0	14.0	0.57	1.84	-	-	-	-	-	-	-	50	36	3	0	39	SI-AR	
IM - 3			93.0	5.0	2.0	0.46	1.17	-	-	-	-	-	-	-	-	76	20	0	0	20	SI
IM- 15			66.0	32.0	2.0	0.84	1.83	-	-	-	-	-	-	-	-	-	-	-	-	-	-
OK- 10			56.0	25.5	18.50	0.55	2.79	-	-	-	-	-	-	-	-	-	-	-	-	-	-
OK- 12			80.0	20.0	0.0	0.11	0.52	-	-	-	-	-	-	-	-	-	-	-	-	-	-
OK- 14			47.0	43.0	10.0	0.53	1.93	-	-	-	-	-	-	-	-	-	-	-	-	-	-
OK-16			74.0	23.0	3.0	0.30	1.11	-	-	-	-	-	-	-	-	-	-	-	-	-	-
OK- 18			18.0	57.0	25.0	0.08	2.33	-	-	-	-	-	-	-	-	-	-	-	-	-	-
OK- 20			76.0	24.0	0.0	-0.19	0.53	-	-	-	-	-	-	-	-	-	-	-	-	-	-
OK- 22			64.5	34.0	1.50	0.05	0.92	-	-	-	-	-	-	-	-	-	-	-	-	-	-
OK- 25		82.0	18.0	0.0	-0.06	0.53	-	-	-	-	-	-	-	-	-	-	-	-	-	-	
AU-3		95.0	3.0	2.0	0.07	1.15	-	-	-	-	-	-	-	-	-	-	-	-	-	-	
AU-6		44.0	41.0	15.0	-0.30	2.70	-	-	-	-	-	-	-	-	-	-	-	-	-	-	
AU-8		36.0	34.0	30.0	-0.02	2.99	-	-	-	-	-	-	-	-	-	-	-	-	-	-	
OK 8A	L3	Thin sheet-like sandy mudstone - muddy sandstone	-	-	-	-	-	-	-	-	-	-	-	-	-	-	-	-	-	-	
OK 8B			-	-	-	-	-	-	-	-	-	-	-	-	-	-	-	-	-	-	-
OK 23A			-	-	-	-	-	-	-	-	-	-	-	-	-	-	-	-	-	-	-
OK 23B			-	-	-	-	-	-	-	-	-	-	-	-	-	-	-	-	-	-	-
OK 23C			-	-	-	-	-	-	-	-	-	-	-	-	-	-	-	-	-	-	-
U1 4A	L4	Oolitic Ironstone and Fe-rich mudstone	0.0	53.0	47.0	0.03	2.01	-	-	-	-	-	-	-	54.5	32.7	0	0	32.7	SI-AR	
U1 4B			0.0	56.0	44.0	0.07	2.05	-	-	-	-	-	-	-	-	50	43	0	0	43	SI-AR
OK 6A			86.0	12.0	2.0	0.23	1.72	-	-	-	-	-	-	-	-	-	-	-	-	-	-
OK 6B			16.0	72.0	12.0	0.28	1.64	-	-	-	-	-	-	-	-	41.4	38.4	0	0	38.4	SI-AR
OK 6C			42.5	48.5	9.0	0.0	2.52	-	-	-	-	-	-	-	-	0	0	0	0	0	-
OK 6D			50.0	42.0	8.0	0.14	2.51	-	-	-	-	-	-	-	-	1	22.8	0	0	22.8	-
Im-12		72.0	21.0	7.0	0.65	2.05	-	-	-	-	-	-	-	-	-	-	-	-	-	-	
Im-17		10.0	43.0	47.0	-0.21	2.74	-	-	-	-	-	-	-	-	-	-	-	-	-	-	
OK 1A			40.0	42.0	18.0	-0.17	2.99	-	-	-	-	-	-	-	-	-	-	-	-	-	

OK 1B	L5 & L6	Channel Sand/Clay	5.0	75.0	20.0	-0.52	1.52	-	-	-	-	-	-	-	-	-	-	-	-	-
OK 1C			38.0	46.0	16.0	0.04	2.44	-	-	-	-	-	-	-	-	-	-	-	-	-
OK 3A			78.0	16.0	6.0	0.54	2.83	-	-	-	-	-	-	-	-	-	-	-	-	-
OK 3B			88.0	8.0	4.0	0.59	1.67	-	-	-	-	-	-	-	-	-	-	-	-	-
OK 4A			100	0.0	0.0	0.03	0.85	-	-	-	-	-	-	-	-	-	-	-	-	-
OK 4B			86.0	12.5	1.5	0.37	1.59	-	-	-	-	-	-	-	-	-	-	-	-	-
OK 5			72.0	25.5	2.5	0.69	2.11	-	-	-	-	-	-	-	-	-	-	-	-	-
IM 1A			27.0	46.0	27.0	-0.08	2.90	-	-	-	-	-	-	-	-	-	-	-	-	-
IM 1B			65.0	25.0	10.0	0.79	2.40	-	-	-	-	-	-	-	-	-	-	-	-	-
IM 1C			93.5	6.50	0.0	0.42	1.08	-	-	-	-	-	-	-	-	-	-	-	-	-
IM 1D			87.0	8.0	5.0	0.54	1.61	-	-	-	-	-	-	-	-	-	-	-	-	-
IM 1E			36.5	42.5	21.0	0.25	2.81	-	-	-	-	-	-	-	-	-	-	-	-	-
IM 20			56.0	25.0	19.0	0.5	2.82	-	-	-	-	-	-	-	-	-	-	-	-	-
IM 21A			81.0	13.0	6.0	0.49	1.89	-	-	-	-	-	-	-	-	-	-	-	-	-
IM 21B			88.0	12.0	0.0	0.33	1.04	-	-	-	-	-	-	-	-	-	-	-	-	-
IM 21C			4.10	62.5	33.4	-0.06	1.62	-	-	-	-	-	-	64	23	13	0	36	SI-AR	
IM 22			73.0	18.0	9.0	0.74	2.65	-	-	-	-	-	-	-	-	-	-	-	-	-
IM 23A			56.0	20.0	24.0	0.59	3.32	-	-	-	-	-	-	-	-	-	-	-	-	-
IM 23B			30.0	32.0	38.0	-0.20	3.53	-	-	-	-	-	-	-	-	-	-	-	-	-
IM 23C			10.0	38.0	52.0	-0.37	2.26	-	-	-	-	-	-	-	-	-	-	-	-	-
AU-10A			96.0	1.50	2.50	0.11	0.81	-	-	-	-	-	-	-	-	-	-	-	-	-
AU-10B			53.0	22.0	25.0	0.62	3.21	-	-	-	-	-	-	-	-	-	-	-	-	-
AU-10C			85.0	7.5	7.50	0.54	1.90	-	-	-	-	-	-	-	-	-	-	-	-	-
OK-1d			52.0	34.0	14.0	0.39	2.60	-	-	-	-	-	-	-	-	-	-	-	-	-
OK-2b			30.0	54.0	16.0	0.11	2.32	-	-	-	-	-	-	-	-	-	-	-	-	-
IM 5D			90.0	7.50	2.50	0.52	1.57	-	-	-	-	-	-	37.4	48.5	15.2	0	63.7	AR-SI	
IM 5A			79.0	14.0	7.0	0.54	2.21	-	-	-	-	-	-	-	-	-	-	-	-	-
IM 5B			86.5	8.50	5.0	0.49	2.07	-	-	-	-	-	-	-	-	-	-	-	-	-
IM 5C			92.0	6.0	2.0	0.44	1.36	-	-	-	-	-	-	-	-	-	-	-	-	-
IM 5E			54.0	33.0	13.0	0.46	2.34	-	-	-	-	-	-	61	24	8	0	32	SI-AR	
IM 7			59.0	36.0	5.0	2.01	0.49	-	-	-	-	-	-	68	24	8	0	32	SI-AR	
IM 8A			46.0	42.0	12.0	2.3	0.36	-	-	-	-	-	-	21	52	27	0	79	AR-SI	
IM 9A			68.0	30.0	2.0	1.87	0.29	-	-	-	-	-	-	62.8	27.3	9.1	0	36.4	SI-AR	
IM 8B			88.0	12.0	0.0	0.94	0.15	-	-	-	-	-	-	-	-	-	-	-	-	-
IM 9B			75.0	21.0	4.0	1.82	0.66	-	-	-	-	-	-	-	-	-	-	-	-	-
IM 6A			55.0	35.0	10.0	2.22	0.34	-	-	-	-	-	-	-	-	-	-	-	-	-
IM 6B			56.0	31.5	12.5	2.47	0.58	-	-	-	-	-	-	-	-	-	-	-	-	-
IM 10A			64.0	29.0	7.0	0.16	1.49	-	-	-	-	-	-	-	-	-	-	-	-	-
IM 10B			96.0	4.0	0.0	0.02	1.04	-	-	-	-	-	-	-	-	-	-	-	-	-
AU-11A	L7	Heterolithics	13.0	61.0	26.00	0.42	2.47	-	-	-	-	-	-	-	-	-	-	-	-	-
AU-11B			2.0	67.0	31.0	0.38	1.98	-	-	-	-	-	-	-	-	-	-	-	-	-
AU-11C			8.0	66.0	26.0	0.33	2.29	-	-	-	-	-	-	-	-	-	-	-	-	-
U1 11			90.0	8.20	1.80	0.37	1.03	-	-	-	-	-	-	50	39	1	0	40	SI-AR	

U1 14			72.0	19.0	9.0	0.66	1.50	-	-	-	-	-	-	-	-	-	-	-	-	-	-	-	-	-	-	-
U1 17			0.0	46.0	54.0	-0.04	1.75	-	-	-	-	-	-	-	-	-	-	50	39	11	0	50	AR-SI			
AU-4a			2.0	58.0	40.0	0.18	1.98	-	-	-	-	-	-	-	-	-	-	54	38	8	0	46	SI-AR			
AU-4B			11.0	38.0	51.0	-0.31	2.66	-	-	-	-	-	-	-	-	-	-	48	31	17	0	48	SI-AR			
AU-5			1.0	55.0	44.0	0.51	1.88	-	-	-	-	-	-	-	-	-	-	54	31	15	0	46	SI-AR			
AU-7			1.0	44.4	54.6	-0.14	1.88	-	-	-	-	-	-	-	-	-	-	48	40	10	0	50	AR-SI			
AU-9			4.0	42.0	44.0	-0.12	1.92	-	-	-	-	-	-	-	-	-	-	58.6	28.3	3.1	0	31.4	SI-AR			
AU 11D			56.0	34.0	10.0	-0.38	2.49	-	-	-	-	-	-	-	-	-	-	-	-	-	-	-	-	-	-	
AU 11E			29.0	47.0	24.0	0.60	3.24	-	-	-	-	-	-	-	-	-	-	-	-	-	-	-	-	-	-	
U1 12			52.0	36.0	12.0	0.54	2.09	-	-	-	-	-	-	-	-	-	-	-	-	-	-	-	-	-	-	
U1 13			67.0	21.0	12.0	0.72	2.07	-	-	-	-	-	-	-	-	-	-	38.6	48.5	11.9	0	60.4	AR-SI			
U1 15			98.0	2.0	0.0	0.13	0.48	-	-	-	-	-	-	-	-	-	-	56.4	29.7	10.9	0	40.6	SI-AR			
U1 16			98.0	2.0	0.0	0.13	0.36	-	-	-	-	-	-	-	-	-	-	-	-	-	-	-	-	-	-	
U1 20A			90.0	10.0	0.0	0.29	0.45	-	-	-	-	-	-	-	-	-	-	-	-	-	-	-	-	-	-	
U1 20B			47.0	25.0	28.0	0.23	3.11	-	-	-	-	-	-	-	-	-	-	-	-	-	-	-	-	-	-	
U1 20C			78.0	13.0	9.0	0.52	1.49	-	-	-	-	-	-	-	-	-	-	-	-	-	-	-	-	-	-	

Table 2.1b

S/N	Lithofacies		Geochemical data																							
			Ni	Co	U	Th	V	La	Cr	Ti	Zr	Hf	Y	Nb	Ta	Sc	Al <sub>2</sub> O <sub>3</sub>	CaO	Fe <sub>2</sub> O <sub>3</sub>	K <sub>2</sub> O	MgO	MnO	Na <sub>2</sub> O	SiO <sub>2</sub>	TiO <sub>2</sub>	
			ppm	ppm	ppm	ppm	ppm	ppm	ppm	ppm	ppm	%	ppm	ppm	ppm	ppm	ppm	ppm	%	%	%	%	%	%	%	%
			0.1	0.2	0.1	0.1	1	0.1	1	0.001	0.1	0.1	0.1	0.1	0.1	1	0.01	0.01	0.01	0.01	0.01	0.0001*	0.001*	0.01	0.01	
U1 1A	L1	Marsh	14.7	3.5	5	14.8	110	50.2	108	0.91	173.2	4.6	24.4	30.3	2.1	9	15.2	0.03	1.35	0.38	0.11	0.005	0.02	72.5	1.68	
U1 1B			-	-	-	-	-	-	-	-	-	-	-	-	-	-	-	-	-	-	-	-	-	-	-	-
U1 1C			11.3	2.1	4.3	11.8	90	43.9	96	0.83	157	4.2	20.6	28	2	6	12.9	0.02	0.82	0.31	0.09	0.004	0.02	77.6	1.58	
U1 2A			11.4	2.1	4.5	13.1	115	47.2	100	0.89	171.8	4.4	22.5	31.8	2.1	7	14.9	0.02	1.7	0.36	0.09	0.004	0.02	73	1.68	
U1 2B			8	1.7	3.8	11.2	102	43	65	0.80	155.8	3.9	20.6	26.7	1.8	7	12.2	0.02	1.03	0.28	0.07	0.004	0.02	78.2	1.48	
U1 2C			10.6	2.2	4.6	12.6	113	47.8	97	0.94	176.6	4.6	22.7	31.4	2.1	9	14.9	0.02	0.82	0.37	0.1	0.004	0.02	74.3	1.79	
U1 3A			10.3	2.2	4.6	12.4	110	48.7	76	0.93	186.1	5	23.8	33.6	2.2	9	14.6	0.02	1.56	0.39	0.1	0.005	0.02	73.2	1.75	
U1 3B			16.3	2.9	4.6	12.3	101	49.6	97	0.95	193.3	5.2	25.8	34.9	2.5	10	17.2	0.02	1.23	0.46	0.12	0.004	0.03	70.7	1.81	
U1 5A			15.1	3.1	5.1	14.8	159	42.8	131	0.90	160.7	4.3	26.8	30.5	2.2	13	22.1	0.03	1.15	0.43	0.12	0.005	0.03	63.6	1.63	
U1 5B			15.3	2.9	4.5	13.4	166	35.9	128	0.85	149.9	4.4	22.6	27.6	2	13	23.7	0.03	1.31	0.43	0.12	0.005	0.03	61.7	1.56	
U1 6A			14.3	3.6	4.4	13.3	166	43.3	104	0.87	155	4.7	20.9	29.4	2.1	12	22.2	0.03	1.25	0.44	0.12	0.003	0.02	63.6	1.6	
U1 6B			-	-	-	-	-	-	-	-	-	-	-	-	-	-	-	-	-	-	-	-	-	-	-	-
U1 7A			50	34.5	4.5	16.3	148	47.2	124	0.76	133.1	4	22	24.4	1.8	15	20.2	0.04	2.63	0.3	0.13	0.008	0.03	61.8	1.47	
U1 7B			26.2	15	4.4	12.6	145	46.1	66	0.87	146	4	22.5	29.1	1.9	12	18.6	0.02	0.86	0.33	0.11	0.005	0.02	66.53	1.6	
U1 8A			37.5	23.9	4.1	15.1	149	38.8	85	0.78	126.5	3.6	19.7	25.5	1.8	13	19.84	0.02	2.07	0.28	0.11	0.006	0.01	63.25	1.36	
U1 8B			31.9	17.9	4.5	14.4	128	52.2	80	0.87	154.9	4.1	24	28.9	2	13	14.4	0.08	1.82	0.3	0.13	0.010	0.03	71.9	1.64	
U1 8C			31.9	16.5	4.3	13.8	103	42.1	86	0.80	142.2	3.9	19.6	25.4	1.8	10	10.8	0.02	0.7	0.21	0.09	0.010	0.02	79.4	1.46	
U1 8D			62.2	27.5	5.4	11.9	172	39.4	66	0.82	161.5	4	23.1	28.8	1.9	12	15.8	0.02	0.95	0.26	0.08	0.005	0.03	71.2	1.55	
U1 9A			-	-	-	-	-	-	-	-	-	-	-	-	-	-	-	-	-	-	-	-	-	-	-	-
U1 9B			37	25.9	5.5	15.3	157	50.7	111	0.93	173.1	4.4	22.1	32	2.2	13	19.3	0.02	2.39	0.33	0.08	0.010	0.02	64.5	1.69	
U1 9C			31.2	20.4	5.2	12.4	151	40.1	91	0.96	178.6	4.5	17.3	33.3	2.4	13	20.9	0.02	1.19	0.35	0.09	0.007	0.03	64	1.74	

U1 10			22.4	7.4	4.1	17.7	184	63.5	142	0.96	182	4.9	20.9	33.2	2.3	12	26.6	0.02	1.25	0.24	0.07	0.003	0.02	55.5	1.77		
U1 18			10.6	2	5.1	16.7	154	56.4	128	0.97	198.7	5.8	20.4	33.2	2.4	17	24.7	0.02	2.52	0.31	0.07	0.004	0.02	59.3	1.82		
U1 19			9.9	1.9	4.7	14.6	137	47.1	93	0.95	180.1	4.7	19.5	31.4	2.1	13	21.94	0.01	1.05	0.23	0.06	0.004	0.01	65.09	1.73		
AU-1A			15.9	3.5	4.7	14.3	113	47.2	102	0.80	138.3	4	30.6	24.3	1.8	13	19.4	0.03	1.53	0.84	0.26	0.005	0.03	67.5	1.51		
AU-1B			-	-	-	-	-	-	-	-	-	-	-	-	-	-	-	-	-	-	-	-	-	-	-		
AU 2			15.6	3.9	4.1	13.4	127	30.1	109	0.81	134	3.8	25	25	1.7	16	22.92	0.03	2.22	1.06	0.34	0.004	0.03	62.04	1.49		
IM 2B	L1	Central Basin	42.7	23	6.8	18.1	159	31.5	103	0.86	111.8	3.4	20.6	30.6	2.3	17	27.9	0.06	4.06	1.19	0.36	0.007	0.03	49.2	1.59		
IM 2C			32.9	13.2	7.2	19.9	161	40.6	105	0.97	123.4	3.8	30.5	32.8	2.4	16	25.4	0.04	3.76	1.21	0.38	0.008	0.04	53.1	1.72		
IM 2D			32.1	16.1	7	20.9	150	41.8	99	0.87	112.6	3.4	26.8	30.7	2.2	16	25.4	0.04	4.15	1.22	0.4	0.007	0.04	53.9	1.62		
IM 2E			46.7	22.5	5.9	18.6	151	42	109	0.84	102.4	3.2	25.9	28.4	2.1	16	25.7	0.09	6.54	1.18	0.5	0.020	0.04	50.6	1.5		
IM 4A				12	5.4	19.5	123	50.4	75	0.71	98.2	2.8	19.9	24.4	1.7	11	19.8	0.03	6.56	0.85	0.29	0.008	0.04	57.4	1.24		
IM 11A			53.5	30.7	9.8	30.9	139	61.3	95	0.66	151.4	4.9	20.5	25	1.8	15	23.8	0.09	10.3	0.72	0.37	0.011	0.03	48.8	1.13		
IM 11B			50.3	21	7	16.1	144	23.6	114	0.69	78.2	2.3	11.4	24.3	1.6	21	31.4	0.08	5.75	1.21	0.48	0.012	0.04	44.3	1.12		
IM 11C			54.7	31.2	8.5	30.3	140	87.2	125	0.66	111.3	3.6	54.8	23	1.6	24	23.7	0.27	7.16	1.37	0.56	0.019	0.04	53.5	1.13		
IM 13A			58.8	32	6.4	23.8	133	50	131	0.60	74.2	2.3	21.3	20.3	1.4	16	25.4	0.16	10.6	1.2	0.68	0.118	0.04	46.6	1.05		
IM 13B			47.7	22.5	6	18.2	146	28.9	113	0.76	89.4	3	14.4	26.6	1.8	21	29	0.06	4.72	1.28	0.49	0.010	0.04	48.3	1.3		
IM 14A			61.9	29.9	8.3	23.1	131	72.1	111	0.64	100.5	2.9	64.8	21.2	1.5	20	23.8	0.75	7.61	1.3	0.53	0.027	0.05	50.8	1.11		
IM 16A			59.1	26.1	4.5	13.4	104	37.5	104	0.39	63.9	1.9	30.6	13.1	0.9	17	22.4	0.37	17.9	1.45	0.7	0.326	0.03	39.6	0.7		
IM 16B			60.9	25.1	4.7	13.2	103	34.8	99	0.46	80.8	2.4	62.2	15.9	1	18	25	0.26	10.2	1.64	0.68	0.108	0.04	44.2	0.82		
IM 16C			46.1	15.1	4.4	13.3	118	27.8	101	0.54	91.9	2.8	31.9	18.2	1.3	16	26.3	0.13	5.67	1.75	0.58	0.027	0.04	48	0.96		
IM 16D			39.2	19.2	4.8	17.9	115	40.2	97	0.57	108	3.3	18.1	19.5	1.3	17	25	0.08	4.16	1.62	0.5	0.010	0.04	53.7	1.02		
IM 18a			45.9	3.15	12.15	20.15	68.5	89	67.5	0.42	93.25	2.7	57.6	13.5	0.9	19	21.97	1.1	1.325	1.275	0.21	0.005	0.05	60.16	0.72		
IM 18C			32.9	6.3	10.8	15.3	94	26.3	94	0.66	78.5	2.3	14.7	22.5	1.5	21	33.6	0.18	2.01	0.97	0.29	0.005	0.03	47.7	1.12		
IM 19A			28.2	7.6	8.6	14.2	111	27.9	107	0.61	98.3	3.1	18.3	20.2	1.5	20	32.6	0.14	2.8	1.32	0.39	0.005	0.03	48.1	1.05		
IM 19B			43.2	13.4	7.5	13	109	20	100	0.57	93	2.8	11.9	19.9	1.3	13	32.1	0.1	3.34	1.32	0.39	0.004	0.03	46.6	0.98		
IM 19D			54.5	36.8	5.6	14.2	102	31.7	105	0.61	99.9	2.7	13.9	20.6	1.3	14	31.2	0.07	4.9	1.11	0.32	0.009	0.04	45	1.08		
IM 19E			26.9	7.4	5.9	10.1	128	13.3	109	0.71	114	3.3	7.9	23.7	1.7	20	32.8	0.05	2.69	1.26	0.36	0.006	0.04	48.9	1.22		
IM 2A			29.2	9.5	6	14	131	37.2	101	0.76	92.9	2.7	16.3	27.3	1.8	13	25.5	0.05	4.55	0.89	0.27	0.005	0.03	51.4	1.34		
IM 4B			24.9	11.8	4.6	18.6	99	50.6	68	0.65	100.6	2.9	19.9	23.6	1.6	9	14.26	0.02	5.89	0.58	0.18	0.009	0.02	62.5	1.1		
IM 14B			-	-	-	-	-	-	-	-	-	-	-	-	-	-	-	-	-	-	-	-	-	-	-		
IM 14C			75.4	27.5	7.7	16.2	110	46.8	99	0.52	70.6	2	36.7	17.6	1.2	19	25.7	0.33	9.54	1.39	0.64	0.026	0.05	44.4	0.91		
IM 18B			33.3	8.8	8.5	9.6	91	11.5	89	0.64	66.4	2	10.5	22.1	1.5	11	31.51	0.23	2.15	0.84	0.24	0.005	0.02	48.73	1.01		
IM 19C			62.6	34.8	7.7	16.1	98	36.1	108	0.58	91.8	2.8	18.8	18.4	1.4	14	30.6	0.1	5.44	1.16	0.34	0.005	0.04	44.9	0.96		
OK 7A	L1	Bay	33.8	16.2	7.2	26.4	95	62.6	92	0.86	120.2	3.6	36.9	32.7	2.5	13	22.7	0.02	4.69	0.55	0.2	0.005	0.02	54	1.51		
OK 7B			21.6	7.8	5.6	24.5	69	60	118	0.63	115.3	3.8	32.1	23.5	2	10	13.1	0.02	3.88	0.28	0.1	0.010	0.02	72.4	1.09		
OK 7C			65.7	36.9	9	19.2	114	40.5	102	0.50	46.6	1.3	39.8	19.9	1.5	17	29.5	0.02	9.67	0.55	0.19	0.023	0.04	38.1	0.9		
OK 7D			57.1	28.8	11.6	20.5	93	39.4	104	0.60	59	1.9	43.3	24	1.8	17	30	0.02	7.69	0.51	0.16	0.006	0.03	40.6	1.06		
OK 7E			43.9	22.9	8.7	19.3	101	42.9	91	0.94	110.1	3.5	32.7	37.8	2.9	16	28.3	0.02	3.46	0.48	0.13	0.003	0.03	47	1.76		
OK 7F			88.4	29.1	8.5	11.9	98	16.9	72	0.72	98.1	2.7	14	28	2.2	15	32.2	0.02	2.89	0.5	0.14	0.007	0.03	45.2	1.31		
OK 7G			52.5	12.5	7.9	26	105	60	70	0.73	184.4	5.8	21.4	30.4	2.6	15	21.8	0.03	2.8	0.56	0.11	0.004	0.04	58.2	1.34		
OK 7H			26.4	6.2	8.2	20	67	36.4	97	0.83	135.2	4.3	12.8	34.1	2.6	11	23.7	0.02	1.7	0.44	0.11	0.006	0.02	59.3	1.53		
OK 7I			26.9	8.9	12	17.3	83	27.1	86	0.87	108.5	3.2	10.1	34.2	2.5	14	28.8	0.03	2.04	0.47	0.12	0.003	0.03	53	1.51		
OK 7J			29.4	6.2	13.7	25.7	104	45.4	119	1.03	169.2	5.2	17.2	43.3	3.2	17	26.1	0.03	2.28	0.53	0.12	0.006	0.03	57.2	1.88		
OK 9			47.2	6	10.8	19.6	88	35.4	88	0.76	111.5	3.5	13.2	31.7	2.5	14	31.9	0.03	1.14	0.51	0.13	0.003	0.02	52.1	1.37		

OK 11A			25.3	5.6	10.3	14.8	103	20.1	105	0.99	150.7	4.6	13.9	37.8	2.7	15	29.1	0.02	2.33	0.77	0.19	0.007	0.03	54.2	1.71		
OK 11B			22.2	5	8	14.4	110	22.6	93	1.05	168.1	5.1	14.1	39.2	2.9	15	30	0.03	2.25	1.06	0.26	0.003	0.03	52.8	1.84		
OK 13A			25.4	5.2	10.5	20.5	86	40.5	99	0.88	112	3.4	16.7	35.1	2.8	16	24.7	0.02	1.85	0.54	0.12	0.005	0.03	60.9	1.56		
OK 13B			29.2	6.6	14	13.3	96	25.1	94	0.99	120.8	3.7	13.2	41.2	3.1	18	29.5	0.02	1.63	0.6	0.13	0.004	0.03	53.4	1.74		
OK 15			27.3	3.1	8.3	36.4	54	73.6	56	0.94	255.4	8.1	24.1	39.1	3.4	12	15.3	0.03	0.88	0.61	0.09	0.005	0.04	74.6	1.7		
OK 17			42.7	4.6	11.8	35.1	61	64.7	84	0.90	185.3	5.7	21.3	36.4	3	24	22.2	0.03	1.07	0.56	0.08	0.006	0.03	64.6	1.64		
OK 19A			29.8	6.1	19.5	23.8	76	43.2	96	0.93	157.2	5	18.9	38.2	3.1	27	26.3	0.02	0.97	0.49	0.1	0.003	0.03	58.3	1.66		
OK 19B			35.3	6.5	12.1	19.7	88	34.3	100	1.04	125.9	3.8	14.6	43.1	3.1	18	29.7	0.02	1.48	0.56	0.13	0.003	0.03	53.9	1.78		
OK 21A			24.1	3.3	12.4	35.3	94	77.7	72	1.14	245.8	7.8	27.9	45.6	3.7	18	19.7	0.04	1.71	0.72	0.15	0.003	0.03	67.3	2		
OK 21B			22.3	4.2	10.8	28	97	71	90	1.11	219.1	6.5	23.1	44.6	3.5	16	22.5	0.03	2.22	0.75	0.17	0.004	0.03	62.9	2.01		
OK 24A			33.9	5.3	31.2	15.9	76	51.9	86	0.96	119.4	3.6	20.6	40	3	16	26.2	0.02	0.89	0.51	0.1	0.003	0.03	57.4	1.65		
OK 24B			25.9	4.2	11.5	25.2	73	64	76	0.88	156	5.1	20.5	34.9	2.9	15	19	0.02	0.92	0.49	0.08	0.005	0.03	69.8	1.53		
U1 9D	L2	Thin sheet-like coarse- sandy mudstone	17.4	10.4	6.6	16.9	116	56	112	0.95	176.9	4.6	23.8	31.8	2.2	14	16.1	0.03	1.28	0.25	0.07	0.009	0.03	72	1.78		
IM - 3			20.8	8.9	3.6	15.3	55	48.2	72	0.24	63.7	1.9	18.1	8.3	0.6	6	6.36	0.26	21.1	0.22	0.32	0.092	0.02	62.9	0.61		
IM- 15			-	-	-	-	-	-	-	-	-	-	-	-	-	-	-	-	-	-	-	-	-	-	-	-	-
OK- 10			-	-	-	-	-	-	-	-	-	-	-	-	-	-	-	-	-	-	-	-	-	-	-	-	-
OK- 12			16.5	1	3.7	19.7	42	50.6	41	0.52	93.6	3	13.9	20.7	1.6	5	7.39	0.02	2.92	0.29	0.04	0.001	0.02	84.36	1.16		
OK- 14			9.6	1.6	5.3	25.5	82	53.8	72	0.66	175.3	5.4	17	27.4	2.5	8	10.38	0.02	13.32	0.48	0.05	0.003	0.02	68.71	1.48		
OK-16			-	-	-	-	-	-	-	-	-	-	-	-	-	-	-	-	-	-	-	-	-	-	-	-	-
OK- 18			26.2	36.8	4.2	13	35	35.8	38	0.27	68.5	2.4	46.4	11.7	1	12	7.23	0.04	53.74	0.2	0.03	0.160	0.01	30.33	0.67		
OK- 20		-	-	-	-	-	-	-	-	-	-	-	-	-	-	-	-	-	-	-	-	-	-	-	-	-	
OK- 22		7.7	1.5	4.4	20.3	50	45.5	58	0.44	151.7	4.8	12.7	20.3	1.8	7	7.97	0.03	15.15	0.58	0.03	0.003	0.03	70.21	1.26			
OK- 25		16	1.1	3.9	28.3	24	67.9	24	0.62	165.9	5.3	15.1	27.3	2.2	4	7.12	0.01	0.28	0.19	0.04	0.001	0.01	87.36	1.5			
AU-3		-	-	-	-	-	-	-	-	-	-	-	-	-	-	-	-	-	-	-	-	-	-	-	-	-	
AU-6		-	-	-	-	-	-	-	-	-	-	-	-	-	-	-	-	-	-	-	-	-	-	-	-	-	
AU-8		-	-	-	-	-	-	-	-	-	-	-	-	-	-	-	-	-	-	-	-	-	-	-	-	-	
OK 8A	L3	Thin sheet-like sandy mudstone - muddy sandstone	-	-	-	-	-	-	-	-	-	-	-	-	-	-	-	-	-	-	-	-	-	-	-	-	
OK 8B			12.5	1.7	2.8	19.5	21	62.4	17	0.48	98.5	3.1	12.4	17.9	1.5	4	4.87	0.04	0.83	0.21	0.03	0.003	0.04	89.5	1.15		
OK 23A			22.8	2.2	4.7	26.8	42	61.3	36	0.78	177.9	5.5	14.4	35.5	3	8	14.41	0.01	0.49	0.93	0.07	0.003	0.05	76.88	1.63		
OK 23B			-	-	-	-	-	-	-	-	-	-	-	-	-	-	-	-	-	-	-	-	-	-	-	-	-
OK 23C		5.2	1.2	3.6	18.6	37	39.3	29	0.57	153	4.7	10.9	25.3	2.1	6	8.04	0.01	2.15	0.77	0.05	0.002	0.04	84.49	1.31			
U1 4A	L4	Oolitic Ironstone and Fe-rich mudstone	19.7	11.6	3.8	11.3	121	40.9	70	0.61	112.4	2.8	24.3	21.2	1.4	21	9.94	0.06	20.52	0.24	0.2	0.140	0.01	57.79	1.25		
U1 4B			35.1	26.1	4.1	17.7	137	45.6	106	0.62	105.6	3.1	23.7	20	1.4	15	16.4	0.02	25.1	0.27	0.09	0.091	0.02	44	1.25		
OK 6A			-	-	-	-	-	-	-	-	-	-	-	-	-	-	-	-	-	-	-	-	-	-	-	-	-
OK 6B			56	4.3	7.6	18.2	54	65	66	0.15	36.6	1	61.5	6.1	0.4	8	15.1	0.18	14.7	0.04	0.05	0.005	0.02	58.9	0.28		
OK 6C			63	7.5	9.6	30.6	64	62.5	88	0.13	29.7	1	52.6	5.7	0.4	12	20.8	0.15	22.4	0.02	0.07	0.013	0.02	43.1	0.27		
OK 6D			79.6	6.9	5	17.9	74	59.3	115	0.05	12	0.4	45.4	2.1	0.2	12	24.03	0.34	28.38	0.02	0.05	0.010	0.01	26.82	0.12		
Im-12		-	-	-	-	-	-	-	-	-	-	-	-	-	-	-	-	-	-	-	-	-	-	-	-	-	
Im-17		18.6	15.3	5.5	5.7	39	26.6	42	0.12	21.4	0.7	47.6	4.1	0.3	16	6.77	0.09	67.4	0.3	0.08	0.066	0.01	11.6	0.22			
OK 1A	L5 &	Channel Sand/Clay	-	-	-	-	-	-	-	-	-	-	-	-	-	-	-	-	-	-	-	-	-	-	-	-	
OK 1B	L6		16.1	5.1	8.6	25.6	72	43.9	63	1.10	105.1	3.1	12.9	44.8	2.9	11	23.57	0.01	0.67	0.06	0.03	0.002	0.01	62.27	1.91		





AU-4B			-	-	-	-	-	-	-	-	-	-	-	-	-	-	-	-	-	-	-	-	-	-	-	-
AU-5			17.9	3.2	4.5	13.7	116	37.3	96	0.89	151.6	4.2	28.7	28.6	1.9	19	22.13	0.03	2.11	1.03	0.32	0.003	0.03	63.24	1.68	
AU-7			15.3	3.1	5	15.4	125	41.3	106	0.94	168.5	4.8	26.5	29.1	2.2	17	23.8	0.03	1.94	1.03	0.31	0.004	0.03	61.7	1.73	
AU-9			12.4	2.5	4.7	18.3	112	51.9	89	0.93	166.4	5.2	27.3	30.6	2.2	20	21	0.03	1.13	0.81	0.24	0.002	0.03	66.2	1.78	
AU - 11D			-	-	-	-	-	-	-	-	-	-	-	-	-	-	-	-	-	-	-	-	-	-	-	
AU- 11E			5.9	2.5	3.1	9.4	86	30.3	50	0.55	102.7	2.8	13.6	15.5	1	7	6.86	0.03	8.56	0.21	0.07	0.006	0.01	78.87	1.19	
U1 12			9.7	2.5	6.6	20.5	140	64.8	144	1.04	228.5	6.7	20.5	32.4	2.2	18	19.8	0.02	2.34	0.24	0.06	0.006	0.02	67.1	1.88	
U1 13			5.8	1.3	3.8	15.8	106	49.7	78	0.831	183.9	5.1	15.7	25.4	1.8	10	14.2	0.02	1.5	0.15	0.04	0.005	0.02	76.1	1.51	
U1 15			1.9	0.6	2	11.9	92	31.4	37	0.61	112.2	3.1	10.5	16.9	1	6	7.33	0.01	1.13	0.07	0.02	0.006	0.008	87.24	1.14	
U1 16			1.9	0.6	1.8	12.8	85	36.3	36	0.59	97.2	2.9	11.7	17.9	1.2	6	8.61	0.01	0.9	0.09	0.02	0.004	0.008	85.9	1.06	
U1 20A			4.6	1.3	3.8	15.3	117	50.4	76	0.90	167.7	4.6	17.3	29.1	2	12	16.23	0.02	1.36	0.16	0.04	0.005	0.011	73.96	1.67	
U1 20B			-	-	-	-	-	-	-	-	-	-	-	-	-	-	-	-	-	-	-	-	-	-	-	
U1 20C			3.1	0.9	4.7	16.2	111	44.9	66	0.89	176.9	4.9	15.9	28	1.9	11	12.37	0.02	1.61	0.12	0.03	0.005	0.009	79.03	1.7	
Turonian Sand <sup>λ1</sup>			-	-	-	-	-	-	-	0.31	-	-	-	-	-	-	16.05	1.87	5.64	2.36	1.25	0.05	2.52	64.29	0.51	
Turonian Shale <sup>λ</sup>			-	-	3.8	18.2	-	67.5	-	0.38	118.2	-	32	14.1	-	-	14.50	14.00	5.68	1.91	2.35	0.06	0.45	50.17	0.64	
Albian Shale <sup>λ</sup>			-	-	3	16.4	-	119.3	-	0.32	62.9	-	34.8	15.8	-	-	11.86	8.94	4.91	1.35	1.22	0.04	0.36	64.73	0.53	
Syenite <sup>λλ</sup>			-	-	-	-	-	-	-	0.47	174	-	15.67	12.33	-	-	13.18	4.38	2.90	5.70	4.60	0.09	2.9	59.01	0.78	
Mica Schist <sup>λλ</sup>			-	-	-	-	-	-	-	0.33	-	-	-	-	-	-	15.87	4.07	4.50	2.89	2.31	-	4.03	65.38	0.55	
Metaconglomerate <sup>λλ</sup>			-	-	-	-	-	-	-	0.32	-	-	-	-	-	-	17.00	3.43	3.60	3.48	1.58	0.01	4.17	65.6	0.54	
UCC			44.0	17.0	2.8	10.7	107.0	30.0	83.0	0.41	190.0	5.8	22.0	12.0	1.0	13.6	15.19	4.1	5.0	3.37	2.2	0.008	6.18	65.89	0.68	

Table 2.1c

S/N	Lithofacies Characterization		Geochemical data																						
			Th/Sc	Zr/Sc	CIA	ICV	La/Th	La/Sc	Th/Co	Y/Ni	SiO <sub>2</sub> /Al <sub>2</sub> O <sub>3</sub>	Th/U	K <sub>2</sub> O/Na <sub>2</sub> O	Th/Cr	Cr/V	Al <sub>2</sub> O <sub>3</sub> /TiO <sub>2</sub>	Zr/Hf								
U1 IA	L1	Marsh	1.64	19.24	97.25	0.24	3.39	5.58	4.23	1.66	4.77	2.96	19.00	0.14	0.98	9.05	37.65								
U1 1B			-	-	-	-	-	-	-	-	-	-	-	-	-	-	-	-	-	-	-	-	-	-	-
U1 1C			1.97	26.17	97.36	0.22	3.72	7.32	5.62	1.82	6.02	2.74	15.50	0.12	1.07	8.16	37.38								
U1 2A			1.87	24.54	97.39	0.26	3.60	6.74	6.24	1.97	4.90	2.91	18.00	0.13	0.87	8.87	39.05								
U1 2B			1.60	22.26	97.44	0.24	3.84	6.14	6.59	2.58	6.41	2.95	14.00	0.17	0.64	8.24	39.95								
U1 2C			1.40	19.62	97.32	0.21	3.79	5.31	5.73	2.14	4.99	2.74	18.50	0.13	0.86	8.32	38.39								
U1 3A			1.38	20.68	97.14	0.26	3.93	5.41	5.64	2.31	5.01	2.70	19.50	0.16	0.69	8.34	37.22								
U1 3B			1.23	19.33	97.12	0.21	4.03	4.96	4.24	1.58	4.11	2.67	15.33	0.13	0.96	9.50	37.17								
U1 5A			1.14	12.36	97.83	0.15	2.89	3.29	4.77	1.77	2.88	2.90	14.33	0.11	0.82	13.56	37.37								
U1 5B			1.03	11.53	97.97	0.15	2.68	2.76	4.62	1.48	2.60	2.98	14.33	0.10	0.77	15.19	34.07								
U1 6A			1.11	12.92	97.84	0.16	3.26	3.61	3.69	1.46	2.86	3.02	22.00	0.13	0.63	13.88	32.98								
U1 6B			-	-	-	-	-	-	-	-	-	-	-	-	-	-	-	-	-	-	-	-	-	-	-
U1 7A			1.09	8.87	98.20	0.23	2.90	3.15	0.47	0.44	3.06	3.62	10.00	0.13	0.84	13.74	33.28								
U1 7B			1.05	12.17	98.05	0.16	3.66	3.84	0.84	0.86	3.58	2.86	16.50	0.19	0.46	11.63	36.50								
U1 8A			1.16	9.73	98.46	0.19	2.57	2.98	0.63	0.53	3.19	3.68	28.00	0.18	0.57	14.59	35.14								

U1 8B			1.11	11.92	97.23	0.28	3.63	4.02	0.80	0.75	4.99	3.20	10.00	0.18	0.63	8.78	37.78
U1 8C			1.38	14.22	97.74	0.23	3.05	4.21	0.84	0.61	7.35	3.21	10.50	0.16	0.83	7.40	36.46
U1 8D			0.99	13.46	98.08	0.18	3.31	3.28	0.43	0.37	4.51	2.20	8.67	0.18	0.38	10.19	40.38
U1 9A			-	-	-	-	-	-	-	-	-	-	-	-	-	-	-
U1 9B			1.18	13.32	98.12	0.24	3.31	3.90	0.59	0.60	3.34	2.78	16.50	0.14	0.71	11.42	39.34
U1 9C			0.95	13.74	98.12	0.16	3.23	3.08	0.61	0.55	3.06	2.38	11.67	0.14	0.60	12.01	39.69
U1 10			1.48	15.17	98.96	0.13	3.59	5.29	2.39	0.93	2.09	4.32	12.00	0.12	0.77	15.03	37.14
U1 18			0.98	11.69	98.60	0.19	3.38	3.32	8.35	1.92	2.40	3.27	15.50	0.13	0.83	13.57	34.26
U1 19			1.12	13.85	98.87		3.23	3.62	7.68	1.97	2.97	3.11	23.00	0.16	0.68	12.68	38.32
AU-1a			1.10	10.64	95.57	0.22	3.30	3.63	4.09	1.92	3.48	3.04	28.00	0.14	0.90	12.85	34.58
AU-1b			-	-	-	-	-	-	-	-	-	-	-	-	-	-	-
AU 2			0.84	8.38	95.34	0.23	2.25	1.88	3.44	1.60	2.71	3.27	35.33	0.12	0.86	15.38	35.26
IM 2B	L1	Central Basin	1.06	6.58	95.61	0.26	1.74	1.85	0.79	0.48	1.76	2.66	39.67	0.18	0.65	17.55	32.88
IM 2C			1.24	7.71	95.17	0.28	2.04	2.54	1.51	0.93	2.09	2.76	30.25	0.19	0.65	14.77	32.47
IM 2D			1.31	7.04	95.13	0.29	2.00	2.61	1.30	0.83	2.12	2.99	30.50	0.21	0.66	15.68	33.12
IM 2E			1.16	6.40	95.15	0.38	2.26	2.63	0.83	0.55	1.97	3.15	29.50	0.17	0.72	17.13	32.00
IM 4A			1.77	8.93	95.56	0.46	2.58	4.58	1.63		2.90	3.61	21.25	0.26	0.61	15.97	35.07
IM 11A			2.06	10.09	96.59	0.53	1.98	4.09	1.01	0.38	2.05	3.15	24.00	0.33	0.68	21.06	30.90
IM 11B			0.77	3.72	95.94	0.28	1.47	1.12	0.77	0.23	1.41	2.30	30.25	0.14	0.79	28.04	34.00
IM 11C			1.26	4.64	93.38	0.45	2.88	3.63	0.97	1.00	2.26	3.56	34.25	0.24	0.89	20.97	30.92
IM 13A			1.49	4.64	94.78	0.55	2.10	3.13	0.74	0.36	1.83	3.72	30.00	0.18	0.98	24.19	32.26
IM 13B			0.87	4.26	95.46	0.27	1.59	1.38	0.81	0.30	1.67	3.03	32.00	0.16	0.77	22.31	29.80
IM 14A			1.16	5.03	91.89	0.48	3.12	3.61	0.77	1.05	2.13	2.78	26.00	0.21	0.85	21.44	34.66
IM 16A			0.79	3.76	92.37	0.96	2.80	2.21	0.51	0.52	1.77	2.98	48.33	0.13	1.00	32.00	33.63
IM 16B			0.73	4.49	92.80	0.55	2.64	1.93	0.53	1.02	1.77	2.81	41.00	0.13	0.96	30.49	33.67
IM 16C			0.83	5.74	93.20	0.35	2.09	1.74	0.88	0.69	1.83	3.02	43.75	0.13	0.86	27.40	32.82
IM 16D			1.05	6.35	93.49	0.30	2.25	2.36	0.93	0.46	2.15	3.73	40.50	0.18	0.84	24.51	32.73
IM 18a			1.08	5.10	90.07	0.11	4.48	4.89	6.46	1.26	2.75	1.68	69.31	0.30	0.99	30.51	34.64
IM 18C			0.73	3.74	96.61	0.14	1.72	1.25	2.43	0.45	1.42	1.42	32.33	0.16	1.00	30.00	34.13
IM 19A			0.71	4.92	95.63	0.18	1.96	1.40	1.87	0.65	1.48	1.65	44.00	0.13	0.96	31.05	31.71
IM 19B			1.00	7.15	95.68	0.19	1.54	1.54	0.97	0.28	1.45	1.73	44.00	0.13	0.92	32.76	33.21
IM 19D			1.01	7.14	96.24	0.24	2.23	2.26	0.39	0.26	1.44	2.54	27.75	0.14	1.03	28.89	37.00
IM 19E			0.51	5.70	96.05	0.17	1.32	0.67	1.36	0.29	1.49	1.71	31.50	0.09	0.85	26.89	34.55
IM 2A			1.08	7.15	96.34	0.28	2.66	2.86	1.47	0.56	2.02	2.33	29.67	0.14	0.77	19.03	34.41
IM 4B			2.07	11.18	95.85	0.55	2.72	5.62	1.58	0.80	4.38	4.04	33.14	0.27	0.69	12.96	34.69
IM 14B			-	-	-	-	-	-	-	-	-	-	-	-	-	-	-
IM 14C			0.85	3.72	93.56	0.50	2.89	2.46	0.59	0.49	1.73	2.10	27.80	0.16	0.90	28.24	35.30
IM 18B			0.87	6.04	96.65	0.14	1.20	1.05	1.09	0.32	1.55	1.13	36.68	0.11	0.98	31.20	33.20
IM 19C			1.15	6.56	95.92	0.26	2.24	2.58	0.46	0.30	1.47	2.09	29.00	0.15	1.10	31.88	32.79
OK 7A	L1	Bay	2.03	9.25	97.47	0.31	2.37	4.82	1.63	1.09	2.38	3.67	27.50	0.29	0.97	15.03	33.39
OK 7B			2.45	11.53	97.62	0.41	2.45	6.00	3.14	1.49	5.53	4.38	14.00	0.21	1.71	12.02	30.34

OK 7C			1.13	2.74	97.97	0.39	2.11	2.38	0.52	0.61	1.29	2.13	13.75	0.19	0.89	32.78	35.85
OK 7D			1.21	3.47	98.17	0.32	1.92	2.32	0.71	0.76	1.35	1.77	17.00	0.20	1.12	28.30	31.05
OK 7E			1.21	6.88	98.16	0.21	2.22	2.68	0.84	0.74	1.66	2.22	16.00	0.21	0.90	16.08	31.46
OK 7F			0.79	6.54	98.32	0.15	1.42	1.13	0.41	0.16	1.40	1.40	16.67	0.17	0.73	24.58	36.33
OK 7G			1.73	12.29	97.19	0.22	2.31	4.00	2.08	0.41	2.67	3.29	14.00	0.37	0.67	16.27	31.79
OK 7H			1.82	12.29	98.01	0.16	1.82	3.31	3.23	0.48	2.50	2.44	22.00	0.21	1.45	15.49	31.44
OK 7I			1.24	7.75	98.19	0.15	1.57	1.94	1.94	0.38	1.84	1.44	15.67	0.20	1.04	19.07	33.91
OK 7J			1.51	9.95	97.79	0.19	1.77	2.67	4.15	0.59	2.19	1.88	17.67	0.22	1.14	13.88	32.54
OK 9			1.40	7.96	98.27	0.10	1.81	2.53	3.27	0.28	1.63	1.81	25.50	0.22	1.00	23.28	31.86
OK 11A			0.99	10.05	97.26	0.17	1.36	1.34	2.64	0.55	1.86	1.44	25.67	0.14	1.02	17.02	32.76
OK 11B			0.96	11.21	96.40	0.18	1.57	1.51	2.88	0.64	1.76	1.80	35.33	0.15	0.85	16.30	32.96
OK 13A			1.28	7.00	97.67	0.17	1.98	2.53	3.94	0.66	2.47	1.95	18.00	0.21	1.15	15.83	32.94
OK 13B			0.74	6.71	97.84	0.14	1.89	1.39	2.02	0.45	1.81	0.95	20.00	0.14	0.98	16.95	32.65
OK 15			3.03	21.28	95.74	0.22	2.02	6.13	11.74	0.88	4.88	4.39	15.25	0.65	1.04	9.00	31.53
OK 17			1.46	7.72	97.28	0.15	1.84	2.70	7.63	0.50	2.91	2.97	18.67	0.42	1.38	13.54	32.51
OK 19A			0.88	5.82	97.99	0.12	1.82	1.60	3.90	0.63	2.22	1.22	16.33	0.25	1.26	15.84	31.44
OK 19B			1.09	6.99	97.99	0.13	1.74	1.91	3.03	0.41	1.81	1.63	18.67	0.20	1.14	16.69	33.13
OK 21A			1.96	13.66	96.14	0.24	2.20	4.32	10.70	1.16	3.42	2.85	24.00	0.49	0.77	9.85	31.51
OK 21B			1.75	13.69	96.53	0.23	2.54	4.44	6.67	1.04	2.80	2.59	25.00	0.31	0.93	11.19	33.71
OK 24A			0.99	7.46	97.91	0.12	3.26	3.24	3.00	0.61	2.19	0.51	17.00	0.18	1.13	15.88	33.17
OK 24B			1.68	10.40	97.24	0.16	2.54	4.27	6.00	0.79	3.67	2.19	16.33	0.33	1.04	12.42	30.59
U1 9D	L2		1.21	12.64	98.11	0.21	3.31	4.00	1.63	1.37	4.47	2.56	8.33	0.15	0.97	9.04	38.46
IM- 3		Thin sheet-like	2.55	10.62	92.71	3.56	3.15	8.03	1.72	0.87	9.89	4.25	11.00	0.21	1.31	10.43	33.53
IM- 15		coarse- sandy	-	-	-	-	-	-	-	-	-	-	-	-	-	-	-
OK- 10		mudstone	-	-	-	-	-	-	-	-	-	-	-	-	-	-	-
OK- 12			3.94	18.72	95.73	0.60	2.57	10.12	19.70	0.84	11.42	5.32	14.50	0.48	0.98	6.37	31.20
OK- 14			3.19	21.91	95.23	1.48	2.11	6.73	15.94	1.77	6.62	4.81	24.00	0.35	0.88	7.01	32.46
OK-16			-	-	-	-	-	-	-	-	-	-	-	-	-	-	-
OK- 18			1.08	5.71	96.61	7.59	2.75	2.98	0.35	1.77	4.20	3.10	14.81	0.34	1.09	10.79	28.54
OK- 20			-	-	-	-	-	-	-	-	-	-	-	-	-	-	-
OK- 22			2.90	21.67	92.57	2.14	2.24	6.50	13.53	1.65	8.81	4.61	19.33	0.35	1.16	6.33	31.60
OK- 25			7.08	41.48	97.14	0.29	2.40	16.98	25.73	0.94	12.27	7.26	19.00	1.18	1.00	4.75	31.30
AU-3			-	-	-	-	-	-	-	-	-	-	-	-	-	-	-
AU-6			-	-	-	-	-	-	-	-	-	-	-	-	-	-	-
AU-8			-	-	-	-	-	-	-	-	-	-	-	-	-	-	-
OK 8A	L3	Thin sheet-like	-	-	-	-	-	-	-	-	-	-	-	-	-	-	-
OK 8B		sandy mudstone -	4.88	24.63	94.38	0.47	3.20	15.60	11.47	0.99	18.38	6.96	5.25	1.15	0.81	4.23	31.77
OK 23A		muddy sandstone	3.35	22.24	93.57	0.22	2.29	7.66	12.18	0.63	5.34	5.70	18.60	0.74	0.86	8.84	32.35
OK 23B			-	-	-	-	-	-	-	-	-	-	-	-	-	-	-
OK 23C			3.10	25.50	90.74	0.54	2.11	6.55	15.50	2.10	10.51	5.17	19.25	0.64	0.78	6.14	32.55

U1 4A	L4	Oolitic Ironstone and Fe-rich mudstone	0.54	5.35	96.98	2.26	3.62	1.95	0.97	1.23	5.81	2.97	24.00	0.16	0.58	7.95	40.14	
U1 4B			1.18	7.04	98.14	1.64	2.58	3.04	0.68	0.68	2.68	4.32	13.50	0.17	0.77	13.12	34.06	
OK 6A			-	-	-	-	-	-	-	-	-	-	-	-	-	-	-	-
OK 6B			2.28	4.58	98.44	1.01	3.57	8.13	4.23	1.10	3.90	2.39	2.00	0.28	1.22	53.93	36.60	
OK 6C		2.55	2.48	99.09	1.10	2.04	5.21	4.08	0.83	2.07	3.19	1.00	0.35	1.38	77.04	29.70		
OK 6D		1.49	1.00	98.48	1.20	3.31	4.94	2.59	0.57	1.12	3.58	2.00	0.16	1.55	200.25	30.00		
Im-12		-	-	-	-	-	-	-	-	-	-	-	-	-	-	-	-	
Im-17		0.36	1.34	94.41	10.07	4.67	1.66	0.37	2.56	1.71	1.04	26.95	0.14	1.08	30.77	30.57		
OK 1A	L5	&Channel Sand/Clay	-	-	-	-	-	-	-	-	-	-	-	-	-	-	-	
OK 1B	L6		2.33	9.55	99.66	0.11	1.71	3.99	5.02	0.80	2.64	2.98	6.38	0.41	0.88	12.34	33.90	
OK 1C			-	-	-	-	-	-	-	-	-	-	-	-	-	-	-	
OK 3A			-	-	-	-	-	-	-	-	-	-	-	-	-	-	-	
OK 3B			4.20	20.10	-	-	5.02	21.10	8.40	2.10	54.26	6.00	2.50	0.38	1.22	5.97	33.50	
OK 4A			-	-	-	-	-	-	-	-	-	-	-	-	-	-	-	
OK 4B			2.65	9.38	98.20	0.41	2.78	7.38	8.15	0.63	13.35	4.08	3.19	0.48	0.46	12.76	34.09	
OK 5			2.12	6.50	97.66	0.25	2.35	4.97	12.70	0.51	16.66	3.02	7.45	0.58	0.81	8.87	32.50	
IM 1A			3.07	14.97	99.15	0.22	2.74	8.40	4.84	1.98	12.67	2.63	7.50	0.44	0.84	10.73	29.93	
IM 1B			-	-	-	-	-	-	-	-	-	-	-	-	-	-	-	
IM 1C			6.90	54.25	97.77	0.40	2.20	15.20	12.55	4.19	31.58	2.94	10.00	1.15	0.60	4.93	33.91	
IM 1D			-	-	-	-	-	-	-	-	-	-	-	-	-	-	-	
IM 1E			5.00	21.55	95.64	0.39	3.38	16.90	5.88	4.81	21.69	4.35	17.28	0.59	0.89	8.10	28.73	
IM 20			-	-	-	-	-	-	-	-	-	-	-	-	-	-	-	
IM 21A			3.56	17.36	99.36	-	3.62	12.88	16.18	4.82	10.68	7.12	5.39	0.64	0.72	8.57	32.15	
IM 21B			-	-	-	-	-	-	-	-	-	-	-	-	-	-	-	
IM 21C			3.60	18.75	99.36	0.17	2.56	9.20	9.39	1.73	7.68	5.84	4.11	0.51	0.84	10.19	33.09	
IM 22			-	-	-	-	-	-	-	-	-	-	-	-	-	-	-	
IM 23A			1.91	11.79	99.82	0.09	3.68	7.03	1.89	0.41	2.11	3.58	1.85	0.28	0.56	16.85	31.21	
IM 23B			-	-	-	-	-	-	-	-	-	-	-	-	-	-	-	
IM 23C			1.46	10.83	99.86	0.07	3.18	4.63	1.28	0.35	1.89	2.79	1.85	0.26	0.72	18.65	30.47	
AU-10A			1.80	8.67	-	-	3.20	5.77	7.71	1.39	25.19	5.40	8.90	0.39	0.50	11.21	37.14	
AU-10B			2.20	8.98	97.46	0.69	3.48	7.65	12.57	2.06	21.65	6.29	8.48	0.40	0.69	9.33	39.89	
AU-10C			5.00	14.80	97.73	0.58	3.40	17.00	16.67	1.94	39.81	7.69	7.42	0.77	0.62	5.20	32.89	
OK-1d			2.71	10.90	99.62	0.10	2.23	6.04	3.81	0.69	2.73	4.93	7.42	0.39	0.90	14.22	32.30	
OK-2b			3.35	13.93	99.31	0.16	3.73	12.50	4.96	1.22	8.33	6.70	7.42	0.64	0.64	11.11	30.94	
IM 5D			-	-	95.52	0.83	2.87	-	4.70	1.12	28.32	2.47	11.68	0.31	1.00	10.06	30.08	
IM 5A			3.73	21.67	97.00	0.50	2.53	9.43	5.33	1.09	14.74	3.29	19.78	0.41	1.00	11.52	34.21	
IM 5B			3.80	35.50	94.83	3.62	3.03	11.50	2.71	2.06	35.72	2.11	9.89	0.27	1.27	9.40	32.27	
IM 5C			-	-	-	-	-	-	-	-	-	-	-	-	-	-	-	
IM 5E			4.15	28.50	96.93	0.50	2.60	10.80	5.93	1.36	21.82	2.59	13.60	0.52	0.89	8.98	33.53	
IM 7			3.06	21.47	96.60	0.32	2.46	7.53	4.86	0.85	4.59	1.89	47.00	0.18	2.29	12.08	35.79	
IM 8A			2.71	23.59	96.17	0.26	2.71	7.34	2.57	0.83	4.94	1.64	25.50	0.16	2.68	10.78	33.69	
IM 9A			2.77	25.02	96.58	0.32	2.45	6.78	4.37	0.97	4.71	1.25	25.14	0.27	1.32	11.24	34.11	

IM 8B			-	-	-	-	-	-	-	-	-	-	-	-	-	-	-
IM 9B			1.99	16.24	97.31	0.26	2.86	5.69	1.85	0.47	3.05	1.08	23.28	0.19	1.06	16.09	32.49
IM 6A			3.40	29.10	96.72	0.31	2.32	7.90	6.18	1.32	5.90	2.29	25.68	0.41	1.16	10.12	37.15
IM 6B			3.62	27.50	96.38	0.41	2.35	8.52	5.03	1.17	7.57	2.21	20.37	0.43	1.17	9.29	34.38
IM 10A			5.07	48.97	95.56	0.32	2.51	12.73	7.60	1.43	9.79	2.34	16.82	0.56	0.63	8.39	31.93
IM 10B			1.57	5.72	93.97	2.45	4.26	6.68	5.70	1.98	7.32	2.29	5.14	0.21	0.59	16.43	31.18
AU-11A	L7	Heterolithics	1.25	11.79	95.78	0.23	2.99	3.72	9.53	3.26	5.31	3.24	27.50	0.22	0.91	8.41	32.62
AU-11B			-	-	-	-	-	-	-	-	-	-	-	-	-	-	-
AU-11C			1.35	14.87	95.83	0.23	3.13	4.24	9.93	3.46	5.73	3.73	25.50	0.26	0.75	7.57	38.95
U1 11			2.50	20.00	98.87	0.21	2.83	7.08	11.54	2.91	8.47	5.56	11.13	0.29	0.69	6.87	37.50
U1 14			1.81	19.20	98.79	0.25	2.56	4.64	18.13	5.83	7.81	4.68	11.66	0.30	0.52	7.59	36.57
U1 17			1.70	17.53	98.64	0.21	3.08	5.23	12.75	2.70	3.88	5.23	10.50	0.19	0.68	9.78	36.89
AU-4a			0.82	8.65	95.24	0.20	3.15	2.59	4.00	0.52	2.84	2.92	26.50	0.15	0.73	14.97	34.19
AU-4B			-	-	-	-	-	-	-	-	-	-	-	-	-	-	-
AU-5			0.72	7.98	95.31	0.24	2.72	1.96	4.28	1.60	2.86	3.04	34.33	0.14	0.83	13.17	36.10
AU-7			0.91	9.91	95.62	0.21	2.68	2.43	4.97	1.73	2.59	3.08	34.33	0.15	0.85	13.76	35.10
AU-9			0.92	8.32	96.02	0.19	2.84	2.60	7.32	2.20	3.15	3.89	27.00	0.21	0.79	11.80	32.00
AU - 11D			-	-	-	-	-	-	-	-	-	-	-	-	-	-	-
AU- 11E			1.34	14.67	96.48	1.47	3.22	4.33	3.76	2.31	11.50	3.03	21.00	0.19	0.58	5.76	36.68
U1 12			1.14	12.69	98.61	0.23	3.16	3.60	8.20	2.11	3.39	3.11	12.00	0.14	1.03	10.53	34.10
U1 13			1.58	18.39	98.68	0.23	3.15	4.97	12.15	2.71	5.36	4.16	7.5	0.20	0.74	9.40	36.06
U1 15			1.98	18.70	98.81	0.33	2.64	5.23	19.83	5.53	11.90	5.95	8.66	0.32	0.40	6.43	36.19
U1 16			2.13	16.20	98.76	0.24	2.84	6.05	21.33	6.16	9.98	7.11	11.13	0.36	0.42	8.12	33.52
U1 20A			1.28	13.98	98.84	0.20	3.29	4.20	11.77	3.76	4.56	4.03	14.84	0.20	0.65	9.72	36.46
U1 20B			-	-	-	-	-	-	-	-	-	-	-	-	-	-	-
U1 20C			1.47	16.08	98.81	0.28	2.77	4.08	18.00	5.13	6.39	3.45	12.72	0.25	0.59	7.28	36.10
Turonian Sand <sup>λ1</sup>			-	-	70.39	0.89	-	-	-	-	4.01	-	0.93	-	-	31.30	-
Turonian Shale <sup>λ</sup>			-	-	46.99	1.73	3.71	-	-	-	3.46	4.79	4.26	-	-	22.73	-
Albian Shale <sup>λ</sup>			-	-	52.70	1.46	7.27	-	-	-	5.46	5.47	3.77	-	-	22.41	-
Syenite <sup>λλ</sup>			-	-	50.38	1.62	-	-	-	-	4.44	-	1.97	-	-	16.90	-
Mica Schist <sup>λλ</sup>			-	-	59.08	-	-	-	-	-	4.12	-	0.72	-	-	28.85	-
Metaconglomerate <sup>λλ</sup>			-	-	60.54	0.99	-	-	-	-	3.86	-	0.83	-	-	31.48	-
UCC			0.79	13.97	52.67	1.42	2.80	2.21	0.63	0.50	4.34	3.82	0.55	0.13	0.78	22.21	32.76

#### 2.4.1.1.3 Dark coloured wavy to curved microfacies (M3)

This microfacies is typically mildly to moderately bioturbated, characteristically wavy to curved and thickly laminated/thinly bedded (where preserved) (Figs. 2.8b5, 8b6), varying texturally from cMs to sMs. The fabric is AR-SI to SI (Fig. 2.6f). Microscale soft sediment deformation structures (ball structures) indicating rapid sedimentation rate were observed in L1 (Figs. 2.8b6). M3 is interpreted as deposits that accumulated more rapidly, arising from discontinuous sedimentation by stronger bottom water currents (lateral accretion) in more proximal, shallower, higher energy condition (Lazar *et al.*, 2015).

The poor sorting of L1 (Fig. 2.6b) is consistent with the findings of Folk (1974), who reported an average standard deviation of 2.0-3.5 $\phi$  for floodplain and shallow marine mudstones. The dominance of the phytoclast palynological organic matter group in L1, the high frequency of occurrence of M2 and M3, as well as the occurrence of sand sized mica on lamina planes is a strong indication of low salinity, high-energy shallow water setting and proximity to higher land plant sources. The observed occurrence of articulate brachiopod and gastropod molds, as well as marine palynomorphs in M1 provides evidence for higher salinity, low energy, and deeper water marine conditions. Thus, we interpret the L1 as a product of brackish water where salinity fluctuations exist. The low Na<sub>2</sub>O, CaO, MgO and K<sub>2</sub>O concentrations (Table 2.1b, Section 2.4.1.4), as well as the occurrence of iron concretions support this interpretation.

We identified three different subfacies of L1 based on inferences drawn from the stratigraphic relationship with L2, L3 and L4 (see Sections 2.4.1.2, 2.4.1.3 and 2.4.1.4), microfacies observations, as well as inferences from the APP, SMP and PQC ternary plots (Figs. 2.6b-d). The subfacies types are L1a, L1b and L1c corresponding to marsh, bay and central basin environments. The marsh and bay environments, which are characterized by stronger terrestrial signature such as, a higher percentage of phytoclasts, relatively enriched

quartz content, and lower percentages of aquatic amorphous organic matter and palynomorphs were deposited under conditions that were more proximal, with lower salinity and higher detrital contribution (Figs. 2.6b-d). The M3 microfacies is particularly common in L1a and occasionally in L1b, which has M2 and M1 (M2>>>M1 in order of occurrence) as its dominant microfacies. The central basin, which shows a stronger marine influence by a higher percentage of palynomorphs (marine palynomorphs in particular) and aquatic amorphous organic matter, a lower percentage of phytoclast and quartz, as well as the occurrence of brachiopod molds, was deposited under conditions more distal, with higher salinity and lower detrital contribution (Figs. 2.6b-d). M2 is dominant microfacies of L1c while M1 was observed in a few instances. This interpretation is corroborated by lower SiO<sub>2</sub> and higher Al<sub>2</sub>O<sub>3</sub> (Table 2.1a) in comparison to other subfacies.

Furthermore, regardless of the low MgO, K<sub>2</sub>O and CaO concentrations in L1, their relative proportion in L1c (Table 2.1a) is significantly higher (0.7-1.18 wt. %, 0.58-1.75 wt. %, and 0.02-1.1 wt.% respectively) than in L1a and L1b (<0.01– 0.33 wt. % , <0.01–1.06 wt. %, and 0.01-0.04 wt.%, respectively). This contrast may be attributable to the transformation of kaolinite to illite-smectite (K-Fe-Mg) clays in L1c resulting from higher salinity prevailing in the more distal central basin. An authigenic transformation is supported by the mean percentage illite (excluding values >30 %) of the L1a, L1b and L1c, which are 11.27 % (n=23), 13.98 % (n=20) and 15.46 % (n=22) respectively, as well as the negative correlation between SiO<sub>2</sub> vs. K<sub>2</sub>O (Appendix 1.2a) (Huggett and Cuadros *in Andrade et al.*, 2014), and the positive correlation between CaO vs MgO, Fe<sub>2</sub>O<sub>3</sub> vs. K<sub>2</sub>O, and Fe<sub>2</sub>O<sub>3</sub> vs. MgO (Appendix 1.2b-d) (Cuadros *et al.*, 2017).



*2.4.1.2 Lithofacies 2 (L2): Thin bedded poorly-moderately sorted, moderately cemented sheet-like sMs-Ss*

This lithofacies displays poor-moderate sorting (Fig. 2.6b) and weak to moderate cementation. It is SI-AR to SI (Fig. 2.6f), sMs-Ss (Fig. 2.6a), which occurs as interbeds in the dark mudstone facies and heterolithic facies (L7) (see Section 2.4.1.7; Figs. 2.7a, 2.7b, 2.7d, 2.8a). L2 is thin and exhibits a sheet-like geometry commonly less than 20 cm thick stretching across the outcrop length (Figs. 2.7a). At the Auchi section (Fig. 2.7d); the base of L2 is bioturbated. The sheet-like geometry, bioturbation and moderate sorting are evidences of a marine signature. Based on texture, fabric and stratigraphic position, L2 is interpreted as shallow marine sandy mudstone brought in during storm events.

*2.4.1.3 Lithofacies 3 (L3): light coloured moderately sorted weakly cemented, weakly to mildly bioturbated sheet-like sMs-mSs*

Lithofacies 3 is characteristically sharp regular-based, massive looking, moderately sorted, and weakly to mildly bioturbated sMs - mSs (Figs. 2.6b, 2.7b, 2.8d, 2.8e). This lithofacies has sheet-like geometry, is commonly thicker than L2 (up to 1.2 m), and extends across the full length of exposure (Figs. 2.7b, 2.8d). It is interbedded with L1 and L2 in the Okpekpe section (Figs. 2.7b, 2.8d). The sheet-like geometry, bioturbation and moderate sorting (Fig. 2.6b) indicate a marine setting. L3 is interpreted as beach-barrier/wash-over fan deposit based on its stratigraphic position and textural characteristics (Figs. 2.7b, 2.8d), which is similar to those described by Reinson (1992).

*2.4.1.4 Lithofacies 4 (L4): MgO – poor oolitic ironstone*

L4 was identified in the Okpekpe section only (Fig. 2.7b), where it overlies L5 (see Section 2.4.1.5) and underlies L1 (Figs. 2.7b, 2.8d, 2.8f). It is 1.26 m thick, stratified, and had solution cavities (Fig. 2.8f). Furthermore, L4 had an oolitic fabric characterized by symmetrical concentric growth rings around a nucleus, which was (partly or wholly) replaced by iron oxide

(and/or iron oxyhydroxide) ranging from 14.7 to 28.4% (Figs. 2.8g1, 2.8g2, Table 2.1b). Ooid diameter ranges from ~300 µm to 2 mm (Figs. 2.8g1, 2.8g2). The basal unit is finer-grained and more compacted with lower iron concentration (Figs. 2.7b, 2.8d, 2.8f, 2.8g2, Table 2.1b). The top unit is coarser-grained, less compacted, richer in iron concentration (Figs. 2.7b, 2.8d, 2.8f, 2.8g1, Table 2.1b), and appears to be separated from the lower unit by a sharp-irregular (erosive) contact (Fig. 2.8d, 2.8f). L4 is interpreted to be a kaolinite-type oolitic ironstone (Mücke, 2000) based on its low MgO content (0.05-0.07%, Table 2.1b), the dominance of woody debris (96%, Table 2.1a), and the absence of marine micro- and macrofossils or bioturbation. Inferences deduced from its geochemistry, texture, fabric and stratigraphic position (Figs. 2.7b, 8d) point to a shallow brackish water setting and lead to its interpretation as a bay deposit. This is consistent with the findings of Umeorah (1987), Mücke *et al.*, (1999), and Mücke (2000), who studied similar aged oolitic ironstones in the Bida Basin.

#### *2.4.1.5 Lithofacies 5 (L5): Poorly sorted cross-bedded, very coarse- to medium-grained mSs to Ss*

This lithofacies has a characteristic sharp-erosive base and channel geometry (Figs. 2.7a, 2.7b, 2.7d, 2.8a, 2.8h-j), with thickness that can be up to 1m in its central part and tapering at the flanks. L1 units are commonly amalgamated in the outcrop, consisting of stacked units eroding into one another (Figs. 2.7a, 2.7b, 2.7d, 2.8a, 2.8j). Quartz pebbles and/or coal and mudstone intraclasts abound at its base (Figs. 2.7a, 2.7b, 2.8j; Appendix 1.3a1-a2), grading into finer mSs of L6 (Appendix 1.3a2; see Section 2.4.1.6). It is light coloured but may be dark due to reworked coaly intraclasts (Fig. 2.8a) and is bioturbated (*Skolithos*, Appendix 1.3b) in places, planar and sigmoidal (Imiegba section, Fig. 2.8a) cross-bedded (Appendix 1.3c) and poorly sorted with grains ranging from very coarse to medium-grained mSs to Ss (Figs. 2.6a-b).

#### 2.4.1.6 Lithofacies 6 (L6): Light coloured sMs to mSs

This lithofacies is poorly sorted, light coloured AR-SI to SI-AR, medium mudstone-sandy mudstone (Figs. 2.6a-b, 2.7a-b, 2.8a). It typically occurs stratigraphically atop L5, which grades and erodes into it (Figs. 2.7a-b, 2.8a, 2.8j). At the Imiegba locality, ripple lamination was observed (Fig. 2.7a). Dark mudstone and coaly intraclasts commonly occur (Figs. 2.7a, 2.7b, 2.8j).

#### 2.4.1.7 Lithofacies 7 (L7): Heterolithic

Lithofacies 7 is characterized by intercalations of mMs, cMs, sMs, mSs and Ss (Fig. 2.7c-d, 2.8k-l). It is SI-AR to SI, weakly bioturbated, lenticular to wavy non-parallel laminated to thin bedded (Figs. 2.6f, 8k-l, Appendix 1.3d-e) and is associated with L5 and L2 (Figs. 2.7c-d). The thickness of coarser mSs and Ss units vary from 1cm to 3cm, whereas the finer mudstone units are commonly less than 1cm (Figs. 2.8k-l, Appendix 1.3d-e). Differential weathering of clay-rich horizons relative to the sand and silt is characteristic of this lithofacies (Appendix 1.3d-e). In the Auchi section, L7 lies stratigraphically on top of L5. The contact between L5 and L7 is sharp here (Fig. 2.7d), whereas in the Uzebba section, L7 overlies L1a.

Process interpretation of L5, L6 and L7 suggests a combination of fluvial and marine effects. The large particle size, the poor sorting, the characteristic sharp-erosive base and channel geometry, the grading upwards motif, as well as inference from the skewness vs. sorting bivariate plot of L5 (Fig. 2.6f) are indicative of confined unidirectional fluvial processes, which predominated during deposition of L5. The coal and dark mudstone intraclasts in L5, L6 and L7 are interpreted as relics of underlying dark mudstone and coal eroded under high energy and deposited as energy conditions waned. That notwithstanding, the bioturbation, lenticular to wavy non-parallel lamination and sigmoidal cross-bedding are evidences of a marine signature in this lithofacies. Consequently, L5 is interpreted as fluvial-tidal channel facies based on its textural characteristics and stratigraphic position similar to

descriptions of Boyd *et al.* (2006). In addition, L5 is subdivided into two subfacies indicating proximal (L5a) to intermediate positions (L5b). L5a is characterized by reworked coaly and mudstone intraclasts which erodes into the marsh facies of L1 (Fig. 2.7a), whereas L5b is characterized by sigmoidal cross bedding which is indicative of stronger tidal influence where it erodes into the central basin mudstones of L1 (Fig. 2.7a).

Based on the stratigraphic relationship between L5 and L6, as well as its textural characteristics, L6 is interpreted as a fluvial-tidal channel floodplain/overbank deposit, which is similar to those described by Ojo and Akande (2009). The textural characteristics, occurrence of lenticular to wavy lamination/ bedding, as well as weak bioturbation and stratigraphic position of L7 suggest an abandoned fluvial-tidal channel. This is similar to the abandoned tidal channel described by Moslow and Tye *in* Reinson (1992).

#### *2.4.1.8 Lithofacies Associations (LFA)*

Two facies associations were identified based on lithofacies descriptions and their stratigraphic relationships.

##### *2.4.1.8.1 Marsh/bay/central basin-beach-barrier/washover fan lithofacies association (L1-L2-L3-L4 LFA)*

This facies association is characterized by dark mudstone interbedded with massive looking, thin poorly-moderately sorted sandy mudstone to sandstone, moderately sorted sandy mudstone to muddy sandstone, and MgO-poor oolitic ironstone. L1 suggests quiet water marsh/bay/central basin depositional conditions (Section 2.4.1.1), occasionally inundated by storms that deposited L2 (Section 2.4.1.2). L3 is characteristic of micro-mesotidal (wave dominated) transgressive coastline environments such as beaches/barrier bars and washover fans partially enclosing the central basin (Section 2.4.1.3). Upon rise in sea level, barriers become drowned, leading to an alternation of brackish water mudstones and beach-barrier sandstones (Reinson, 1992), as observed in the Imiegba and Okpekpe sections with the

intercalations of L1, L2 and L3 (Figs. 2.7a-b). The brackish conditions prevailing allowed for the formation of L4 at the interface between (proximal) fluvial-tidal channel and bay (Figs. 2.7b, 2.8a). The stratigraphic relationship between L4, L1 and L5a (Fig. 2.7b) lends credence to this interpretation and possibly represents a (fluvially dominated) bay head delta (Boyd *et al.*, 2006). The components of this “birds-foot type” bay head delta include L1 and L2 as prodelta facies and L5 as distributary channel (Dalrymple *et al.*, 1992).

#### *2.4.1.8.2 Fluvial-tidal channel lithofacies association (L5-L6- L7 LFA)*

This facies association is characterized by sharp irregular (erosive) based, poorly sorted, planar cross-bedded very coarse to medium-grained muddy sandstone to sandstone with quartz pebble lags and/or coaly and mudstone intraclasts, light coloured medium mudstone-sandy mudstone and heterolithics. L5 and L7 represents channel deposition at active and abandonment phases respectively. Floodplain/ overbank condition is represented by L6. The poor sorting, the facies geometry as well as the characteristic unidirectional channelized flow deposits of L5 are evidences of high-energy fluvial process. The sigmoidal cross-bedding observed in L5, the weak bioturbation, the lenticular to wavy laminations, as well as the improved sorting of sand units in the heterolithics evidence tidal influence.

#### *2.4.1.9 Facies Succession*

The alluvial to fluvial Lokoja Formation (Section 2.1.1) underlying the Mamu Formation signifies deposition due to high-energy mixed gravity and confined flows during basin subsidence resulting from thermal sag. This lithostratigraphic unit outcrops at the proximal parts of the western flank. The Mamu Formation marks the onset of post-Santonian flooding in the western flank of the Anambra Basin.

Table 2.2. Lithofacies characterization summary

S/N	Lithofacies	Interpretation	Facies Association	Gross depositional environment
L1	Dark mudstone with three microfacies: planar to wavy laminated microfacies (M1), lenticular to wavy laminated microfacies (M2), wavy to curved microfacies (M3).	Marsh-bay-central basin	Marsh/ bay/ central basin -barrier-beach-washover	Tidal influenced wave dominated estuary (Reinson, 1992)
L2	Thin sheet-like poorly-moderately sorted, moderately cemented sMs to Ss.			
L3	Light coloured, moderately sorted, weakly cemented, weakly-mildly bioturbated, sMs to mSs.	Barrier/beach/wash-over sand		
L4	MgO-poor, kaolinite-type oolitic ironstone. Iron oxide content ranges from 14.7 -28.4%.	Brackish water interpreted as bay deposit		
L5	Poorly sorted cross-bedded, very coarse- to medium-grained mSs to Ss. Two subfacies with L5a characterized by reworked coaly and mudstone intraclasts corresponding to a proximal setting, and L5b characterized by sigmoidal cross-bedding corresponding to more distal setting with tidal influence.	Fluvial (dominated)-tidal channel deposit	Fluvial-tidal channel – floodplain	
L6	Light coloured sMs to mSs with dark mudstone and coaly intraclasts	Fluvial-tidal channel overbank/floodplain deposit (Ojo and Akande, 2009)		
L7	Weakly bioturbated, lenticular to wavy non-parallel laminated/thinly bedded heterolithics characterized by intercalations of mMs, cMs, sMs, mSs and Ss.	Abandoned meandering fluvial-tidal channel deposit (Boyd et al., 2006)		

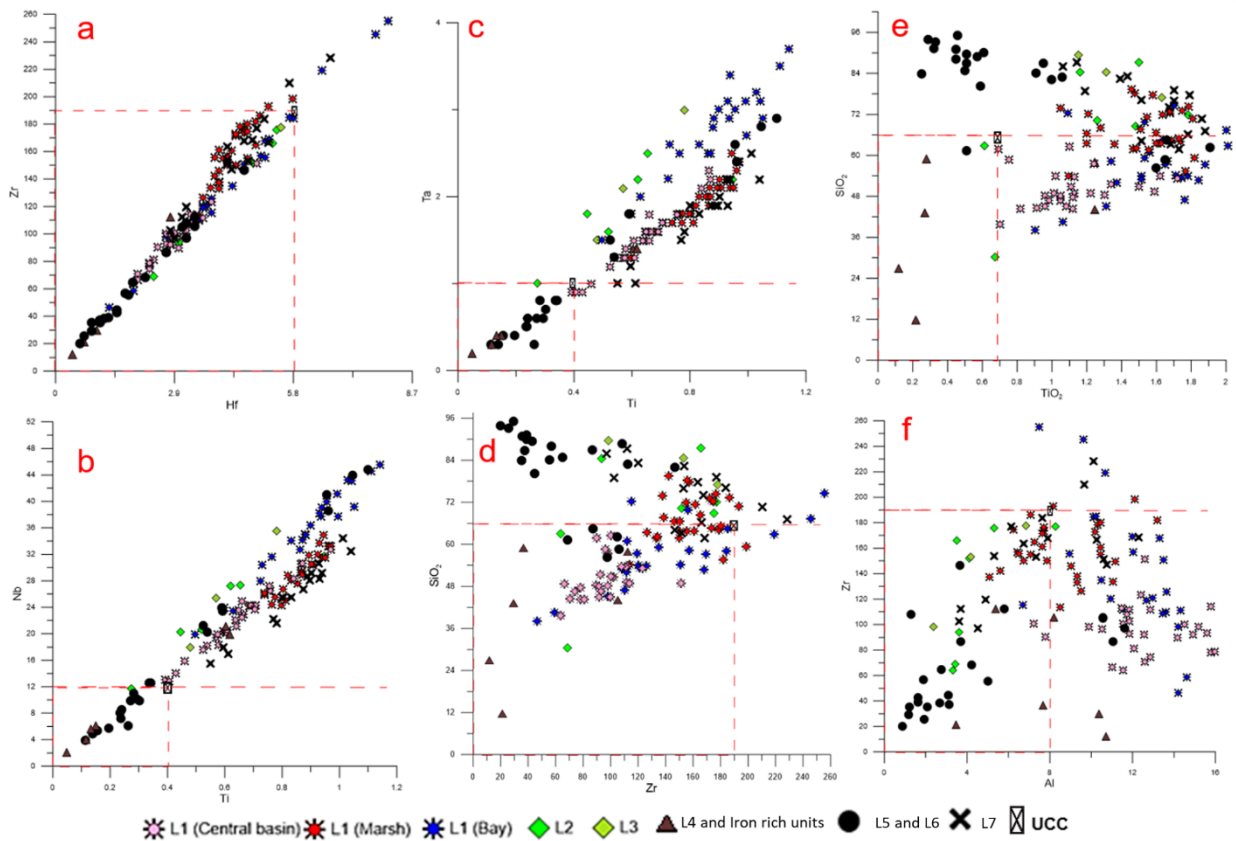


Fig. 2.9. a-c, Strong positive correlation of Zr vs. Hf, Nb vs. Ti, and Ta vs. Ti in binary plots, respectively. d-f, Scatter plot of SiO<sub>2</sub> vs. Zr, SiO<sub>2</sub> vs. TiO<sub>2</sub>, and Zr vs. Al, respectively. Note the red broken line indicating the UCC composition for the elements and oxides

At least two cycles of sedimentation can be observed from the outcrop sections studied: each depositional cycle begins and ends with a regressive phase characterized by deposits of fluvial-tidal channels with evidence of incision of older strata. This phase is succeeded by a transgressive phase beginning with a flooding surface typified by the base of L1. The Okpekpe and Imiegba sections illustrate this succession, as they show the transitioning from channelized flows into open unconfined deeper brackish water. The latter resulted from rising sea levels (outpacing clastic input), which induced flooding and estuarine conditions as represented by L1- L2- L3-L4 LFA. L6 and L7 also represent flooding of L5, with L7 interpreted to represent high-stand conditions in the filling history. The gross depositional environment based on facies analysis is one that has evidences of fluvial and marine processes and as such is interpreted as

a tidally influenced, wave-dominated estuary similar to the partially closed wave dominated estuary of Reinson (1992). A summary of the lithofacies characterization is given in Table 2.2.

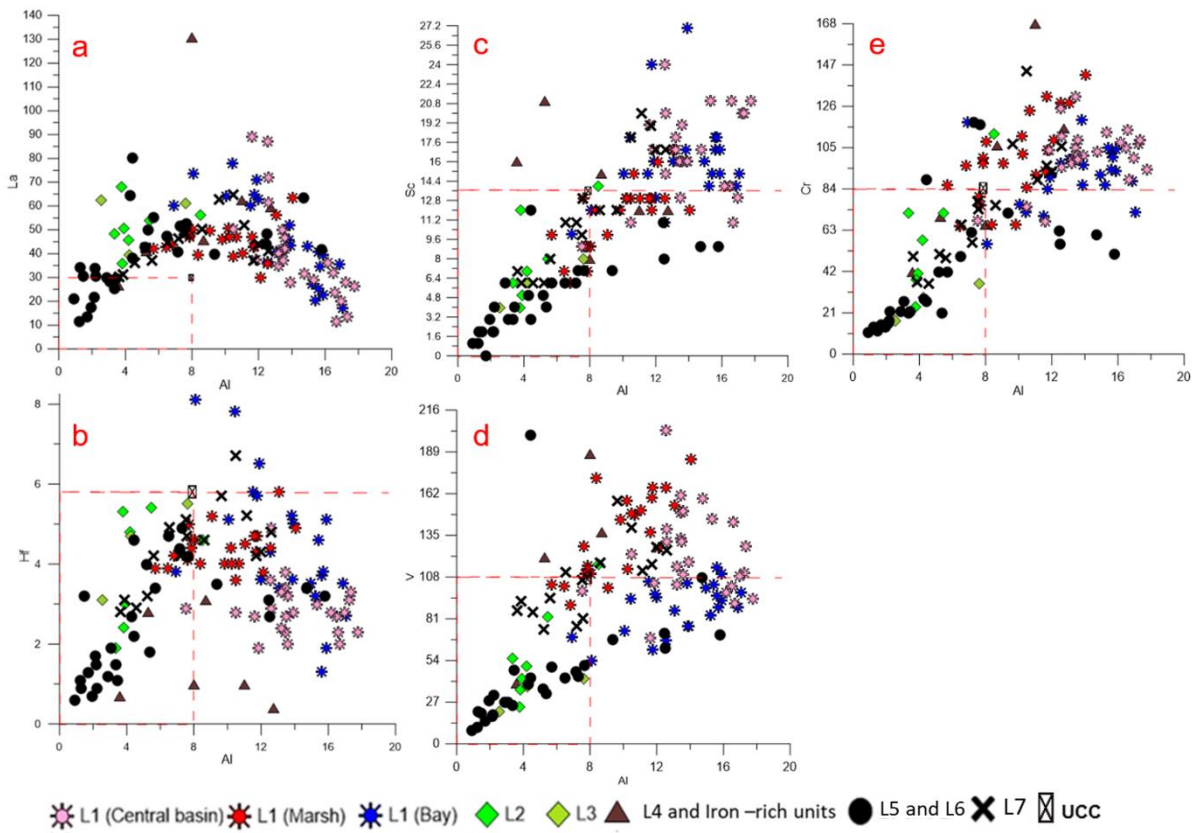


Fig. 2.10. a,b, Binary plots showing very weak positive correlation for La vs. Al and Hf vs. Al respectively. c-e, Binary plots showing moderate to weak positive correlation of Sc vs. Al, V vs. Al and Cr vs. Al. Note the red broken line that indicates the UCC composition for the elements and oxides.

## 2.4.2 Geochemical characterization

### 2.4.2.1 Source and distribution of elements

Bivariate plots of geochemical data (Table 2.1b) reveal the existence of a strong correlation between Zr vs. Hf, Nb vs. Ti, and Ta vs. Ti (Figs. 2.9a-c) and moderate correlation between Nb vs. Zr, and Ta vs. Zr (Appendix 1.4a-b), implying that Ta, Nb, Hf, Ti and Zr are concentrated in the heavy mineral fraction of the sediments (i.e. rutile, ilmenite, etc. and zircon respectively). This hypothesis is supported by the moderate positive correlation between Ti vs. Al (Appendix 1.4c) and the moderate positive correlation between Ti vs. Zr (Appendix 1.4d)



The correlations suggest chemical immobility of Ti and some contribution of Ti from zircon (Zaid, 2015), implying that rutile is not the only source of Ti (Wang *et al.*, 2018).

Furthermore, the broad distribution between SiO<sub>2</sub> vs. Zr (Fig. 2.9d) and SiO<sub>2</sub> vs. TiO<sub>2</sub> (Fig. 2.9e) indicates that the amount of quartz has no effect on Ti and Zr concentrations in the sediments. This is supported by the very weak correlation between Zr vs. Al, La vs. Al, Hf vs. Al, Y vs. Al, Co vs. Al, and Th vs. Al in the binary plots (Figs. 2.9f, 2.10a-b, and Appendix 1.4e-f, 1.5a), which suggests insignificant sorting during weathering and sediment transport. The observation agrees well with the hypothesis that Zr, La, Hf, Y, Co, and Th are derived from variable sources and occur in both the coarse quartz-rich sandy fraction and the finer kaolinite-rich mudstone fraction. Better positive correlation between Sc vs. Al, V vs. Al, Cr vs. Al, Ti vs. Al, Ni vs. Al, Nb vs. Al, Ta vs. Al, and U vs. Al was noted in the binary plots (Figs. 2.10c-e, and Appendix 1.4c, 1.5b-e), indicating some concentration in the kaolinite-rich mudstone fraction. In addition, the strong negative correlation between SiO<sub>2</sub> vs. Al<sub>2</sub>O<sub>3</sub> (Appendix 1.5f), and total clay vs. quartz (Fig. 2.6f) suggests that quartz is mainly derived from detrital sources (Amedjoe *et al.*, 2018).

#### 2.4.2.2 Paleoclimate, provenance and tectonic setting

Several proxies including mineralogical composition (i.e. quartz content and clay mineral type), and major, trace and rare earth element concentrations, palynology, molecular and isotope geochemistry amongst others can be used for paleoclimate, provenance and paleotectonic studies of sedimentary rocks (Potter *et al.*, 2005; Basu *et al.*, 2016). In this study, we decided to use mineralogy, major element, and trace element proxies.

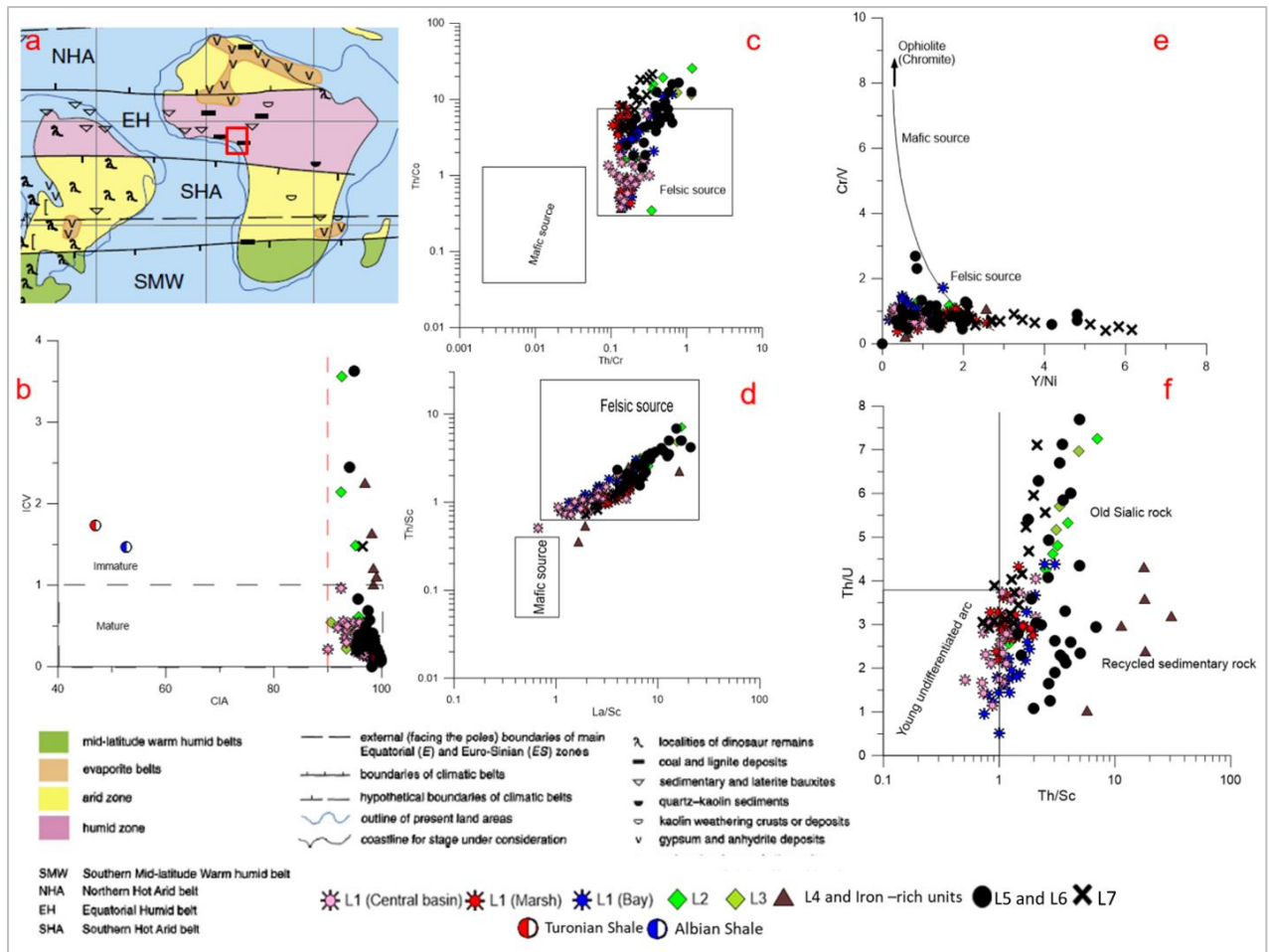


Fig. 2.11. a, Maastrichtian palaeogeographic and paleoclimatic reconstruction of Africa (adapted from Chumakov et al. in Hay and Floegel, 2012); note legend at bottom of figure. The red box shows Nigeria under humid tropical climate. b, ICV vs. CIA binary plot. Notice the high CIA and mineralogical maturity of the post-Santonian Mamu Formation, whereas the pre-Santonian mudstones (data from Amajor, 1987a) indicate low CIA and mineralogical immaturity. c-f, Th/Co vs. Th/Cr, Th/Sc vs. La/Sc, Cr/V vs. Y/Ni (after Hiscott, 1984), and Th/U vs. Th/Sc used to constrain provenance and paleotectonics of the sediments. Th/Co, La/Sc, Th/Cr and Th/Sc data ranges for felsic and mafic rocks as well as young undifferentiated arc, recycled sedimentary rock and old sialic rock obtained from Cullers (2000) (see Table 2.3).

Table 2.3: Ratios of trace elements from felsic and mafic rocks (adapted from Cullers, 2000).

Provenance	Trace element ratios				
	La/Sc	Th/Sc	La/Co	Th/Co	Th/Cr
Felsic rocks	0.7-27.7	0.64-20.5	1.4-22.4	0.3-19.4	0.067-4
Mafic rocks	0.4-1.1	0.05-0.4	0.14-0.38	0.04-1.4	0.002-0.0046

#### 2.4.2.2.1 Paleoclimate

The low content of Na<sub>2</sub>O, CaO, MgO and K<sub>2</sub>O, as well as the dominance of kaolinite as the main clay mineral and minor illite in the sediments (Table 2.1a) signifies intensive chemical weathering, which corresponds to tropical conditions prevailing in the source area that lead to intense leaching (Singer, 1984; Rimstidt *et al.*, 2017). This interpretation is supported by the concentration of Sc, V, Cr, Ti, Ni, Nb, Ta, and U in the kaolinite-rich mudstone fraction (section 2.4.2.1)(Feng and Kerrich, 1990; Zaid, 2015), the Maastrichtian paleoclimatic reconstruction (Chumakov *et al. in* Hay and Floegel, 2012), which placed the Anambra Basin (and Nigeria as a whole) within the tropical climate (Fig. 2.11a) belt as well as a high chemical index of alteration ( $CIA = (Al_2O_3 / (Al_2O_3 + CaO + Na_2O + K_2O)) \times 100$ ) (Nesbitt and Young, 1982; Potter *et al.*, 2005) exceeding 90% (Fig. 2.11b). In addition, a low index of compositional variability ( $ICV = (Fe_2O_3 + K_2O + Na_2O + CaO + MgO + MnO + TiO_2) / Al_2O_3$ ) (<1%, Fig. 2.11b) is indicative of an advanced mineralogical maturity (Cox *et al.*, 1995; Wang *et al.*, 2018) of the sediments. In contrast, geochemical data from some pre-Santonian strata show low CIA and high ICV values of pre-Santonian mudstones (Fig. 2.11b), which suggest less intense chemical weathering and mineralogical immaturity (data adapted from Amajor, 1987a).

#### 2.4.2.2.2 Provenance and Paleotectonics

La, Sc, Th, Hf, Co, Ta, V, Cr, Ni, Zr, Y, Nb, Ta, etc., are conservative elements, being relatively immobile/insoluble during weathering, diagenesis and transportation of source rocks (Bhatia and Crook, 1986; Wronkiewicz and Condie, 1990; Cullers, 1995, 2000; Potter *et al.*, 2005). We assume that the disparity in the trace element geochemistry of the provenance and sediments are subordinate to insignificant (see Section 2.4.2.1). Enrichment of Th, U, Ta, Nb, Zr, Y, Hf and La (high field strength trace elements [HFSTE] with a partition coefficient < 1)

occurs in felsic igneous rocks rather than in mafic rocks due to their preferential partitioning in silicic melts upon crystallization of mineral phases (Feng and Kerrich, 1990; Best, 2003; Ali *et al.*, 2014; Hassan, 2017). Conversely, Cr, Co, Ni, V, Sc (transition trace elements [TTE] with a partition coefficient  $>1$ ) are compatible elements abundant in mafic igneous rocks, where they readily substitute for major elements in mafic to ultramafic mineral phases. Consequently, their ratios (HFSTE *vs.* TTE) provide insight into the composition of the provenance and tectonic settings of sedimentary rocks, as indicated by the classification given by Cullers (2000).

Bivariate plots of Th/Co *vs.* Th/Cr, Th/Sc *vs.* La/Sc, Th/Co *vs.* La/Sc, Th/Co *vs.* Th/Sc, Th/Cr *vs.* La/Sc (Figs. 2.11c-d, Appendix 1.6a-c), based on the data ranges from Cullers (2000) (Table 2.3) reveal a dominantly felsic source for the sediments. Binary plots of Cr/V *vs.* Y/Ni, and TiO<sub>2</sub> *vs.* Zr (Fig. 2.11e, Appendix 1.6d) favour a felsic-intermediate provenance for the post-Santonian sediments and pre-Santonian rocks (data adapted from Amajor, 1987a). High Zr, CIA, Si/Al, Th/Sc ( $\geq 1$ ) and Th/U ( $> 3.8$ ) and low ICV (Fig. 2.11b), which characterize terranes with old sialic and/or recycled sedimentary rocks (McLennan *et al.*, 1993) as well as Th/Sc *vs.* Th/U bivariate plot (Fig. 2.11f), which imply that the provenance of the Campano-Maastrichtian Mamu Formation sediments is dominantly from recycled pre-Santonian rocks. In addition, the implication of felsic-intermediate rocks in the source area (Figs. 2.11c-e, Appendix 1.6a-d) suggests an extensional tectonic regime devoid of orogenic volcanic rocks at the time of sediment accumulation in a passive margin setting as depicted in the binary plot of K<sub>2</sub>O/Na<sub>2</sub>O *vs.* SiO<sub>2</sub> (Fig 2.12a).

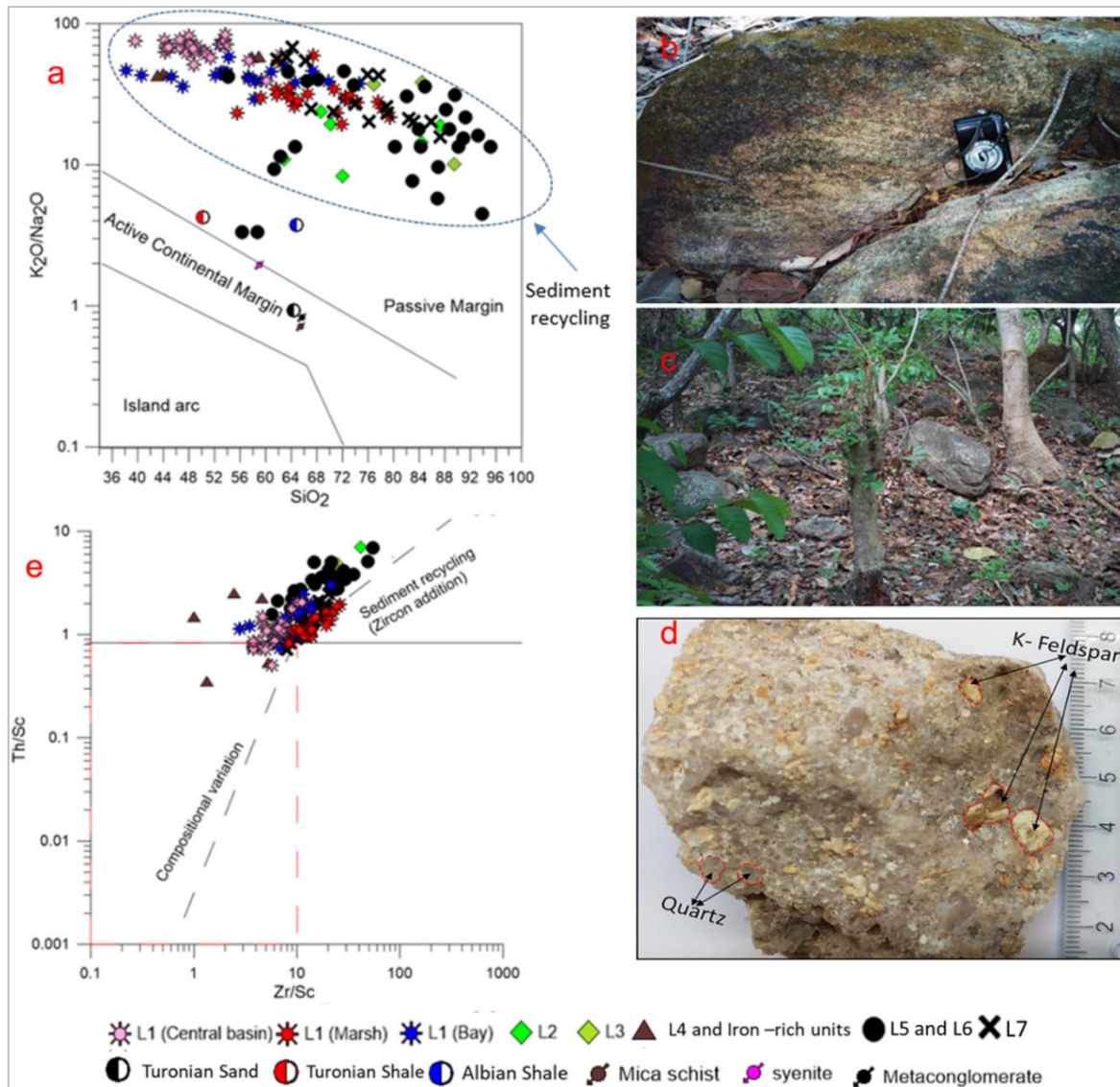


Fig. 2.12. a,  $Th/Sc$  vs.  $Zr/Sc$  binary plot (after McLennan et al., 1993) implying that the sediments are sourced from basement rocks and pre-Santonian rocks. b-c, pre-Santonian arkosic sandstone outcrop near Ikpeshi. d, Hand specimen of pre-Santonian arkosic sandstone. Note the sub-angular pebbly quartz and feldspar grains. e,  $K_2O/Na_2O$  vs.  $SiO_2$  (after Roser and Korsch, 1986) used to constrain paleotectonics of the sediments as well as pre-Santonian and Precambrian rocks. Note that basement rocks plot in the active continental margin field. Data for pre-Santonian and Precambrian basement rocks obtained from Amajor (1987a), Igwe (2017) and Imarhiagbe (2017) respectively.

Furthermore, the binary plot of  $K_2O/Na_2O$  vs.  $SiO_2$  (Fig 2.12a) also shows a clear contrast between the provenance and paleotectonic signatures of the pre and post-Santonian units. Whereas the post-Santonian units are more distinct from the basement signature due to sediment recycling, the signature of the basement and pre-Santonian rocks are quite similar. This suggests a dominant basement source for the pre-Santonian rocks (Amajor, 1987b; Igwe,

2017), which explains the high ICV and low CIA values reported for the pre-Santonian rocks and vice versa. This hypothesis is consistent with the current understanding of the tectonic setting of pre-and post-Santonian Benue Trough evolution (Edegbai *et al.*, 2019). Edegbai's unpublished data reveal the presence of boulders of pebbly to coarse grained silica-cemented arkosic sandstone outlier (Figs. 2.12 b-d) close to Ikpeshi (N07° 07' 35.8'', E006° 13' 00.4'') in the western section of the Anambra basin, which has similar mineralogy and textural characteristics of pre-Santonian sandstone units described elsewhere (Hoque, 1977; Kogbe, 1981; Amajor, 1987b; and Shettima *et al.*, 2018). This arkosic sandstone is interpreted to be a relic of pre-Santonian rocks that sourced a large proportion of the post-Santonian sediments in the western Anambra Basin. In addition, the bivariate plot of Th/Sc vs. Zr/Sc (Fig. 2.12e; McLennan *et al.*, 1993) suggests some contribution from the basement rocks around the Benin Flank, which comprise three main lithological units – the Migmatite-Gneiss-Quartzite complex, the metasedimentary rocks, and the Older Granite suite (Woakes *et al.*, 1987; Odeyemi, 1988).

Recent paleo-drainage models (Bonne, 2014; Markwick, 2018) suggest that the paleo-River Niger and paleo-River Benue drainage systems were important sediment transport sources to the Anambra Basin during the Campanian to Maastrichtian stages. These models imply different provenance signatures for the post-Santonian rocks in the western and eastern sections of the Anambra Basin. The western section of the Anambra Basin, as confirmed by this study, received a large proportion of its sediment contribution from pre-Santonian rocks, and a minor contribution from Pre-Cambrian basement, which is perhaps a consequence of a strong contribution from the paleo- River Niger drainage system. Conversely, sediment contribution in the eastern section of the Anambra Basin derived predominantly from reworked pre-Santonian rocks perhaps due to strong contribution from the paleo-River Benue drainage system (Edegbai *et al.*, 2019; M. E. Okiotor, pers. comm., 2015; Amajor, 1987b).

## 2.5 Conclusion

The major findings of this study are listed below:

- (1) MgO-poor oolitic ironstones in the Benin Flank of the western Anambra Basin have been documented for the first time.
- (2) Inferences drawn from mineralogical, palynological and sedimentological observations indicate that wave dominated estuarine conditions were prevalent in the western section of the basin during the Campano-Maastrichtian ages.
- (3) The estuarine depositional conditions were responsible for the widespread facies variability of the Mamu Formation reported elsewhere in the Anambra Basin.
- (4) Multiple proxies (based on mineralogical and palynological observations) indicate that the dark mudstone lithofacies of the Mamu Formation is heterogeneous, varying from central basin, to bay, and marsh environments. This is crucial for its hydrocarbon potential especially, as the central basin mudstone may hold potential for oil generation from type II/III kerogen, inferred from the high percentage of palynomorphs. This result stands in contrast to the consensus that favours a gas prone kerogen type III source.
- (5) Tropical conditions characterized by intense leaching in the source area prevailed during the mid-Maastrichtian.
- (6) The CIA and ICV of the pre- and post-Santonian units imply that the post-Santonian sediments are mineralogically mature and more severely chemically weathered in contrast to the post-Santonian rocks that are mineralogically immature and less chemically weathered.
- (7) A clear distinction exists between the provenance signatures of the pre and post-Santonian units. The post-Santonian rocks show a mixed provenance with felsic-intermediate composition which gives evidence of sediment recycling from pre-

Santonian rocks as well some contribution from Precambrian basement rocks, whereas the signature of the pre-Santonian rocks imply a basement source for the pre-Santonian rocks. The bivariate plot of Th/Sc vs. Zr/Sc. substantiates this hypothesis

- (7) A passive margin tectonic regime inferred from mineralogical and geochemical analyses is consistent with the current understanding of the tectonic setting of pre-and post-Santonian Benue Trough evolution.

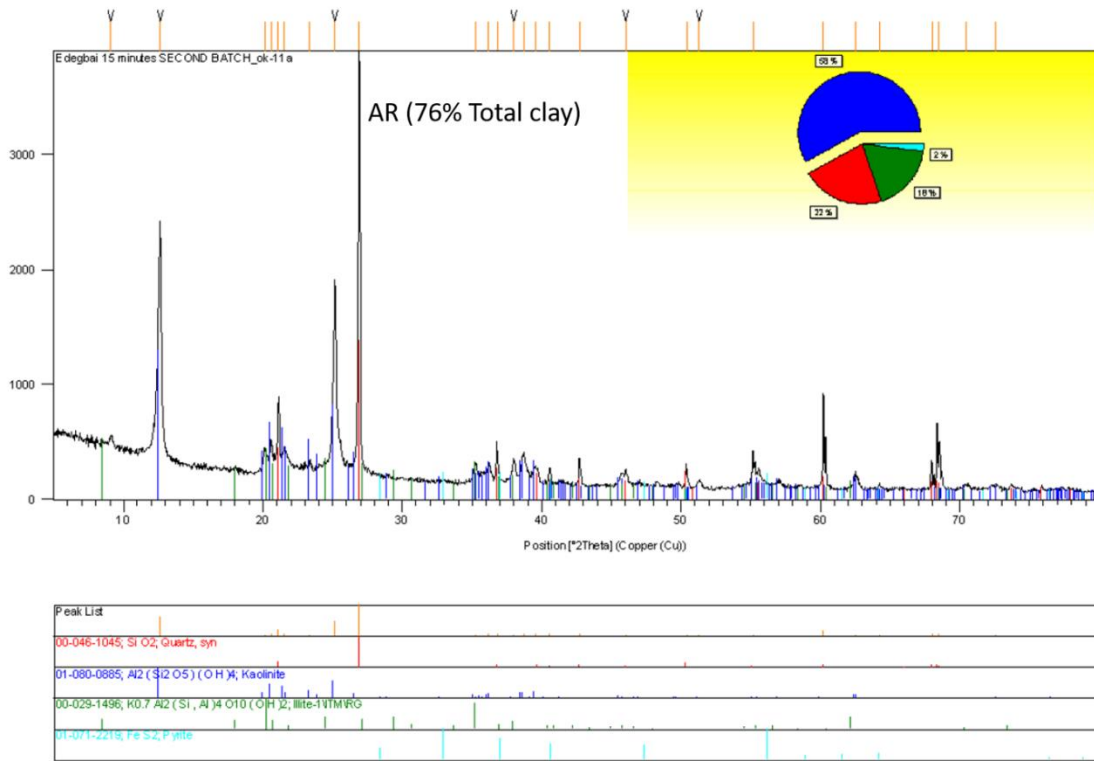
### **Acknowledgement**

The first author is grateful to the University of Benin Research and Publications Committee, the Fulbright Commission (15160892), the Niger Delta Development Commission (NDDC/DEHSS/2015PGFS/EDS/011), and the DAAD (ST32 - PKZ: 91559388) who have contributed to his educational development over the years. The help of Julius Imarhiagbe who provided great assistance during fieldwork is appreciated. The guidance and instruction provided by Drs. David Wronkiewicz, Jonathan Obrist Farner, Marek Locmelis and Eric Bohannan whilst the first author was on Fulbright fellowship at the Missouri S&T are also worthy of mention. The authors are grateful for the contributions of Drs. Kenny Ladipo and Sam Coker, which greatly improved the first draft of this paper.

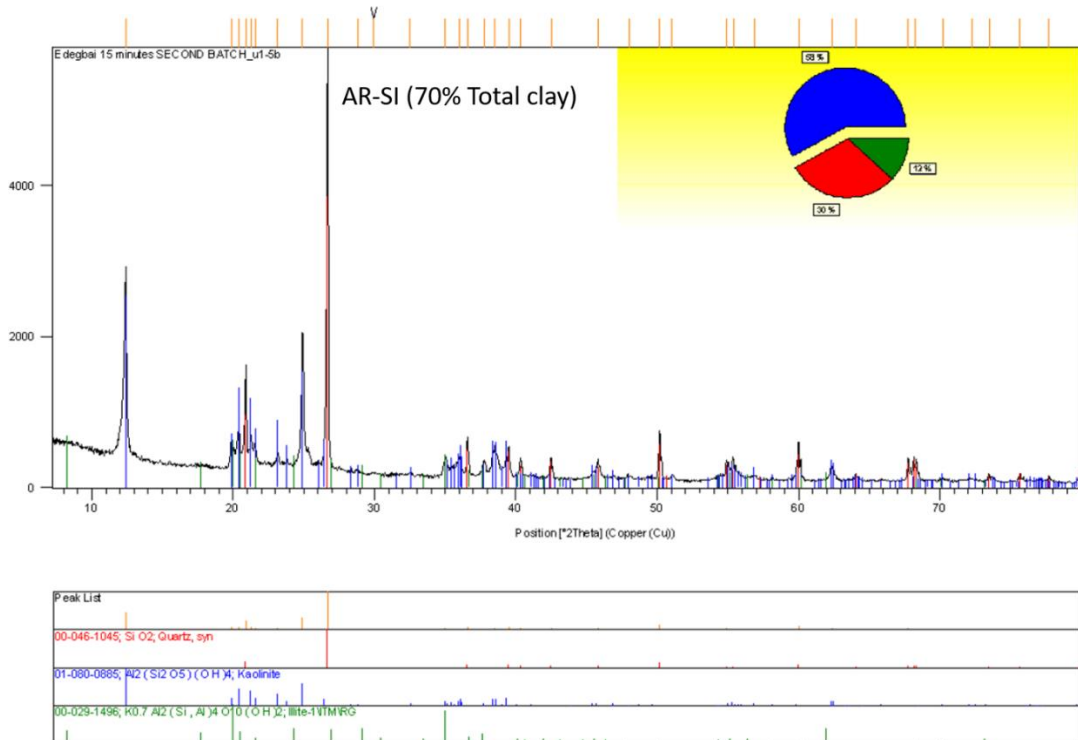


Appendix 1.1. a-d, Representative X-ray diffractograms for the identified mineralogical groups.

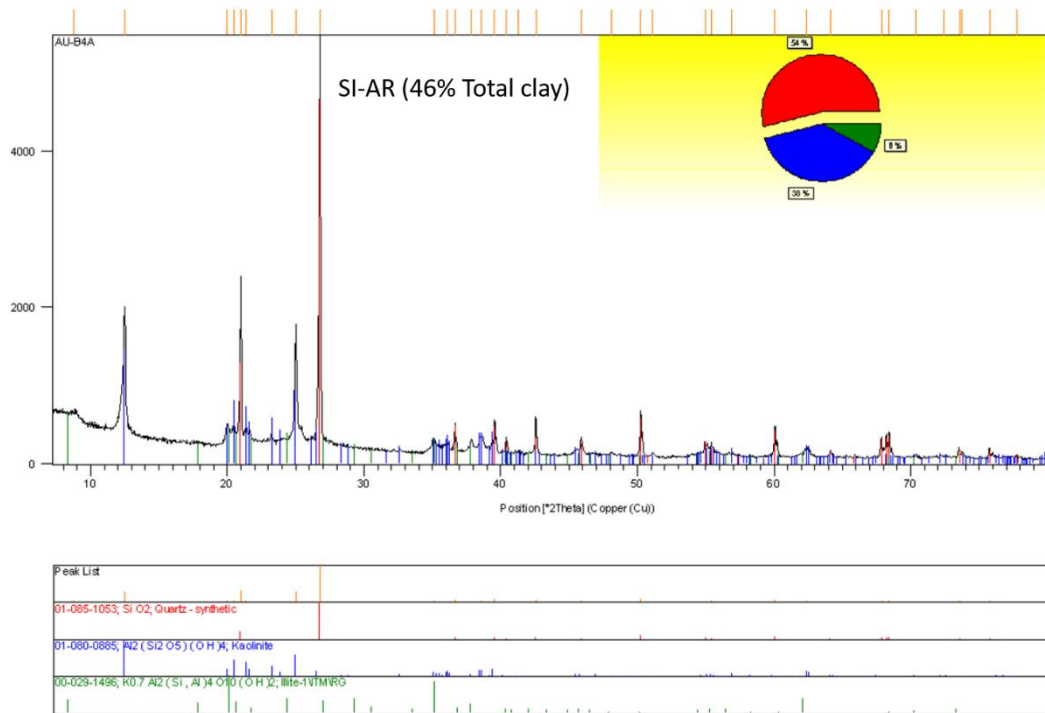
Appendix 1.1a



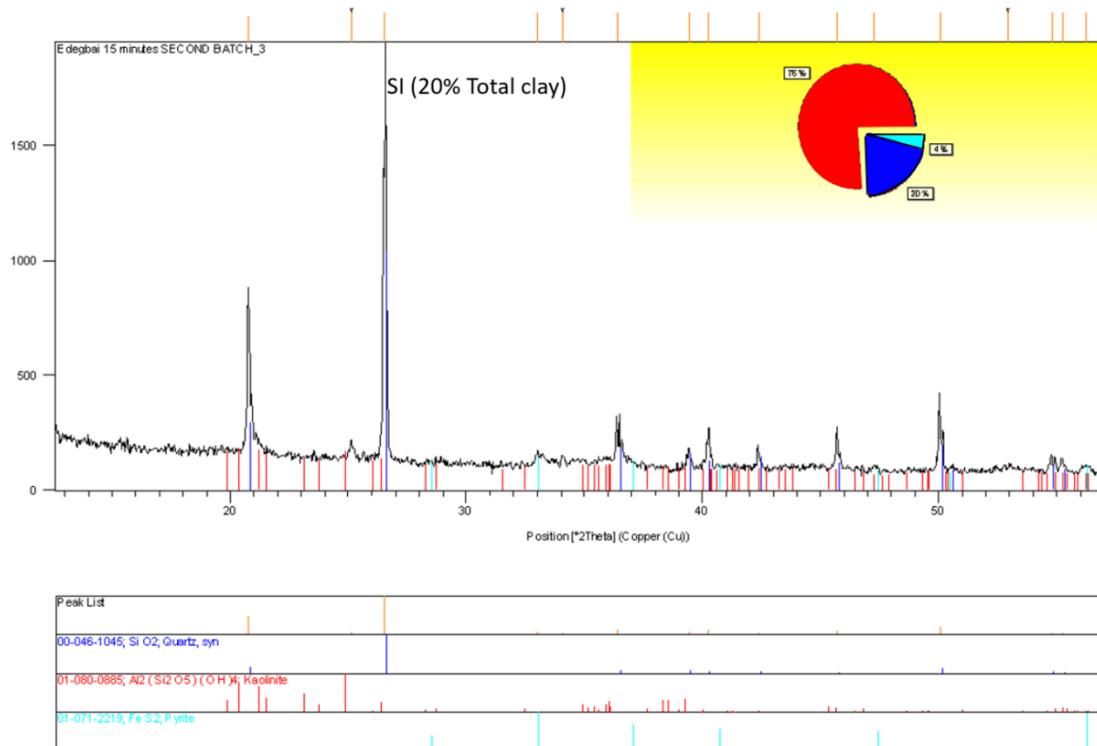
Appendix 1.1b



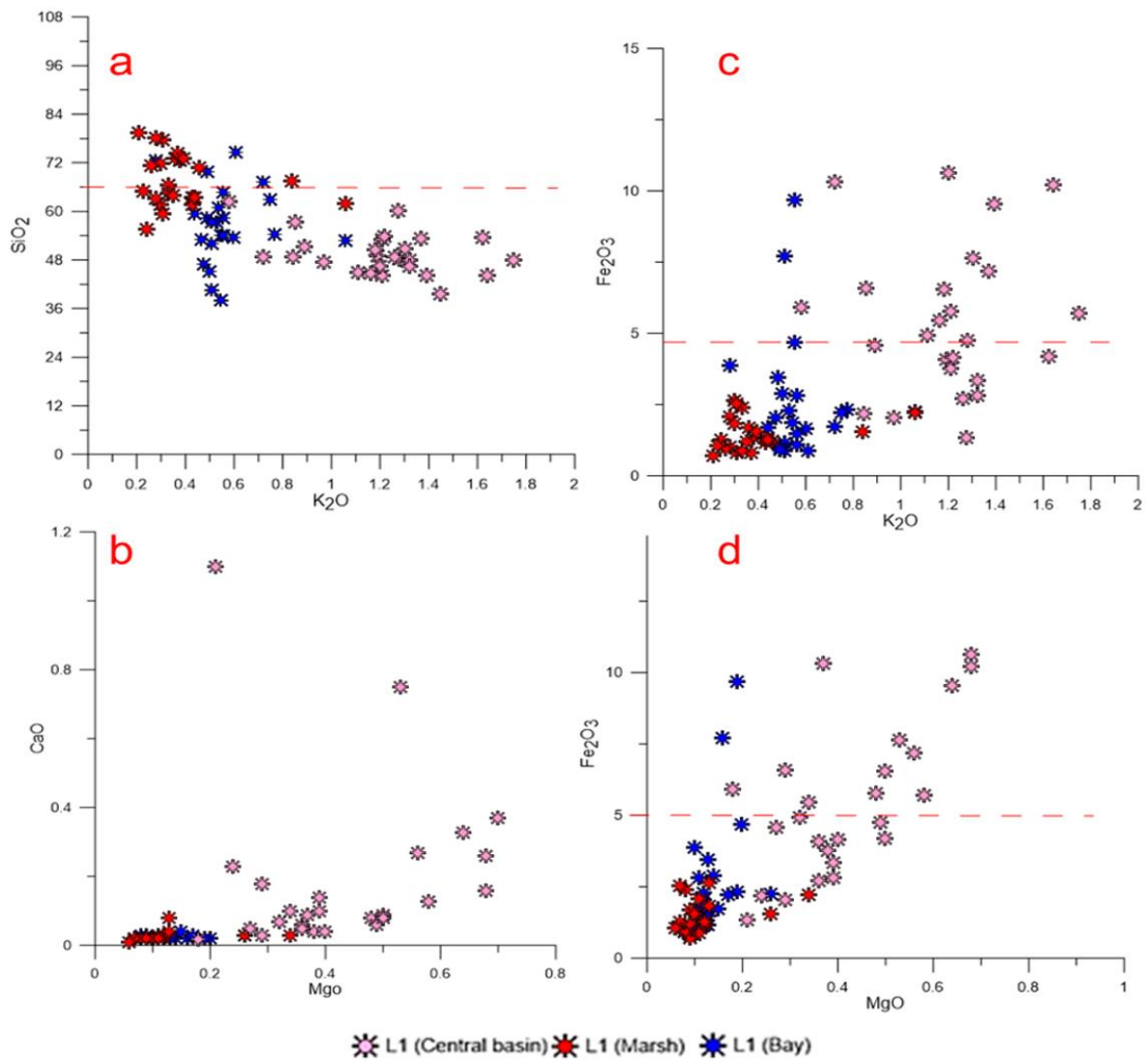
### Appendix 1.1c



### Appendix 1.1d



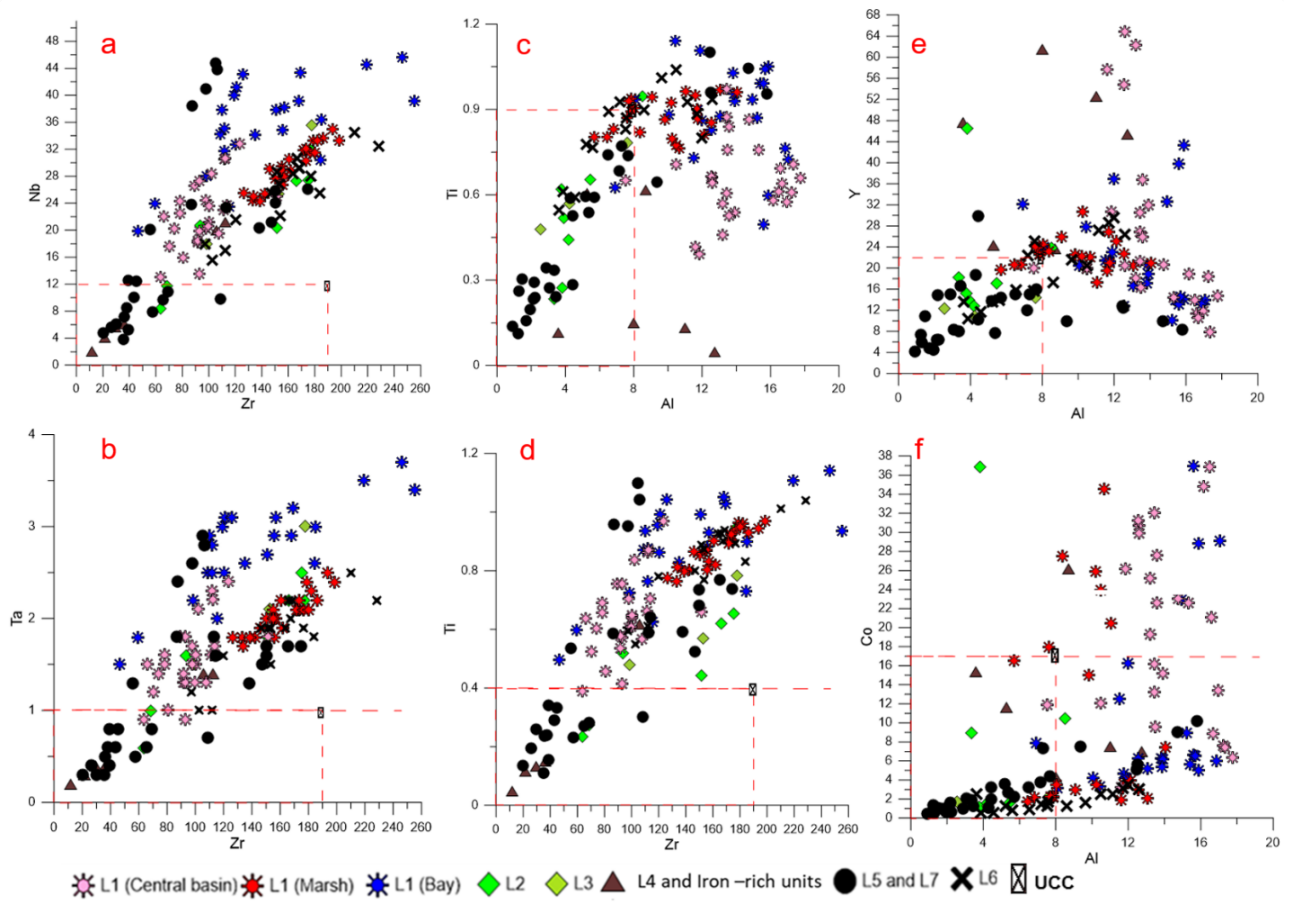
Appendix 1.2. a -d, binary plots of SiO<sub>2</sub> vs. K<sub>2</sub>O, CaO vs. MgO, Fe<sub>2</sub>O<sub>3</sub> vs. K<sub>2</sub>O, and Fe<sub>2</sub>O<sub>3</sub> vs. MgO (Cuadros et al., 2017) used to constrain paleosalinity conditions of L1a, L1b and L1c. Note the red broken line, which indicates the UCC value for the oxides.



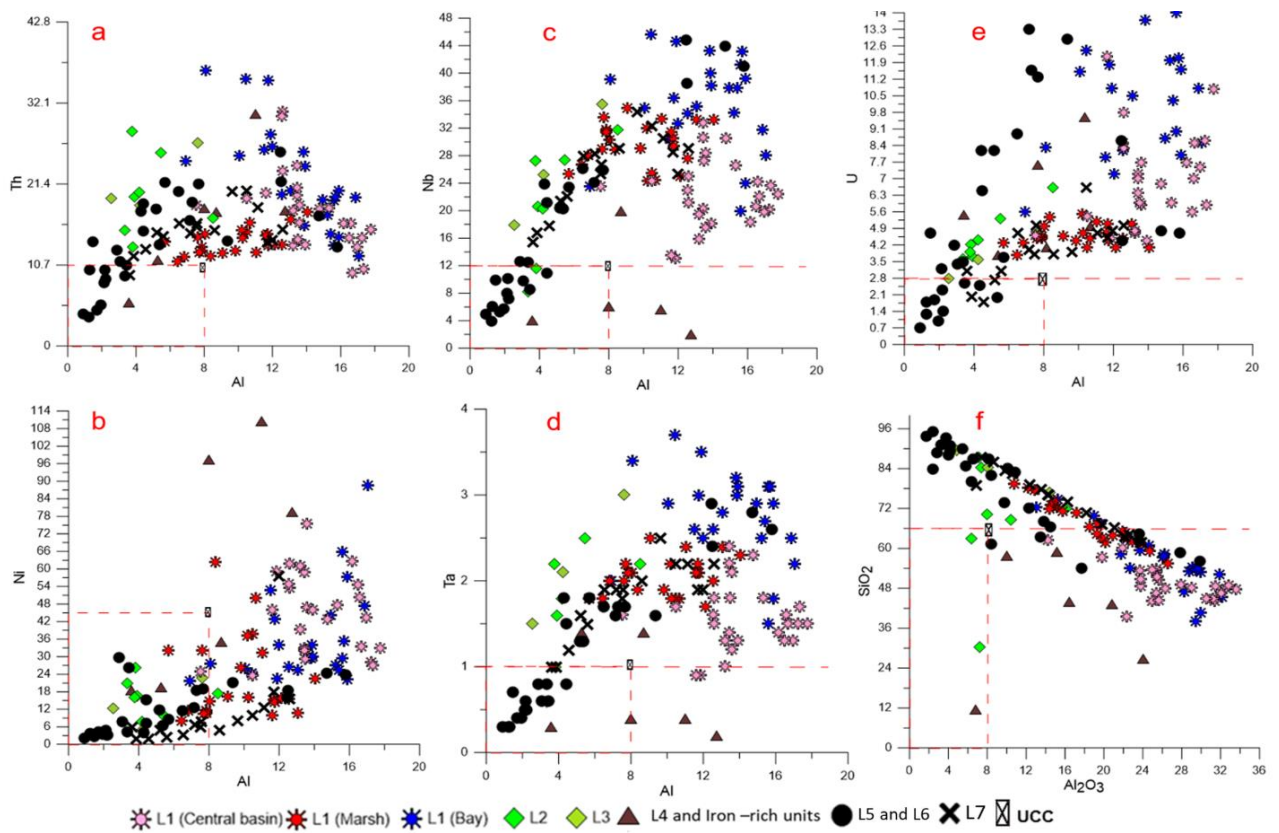
Appendix 1.3a<sub>1</sub>,a<sub>2</sub>, quartz pebble lags at the base of L5. Notice the normal grading in 3a1. b, Weak to mild bioturbation in L5 (Skolithos). c, L5 at Imiegba section showing sigmoidal cross bedding indicative of tidal influence. d, Uzebba section showing L7. e, Close-up section of L6 showing the thin mSs beds alternating with cMs-sMs laminae.



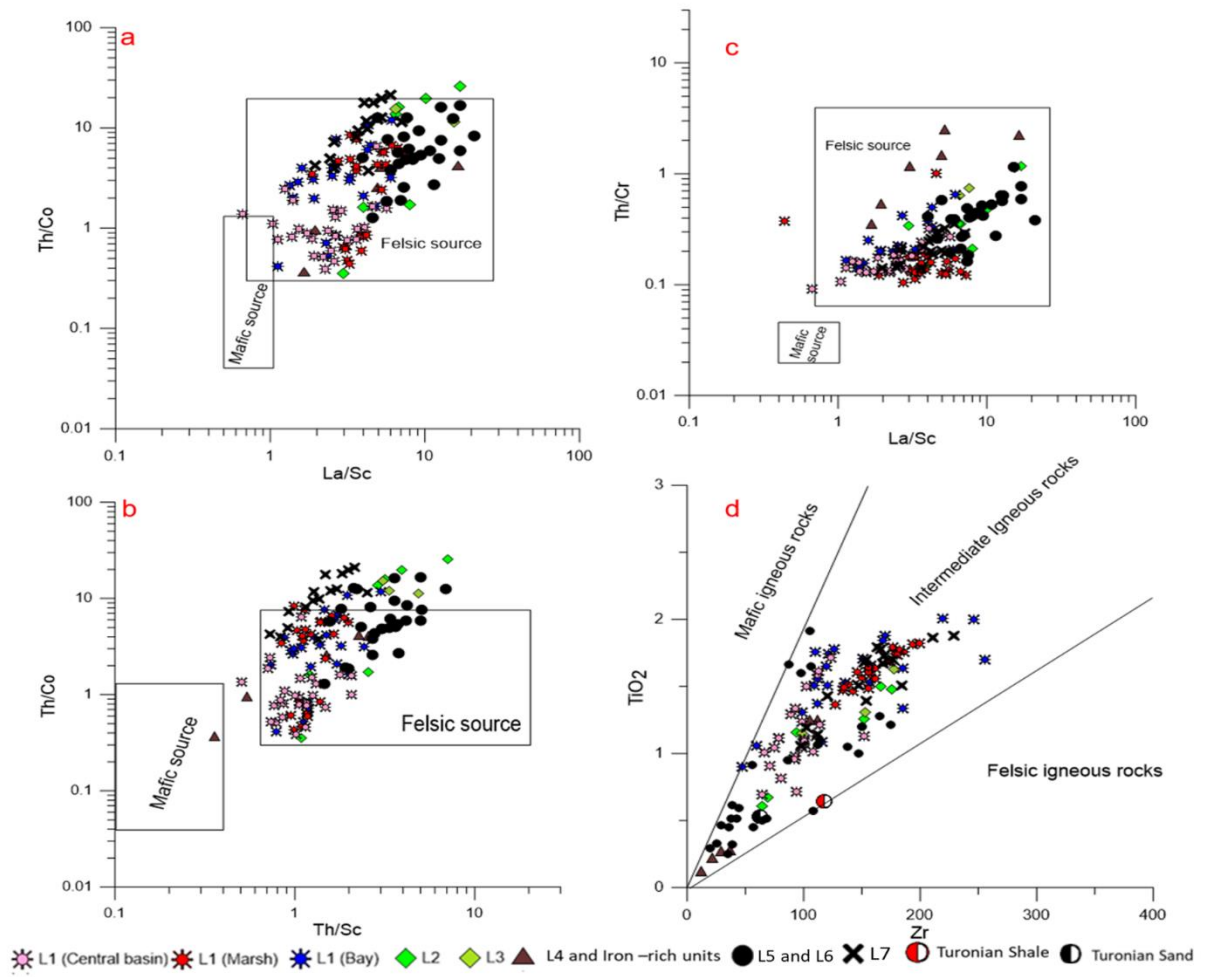
Appendix 1.4a-f, binary plots of Nb vs. Zr, Ta vs. Zr, Ti vs. Al, Ti vs. Zr, and Co vs. Al used to constrain the source and distribution of trace elements in the samples. Note the red broken line, which indicates the UCC value for the elements and oxides.



Appendix 1.5a-e, binary plots of Th vs. Al, Ni vs. Al, Nb vs. Al, Ta vs. Al, U vs. Al and SiO<sub>2</sub> vs. Al<sub>2</sub>O<sub>3</sub> used to constrain the distribution of trace elements as well as the origin of quartz in the samples. Note the red broken line, which indicates the UCC value for the elements and oxides



Appendix 1.6a-d,  $Th/Co$  vs.  $La/Sc$ ,  $Th/Co$  vs.  $Th/Sc$ ,  $Th/Cr$  vs.  $La/Sc$ , of  $TiO_2$  vs.  $Zr$  discriminant plots used to constrain the provenance of Mamu Formation.



## Chapter Three

Organic facies characterization and paleoredox conditions of the Campano-Maastrichtian dark mudstone unit, Benin flank, western Anambra Basin: implications for Maastrichtian Trans-Saharan seaway paleoceanographic conditions

Accepted for publication as:

*Edegbai, A.J., Schwark, L., Oboh-Ikuenobe, F.E., 2020. Nature of dispersed organic matter and paleoxygenation of the Campano-Maastrichtian dark mudstone unit, Benin flank, western Anambra Basin: implications for Maastrichtian Trans-Saharan seaway paleoceanographic conditions. <https://doi.org/10.1016/j.jafrearsci.2019.103654>*

### A B S T R A C T

The Campano-Maastrichtian age is an important time in the Geological evolution of Nigeria as it marked the re-establishment of the Trans-Saharan seaway that was broken due to Santonian inversion tectonics. In this paper, we conducted a high-resolution investigation of the dark mudstone unit of the Campano-Maastrichtian Mamu Formation exposed in 4-outcrops in the western segment of the Anambra basin, Nigeria, using multidisciplinary tools involving geochemistry, palynofacies, and microfabric analyses. Our objectives were to determine the nature of organic matter preserved in the sediments and the paleo-oxygenation conditions of the Trans-Saharan seaway. Our findings reveal that the Trans-Saharan seaway was of low salinity, characterized by the dominance of terrestrial organic matter in the more proximal marsh and bay sub-environments (organic facies C and CD) and mixed terrestrial – marine organic matter (organic facies BC and C) in the more distal central basin. Bottom water paleo-oxygenation was predominantly oxidic. However, palynofacies and microfabric evidences as well as inferences from Fe-TS-TOC relationship suggests pyrite formation occurred in at least



two phases. The first phase of syngenetic to early diagenetic pyrite formation, which was due to bacterial sulphate reduction that occurred in the anoxic zone below the sediment water interface, whereas secondary (late diagenetic) pyrite growth which formed the bulk of pyrite preserved occurred at the base of the bottom water. Furthermore, we hypothesize that pyrite formation occurred faster, and was better preserved in the central basin than in the other sub-environments. This is attributed to the presence of more reactive organic matter (marine palynomorphs), higher salinity (more sulphate), mineralogy (higher clay content), and microfabric (thinner lamination with low degree of bioturbation).

### **3.0 Introduction**

This study is part of a high-resolution project aimed at comparing the sediment provenance and prevalent paleoceanographic conditions for the rift (pre-Santonian) versus post rift (post-Santonian) stages in the Nigerian section of the West African Rift System (WARS). The Mamu Formation of the western Anambra Basin, which is part of the coeval Campano-Maastrichtian lithostratigraphic units of Nigeria, formed due to the Trans-Saharan seaway connection re-established between the Tethys and Atlantic oceans (Fig. 3.1). Characterization of the sedimentological, mineralogical, geochemical and preliminary palynofacies aspects of the Mamu Formation by Edegbai et al. (2019b) suggests its formation under wave-dominated estuarine conditions in a humid tropical paleoclimate. In addition, they inferred the provenance of the sediments as dominantly from reworked pre-Santonian rocks with minor contribution from Precambrian basement rocks.

Of particular interest is the dark mudstone lithofacies – the focus of this study – interpreted as brackish water deposits in central basin, marsh and bay sub-environments (Edegbai et al., 2019b). Several studies published in the last ten years on the source quality of this dark mudstone lithofacies reveal that organic matter is dominantly of Type III kerogen

(e.g., Aganbi, 2010; Ogala, 2011; Nton and Awarum, 2011; Chiaganam et al., 2013; Edegbai and Emofurieta, 2015; Ogbamikhumi and Igbinijie, 2017). However, very little data exist on the paleoredox conditions prevailing during deposition of this dark mudstone lithofacies. Based on micropaleontological evaluation in the eastern section of the Anambra Basin, Gebhardt (1998) reported dominantly oxic to dysoxic paleoredox conditions of the dark mudstone, while Adedosu et al (2010) reported oxic to suboxic paleoredox condition based on studies of biomarkers and n-alkane distribution of bitumen extracts from coal and mudstone units in the eastern section. Akinyemi et al. (2013) and Adebayo et al. (2015) used trace element geochemistry data in the western and eastern sections of the basin, respectively, to infer dominantly oxic paleoredox conditions for the dark mudstone units and suboxic to anoxic paleoredox conditions for the interbedded coal units.

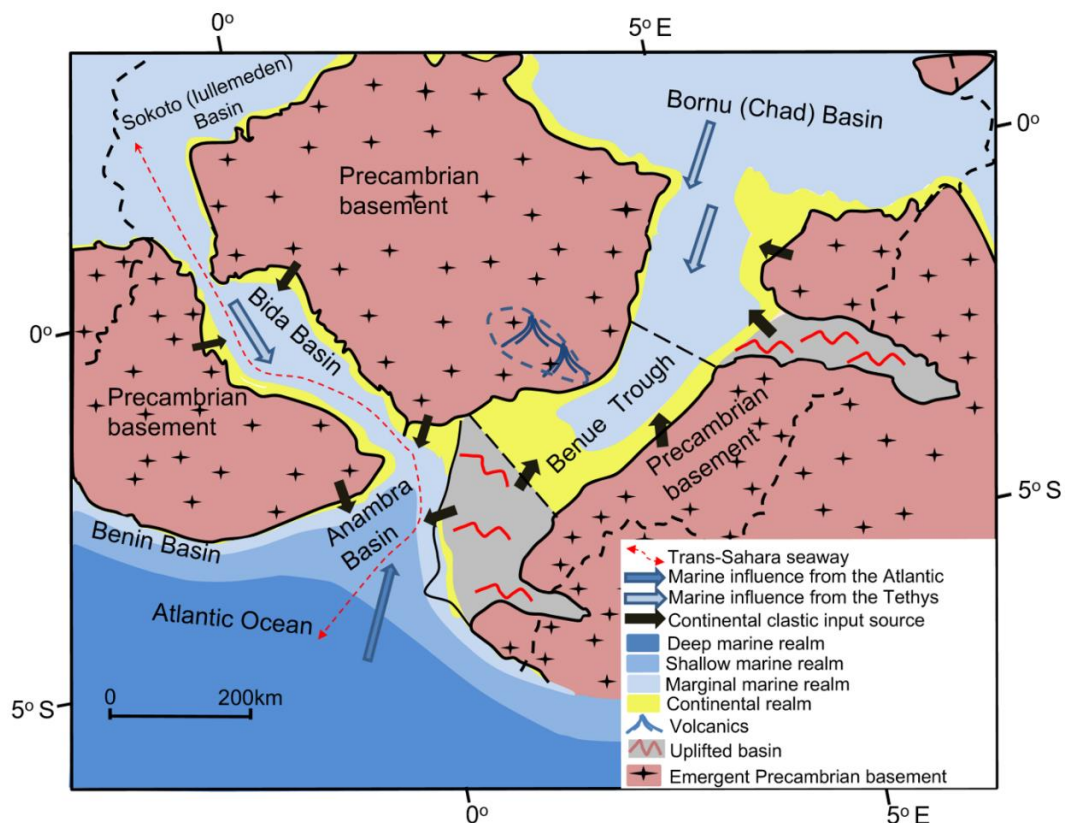


Fig. 3.1. Conceptual early Maastrichtian paleogeography of Nigeria (Edegbai et al., 2019a).

The objectives of this study are to provide a high-resolution characterization of the organic facies using multi-proxy techniques comprising bulk and isotope geochemistry and

palynofacies, and to decipher the prevailing paleoredox condition of the Mamu Formation. The data will provide insights into the nature of organic matter and bottom water paleo-oxygenation condition of the Maastrichtian Trans-Saharan seaway.

### **3.1 Geologic overview**

#### *3.1.1 Tectonics and Stratigraphy of the Anambra Basin*

The Anambra Basin (Fig. 3.2a, b) was formed during the penultimate phase of the Benue Trough evolution. Its formation was a consequence of slow subsidence induced by thermal relaxation that followed the continent-wide (largely) Santonian inversion episode, which was characterized by uplift, volcanism, folding and faulting of older rocks (Benkhelil and Robineau, 1983). This tectonism was more severe in the southern end than in the other parts of the Benue Trough (Guiraud and Bosworth, 1997). The Anambra Basin covers an area of about 55,000 km<sup>2</sup> and is flanked by the Benin hinge line (Okitipupa structure), the Southern Benue Trough and Oban Massif, and the Niger Delta Basin at its western, eastern, and southern boundaries, respectively (Fig. 3.2a). The basin has a Campanian to Danian basin fill (Fig. 3.2b) consisting of the dominantly marine sediments of the basal Nkporo Group (Nkporo, Owelli and Enugu formations) in the eastern section, whereas to the North and West of the basin alluvial to fluvial sediments of the Lokoja Formation are present (NGSA, 2006; Nwajide, 2013; Edegbaei et al., 2019a). The largely estuarine to open shelf Mamu Formation (Ladipo, 1988; Edegbaei et al., 2019b; Dim et al., 2019), shallow marine Ajali Formation (Ladipo, 1986; Umeji, 2000; Nwajide, 2013); and estuarine-deltaic Nsukka Formation (Nwajide, 2013) overlie the Nkporo Group in stratigraphic order.

Gravity measurements and well data (Agagu and Adighije, 1983; Total, 1988) suggest a thick basin fill (inclusive of pre-Santonian rocks in the Southern Benue Trough) in the eastern section (up to 8000 m) that pinch-out (to about 2000 m) at the basin margin (Fig. 3.2b).

### *3.1.2. Lithostratigraphy of the Mamu Formation in the western section*

Following the integration of data from outcrop descriptions, sedimentological, mineralogical, palynofacies and geochemical analyses, Edegbai et al. (2019b) identified seven lithofacies units and two lithofacies associations, which are summarized in Table 3.1. Detailed outcrop descriptions and high-resolution sampling were carried out on measured sections exposed as road cuts at Okpekpe, Uzebba, Imiegba and Auchi (Figs. 3.2c, 3.3a-d). Graphic logs with sample points of the measured sections are presented in Figures 3.3a-d. For a discussion of facies description and analysis of the outcrop sites, see Edegbai et al. (2019b).

## **3.2 Materials and Methods**

### *3.2.1 Kerogen analysis*

We selected 70 dark mudstone samples for kerogen analysis (seven of which were composite samples) (Fig. 3.3a-d). This entailed kerogen slide preparation and identification of the various organic matter groups, which were carried out at the palynology processing facility and digital microscope laboratory at Missouri University of Science and Technology, USA. For kerogen slide preparation, approximately 15 g of each sediment was treated with HCl and HF to digest carbonates and silicates, respectively (Traverse, 2007), followed by screening the organic residue with a 10- $\mu$ m nylon sieve. Aquamount® mountant and Depex® sealant were used for preparing permanent slides. Slides were examined under a transmitted light microscope to identify and point count a minimum of 300 organic matter particles per sample (except in barren samples), followed by normalization to 100%. A simple characterization of the organic matter components was carried out, which consists of aquatic amorphous organic matter, phytoclast (comprising woody and non-woody debris, cuticles as well as terrestrial amorphous organic matter), and palynomorph (comprising dinoflagellate cysts, acritarchs,

foraminiferal test linings, spores, pollen, and fungal remains) (APP) ternary plots (Tyson, 1995) (Figs. 3.4a - f, 3.5).

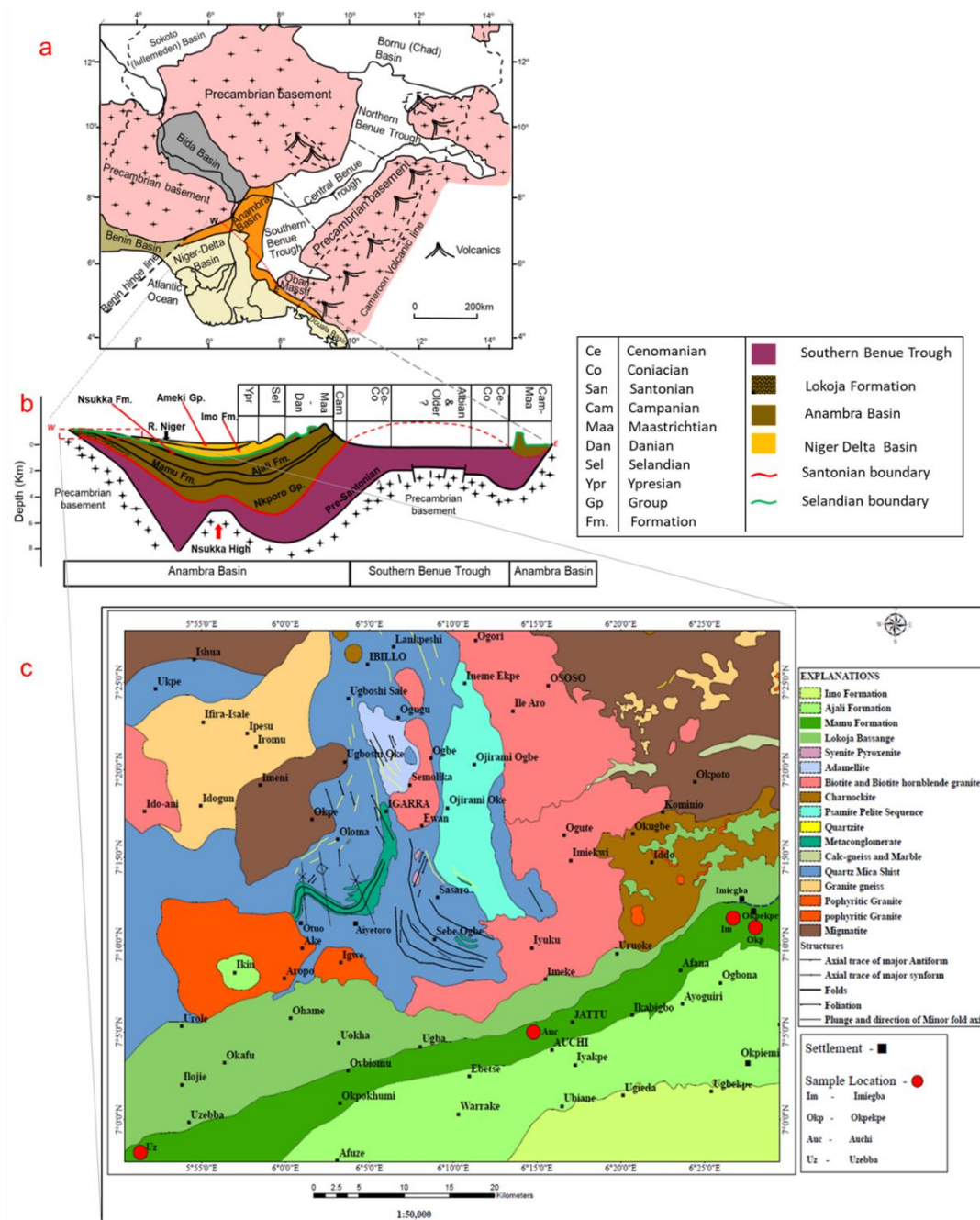


Fig. 3.2. a, Map of Nigeria showing areas underlain by basement and sedimentary rocks. b. West -East Cross section showing the basin fill of the Southern Benue Trough, Anambra and Niger-Delta basins (Modified from Total, 1988). c, Geological map of the Benin Flank (modified from NGSA, 2006).

Table 3.1: lithofacies description and analysis of the Mamu Formation in the Benin Flank (Edegbai et al., 2019b)

S/N	Lithofacies	Interpretation	Facies Association	Gross depositional environment
L1	Dark mudstone with three microfacies: planar to wavy laminated microfacies (M1), lenticular to wavy laminated microfacies (M2), wavy to curved microfacies (M3).	Marsh-bay-central basin	Marsh/bay/central basin - barrier-beach-washover	Tidal influenced wave dominated estuary (Reinson, 1992)
L2	Thin sheet-like poorly-moderately sorted, moderately cemented sMs to Ss.			
L3	Light coloured, moderately sorted, weakly cemented, weakly-mildly bioturbated, sMs to mSs.			
L4	MgO-poor, kaolinite-type oolitic ironstone. Iron oxide content ranges from 14.7 -28.4%.	Brackish water interpreted as bay deposit		
L5	Poorly sorted cross-bedded, very coarse- to medium-grained mSs to Ss. Two subfacies with L5a characterized by reworked coaly and mudstone intraclasts corresponding to a proximal setting, and L5b characterized by sigmoidal cross-bedding corresponding to more distal setting with tidal influence.	Fluvial (dominated)-tidal channel deposit		
L6	Light coloured sMs to mSs with dark mudstone and coaly intraclasts	Fluvial-tidal channel overbank/floodplain deposit (Ojo and Akande, 2009)	Fluvial-tidal channel – floodplain	
L7	Weakly bioturbated, lenticular to wavy non-parallel laminated/thinly bedded heterolithics characterized by intercalations of mMs, cMs, sMs, mSs and Ss.	Abandoned meandering fluvial-tidal channel deposit (Boyd et al., 2006)		

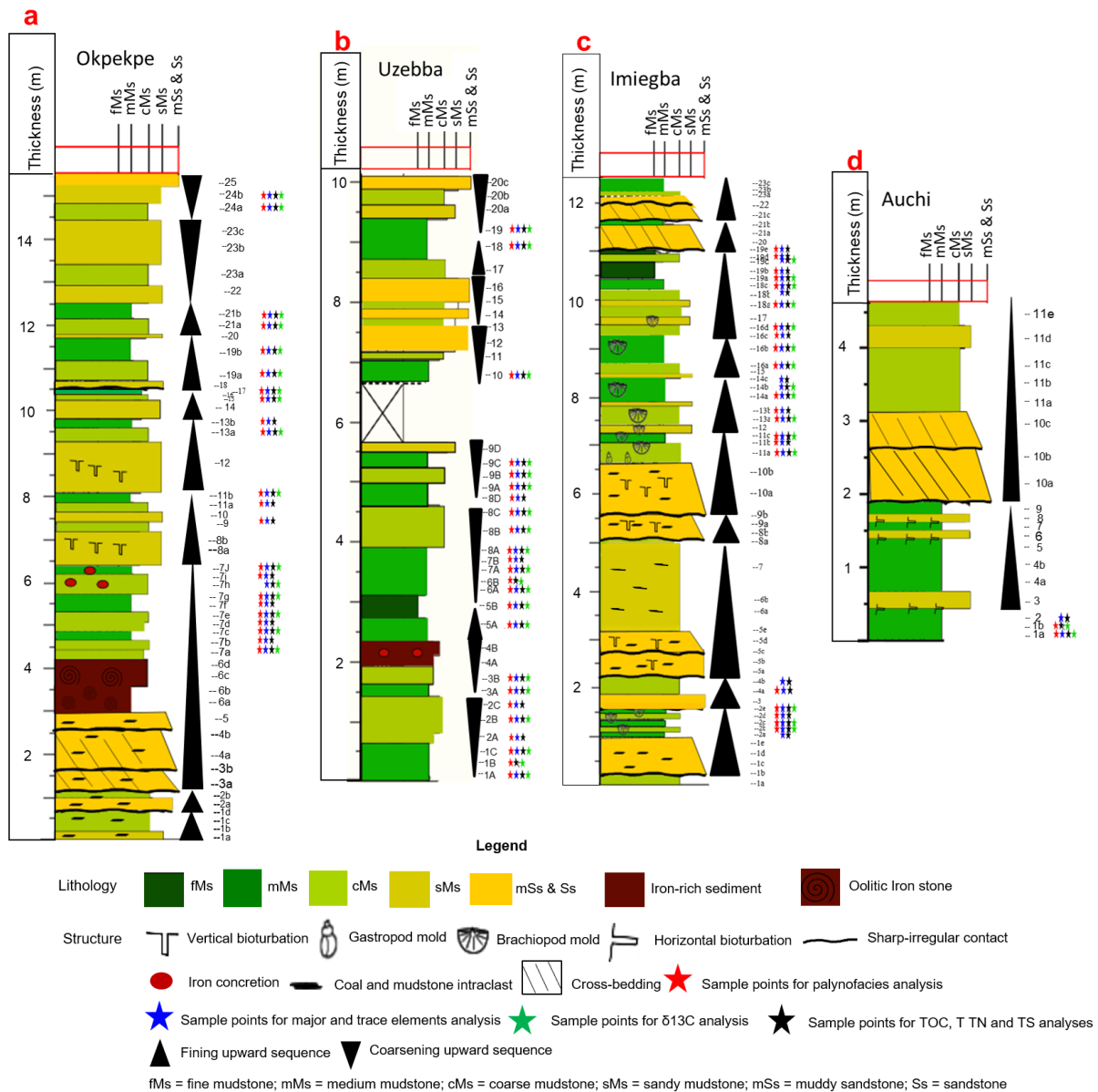


Fig. 3.3. Graphic logs of the measured sections

### 3.2.2 Geochemical analyses

#### 3.2.2.1 Major and trace element measurements

Seventy-three dark mudstone samples (Figs. 3.3a-d) were analyzed using inductively coupled plasma mass spectrometry (ICP-MS) to determine their major and trace element concentrations. Analysis was carried out at the Bureau Veritas Mineral Laboratories (AcmeLabs) in Canada. The ICP-MS measurement was carried out using a PerkinElmer ELAN

9000 ICP-MS following sample preparation that entailed multi-acid digestion ( $\text{H}_2\text{O}$ - $\text{HF}$ - $\text{HClO}_4$ - $\text{HNO}_3$  with 2:2:1:1 proportions) of 0.25 g of pulverized sample, followed by addition of  $\text{HCl}$  (50%) to the residue before heating.

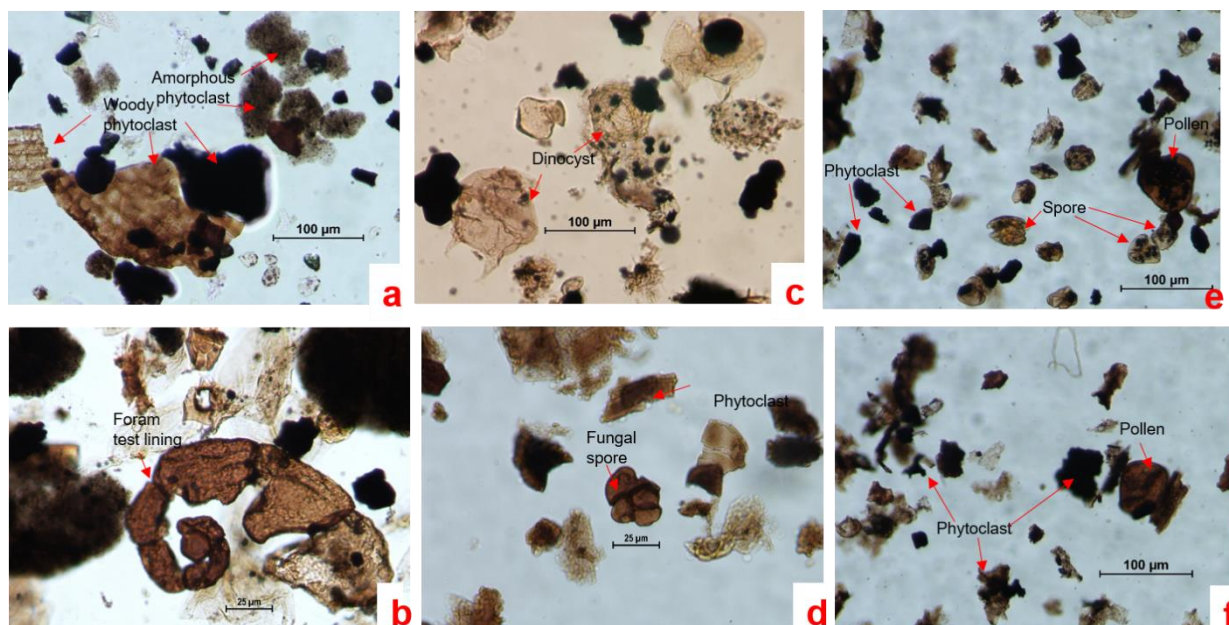


Fig 3.4. Photomicrographs showing various types of organic constituents identified (Edegbai et al., 2019b)

### 3.2.2.2 Carbon, Nitrogen, Sulphur content and stable organic carbon isotope measurements

Total carbon (TC), Total inorganic carbon (TIC), Total organic carbon (TOC), Total Sulphur (TS), and Total Nitrogen (TN) measurements were carried out on 77 samples in the Stable Isotope Mass Spectrometry Laboratory at the University of Florida (UF), USA, and the Organic Geochemistry Departmental Laboratory at Kiel University (CAU), Germany (Fig 3.3a-d). Selected samples with high, intermediate and low TOC values were measured in both laboratories to check for data consistency (see Table 3.2). Stable organic carbon isotope ( $\delta^{13}\text{C}_{\text{org}}$ ) measurements were carried out on 53 samples at UF. The analytical techniques employed by both laboratories are detailed below.



Table 3.2: Raw data used for quality checks

*x* = data from University of Florida; *y* = data from Kiel University

S/N	TN (wt. %)	TC (wt. %)	TS (wt. %)	TOC (wt. %)		S/N	TN (wt. %)	TC (wt. %)	TS (wt. %)	TOC (wt. %)
U1-5b (x)	0.07	1.27	0.04	1.27		Im-2e (x)	0.06	1.09	1.12	1.09
(y)	0.08	1.11	0.12	1.14		(y)	0.04	0.45	0.67	0.45
<i>Mean</i>	<i>0.08</i>	<i>1.19</i>	<i>0.08</i>	<i>1.21</i>		<i>Mean</i>	<i>0.05</i>	<i>0.77</i>	<i>0.90</i>	<i>0.77</i>
<i>SD</i>	<i>0.01</i>	<i>0.11</i>	<i>0.06</i>	<i>0.09</i>		<i>SD</i>	<i>0.01</i>	<i>0.45</i>	<i>0.32</i>	<i>0.45</i>
U1-6b (x)	0.07	1.04	1.27	1.04		IM 2b (x)	0.06	1.09	1.99	1.09
(y)	0.08	1.25	0.51	1.29		(y)	-	-	-	0.92
<i>Mean</i>	<i>0.08</i>	<i>1.15</i>	<i>0.89</i>	<i>1.17</i>		<i>Mean</i>				<i>1.01</i>
<i>SD</i>	<i>0.01</i>	<i>0.15</i>	<i>0.54</i>	<i>0.18</i>		<i>SD</i>				<i>0.12</i>
U1-8b (x)	0.07	1.24	1.26	1.24		OK 7e (x)	0.08	2.83	1.94	2.82
(y)	0.06	1.07	1.21	1.15		(y)	0.11	3.03	1.96	3.10
<i>Mean</i>	<i>0.07</i>	<i>1.16</i>	<i>1.24</i>	<i>1.20</i>		<i>Mean</i>	<i>0.10</i>	<i>2.93</i>	<i>1.95</i>	<i>2.96</i>
<i>SD</i>	<i>0.01</i>	<i>0.12</i>	<i>0.04</i>	<i>0.06</i>		<i>SD</i>	<i>0.02</i>	<i>0.14</i>	<i>0.01</i>	<i>0.20</i>
U1-10 (x)	0.07	2.12	0.69	2.12		OK 11b (x)	0.05	0.42	0.01	0.42
(y)	0.04	0.14	0.05	2.56		(y)	-	-	-	0.43
<i>Mean</i>	<i>0.06</i>	<i>1.13</i>	<i>0.37</i>	<i>2.34</i>		<i>Mean</i>				<i>0.43</i>
<i>SD</i>	<i>0.02</i>	<i>1.40</i>	<i>0.45</i>	<i>0.31</i>		<i>SD</i>				<i>0.01</i>
Au-1a (x)	0.06	0.76	0.01	0.76		OK 13a (x)	0.05	0.96	0.00	0.95
(y)	0.08	1.05	0.05	0.78		(y)	-	-	-	0.89
<i>Mean</i>	<i>0.07</i>	<i>0.91</i>	<i>0.03</i>	<i>0.77</i>		<i>Mean</i>				<i>0.92</i>
<i>SD</i>	<i>0.01</i>	<i>0.21</i>	<i>0.03</i>	<i>0.01</i>		<i>SD</i>				<i>0.04</i>

### 3.2.2.2.1 UF analytical techniques

The TC, TN, and TS measurements were carried out using a Carlo Erba NA1500 CNHS analyzer. The TC and TN analytical procedure entailed heating up tin capsules containing approximately 50 mg of powder sample material in a quartz column containing chromium oxide and silver cobaltous/cobaltic oxide at 1020°C. The flash combustion resulting released

effluent gases, which were streamed through reduced copper wires at 650 °C (to remove oxygen and reduce NO<sub>2</sub> to N<sub>2</sub>) and a Mg(ClO<sub>4</sub>)<sub>2</sub> trap (to remove water). The CO<sub>2</sub> and N<sub>2</sub> were subsequently separated via a 0.7-meter GC column held at 120 °C, and measured by a thermal conductivity detector. The TS analysis followed a similar procedure, except that approximately 20 mg of sample was loaded with 8-10 mg of V<sub>2</sub>O<sub>5</sub> (for melting point reduction) into tin capsules. In addition, a single reactor with Nb<sub>2</sub>O<sub>5</sub> and reduced copper wires 650 °C was utilized. A CO<sub>2</sub> coulometer (UIC 5014) coupled to an AutoMate automated carbonate preparation device was used to measure the TIC of the samples. The experiment involved loading approximately 15 mg of powder sample into sample vials, which were purged free of oxygen using CO<sub>2</sub>-free N<sub>2</sub> carrier gas before injecting with HCl. The CO<sub>2</sub> released, a measure of the amount of carbonate present, was streamed through an AgNO<sub>3</sub> scrubber, where the TIC was measured. TOC was measured indirectly by computing the difference between TC and TIC (i.e. TOC = TC – TIC).

The  $\delta^{13}\text{C}_{\text{org}}$  measurements were carried out on 53 samples using a Thermo Electron Delta V Advantage isotope ratio mass spectrometer attached to the Carlo Erba NA1500 CNHS elemental analyzer through a ConFlo II interface. The analytical procedure comprised streaming the CO<sub>2</sub> gas from the GC column to the Thermo Electron Delta V Advantage isotope ratio mass spectrometer operating in a continuous flow mode through the attached ConFlo II interface. Measurements were made in reference to UF in-house standards and were expressed relative to the Vienna Pee Dee Belemnite (VPDB).

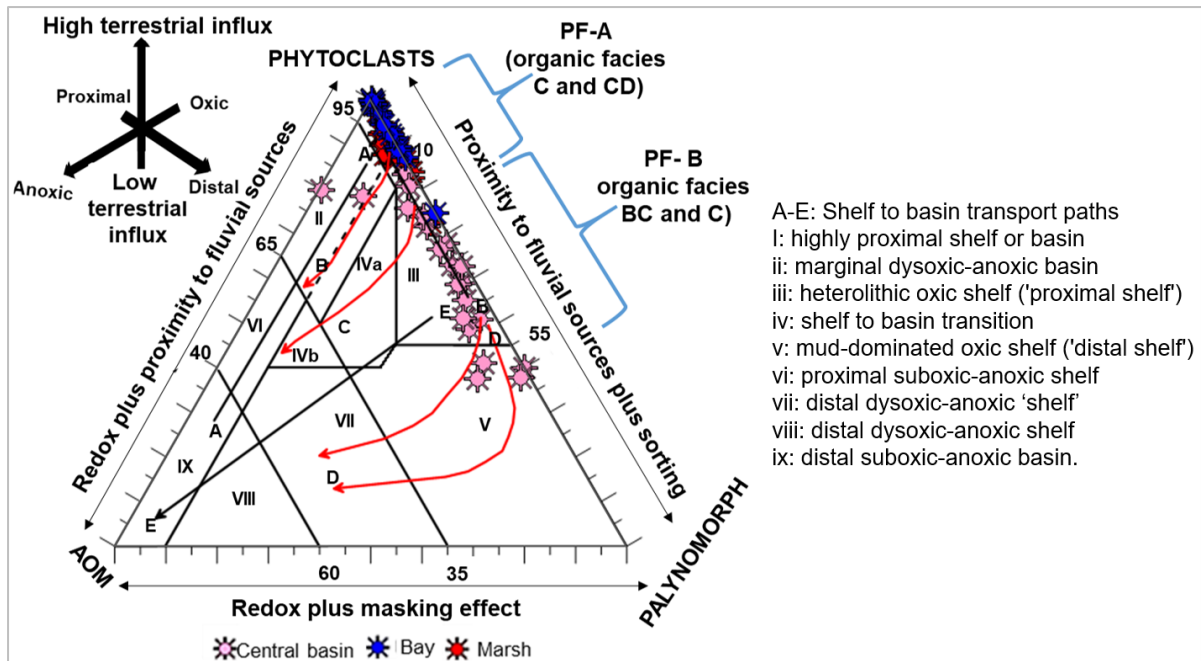


Fig. 3.5. APP plot showing different palynofacies groups (Tyson, 1995)

### 3.2.2.2.2 CAU analytical techniques

The experimental procedure for TOC measurements involved decalcifying 150-200 mg of powder samples first with 10% HCl, then with 25% HCl before drying at 50<sup>0</sup>C overnight. TOC was measured afterwards using an ELTRA CS-580A analyzer. The TC, TN and TS experimental procedure consisted of loading approximately 10 mg of powder sample and WO<sub>3</sub> into tin capsules. Thereafter, the samples were measured using an Elementar Vario EL III CNS analyzer, which followed a similar procedure as the Carlo Erba NA1500 CNHS elemental analyzer.

### 3.2.3 Microfabric analysis

Samples representative of the identified microfacies were cut into billets and sent for petrographic slide preparation at Precimat (precimat.com) in Carrollton Texas, USA. Microfabric analysis was carried out on the billets and petrographic slides using petrographic microscopes at the digital microscope laboratory at Missouri University of Science and Technology.

### 3.3 Results

A summary of the results of palynofacies and geochemical analyses is presented in Table 3.3.

#### 3.3.1. *Palynofacies analysis*

Palynofacies analysis provides a direct means of visually estimating the relative abundances of the particulate organic matter types (Tyson, 1995), which is critical in organic facies characterization. The phytoclast group (especially the structured wood debris) is the most dominant organic matter type with relative abundances varying from 37.22% to 100% (Table 3.3). The mean phytoclast percentages for the central basin, bay and marsh sub-environments are 60.86% (n = 21; SD = 14.95), 93.42% (n = 22; SD = 6.88) and 88.59% (n = 27; SD = 4.94), respectively. The mean palynomorph relative abundances for the central basin, bay and marsh sub-environments are 34.29% (n = 21; SD = 16.20), 6.27% (n = 22; SD = 6.77) and 10.13% (n = 27; SD = 4.81), respectively. Finally, the mean aquatic amorphous organic matter percentages for the central basin, bay and marsh sub-environments are 4.85 % (n = 21; SD = 4.60), 0.08% (n = 22; SD = 0.19) and 1.28% (n = 27; SD = 0.95), respectively. The phytoclast data is more variable in the central basin than in the bay and marsh sub-environments.

#### 3.3.2. *TOC, TN, and TS analyses*

The TOC values of the dark mudstone samples vary from 0.24 to 2.96%, with 11% of the dark samples having TOC >2% (Table 3.3). The mean TOC for the central basin, bay and marsh sub-environments are 1.09 %, 1.39 % and 1.13 %, respectively (n = 27, 23, and 27, respectively). The measure of scatter around the mean TOC is greatest in the bay sub-environment (SD = 0.91%), intermediate in the marsh (SD = 0.36%), and least in the central basin sub-environment (SD = 0.27%).

Table 3.3. Data from palynofacies and geochemical analyses (composite samples are indicated with thick borders)

Sample No.	Lithofacies		Palynofacies data (%)			Geochemistry data																	
			Phytoclasts	Palynomorphs	AOM	TOC	TN	TC	TS	TOC/TN	$\delta^{13}C_{org}$ (permil, vs VPDB)	Mo	MoEf	Cu	CuEf	Ni	NiEf	Fe	U	UEf	V	VEf	Al
U1 IA	L1	Marsh	92.31	5.71	1.99	1.35	0.06	1.35	0.65	22.5	-26.69	3	2.66	7.1	0.18	14.7	0.25	0.94	5	4.44	110	0.98	7.7
U1 1B			92.74	6.05	1.21	1.33	0.06	1.33	0.93	22.17	-26.79	-	-	-	-	-	-	-	-	-	-	-	-
U1 1C			91.22	7.43	1.35	1.19	0.05	1.19	0.17	23.8	-26.71	2.6	2.77	8.7	0.27	11.3	0.23	0.59	4.3	4.59	90	0.96	6.41
U1 2A			83.66	15.18	1.17	1.22	0.07	1.20	0.13	18.27	-	2.2	1.97	7.7	0.20	11.4	0.20	1.24	4.5	4.04	115	1.03	7.62
U1 2B			86.11	13.54	0.35	0.99	0.05	0.99	0.07	19.8	-26.73	0.9	0.95	4.6	0.14	8	0.16	0.79	3.8	4.0	102	1.07	6.49
U1 2C			82.49	16.50	1.01	1.17	0.06	1.16	0.21	18.90	-	2.3	2.05	4.2	0.11	10.6	0.18	0.58	4.6	4.09	113	1.0	7.69
U1 3A			88.93	10.42	0.65	1.24	0.06	1.24	0.06	20.67	-26.53	1.1	1.07	6	0.17	10.3	0.19	1.01	4.6	4.46	110	1.07	7.06
U1 3B			88.20	11.15	0.66	1.2	0.06	1.2	0.13	20	-26.51	1.9	1.60	5.8	0.14	16.3	0.26	0.91	4.6	3.87	101	0.85	8.13
U1 5A			88.49	10.20	1.32	1.78	0.08	1.79	0.05	22.25	-26.56	2.5	1.64	6.5	0.12	15.1	0.19	0.86	5.1	3.35	159	1.04	10.42
U1 5B			90.29	9.06	0.65	1.20	0.07	1.19	0.08	16.20	-26.59	2	1.23	5.1	0.09	15.3	0.18	0.97	4.5	2.76	166	1.02	11.16
U1 6A			83.62	15.87	0.48	1.09	0.06	1.09	0.13	18.17	-26.54	1.1	0.72	6.6	0.13	14.3	0.18	0.88	4.4	2.88	166	1.09	10.43
U1 6B			83.62	15.87	0.48	1.04	0.08	1.14	0.89	13.59	-26.46	-	-	-	-	-	-	-	-	-	-	-	-
U1 7A			87.83	9.54	2.63	1.12	0.06	1.12	-	18.67	-26.32	2.1	1.54	27.4	0.58	50	0.70	1.75	4.5	3.31	148	1.09	9.31
U1 7B			87.83	9.54	2.63	1.03	0.06	0.99	0.89	18.29	-	1	0.76	11.3	0.25	26.2	0.38	0.65	4.4	3.33	145	1.10	9.03
U1 8A			92.05	5.96	1.99	1.16	0.06	1.16	2.51	19.33	-26.49	0.8	0.58	15.6	0.32	37.5	0.52	1.4	4.1	2.95	149	1.07	9.5
U1 8B			90.61	8.74	0.65	1.20	0.06	1.16	1.23	19.05	-26.67	1.4	1.35	10.6	0.30	31.9	0.59	1.31	4.5	4.35	128	1.24	7.07
U1 8C			90.61	8.74	0.65	0.97	0.05	0.97	0.63	19.4	-26.57	3.8	4.66	6.8	0.24	31.9	0.75	0.51	4.3	5.27	103	1.26	5.58
U1 8D			89.91	8.83	1.26	1.07	0.06	1.04	0.88	17.68	-	0.7	0.63	6.8	0.18	62.2	1.07	0.66	5.4	4.84	172	1.54	7.63
U1 9A			89.91	8.83	1.26	1.2	0.06	1.2	0.64	20	-26.55	-	-	-	-	-	-	-	-	-	-	-	-
U1 9B			86.58	11.82	1.60	1.09	0.06	1.09	0.83	18.17	-26.52	2.5	1.68	16.3	0.32	37	0.48	1.69	5.5	3.70	157	1.06	10.16
U1 9C			90.23	7.82	1.95	0.8	0.06	0.8	0.88	13.33	-26.39	1.3	0.86	14.2	0.27	31.2	0.40	0.84	5.2	3.46	151	1.0	10.28
U1 10			72.36	25.47	2.17	2.55	0.04	2.55	0.72	64.58	-26.08	2	1.04	14	0.21	22.4	0.22	0.88	4.1	2.13	184	0.95	13.19
U1 18			89.61	7.47	2.92	0.98	0.05	0.98	0.04	19.6	-25.89	1.5	0.85	31.4	0.51	10.6	0.11	1.69	5.1	2.88	154	0.87	12.1
U1 19			87.54	8.85	3.61	1.23	0.06	1.23	0.03	20.5	-26.05	1.1	0.72	33.1	0.63	9.9	0.12	0.7	4.7	3.08	137	0.90	10.42
AU-1a			89.12	10.88	0.0	0.77	0.07	0.91	0.03	11.34	-25.94	1.9	1.39	36.2	0.77	15.9	0.22	1.07	4.7	3.45	113	0.83	9.32
AU-1b			97.37	2.63	0.0	0.54	0.04	0.54	0.06	14.98	-25.65	-	-	-	-	-	-	-	-	-	-	-	-
AU-2			98.70	1.30	0.0	0.34	0.03	0.34	0.03	12.27	-	1	0.62	23.1	0.41	15.6	0.18	1.49	4.1	2.54	127	0.79	11.04
IM 2B	L1	Central Basin	58.61	38.74	2.65	1.01	0.06	1.09	1.99	16.76	-25.97	1.8	0.96	25.9	0.40	42.7	0.43	2.68	6.8	1.57	159	0.85	12.86
1M 2C			62.87	34.53	2.61	0.93	0.06	0.93	1.34	15.5	-25.82	1.5	0.83	19.6	0.31	32.9	0.35	2.55	7.2	1.72	161	0.89	12.41
1M 2D			54.85	41.21	3.94	1.02	-	-	-	-	-	0.6	0.36	28.7	0.49	32.1	0.37	2.7	7	1.81	150	0.89	11.49

1M 2E			71.33	25.33	3.33	1.09	0.05	0.77	0.89	21.34	-25.62	1.3	0.75	22.7	0.38	46.7	0.51	4.29	5.9	1.47	151	0.87	11.87	
IM 4A			83.17	15.18	1.65	1.51	0.03	1.51	3.39	43.95	-	1	0.69	14.7	0.29	23.5	0.31	4.23	5.4	1.62	123	0.85	9.9	
IM 11A			67.65	31.05	1.31	1.17	0.06	1.18	3.42	19.5	-26.17	1	0.54	30.5	0.48	53.5	0.55	6.92	9.8	2.30	139	0.75	12.61	
IM 11B			50.50	46.18	3.32	1.40	0.07	1.40	2.97	19.39	-	1	0.43	32.1	0.40	50.3	0.42	3.95	7	1.31	144	0.62	15.81	
IM 11C			73.63	23.47	2.89	0.94	0.06	0.95	1.62	15.67	-25.50	0.6	0.35	28.1	0.47	54.7	0.60	4.73	8.5	2.13	203	1.17	11.85	
IM 13A			75.49	19.61	4.90	1.21	0.07	1.22	1.6	17.29	-25.74	1.2	0.64	31.1	0.48	58.8	0.60	7.08	6.4	1.47	133	0.71	12.86	
1M 13B			80.39	17.32	2.29	1.28	0.08	1.26	1.52	16.08	-	1.1	0.53	35.1	0.49	47.7	0.44	3.27	6	1.25	146	0.70	14.18	
IM 14A			58.50	37.91	3.59	1.22	0.06	1.23	1.82	20.33	-25.37	2	1.18	32.2	0.55	61.9	0.70	4.99	8.3	2.13	131	0.77	11.56	
IM 16A			39.76	60.24	0.0	1.18	0.04	1.18	3.07	29.12	-26.01	2.2	1.30	28.9	0.49	59.1	0.67	12.52	4.5	1.16	104	0.62	11.54	
IM 16B			48.46	45.06	6.48	1.51	0.09	1.54	2.03	16.78	-25.60	1.7	0.96	24.3	0.40	60.9	0.66	6.54	4.7	1.15	103	0.58	12.08	
1M 16C			40.69	51.74	7.57	1.34	0.10	1.32	2.33	13.18	-	1.5	0.82	19.2	0.30	46.1	0.48	3.78	4.4	1.04	118	0.64	12.58	
1M 16D			37.22	52.37	10.41	1.1	0.07	1.11	1.1	15.71	-25.75	0.5	0.29	17.9	0.30	39.2	0.44	2.82	4.8	1.21	115	0.67	11.73	
IM 18a			79.55	0.65	19.81	0.32	0.03	0.33	0.27	10.67	-23.85	1.1	0.82	9.75	0.21	45.9	0.65	0.85	12.15	3.92	68.5	0.51	9.18	
IM 18C			66.34	30.39	3.27	0.61	0.04	0.62	0.01	15.25	-26.14	1.5	0.64	24.2	0.30	32.9	0.27	1.34	10.8	2.00	94	0.40	16	
IM 19A			62.46	36.57	0.97	0.83	0.06	0.84	0.13	13.83	-25.84	2	0.90	36.5	0.47	28.2	0.24	1.85	8.6	1.68	111	0.50	15.19	
IM 19B			37.46	60.59	1.95	0.8	0.05	0.81	0	16	-26.48	1	0.44	43.1	0.55	43.2	0.36	2.34	7.5	1.42	109	0.48	15.62	
IM 19D			50.83	42.57	6.60	1.03	0.07	1.03	1.42	14.89	-	1	0.47	209.1	2.84	54.5	0.49	3.19	5.6	1.14	102	0.48	14.52	
IM 19E			78.25	9.42	12.34	1.15	0.06	1.18	0.94	17.99	-	1.9	0.82	19.3	0.24	26.9	0.22	1.81	5.9	1.11	128	0.55	15.79	
IM 2A			-	-	-	1.10	0.05	1.06	2.64	21.06	-	1.7	0.98	11.3	0.19	29.2	0.32	3.04	6	1.50	131	0.75	11.87	
IM 4B			-	-	-	0.83	0.04	0.91	4.12	18.79	-	1.4	1.32	22.8	0.62	24.9	0.45	4.27	4.6	1.89	99	0.94	7.23	
IM 14B			-	-	-	1.14	0.07	1.15	2.41	16.29	-26.41	-	-	-	-	-	-	-	-	-	-	-	-	-
IM 14C			-	-	-	1.25	0.08	1.20	3.39	16.59	-	3.3	1.79	44	0.69	75.4	0.78	6.09	7.7	1.81	110	0.60	12.61	
IM 18B			-	-	-	1.10	0.06	1.10	0.50	18.87	-	2.2	1.36	111.1	1.99	33.3	0.39	1.35	8.5	2.28	91	0.56	11.04	
IM 19C			-	-	-	1.40	0.07	1.38	2.42	18.82	-	1.3	0.60	147.4	1.95	62.6	0.55	3.81	7.7	1.53	98	0.45	14.92	
OK 7A	L1	Bay	90.72	9.28	0.0	2.52	0.09	2.52	1.56	28.0	-27.59	3.2	2.0	18.30	0.33	33.80	0.40	3.30	7.20	4.50	95.0	0.59	10.93	
OK 7B			90.72	9.28	0.0	0.95	0.06	0.99	0.83	16.58	-	6.4	6.54	13.0	0.38	21.60	0.42	2.77	5.60	5.72	69.0	0.71	6.69	
OK 7C			90.86	6.58	0.0	2.35	0.09	2.36	4.43	26.11	-27.87	7.9	3.80	40.70	0.57	65.70	0.60	6.23	9.0	4.33	114.0	0.55	14.21	
OK 7D			90.86	6.58	0.0	2.86	0.12	2.83	4.39	24.02	-	2.9	1.36	38.80	0.52	57.10	0.51	4.96	11.60	5.42	93.0	0.43	14.63	
OK 7E			71.38	28.44	0.19	2.96	0.10	2.93	1.95	30.90	-27.14	2.5	1.26	25.70	0.37	43.90	0.42	2.36	8.70	4.37	101.0	0.51	13.62	
OK 7F			85.11	14.89	0.0	2.19	0.09	2.17	1.17	25.26	-	1.5	0.72	26.70	0.37	88.40	0.81	1.93	8.50	4.09	98.0	0.47	14.20	
OK 7G			88.34	11.66	0.0	2.48	0.09	2.49	1.63	27.56	-26.77	1.8	1.22	18.0	0.35	52.50	0.68	1.84	7.90	5.35	105.0	0.71	10.10	
OK 7H			-	-	-	2.59	0.09	2.60	0.01	28.78	-26.35	2.6	1.69	15.70	0.30	26.40	0.33	1.20	8.20	5.34	67.0	0.44	10.50	
OK 7I			88.40	11.11	0.49	1.78	0.07	1.75	0.06	24.51	-	2.8	1.42	30.0	0.44	26.90	0.26	1.38	12.0	6.09	83.0	0.42	13.47	
OK 7J			88.40	11.11	0.49	1.82	0.07	1.83	0.0	26.0	-25.92	4.3	2.45	29.90	0.49	29.40	0.32	1.59	13.70	7.81	104.0	0.59	11.99	
OK 9			96.79	3.21	0.0	0.24	0.05	0.47	0.10	4.76	-	1	0.48	19.10	0.26	47.20	0.43	0.79	10.80	5.16	88.0	0.42	14.32	
OK 11A			99.39	0.61	0.0	0.70	0.07	0.72	0.07	9.72	-	3.3	1.67	17.80	0.26	25.30	0.25	1.73	10.30	5.22	103.0	0.52	13.49	
OK 11B			99.77	0.23	0.0	0.42	0.05	0.42	0.01	8.50	-24.73	2.1	1.08	13.80	0.20	22.20	0.22	1.55	8.0	4.11	110.0	0.57	13.31	
OK 13A			98.86	1.14	0.0	0.92	0.05	0.91	0.04	17.32	-25.57	3.5	2.07	27.10	0.46	25.40	0.29	1.25	10.50	6.22	86.0	0.51	11.54	
OK 13B			98.66	1.34	0.0	1.30	0.08	1.36	0.06	15.85	-	1.8	0.95	29.90	0.45	29.20	0.29	1.11	14.0	7.37	96.0	0.51	12.99	
OK 15			98.79	1.21	0.0	0.38	0.03	0.38	0.03	12.67	-25.47	1.5	1.37	13.70	0.36	27.30	0.48	0.63	8.30	7.59	54.0	0.49	7.48	
OK 17			91.56	8.44	0.0	1.04	0.06	1.04	0.01	17.33	-25.51	1.8	1.20	36.70	0.71	42.70	0.55	0.72	11.80	7.89	61.0	0.41	10.23	

OK 19A			99.36	0.64	0.0	1.16	0.06	1.17	0.00	19.33	-25.65	1.1	0.63	59.30	0.97	29.80	0.32	0.64	19.50	11.08	76.0	0.43	12.03
OK 19B			100.0	0.0	0.0	0.68	0.05	0.69	0.01	13.60	-25.17	1.9	0.95	32.70	0.47	35.30	0.34	1.05	12.10	6.06	88.0	0.44	13.66
OK 21A			93.79	6.21	0.0	0.27	0.03	0.28	0.03	9.0	-24.95	1	0.71	20.30	0.42	24.10	0.33	1.19	12.40	8.80	94.0	0.67	9.64
OK 21B			100.0	0.0	0.0	0.40	0.04	0.41	0.01	10.0	-25.01	1.7	1.09	17.80	0.33	22.30	0.27	1.60	10.80	6.92	97.0	0.62	10.67
OK 24A			94.12	5.29	0.59	1.37	0.06	1.37	0.0	22.83	-26.26	1.5	0.81	63.60	0.99	33.90	0.35	0.63	31.20	16.84	76.0	0.41	12.67
OK 24B			99.35	0.65	0.0	0.59	0.03	0.59	0.05	19.67	-25.48	1.9	1.45	26.40	0.58	25.90	0.38	0.65	11.50	8.78	73.0	0.56	8.96
WSA			-	-	-	-	-	-	-	-	-	1.3	-	45	-	68	-	4.83	3	-	130	-	8.89

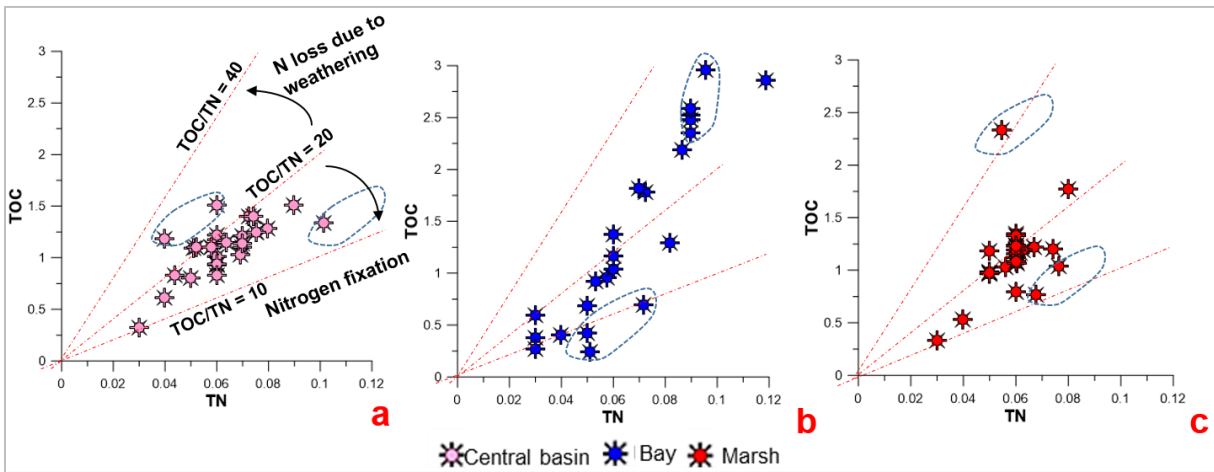


Fig. 3.6. TOC vs. TN binary plots for the central basin (a), bay (b) and marsh mudstones (c)

The TN values are very low, ranging from 0.03 (at low TOC) to 0.1% (Table 3.3). The mean TN for the central basin, bay and marsh sub-environments are 0.06% (n = 26; SD = 0.02), 0.07% (n = 23; SD = 0.02) and 0.06% (n = 27; SD=0.01), respectively. The Mean TOC/TN ratios vary from 17.92 and 19.06, respectively in the central basin and bay sub-environments to 19.22 in the marsh sub-environment (Table 3.3). The variability around mean TOC/TN values is greatest in the bay and marsh sub-environments (SD = 7.60, and 5.75, respectively) and lowest in the central basin sub-environment (SD = 3.93).

Thirty-six percent of the dark mudstone samples reported TS > 1% (Table 3.3). Of this number, 70% of the samples are from central basin sub-environment. The highest TS values (> 4%) are recorded in samples Ok-7c, Ok-7d and Im-4b. TS varies from 0.00 % to 4.39%. The mean TS for the central basin, bay and marsh sub-environments are 1.82% (n = 26), 0.72% (n = 23) and 0.48 % (n = 27), respectively. TS data is more variable in comparison to the TOC values of given mudstone samples. The measure of scatter around the mean TS is greatest in the bay and central basin sub-environments (SD = 1.32 and 1.16, respectively) and least in the marsh sub-environment (SD = 0.56).



### 3.3.3. Stable carbon isotope geochemistry

The  $\delta^{13}\text{C}_{\text{org}}$  values of our samples vary in the range of  $-23.85$  ‰ (central basin mudstone) to  $-27.87$  ‰ (bay mudstone) (Table 3.3). Mean  $\delta^{13}\text{C}_{\text{org}}$  are  $-25.75$  ‰ ( $n = 15$ ,  $\text{SD} = 0.61$ ),  $-25.97$  ‰ ( $n = 16$ ,  $\text{SD} = 0.95$ ) and  $-26.42$  ‰ ( $n = 22$ ,  $\text{SD} = 0.31$ ) for the central basin, bay and marsh mudstones, respectively.

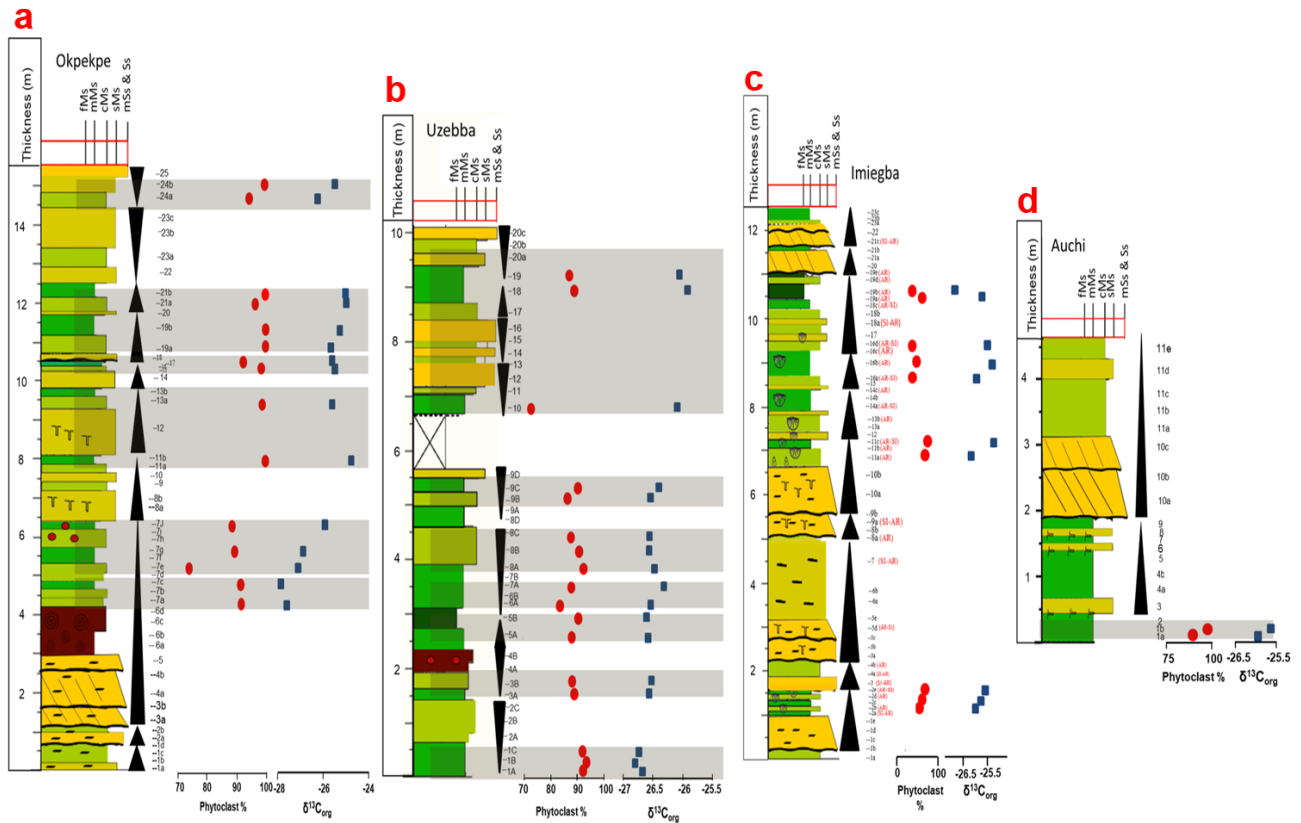


Fig. 7a-d. Graphic logs showing the relationship between phytoclast % and  $\delta^{13}\text{C}_{\text{org}}$  in samples from same bed. Note the heavier  $\delta^{13}\text{C}_{\text{org}}$  values corresponding with high phytoclast abundance.

### 3.3.4. Major and trace element geochemistry

All the samples have U contents greater than the “world shale average” (WSA) (Wedepohl, 1971, 1991; WSA: U= 3 ppm), whereas 97.26%, 93.15%, 89%, 68.49%, 30.14%, and 16.44% of the dark mudstone samples, respectively have Ni, Cu, Fe, V, Mo and Al contents less than the WSA (WSA = 68 ppm; 45 ppm, 4.83%, 130 ppm, 1.3 ppm, and 8.84% for Ni, Cu, Fe, V, Mo, and Al,

respectively) (Table 3.3). The mean contents of U, Ni, Cu, Fe, V, Mo and Al of the central basin (n =26), bay (n = 23) and marsh sub-environments (n = 23) are respectively U: 6.99 ppm, 11.46 ppm, and 4.61 ppm; Ni: 44.89 ppm, 36.36 ppm, and 22.16 ppm; Cu: 41.14 ppm, 27.61 ppm, and 13.44 ppm; Fe: 3.96%, 1.79% and 1.02%; V: 123.90 ppm, 88.30 ppm, and 134.78 ppm; Mo: 1.44 ppm, 2.61 ppm, and 1.77 ppm; and Al: 14.08%, 13.40% and 9.79%. Enrichment factors of the aforementioned trace elements were computed using  $EF_{\text{element X}} = X/AI_{\text{sample}} / X/AI_{\text{WSA}}$ .

### **3.4 Discussion**

#### *3.4.1 Organic matter characterization*

Palynofacies characterization based on the relative abundances of aquatic amorphous organic matter, phytoclasts and palynomorphs (APP) (Fig. 3.5) reveal two palynofacies groups – PF-A and PF-B. PF-A is characterized by high percentages of phytoclasts, which predominate over the other organic matter groups. This is compatible with the organic facies C and CD (Jones *in* Tyson, 1995), which is typical of areas proximal to fluvial sources with high phytoclast dilution and shallow water depth. In this study, this palynofacies group characterizes the marsh and bay mudstones mostly plotting in field I of the APP ternary plot (Fig. 3.5). PF-B is characterized by moderate percentage of phytoclasts, moderate percentage of palynomorphs, and low amounts of aquatic amorphous organic matter (Fig. 3.5). These results are compatible with the organic facies BC and C (Jones *in* Tyson, 1995), and are typical of areas with deeper water that are more distal from fluvial sources with mixed organic matter. This palynofacies characterizes the central basin mudstones, which plot in fields III and V of the APP ternary plot (Fig. 3.5).

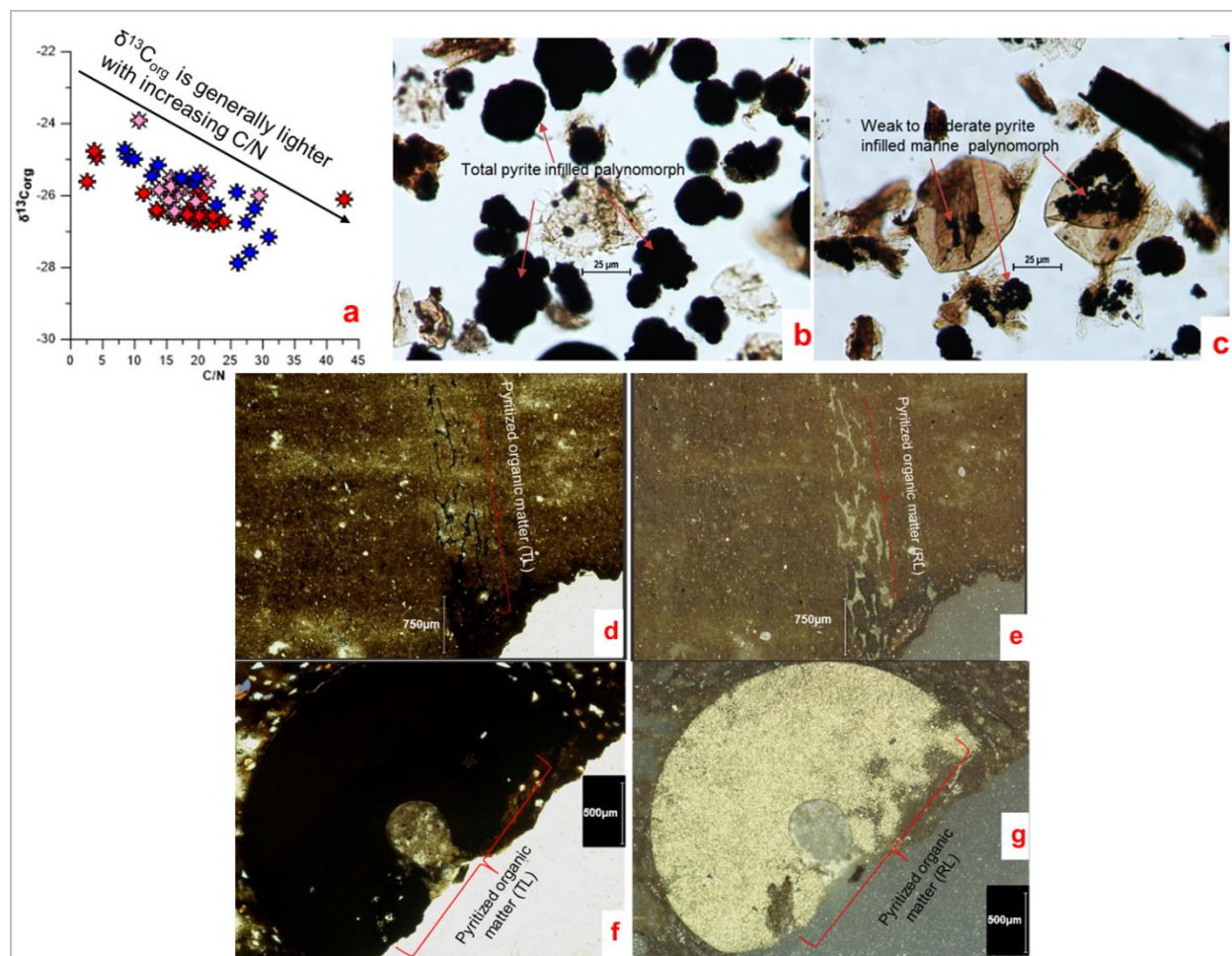


Fig. 3.8. a,  $\delta^{13}C_{org}$  vs. TOC/TN binary plot. b-c, palynological evidence of pyritization. d-g, petrographic evidence of pyritization under transmitted light (TL) and reflected (RL)

The mean TOC values observed for the dark mudstones are within the range of TOC data (<2%) reported for areas with high clastic dilution (Tyson, 1995). These data compare favourably with data from the eastern segment of the Anambra Basin and coeval mudstones of the Gombe and Patti formations in the Northern Benue Trough and the Bida Basin, respectively (Total, 1984; Idowu and Enu, 1992; Akande et al., 1998, 2005; Obaje et al., 2004, 2006; Nton and Okunade, 2013; Abubakar, 2014; Ayinla et al., 2017). Disregarding data modified by weathering (where up to 50% TN may be lost) and inorganic N-sources due to nitrogen fixation in clay mineral matrix of the mudstone (Müller, 1977), the TOC vs. TN bivariate plot (Fig. 3.6a-c) show a very strong

positive covariation observed for the central basin ( $R^2 = 0.71$ ), bay ( $R^2 = 0.80$ ) and marsh ( $R^2 = 0.50$ ) sub-environments. This implies that the TN is mostly organic (Meyers, 1994; Tyson, 1995). Furthermore, the bulk of the data points cluster around the  $\text{TOC}/\text{TN} \geq 20$  line (Fig. 3.6a-c), which further confirms the dominance of land derived organic matter (Meyers, 1994).

$\delta^{13}\text{C}_{\text{org}}$  is more enriched in marine biomass than in terrestrial biomass (Arthur et al., 1985). This attribute is useful in differentiating sediments with land derived organic matter from sediments with marine organic matter. Whilst this observation holds true for Tertiary and Quaternary sediments, the reverse is the case for Cretaceous and older strata. The main reason advanced for this observation in the Cretaceous is C-isotopic fractionation during photosynthesis, which was a consequence of high levels of atmospheric  $\text{CO}_2$  (Arthur et al., 1985). Arthur et al., (1985) reported  $\delta^{13}\text{C}_{\text{org}}$  data ranges of -29 to -27, and -25 to -24 respectively for marine and land derived organic matter in Cretaceous strata. Discounting samples with  $\text{TOC} < 0.5$  wt. %, there is no clear distinction between marine derived organic matter from terrestrially derived organic matter across the three sub-environments using  $\delta^{13}\text{C}_{\text{org}}$  data. However, when comparing  $\delta^{13}\text{C}_{\text{org}}$  in samples from a single bed, subtle differences were observed. Samples with higher percentage of phytoclasts show enrichment in  $\delta^{13}\text{C}_{\text{org}}$  and vice versa (Fig. 3.7a-d).

$\text{TOC}/\text{TN}$  and  $\delta^{13}\text{C}_{\text{org}}$  data are complementary, and are useful in characterizing different organic matter sources in Tertiary to recent sediments (Meyers, 1994, 1997; Lamb et al., 2006; Bauersachs et al., 2014) as these provide a good contrast of different organic matter sources. Binary plot of  $\text{TOC}/\text{TN}$  vs.  $\delta^{13}\text{C}_{\text{org}}$  shows an inverse relationship suggesting that organic rich units are depleted in  $^{13}\text{C}_{\text{org}}$  and vice versa (Fig. 3.8a). In general, we can report that the dominance of land-derived organic matter as well as the low preservation mask the  $\delta^{13}\text{C}_{\text{org}}$  and TN signatures of

aquatic-derived organic matter in the central basin. As a result, these methods may not be well suited for studying organic source variability in estuarine sediments.

### 3.4.2 *Paleoredox evaluation*

The relative proportions of organic matter constituents are a reflection of paleoredox conditions (Tyson, 1995). Oxidic conditions in proximal depositional settings are characterized by high percentages of phytoclasts and low proportions of aquatic amorphous organic matter, whereas oxidic conditions in distal and more marine settings are characterized by lower relative proportions of phytoclasts, higher percentages of palynomorphs and low relative abundances of aquatic amorphous organic matter (Tyson, 1995; Santos et al., 2013). Conversely, proximal anoxic conditions are characterized by moderate percentages of aquatic amorphous organic matter, low to moderate percentages of palynomorphs and moderate percentages of phytoclasts, in contrast to high relative proportions of aquatic amorphous organic matter, moderate percentages of palynomorphs and low relative proportions of phytoclasts in anoxic conditions in distal settings.

The PF-A palynofacies group suggests proximal oxidic settings (bay and the marsh mudstones) with predominantly terrestrial organic matter, where high percentages of phytoclasts diluted the palynomorphs, coupled with the low relative abundances of aquatic amorphous aquatic organisms (Fig. 3.5) (Tyson, 1995). A more distal oxidic realm characterized by moderate to high relative proportions of palynomorphs in the central basin mudstone is inferred for PF-B (Fig. 3.5). In addition, a careful observation of the palynomorph assemblages and petrographic slides reveal the occurrence of opaque minerals interpreted as pyrite (Fig. 3.8b-g). The moderate to total infilling of palynological organic matter (especially palynomorphs) by pyrite and their variable grain sizes [(estimated to be commonly  $>5\mu\text{m}$  (Fig. 3.8b-c)] suggest diagenetic replacement under reducing conditions (Szczepanik et al., 2017).

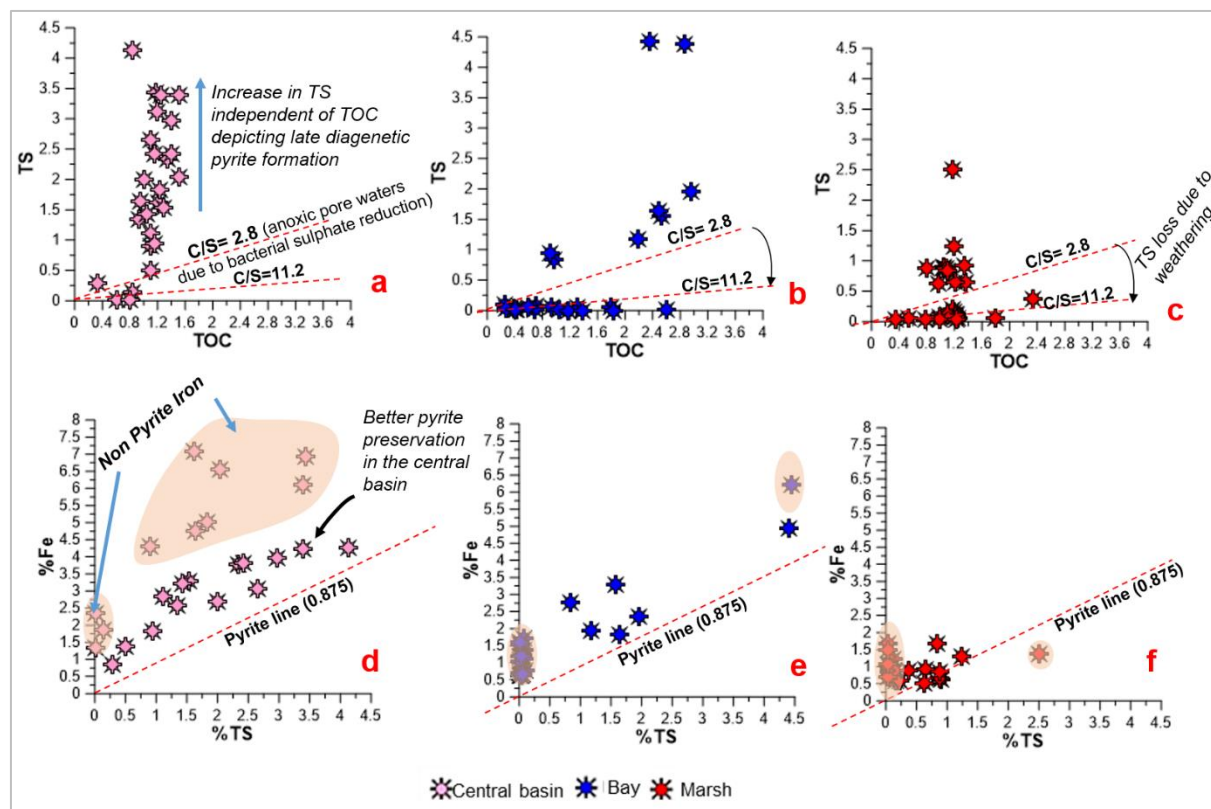
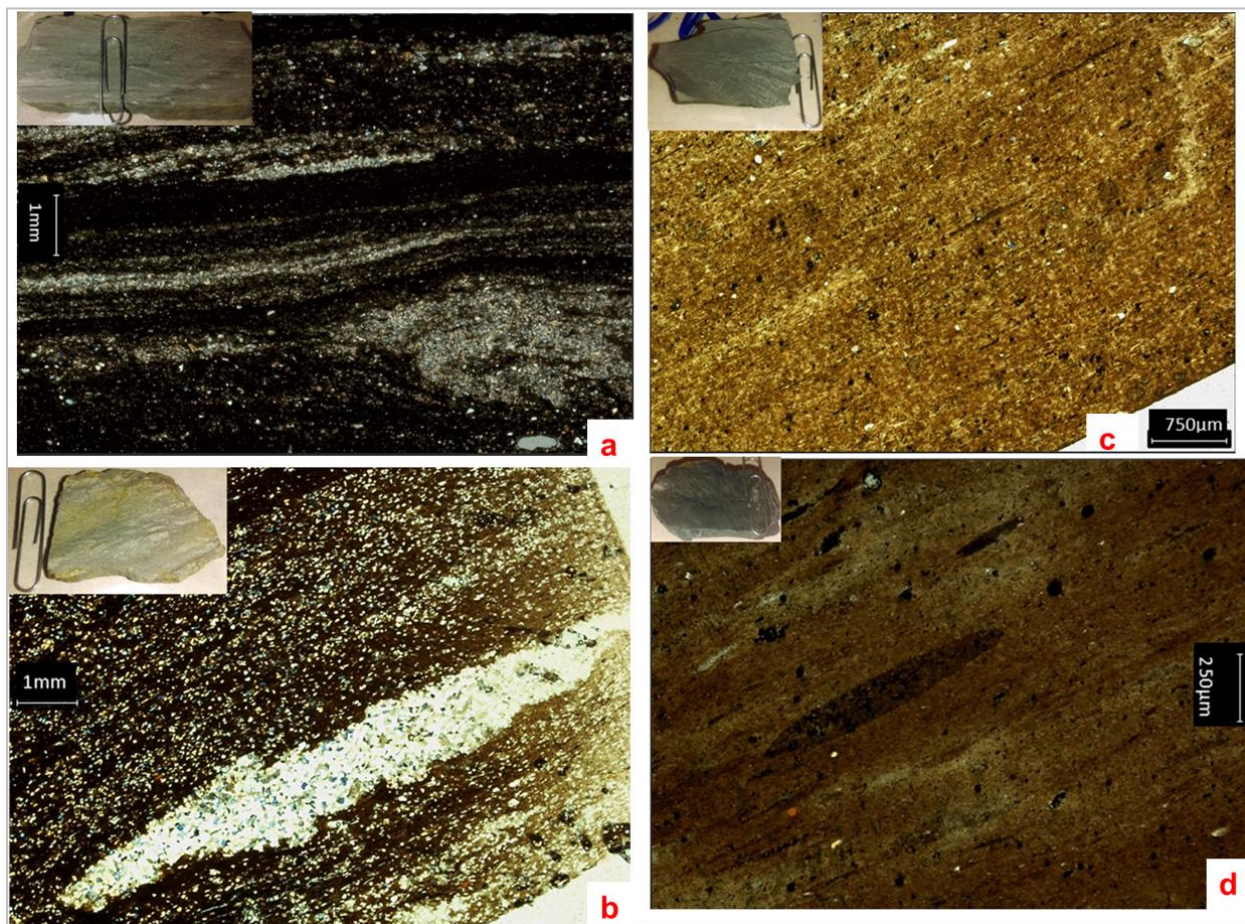


Fig. 3.9. Binary plots of TS vs. TOC (a-c) and Fe vs. TS (d-f) in the marsh, bay and central basin sub-environments.

In general, lower TS values are observed in the marsh mudstones (Table 3.3). As noted earlier, TS values are more variable than the TOC and TN data recorded from same set of samples. This is attributed to weathering of the mudstones (Ruebsam et al., 2018), especially in the bay and marsh where up to 75% TS was potentially lost (Fig. 3.9a-c). Raiswell and Berner (1985) (and references therein) posited that under anaerobic depositional setting, the principal limiting factor for pyrite formation is the abundance of organic matter required for bacterial sulfate reduction. Consequently, a TS vs. TOC bivariate plot showing a positive covariation with a regression line that passes through the origin ( $m \sim 0.36$ ) is characteristic of anoxic pore water conditions in a normal marine depositional setting. In contrast, under euxinic conditions, the abundance of detrital iron present is the principal limiting factor favouring pyrite formation. As such, TOC vs. TS

bivariate plot show a positive covariation with a regression line that passes through a positive S - intercept.



*Fig. 3.10. Microfabric of dark mudstone used as paleoredox proxy.*

Notwithstanding the weathering effects, we can make some valid inferences from the TS vs. TOC bivariate plot for dark mudstones (Fig. 3.9a-c). This plot shows two trends interpreted as primary and secondary anoxic trends. The primary anoxic trend with a C/S-ratio of 2.8 is typical for normal marine conditions with the anoxic zone positioned cms below the water/sediment interface as put forward by Raiswell and Berner (1985) (and references therein). We hypothesize that reducing conditions favouring syngenetic to early diagenetic pyrite formation were attained in the pore waters below the sediment/water interface. We interpret this as a scenario where the main

limitation for pyrite formation was the amount of bacterially decomposable organic matter available for sulphate reduction and anoxicity (Berner, 1984; Westrich and Berner, 1984). The secondary anoxic trend shows an increase in TS independent of TOC, signifying the existence of anoxic conditions at the base of the bottom water favouring late diagenetic pyrite growth, which is perhaps the more dominant mode of pyrite formation as illustrated by the replacement textures observed from microfabric and palynofacies analysis (Fig. 3.8b-g). The source of this H<sub>2</sub>S is thought to come from the anoxic zone below the sediment water interface explained above.

The central basin as observed through visual kerogen analysis possess more palynomorphs (especially dinoflagellate cysts). Reactive organic matter flux is believed to have spurred sulphate reduction, thus promoting pyrite formation faster in the central basin than in the marsh and bay sub-environments, which possess higher proportions of less reactive phytoclasts rich in lignin (Westrich and Berner, 1984). The favourability of diagenetic pyrite formation in the marsh and bay is further limited by lower salinity, which is due to the low sulphate concentration typical of very high dilution in proximal realms of brackish water bodies (Berner, 1984) as revealed by the generally lower TS concentration and TS variability recorded especially from the marsh sub-environment. Other important factors are grainsize and fabric, which are also influenced by proximity and mineralogy, as well as degree of bioturbation (Berner, 1984; Szczepanik et al., 2017), all of which are more conducive in the central basin mudstones (this study, and Edegbai et al., 2019b). The Fe vs. TS binary plots for the marsh, bay and central basin sub-environments (Fig. 3.9 d-f) confirms this even further and shows better pyrite preservation in the central basin.

The relationship between the degree of bioturbation, sediment fabric and redox conditions is well known (Potter et al., 2005). Hereby, the degree of bioturbation increases with the amount of dissolved oxygen present in the water column and in pore waters below the sediment water



interface, as well as with reduction in water depth. Thus, better development and preservation of lamination increase with anoxicity. The marsh and proximal parts of the bay sub-environment show much thicker laminations/thin beds and weak to sparse bioturbation with a grain-supported fabric (Figs. 3.10a, b), whereas the more distal bay and central basin sub-environments preserve thin, well-developed lamination with zero to weak bioturbation (Figs. 3.10c, d). Consequently, we infer increasing anoxicity from the marsh to the bay and central basin sub-environments from the analysis of representative thin sections.

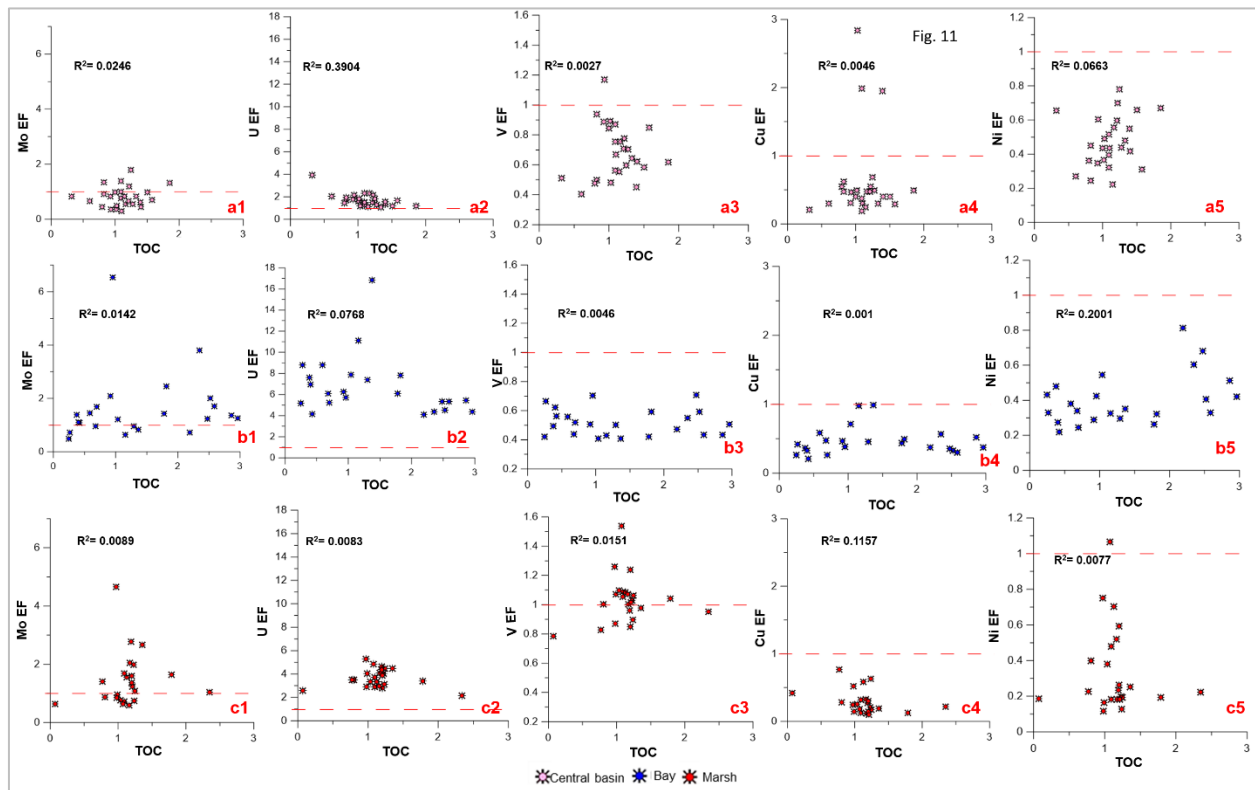


Fig. 3.11. Binary plots of Enrichment factors of Mo, U, V, Cu and Ni vs. TOC. a1-a5, b1-b5, and c1 to c5 represent data from the central basin, bay and marsh sub-environments respectively.

Tribovillard et al. (2006) illustrated the different relationships that exist between the enrichment of redox sensitive trace elements (i.e., Ni, Cu, V, U, Mo) and organic richness (TOC) under oxic, suboxic, anoxic and euxinic conditions. No covariation exists between the enrichment of redox sensitive trace elements and TOC under oxic-suboxic conditions due to their sequestration

with the detrital fraction. TOC is the limiting factor for the enrichment of Ni and Cu due to the formation of organometallic complexes, which occur under anoxic to euxinic conditions. Consequently, a strong covariation exists between Ni, Cu and TOC due to the increase in TOC under anoxic conditions. Sequestration of V and U occur under anoxic conditions as more organometallic complexes producing suitable substrates for their sequestration are formed. Thus, a good covariation exists between V, U and TOC. Under euxinic conditions, the presence of hydrogen sulphide allows for strong enrichment of Mo bound in sulphides, oxyhydroxide and thiomolybdate phases, respectively. S therefore replaces organic richness as the limiting condition for U, V and Mo sequestration, and consequently, a weak covariation occurs between Mo, V, U enrichment and TOC.

In this study, we refrained from using conventional ratios of trace elements affected by redox conditions and those that are not (e.g., V/Cr, U/Th) since high clastic dilution can lead to misinterpretation of paleoredox condition (Potter et al., 2005; Hans Brumsack, *pers. comm.*, 2018). Instead, we elected to exploit the relationship between TOC and the enrichment factors of redox sensitive trace elements explained above. Bivariate plots of enrichment factors of Ni, Cu, V, U, and Mo vs. TOC (Fig. 3.11) show very weak covariations, further confirming the inferences of oxic bottom water paleo-oxygenation conditions hypothesized from palynofacies and microfabric analyses, as well as Fe-TOC-S relationship.

### **3.5 Conclusion**

This study has revealed that the re-established Trans-Saharan seaway in the Maastrichtian was shallow and characterized by low salinity brackish water deposits with largely terrigenous organic matter influx. In the more distal sub-environments and with rising sea level, some contribution from aquatic organic matter is evident in the palynofacies of the central basin

mudstones. In addition, results of the multiproxy approach used in this study suggest predominant oxic bottom water conditions for the Maastrichtian Trans-Saharan seaway. Palynofacies and microfabric evidences as well as inferences from Fe-TS-TOC relationship suggests conditions favourable for pyrite formation were attained. Sequentially, we hypothesize that primary (syngenetic to early diagenetic) pyrite formation occurred in the anoxic zone below the sediment water interface, whereas secondary (late diagenetic) pyrite formation which formed the bulk of pyrite preserved occurred at the base of the bottom water.

### **Acknowledgement**

The first author is grateful to the University of Benin Research and Publications Committee, the Fulbright Commission (15160892), the Niger Delta Development Commission (NDDC/DEHSS/2015PGFS/EDS/011), and the DAAD (ST32 - PKZ: 91559388) who have contributed to his educational development over the years. The efforts of Julius Imarhiagbe who was of great assistance during fieldwork is appreciated. Furthermore, the first author wishes to acknowledge the motivation, guidance and instruction provided by Prof. W.O. Emofurieta during the early phase of this research.

## Chapter Four

Differentiation of sediment source regions in the Southern Benue Trough and Anambra Basin, Nigeria: insights from major and trace element geochemistry

Together with:

L. Schwark. Submitted to *Journal of African Earth Sciences*

### A B S T R A C T

It is widely accepted that the lithic fill of the Anambra Basin, Southern Nigeria was sourced from the reworked pre-Santonian rocks of the Benue Trough. However, this hypothesis cannot account for the large sand volumes within the basin especially as the lithic fill of the Southern Benue Trough comprises mudstones, carbonates and subordinate sandstone units. In this study, we set out to investigate the provenance of the Mamu Formation as well as pre-Santonian Awgu and Eze-Aku groups by undertaking geochemical evaluation of cuttings from 5-wells spread across the Anambra Basin. The results of the well data, which was integrated with our previously generated data on the western margin of the Anambra basin as well as published data on the eastern margin reveal that the pre-Santonian units are characterized by a lower degree of chemical alteration and were sourced from basement complex rocks. By contrast, the more chemically altered Mamu Formation is sourced from recycled Southern Benue Trough strata, basement complex rocks as well as, anorogenic granites. In addition, the pre-Santonian units show spatio-temporal compositional variability, which is due to a large proportion of detrital contribution accruing from mafic rocks in the latest Cenomanian to early Turonian, whereas from middle Turonian to Coniacian the detrital contribution was more from felsic sources. Furthermore, the observed spatial geochemical variability of the Mamu Formation is adduced to be a consequence of detrital contribution from

three source regions: the eastern, western and northern provenance regions. The eastern provenance region is characterized by a stronger mafic signature, low levels of Nb, Ta, Sn and Ti, high levels of W, Pb and Zn, strong Pb-Zn covariation as well as enrichment of Zn over Pb ( $Pb/Zn < 1$ ), whereas the western and northern regions show higher levels of Nb, Ta, Sn and Ti. In addition, the western provenance is characterized by higher Pb over Zn ( $Pb/Zn > 1$ ) and lower W concentration, which is distinct from the northern provenance with  $Pb/Zn < 1$  and higher W concentration. Discriminant plots show clear evidence of mixing of provenance regions especially in the Idah-1 and Amansiodo-1 well whose sediments show secondary Pb, Sn and W mineral enrichment respectively.

#### **4.0. Introduction**

Several hypotheses have been put forward to explain the provenance of the Anambra basin's lithic fill. The leading hypothesis posits that the lithic fill of the Anambra Basin was sourced from reworked pre-Santonian rocks of the Benue Trough (Ladipo, 1986; Amajor, 1987; Obi and Okogbue, 2004). This is preferred over sourcing from the basement complex in the eastern highlands (Oban Massif and Cameroun highlands) (Hoque, 1977). The main drawback of the former is its inability to account for the large sand volumes in the post-Santonian units (Edegbai et al., 2019a), especially the dominantly sandy Ajali Formation (Nwajide, 2013) since the pre-Santonian rocks in the Southern Benue Trough are predominantly made up of mudstone and limestone units. The latter hypothesis does not convincingly explain the clear evidence of sediment recycling inferred from the textural, mineralogical and geochemical characteristics, which has been observed in the post-Santonian units (Amajor, 1987; Odigi, 2007; Tijani et al., 2010; Edegbai et al., 2019b).

Besides the aforementioned hypotheses, further data and reports, support that more than one provenance region exists. Petters (1978) opined that sediment contribution from the palaeo-River Niger and the Southern Benue Trough exists. This hypothesis has been somewhat reinforced by recent palaeogeographic and palaeo-drainage models of Bonne (2014), Markwick (2018), and Edegbai et al. (2019a). Tijani et al. (2010), who undertook textural and geochemical analysis of the Ajali Formation, hypothesized a sediment provenance in the Adamawa-Oban Massif highlands as well as from the pre-Santonian strata of the Southern Benue Trough. Our previous findings in the western segment of the Anambra basin (Edegbai et al., 2019b) using high resolution multidisciplinary techniques suggested some detrital contribution from basement complex rocks in the southwest (minor) as well as the pre-Santonian rocks (major).

It is against this background that we undertook this study, which seeks to investigate the provenance of the Awgu and Eze-Aku groups, and the Mamu Formation as a basis for deciphering the provenance regions of the Anambra Basin's lithic fill using geochemical data from outcrops in the western and eastern margin (Edegbai et al., 2019b; Odoma et al., 2015) as well as from 5 wells spread across the Anambra Basin. Furthermore, data from regional geochemical analysis of sediments from streams draining parts of southwestern and northcentral Nigeria (Lapworth et al., 2012), reports from Pb-Zn deposits in the Benue Trough (Olade et al., 1979; Olade, 1987) as well as reports from mineralized pegmatite (Kinnaird, 1984) and biotite granite (Imeokparia, 1982a, 1982b) domains in southwestern and northcentral Nigeria, respectively, complemented this study.

#### **4.1 Geologic overview**

The Benue Trough is a NE-SW trending depression approximately 1000km by 50-100km in dimension, which comprises of a suite of depocenters broadly grouped into Northern, Central and Southern Benue Trough (Fig. 4.1) (Nwajide, 2013). It is part of a much larger west rift system

(WARS) that formed due to stresses arising from the opening of the South Atlantic Ocean in the Barremian age (Fairhead, 1988; Fairhead and Green, 1989; Benkhelil, 1989). The opening of the Equatorial Atlantic Ocean consequent upon the final separation of the African plate from the South American plate in the Albian (Moulin et al., 2010) resulted in flooding of the Southern Benue Trough, leading to the deposition of the Asu-River Group. Due to global sea level rise, this flooding, which peaked in the Cenomanian-Turonian boundary continued into the Turonian (Adeleye, 1975; Reyment and Dingle, 1987), were floodwaters from the equatorial Atlantic Ocean connected with floodwaters from the Tethys Ocean to establish the Trans-Saharan seaway through the Benue Trough. This resulted in the deposition of the Eze-Aku and Awgu groups (Petters, 1978; Petters and Ekweozor, 1982).

The Eze-Aku and Awgu groups belong to one depositional episode spanning latest Cenomanian to Coniacian (Petters and Ekweozor, 1982). Gebhardt (1999) reported that these units could only be differentiated based on fossil content. In the southern Benue Trough, the Eze-Aku group comprises chiefly of highly fossiliferous calcareous mudstone intercalated with sands, and limestone units deposited in environments ranging from continental to deep marine environments (Banerjee, 1980; Umeji, 1984; Gebhardt, 1999; Kuhnt et al., 1990; Igwe and Okoro, 2016; Dim et al., 2016). The Awgu Group consists of limestone, mudstone interstratified with thin limestone and marl units (Petters and Ekweozor, 1982), as well as subordinate sands. Coal units have been documented at the top of the stratigraphic succession. These units are interpreted to have been deposited in delta plain to marine conditions (Gebhardt, 1999; Petters, 1978; Nwajide, 2013).

The Trans-Saharan seaway was short lived and eventually broken in the Santonian primarily due to a change in stress regime, which brought about reactivation of NE-SW trending

faults, folding, volcanism as well as exhumation of pre-Santonian strata of which the southern Benue trough was the most affected (Guiraud and Bosworth, 1997).

After the Santonian inversion, came a phase of renewed subsidence west of the Southern Benue Trough, which formed the Anambra Basin. The Anambra Basin (Fig. 4.1) represents the sag phase of the Benue Trough evolution. The oldest and youngest parts of its lithic fill comprises of the Nkporo Group whose facies is dominantly marine, but shows fluvial to fluvio-marine character at the marginal parts of the basin (Nwajide, 2013; Edegbai et al., 2019a), and the brackish Nsukka Formation (Nwajide, 2013) respectively.

The Mamu Formation comprises of mudstone, sand, limestone, carbonaceous and calcareous mudstone, as well as coal and minor ironstone units, which exhibit spatio-temporal variability with respect to thickness and facies (Edegbai et al., 2019b; Dim et al., 2019; Okoro and Igwe, 2018a, 2018b; Simpson *in* Nwajide 2013; Gebhardt, 1998; Akande and Mücke, 1993). In recent times, these units have been adduced to represent estuarine to shallow marine depositional conditions (Igwe and Okoro, 2018b; Dim et al., 2019; Edegbai et al., 2019b). In addition, variable ages ranging from middle Maastrichtian in the North (Gebhardt, 1998) to late Campanian to middle Maastrichtian in the South implying later sedimentation of the Mamu in northern Anambra-Basin have been reported (Zaborski, 1983; Gebhardt, 1998; Okoro and Igwe, 2018a).

## **4.2 Materials and Methods**

### *4.2.1 Elemental analysis*

Ninety drill cuttings and core samples from the Nzam-1, Idah-1, Owan-1, Amansiodo-1 wells (Fig. 4.3a-f) representing the post-Santonian Mamu Formation as well as the pre-Santonian Eze-Aku and Awgu groups were obtained from the Nigerian Geological Survey Agency storage



Core Shed, Kaduna, Nigeria. A combination of cluster and systematic sampling techniques (modified by sample availability and stratigraphic control based on well logs and original reports from oil companies) was employed. Sample preparation entailed homogenization and mechanical pulverization into powder, succeeded by near total multi-acid digestion and elemental analysis using ICP-MS at Activation Laboratories, Ontario, Canada.

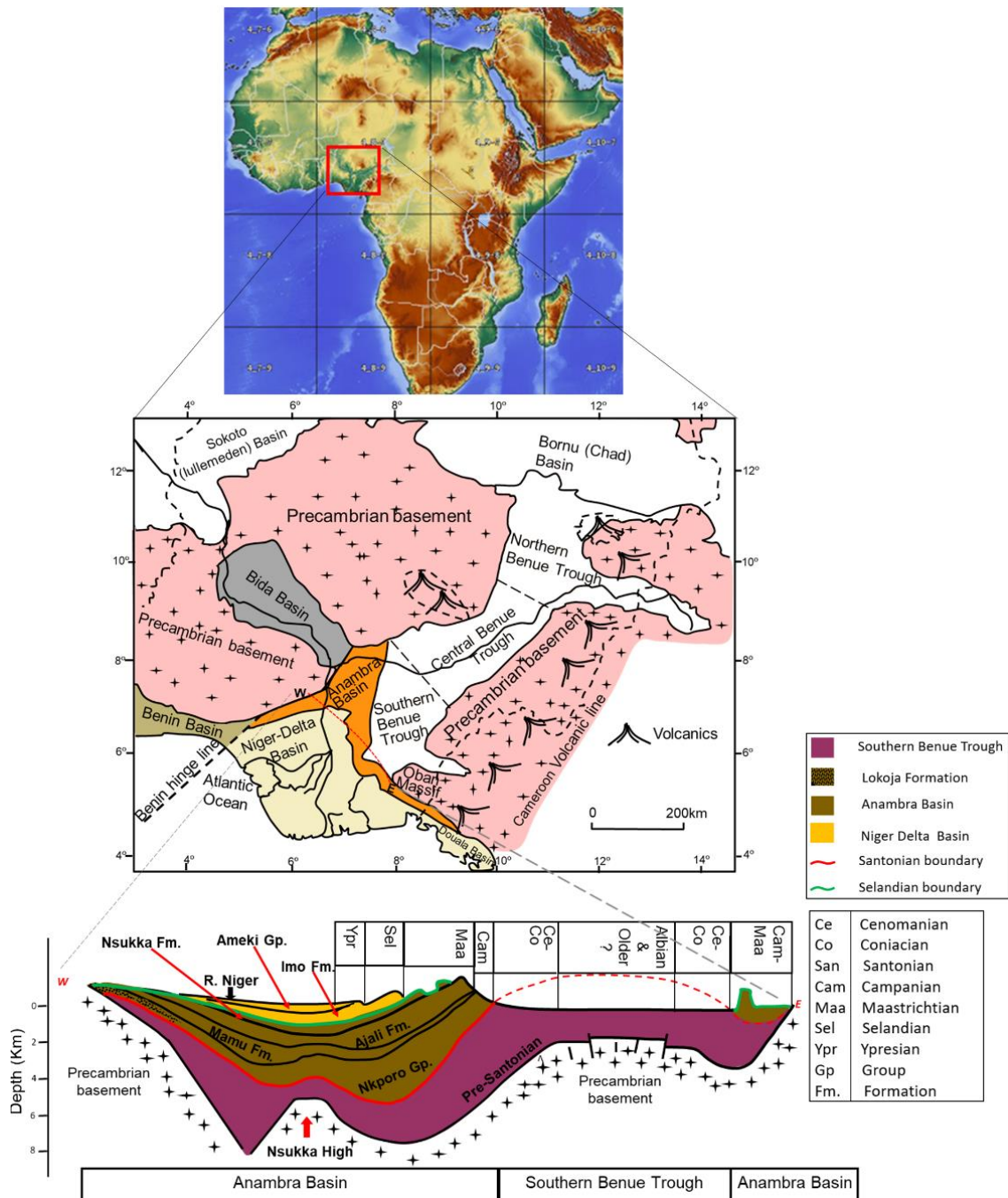


Fig. 4.1 Map of Nigeria showing areas underlain by sedimentary and basement rocks. Below is a W-E cross section showing lithostratigraphic packages of southern Nigeria ranging from Barremian to Ypresian (Edegbai et al., 2019b).

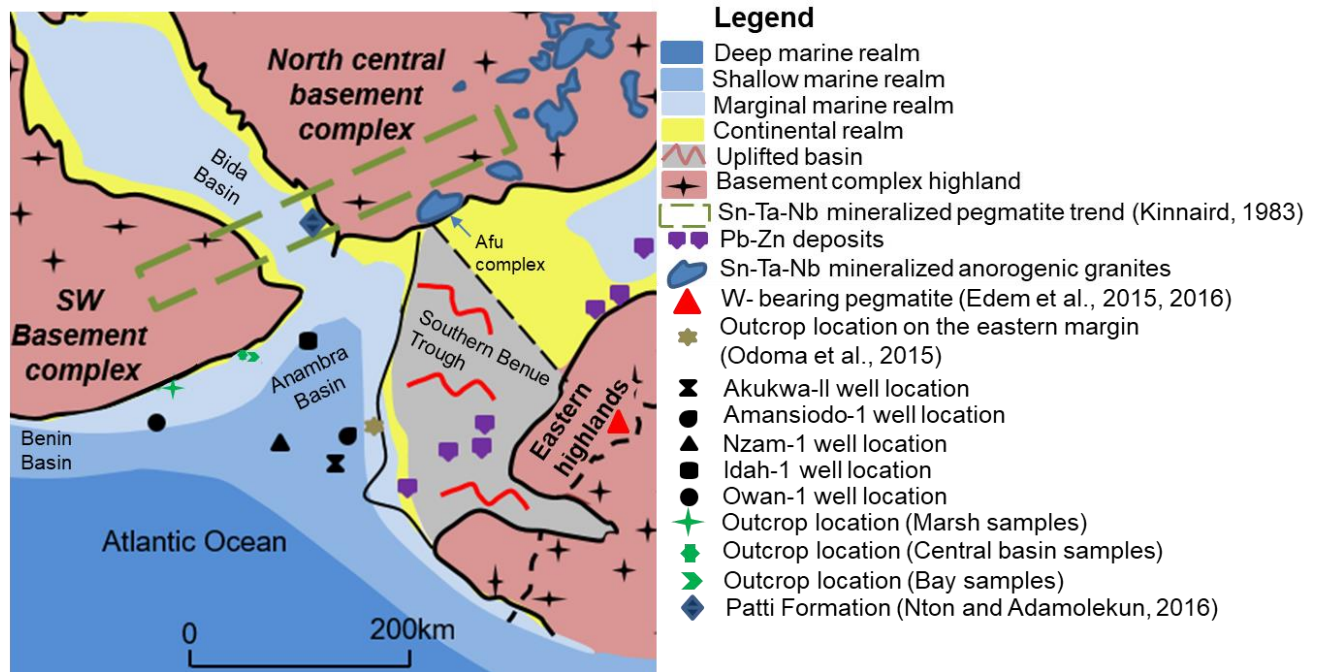


Fig. 4.2. Conceptual early Maastrichtian paleogeographic model with sample locations, ore deposits and mineralized granites or pegmatites

#### 4.2.2 Total organic carbon (TOC) analysis

Eighty-two drill cuttings and core samples from the Nzam-1, Idah-1, Owan-1, Amansiodo-1 wells (Fig. 4.3a-f) were measured for TOC using an ELTRA CS-580A analyzer at the Organic Geochemistry Departmental Laboratory at Kiel University, Germany. Sample preparation entailed mechanical homogenization and pulverization, followed afterwards by decalcification of 150-200 mg with 10% HCl and 25% HCl (for calcite and dolomite dissolution respectively) before drying on a hot plate at moderate temperature.

The results of major and trace element analysis as well as TOC analysis were integrated before comparison with previously generated data from outcrops at the western flank by the authors [some of which have been published (Edegbai, 2019b)] as well as data from the eastern margin

(Odoma et al., 2015). As observed by Cullers and Stone (1991), argillaceous sediments and fine sands better preserve the provenance signature of source units than coarser units do. Consequently, for the purpose of our study, only data from the outcropping dark mudstone lithofacies in the western flank, which has been subdivided into marsh, bay and central basin subenvironments in order of proximity (Edegbaei et al., 2019b), was integrated with data from the drill cuttings.

### **4.3 Results**

A summary of the elemental analysis results is presented in Appendix 2.1a-c.

#### *4.3.1 Major elements (Ca, Fe, K, Mg, Mn, Na, Ti and Al)*

##### *4.3.1.1 Outcropping Mamu Formation:*

On the western margin, Al, and Fe are the most abundant in the suite of major elements under consideration (Appendix 2.1a, Fig. 4.4a-b). 65.2%, 95.7%, 96.1% of samples from the marsh, bay and central basin subenvironments are above the average upper continental crust (UCC, McLennan, 2001) limit for Al. The samples from the central basin subenvironment are the most enriched in Fe with 50% of the samples below the UCC limit for Fe. 8.7% of the bay samples are above the UCC limit for Fe, while all the samples from the marsh subenvironment have concentrations below the UCC limit for Fe. In addition, except for one sample from the central basin subenvironment, the Ti concentration in all the dark mudstone samples are above UCC. Furthermore, all the dark mudstone samples have concentrations below the UCC limits for Ca, K, Mg, and Na. In broad terms, the more distal and saline central basin subenvironment have the highest concentration of Ca, Fe, K, Mg, Mn, Na and Al of all the dark mudstone samples (Appendix 2.1a, Fig. 4.4a-b) and are very similar in median values to those reported by Odoma et al. (2015)

(Appendix 2.1a, Fig. 4.4a-b), whereas the lowest concentrations are recorded from the more proximal less saline marsh subenvironment (Appendix 2.1a, Fig. 4.4a-b).

Outcrop data from Odoma et al. (2015) on the eastern margin suggests that Al and Fe are the most abundant major elements (Appendix 2.1a, Fig. 4.4a-b). The concentrations of Ca, K, Mg and Na concentration in the samples are below the respective UCC limits. 88.9% and 66.7% of the samples have Al and Fe concentrations below the respective UCC, while all the samples have Ti concentration above the UCC for Ti (Appendix 2.1a, Fig. 4.4a-b).

#### *4.3.1.2 Well data:*

##### *4.3.1.2.1 Mamu Formation:*

Al and Fe are the most abundant among the major elements being discussed (Appendix 2.1a, Fig. 4.4a-b). In the Owan-1 well, all samples are below the UCC limits for Ca, Fe, K, Mg, and Na, while 71.4 % and 14.3 % of the samples have concentrations above the respective UCC limit for Ti and Al. In the Amansiodo-1 well, all the samples have Fe, Ti, Al, K, Mg, and Na concentrations below the respective UCC limits. In addition, 33.3% of the samples have Ca concentration above the UCC limit. All the samples from the Idah-1 and Nzam-1 wells have concentrations below the UCC limits for Ca, K, Mg and Na. Furthermore, all the samples from the Nzam-1 well have Ti concentrations above the UCC limit, as do bulk of the samples (90.5%) from the Idah-1 well. With respect to Fe and Al concentrations, 87.5% and 75% of samples from the Nzam-1 well, as well as 85.7% and 61.9% of samples from the Idah-1 well have Fe and Al concentrations greater than the respective UCC.

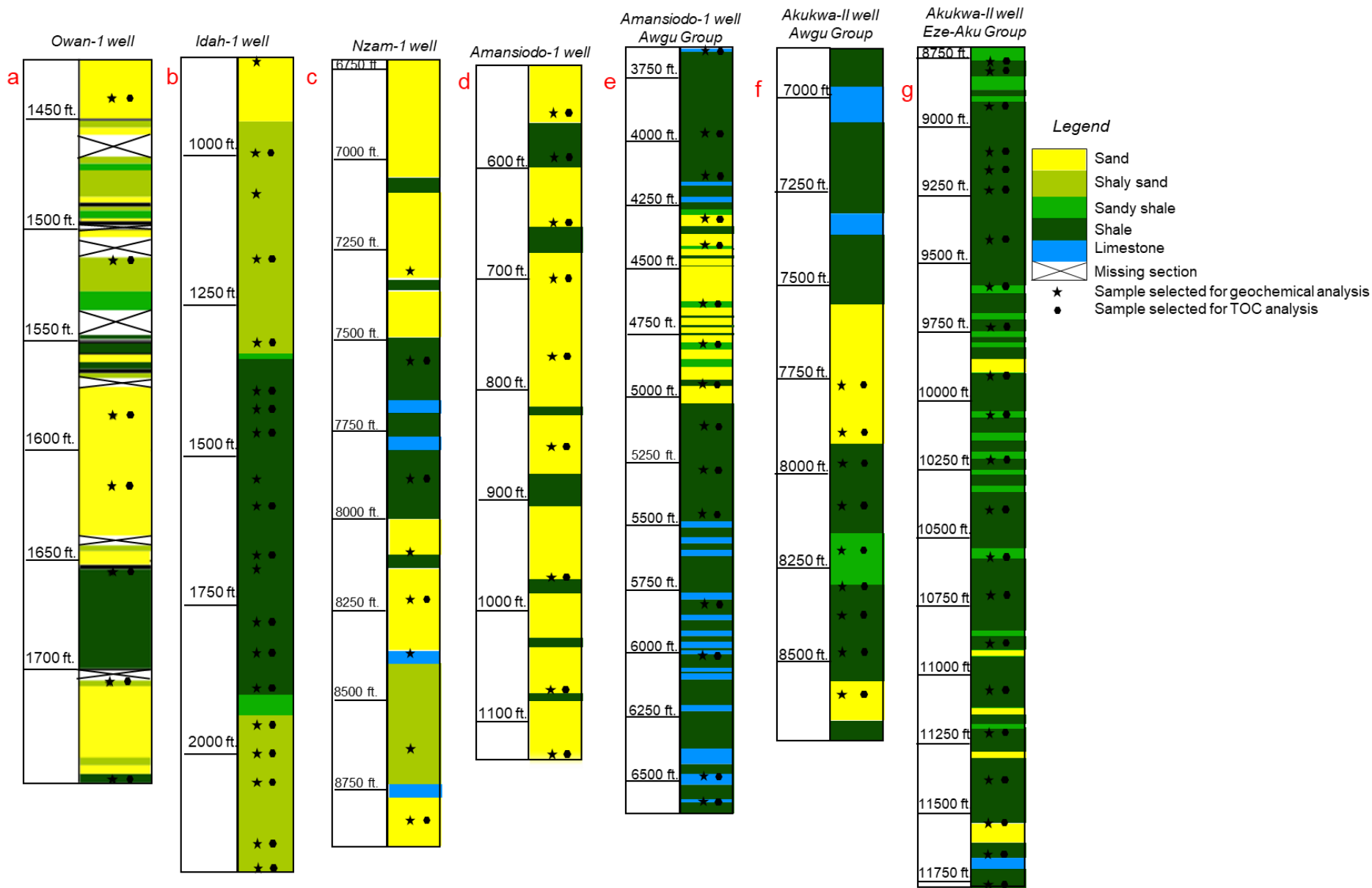


*Fig. 4.3. a-d, Lithology of the Mamu Formation penetrated by Owan-1, Idah-1, Nzam-1 and Amansiodo-1 wells respectively. d-e, Lithology of the Awgu Group penetrated by the Amansiodo-1 and Akukwa-II wells. f, Lithology of the Eze-Aku Group penetrated by the Akukwa-II well. See Edegbai, et al., (2019b) for the lithology of outcropping units of the Mamu Formation on the western margin*

The data from Amansiodo-1 (closest to the eastern boundary) and the Owan-1 (on the closest to western margin) wells show very distinct major element distribution in comparison to results from the more central Nzam-1 and Idah-1 wells. The Amansiodo-1 samples possess the largest median concentrations of Ca as well as much lower concentrations of the other major elements. The median values of the major element data from Owan-1 are very comparable with the marsh outcrop samples, which are also depleted in Ca and Mg (Appendix 2.1a, Fig. 4.4a-b).

The samples from Idah-1 and Nzam-1 wells show greater Ca, Fe, K, Mg, Mn, Na and Ti concentrations (Appendix 2.1a, Fig. 4.4a-b), which is distinct from the samples of the marginal wells. The Idah-1 well also shows subtle variation in major element concentration when compared to the southern Nzam-1 well. Greater concentrations of Ca, Mg, Mn and Ti abound in the Idah-1 well in comparison to the Nzam-1 well, which shows greater concentrations of K, Na and Al (Appendix 2.1a, Fig. 4.4a-b).

#### *4.3.1.2.2 Pre-Santonian Units.*

Geochemical data from the Awgu Group show Al and Fe as the most abundant major elements among the major element suite being discussed (Appendix 2.1a, Fig. 4.4a-b). All but one of the samples (from the Akukwa-II well) have Fe, Ti and Al concentrations above the respective UCC limits. In addition, with the exception of one sample from the Amansiodo-1 well, all the samples have Ca, K, Mg and Na concentrations below their respective UCC limits (Appendix 2.1a, Fig. 4.4a-b). Furthermore, the major element distribution in the Awgu Group shows slight

variability. Whereas samples from the Amansiodo-1 well are slightly more enriched in Fe, K, Ti and Al, the Akukwa-II well samples are slightly more enriched in Ca and Na (Appendix 2.1a, Fig. 4.4a-b).

In the Eze-Aku Group, Al and Fe are the most abundant major elements among the major element suites being discussed (Appendix 2.1a, Fig. 4.4a-b). All the samples have K and Na concentrations below their respective UCC limits. 85% and 95.2% of the samples have Ca and Mg concentrations below the respective UCC limits. In addition, the concentration of Al in bulk of the samples (90.5%) is above the UCC limit.

In general, samples from the Eze-Aku Group show slight enrichment in Na and Ca over the samples from the Awgu Group, which are more enriched in Fe, K, Mg, Ti and Al. In addition, the major element distribution in the pre-Santonian units are quite comparable to those observed from the centrally positioned Nzam-1 and Idah-1 wells (Appendix 2.1a, Fig. 4.4a-b).

#### 4.3.2 *High Field strength elements (HFSE: Th, U, Ta, Nb, Zr, Y, Hf)*

##### 4.3.2.1 *Outcropping Mamu Formation*

All the dark mudstone samples on the western margin have U and Nb concentrations above the respective UCC limit (Appendix 2.1b, Fig. 4.4c-d). The Th and Ta concentrations of all the samples from marsh and bay subenvironments, and the bulk of the samples (92.3% and 88.5% respectively) from the central basin subenvironment are above the respective UCC limits for Th and Ta. In addition, a very large proportion of the dark mudstone samples have concentrations below the UCC for Zr and Hf. Furthermore, 56.5%, 34.8%, and 38.5% of samples from the marsh, bay and central basin subenvironments respectively have Y concentration above the UCC limit.

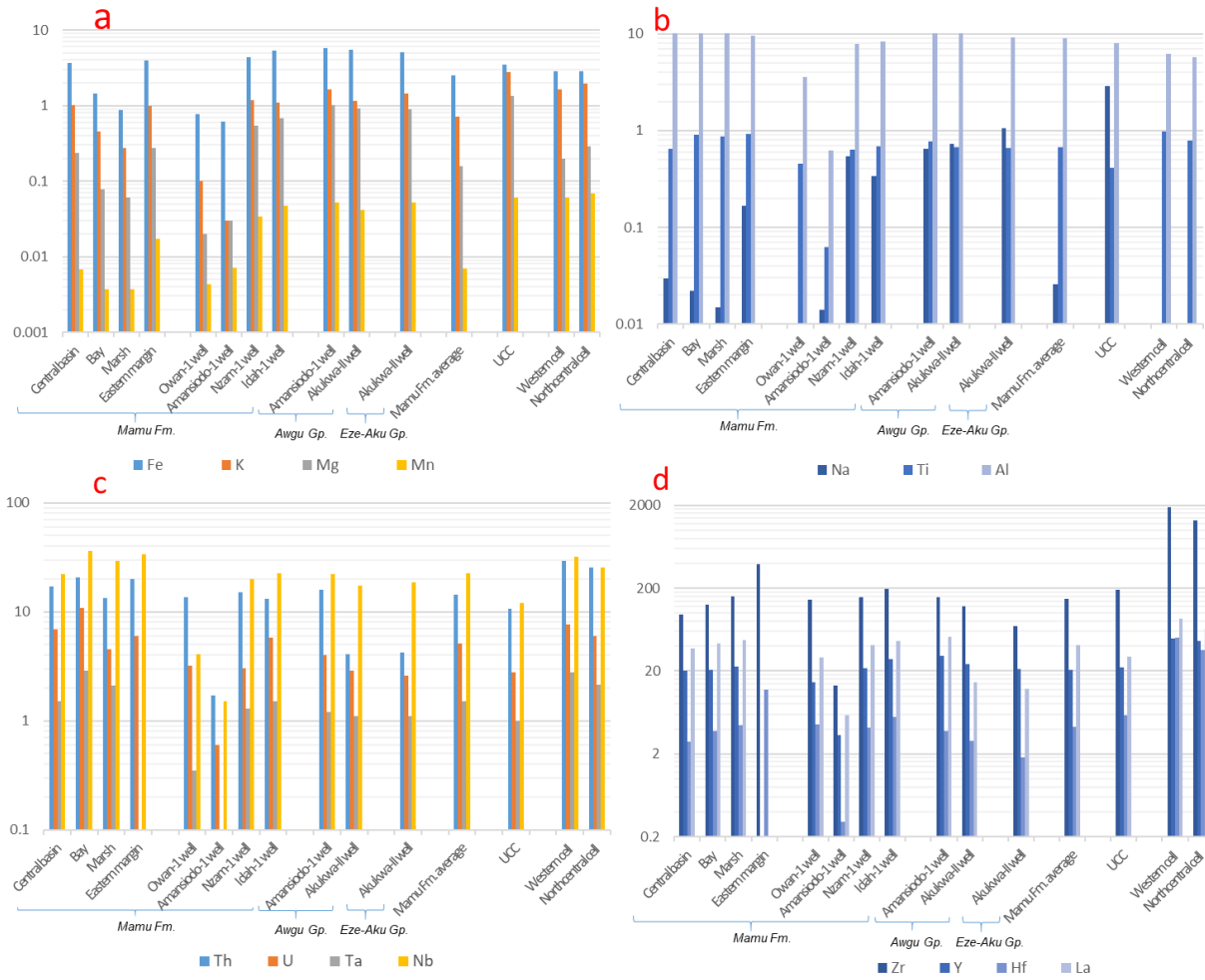


Fig. 4.4. Variograms showing the median concentrations of major and high field strength elements for all sample locations as well as regional data from western and northcentral Nigeria (Lapworth et al., 2012)

On the eastern margin, data from Odoma et al. (2015), show that all the samples are enriched above the UCC concentration for Th, U, Nb, Zr and Hf (Appendix 2.1b, Fig. 4.4c-d). In general, with the exception of Zr and Hf, which are much higher, the concentration of the other HFSE being discussed are more comparable to the outcrops at the Benin flank than the well data (Appendix 2.1b, Fig. 4.4c-d).



#### 4.3.2.2 Well data

##### 4.3.2.2.1 Mamu Formation

As observed in the major element distribution, the Amansiodo-1 well samples show very distinct geochemical distribution of the HFSE (Th, U, Ta, Nb, Zr, Y, and Hf) as indicated by very low concentrations that are at least one order lower than those obtained from the outcropping units (Appendix 2.1b, Fig. 4.4c-d). The HFSE abundance from the Owan-1 well, though much higher than the data from the Amansiodo-1 well, is subordinate to the outcropping units (Appendix 2.1b, Fig. 4.4c-d).

In the more centrally located Nzam-1 and Idah-1 wells, a very large proportion of the samples show enrichment in Th, U, Ta, and Nb above the respective UCC (Appendix 2.1b, Fig. 4.4c-d). In the Idah-1 well, 57%, 85.7% and 28.6 % of the samples have concentration above the respective UCC for Zr, Y, and Hf (Appendix 2.1b, Fig. 4.4c-d). The Zr, Y and Hf concentrations that are higher than the outcropping units on the western margin are subordinate to the Zr and Hf on the eastern margin (Odoma et al., 2015). By contrast, the outcropping units on the western margin show more enrichment in Th, U, Ta, and Nb than the sediments in the Nzam-1 and Idah-1 wells (Appendix 2.1b, Fig. 4.4c-d). Furthermore, with the exception of Th, the median concentrations of the HSFSE being discussed decreases from samples from Idah-1 well location to the samples from Nzam-1 well (Appendix 2.1b, Fig. 4.4c-d). In the Nzam-1 well, the bulk of the samples, which show enrichment in Th, U, Ta and Nb above the respective UCC limit, show depletion in Zr, Y, and Hf concentrations.

#### 4.3.2.2.2 *Pre-Santonian units:*

The Awgu Group samples from the Amansiodo-1 well show more enrichment in Th, U, Ta, Nb, Zr, Y and Hf in comparison to samples from the Akukwa-II well (Appendix 2.1b, Fig. 4.4c-d). The median values of the HFSE are comparable to the Mamu Formation data from the Idah-1 and Nzam-1 wells. In addition, a large proportion of the samples from the Amansiodo-1 well show enrichment above the respective UCC for Th, U, Ta and Nb and Y (Appendix 2.1b, Fig. 4.4c-d). Conversely, the samples are depleted below the respective UCC composition for Zr and Hf (Appendix 2.1b, Fig. 4.4c-d). A much lower proportion of the samples from the Akukwa- II well show enrichment above the respective UCC limits for U, Ta, Nb and Y. Furthermore, none of the samples are enriched above the UCC concentrations for Th, Zr and Hf (Appendix 2.1b, Fig. 4.4c-d).

In broad terms, when compared with the post-Santonian Mamu Formation (excluding the samples from Owan-1 well and the Amansiodo-1 well), the Awgu Group is depleted in Th, U, Ta, Nb, Zr and Hf concentrations (Appendix 2.1b, Fig. 4.4c-d). In contrast, the concentration of La and Y is much higher than in post-Santonian units (Appendix 2.1b, Fig. 4.4c-d).

The bulk of the samples from the Eze-Aku Group show depletion in Th, U and Hf concentrations below the respective UCC composition (Appendix 2.1b, Fig. 4.4c-d). In addition, none of the samples shows enrichment in Zr and Hf above the respective UCC limits (Appendix 2.1b, Fig. 4.4c-d). Conversely, a larger proportion of the samples are enriched in Ta and Nb above the respective UCC limits. The HFSE distribution within the Eze-Aku Group is very comparable to the data from the Awgu Group in the Akukwa II well, except that much lower Zr concentrations are present (Appendix 2.1b, Fig. 4.4c-d).

### 4.3.3 *Transition trace elements [(TTE) Ni, Co, V, Cr and Sc]*

#### 4.3.3.1 *Outcropping Mamu Formation*

A large proportion of the marsh and bay samples are depleted in Ni, Co and Sc content. Conversely, the bulk of the samples show enrichment in Cr (Appendix 2.1b, Fig. 4.5a-b). There is a distinction in the V content of the marsh and bay samples. Whereas the bulk of the Marsh samples are enriched above the UCC limit for V, only 8.7 % of the Bay samples show V enrichment above the UCC limit. In comparison to the marsh and bay units, the central basin samples are much more enriched in TTE, only subordinate to the marsh unit in V concentration (Appendix 2.1b, Fig. 4.5a-b).

On the eastern margin, data from Odoma et al. (2015) shows depletion of Ni and Co, whereas a substantial proportion of the samples show enrichment above the Cr and Sc of the respective UCC composition (Appendix 2.1b, Fig. 4.5a-b). In addition, 44.4% of the samples are enriched above the UCC mean for V.

In general, the central basin unit shows the most enrichment in TTE when compared with the other outcrop units (Appendix 2.1b, Fig. 4.5a-b), which is perhaps due to the redox conditions prevailing. The V and Cr content in the eastern margin is much lower than the marsh and central basin units in the western margin are (Appendix 2.1b, Fig. 4.5a-b). Furthermore, excluding the central basin unit, all other outcrop samples are depleted in Ni and Co concentrations (Appendix 2.1b, Fig. 4.5a-b).

#### 4.3.3.2 Well data

##### 4.3.3.2.1 Mamu Formation

The TTE distribution in samples from the Owan-1 and Amansiodo-1 wells are very distinct from the more centrally located wells due to their lower TTE concentrations. The samples from the Nzam-1 well show significant enrichment above the samples from the Idah-1 well (Appendix 2.1b, Fig. 4.5a-b). The Ni concentration in the majority of the well samples are below the UCC limit. In addition, the V, Cr and Sc abundances of all samples from the Owan-1 and Amansiodo-1 wells as well as the majority of the samples from the Idah-1 well fall below the respective UCC limit (Appendix 2.1b, Fig. 4.5a-b). The Co content in bulk of the samples are above the UCC mean.

In general, the outcropping units on the western margin contain higher levels of V, Cr and Sc than their well counterparts (Appendix 2.1b, Fig. 4.5a-b).

##### 4.3.3.2.2 Pre-Santonian Units:

Excluding the Cr concentration, which is depleted in the samples from Akukwa - II well, the TTE distribution in the Awgu Group is quite similar with a dominance of samples enriched above the respective UCC limits. Excluding the Ni concentration, which are much lower, the Eze-Aku unit shows similar distribution of TTE with those of the Awgu Group in the Akukwa –II well (Appendix 2.1b, Fig. 4.5a-b).

In broad terms, higher V, Co, Ni, and Sc concentrations persist in the pre-Santonian units when compared with the Mamu Formation, which is more enriched in Cr.

#### 4.3.4 *Pb, Sn, W, Zn, Mo and Cu bivalent metals*

##### 4.3.4.1 *Outcropping Mamu Formation*

The marsh unit contains significantly lower Pb, Sn, Zn and Cu concentration when compared with the bay and central basin units (Appendix 2.1a, Fig. 4.5c-d). The bay unit shows more enrichment in Pb, Sn, Mo and W when compared with the central basin unit that has a much higher Zn concentration (Appendix 2.1a, Fig. 4.5c-d). A large proportion of the central basin samples have Sn, W, Mo and Zn below the respective UCC limits, whereas 58% of the samples show enrichment in Cu above the UCC limit. In addition, sizeable proportions of the marsh samples have W, Zn, and Cu below the respective UCC limits, whereas a majority of the bay samples shows enrichment in W, Mo, and Cu as well as depletion of Zn when compared with the respective UCC means. Furthermore, all the samples show enrichment in Pb above the UCC limit, whereas a sizeable proportion show enrichment in Mo above the UCC limit.

On the eastern margin (Odoma et al., 2015), all the samples show enrichment in Pb above the UCC limit (Appendix 2.1a, Fig. 4.5c-d). In addition, 53% and 26% of the samples show enrichment in Zn and Cu, respectively, when compared with the UCC.

In general, the outcropping units along the western margin show higher levels of Pb and Sn than the eastern margin, which shows more enrichment in Zn (Appendix 2.1a, Fig. 4.5c-d).

##### 4.3.4.2 *Well data*

###### 4.3.4.2.1 *Mamu Formation*

All the well samples show enrichment at or above the UCC concentration of W, whereas the bulk of the well samples show depletion in Mo. Excluding a few samples from the Idah-1 well,

all others are depleted in Sn and Cu when compared with the respective UCC average (Appendix 2.1a, Fig. 4.5c-d). A very large proportion of the samples from the Idah-1 and Nzam-1 wells shows enrichment above the UCC limits for Pb and Zn (Appendix 2.1a, Fig. 4.5c-d). The samples from Idah-1 well in particular shows very high levels of Pb and Zn as well as Sn in some intervals. The Owan-1 and Amansiodo-1 wells show some distinction, as a large proportion of the samples from both wells is depleted in Zn when compared with the centrally located wells (Appendix 2.1a, Fig. 4.5c-d). In addition, all the samples from the Amansiodo-1 well show enrichment above the UCC for Pb, whereas only 28.6% of samples from the Owan-1 well have Pb concentration above the UCC.

#### 4.3.4.2.2 *Pre-Santonian Units*

All the samples from the Awgu Group across the wells are enriched in Pb, W and Zn above the respective UCC, whereas by contrast, are depleted in Sn (Appendix 2.1a, Fig. 4.5c-d). The samples from Akukwa-II well show higher levels of Zn, W, Mo and Cu, thus contrasting with samples from the Amansiodo-1 well. In addition, nearly all the samples from the Akukwa-II well are enriched above the UCC limits for Mo and Cu, whereas a lower proportion of samples from the Amansiodo-1 well (60% and 53.3% respectively) are enriched above the respective UCC.

A very large proportion of the samples from the Eze-Aku Group show enrichment in Pb, W, Zn, Mo, and Cu, whereas all the samples are depleted in Sn (Appendix 2.1a, Fig. 4.5c-d). In addition, the Eze-Aku group is more enriched in Mo, W, and Zn when compared with samples from the Awgu Group.

In general, the pre-Santonian units show enrichment in W, Zn, Mo, and Cu when compared with data from the post-Santonian Units (Appendix 2.1a, Fig. 4.5c-d). There is significantly more

enrichment of Pb in the Mamu Formation when compared with data from the pre-Santonian Awgu and Eze-Aku Groups.

## 4.4 Discussion

### 4.4.1. Degree of chemical alteration

The order of stability of major elements as suggested by Anderson and Hawkes (1958) implies that Si, Fe, Ti and Al are the most stable elements. Thus, the proportion of major elements can provide some clues as to the degree of chemical alteration in the source region. The most depleted elements are Na, Ca, and Mg, which is indicative of a high degree of initial weathering. The exception is the Eze-Aku Group in the Akukwa-II well and the Mamu Formation in Amansiodo-1 well that are enriched in non-silicate Ca, Na/K, Mg/K, K/Al and Na/Al, which reflects the proportion of less stable minerals like plagioclase, biotite, chlorite, smectite, vermiculite and illite relative to more stable K-feldspar, illite and Kaolinite has been shown to track the degree of weathering of crustal material (Nesbitt et al., 1980).

A higher degree of chemical alteration is inferred for the outcropping units on the western and eastern margins as well as the samples from the Owan well based on the low Na/Al, K/Al, Mg/K and Na/K. This is illustrated further by the major element distribution [(Na, Ca, Mg) <K<Ti<Fe<Al] as well as low Mg/Ti (Appendix 2.1a, c, Fig. 4.4a-b, 4.6a-c). In addition, higher Na/Al, K/Al, Mg/K (Appendix 2.1c, Fig. 4.6c) recorded for the central basin mudstones as well as the samples from the eastern margin (Odoma et al., 2015) suggests relatively lower degrees of chemical alteration. This is adduced to authigenic illite and smectite formation arising from an increase in salinity (Edegbai et al., 2019b; Edegbai et al. (in review)).

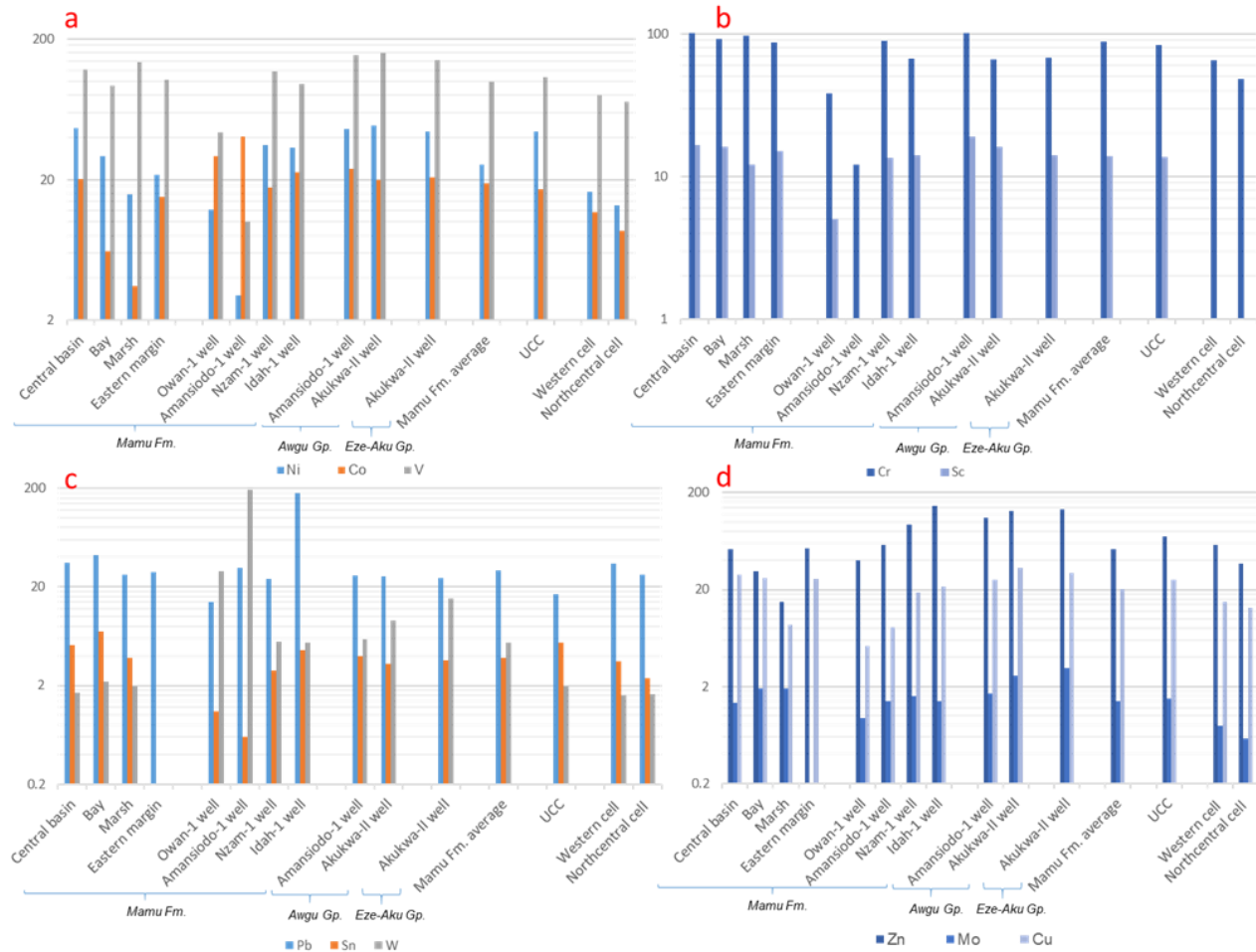


Fig. 4.5. Variograms showing the median concentrations of TTE as well as Pb, Sn, W, Zn, Mo, and Cu for all sample locations as well as regional data from western and northcentral Nigeria (Lapworth et al., 2012).

Furthermore, in comparison with the outcropping units, data from the Amansiodo-1 well as well as the more centrally placed Nzam-1 and Idah-1 wells show much higher Na/Al, K/Al, Mg/K, Na/K, Mg/Ti values (Appendix 2.1c, Fig. 4.6c). This indicates a lower degree of chemical alteration regardless of carbonate dilution (calcite cement) in the Amansiodo-1 well (Na<K<Mg<Ti<Al<Fe <Ca) that has modified the major element distribution pattern. We hypothesize that the higher salinities in these areas as suggested by early Maastrichtian paleogeographic reconstruction (Edegbai et al., 2019a) may account for some increment in the Na/Al, K/Al, Mg/K, Na/K, Mg/Ti values as well as the extent of mixing from provenance regions



(discussed in section 4.3.1.2.1). In addition, data from the eastern margin as well as the central basin mudstones, which show higher K relative to Ti (which increases with higher Mg/Ti) further illustrates this.

The data from the Awgu Group is comparable to those observed in the Nzam-1 and Idah-1 wells) except in Mg/Ti, which is much higher (Appendix 2.1c, Fig. 4.6c). The observed major element trend (Ca<Na<Ti<Mg<K<Fe<Al) at the Amansiodo-1 well is distinct from that of the Awgu (Ca<Ti<Na<Mg<K<Fe<Al) and Eze-Aku (Ti<Mg<Na<K<Ca<Fe<Al) groups observed at the Akukwa-II well, which have lower Ti relative to Na, Mg and K (Appendix 2.1a, Fig. 4.4a-b, 4.6c). This implies a higher degree of chemical alteration of the Awgu Group in the Amansiodo well.

In general, regardless of carbonate dilution in the samples from the Eze-Aku Group, we can infer that a much lower degree of chemical alteration and consequently mineralogical immaturity persists in the pre-Santonian units when compared with the Mamu Formation. This is based on the much higher Na/Al, K/Al, Mg/K, Na/K, Mg/Ti (Appendix 2.1c, Fig. 4.6c), as well as higher percentages of smectite, illite and mixed layered clays reported for these units, in comparison to those reported for the Mamu Formation (Petters and Ekweozor, 1982; Odigi, 2007; Edegbai et al., 2019b). Furthermore, our findings are consistent with published results of petrographic analysis, which reported textural and mineralogical immaturity of the pre-Santonian units as distinct from the more texturally and mineralogically mature post-Santonian units of which the Mamu Formation subsists (Hoque, 1977; Amajor, 1987; Odigi, 2007; Igwe, 2017). This is in spite of the humid equatorial climatic conditions that prevailed at during the Cenomanian-Turonian and Campanian- Maastrichtian stages (Chumakov et al., *in* Hay and Floegel, 2012).

#### 4.4.2 *Source rock composition*

Some trace elements common to felsic and mafic rocks have reduced mobility when subjected to weathering, erosion, transportation, and diagenesis (Bhatia and Crook, 1986; Wronkiewicz and Condie, 1990; McLennan and Taylor, 1991; Cullers, 1995, 2000; Potter et al., 2005). Consequently, their concentrations in sedimentary rocks can give valuable insight in provenance studies Cullers (2000). In our earlier investigation, we successfully used this technique to determine the provenance of the outcropping units at the western margin (Edegbai et al., 2019b).

To reduce the uncertainty regarding the accuracy of provenance determination using trace elements, we utilized trace elements whose concentrations are least affected by redox conditions. The Th/Sc vs. La/Sc, TiO<sub>2</sub> vs. Zr, Th/Sc vs. Sc, as well as Th/Sc vs. Zr/Sc discriminant plots (Cullers, 2000; McLennan and Taylor, 1991; McLennan et al., 1993) (Fig. 4.7a-h) highlight intra- and interformational variation in the geochemical characteristics of the pre-Santonian units and the Mamu Formation, which are useful in determining the chemical composition of source units. . Furthermore, we assume that the sediments preserve the geochemistry of the sediment provenance regions.

Samples from the pre-Santonian units show a uniform Sc concentration (averaging ~ 15ppm) (Fig. 4.7e-f), whereas the Th, Zr and La content of these units are highly variable (Fig. 4.7a-h, Appendix 2.1b). The geochemical characteristics of the pre-Santonian units suggests a basement source rock with compositional variability as shown by the Th/Sc < 1 (Fig. 4.7c-f) (McLennan and Taylor, 1991). This is illustrated further by the Th/Sc vs. Zr/Sc binary plot (McLennan et al., 1993) (Fig. 4.7g-h), which indicate that these units were not sourced from reworked older sedimentary rocks.

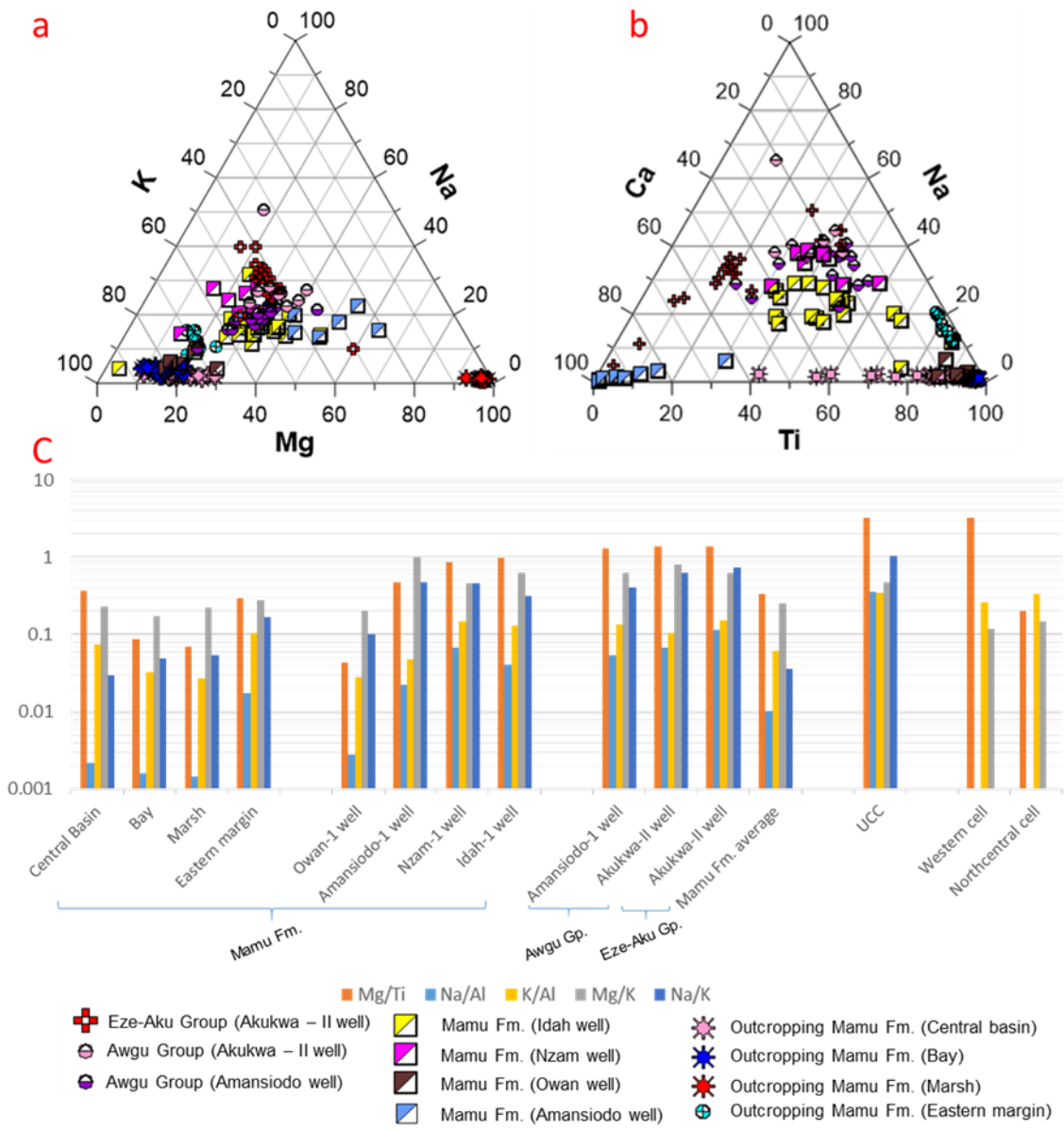


Fig.4.6.a,b Ternary plots showing the distribution of K, Na, Mg, Ca, Na and Ti concentrations of all sample locations as well as a variogram of median values of Mg/Ti, Mg/K, Na/Al, and K/Al

#### 4.4.2.1 Pre-Santonian Units

Intraformational compositional variability is visible in the Awgu Group (across the Amansiodo-1 and Akukwa-II wells) as well as the Eze-Aku Group. In the Akukwa-II well, a mafic to intermediate source rock composition is inferred due to the much lower Th, Zr, La and other HFSE concentrations, whereas in the Amansiodo-1 well, which has much higher concentration of

HFSE, an intermediate to felsic source rock composition is inferred (Appendix 2.1b, Fig. 4.4c-d, 4.7a-d). The observed spatial variation in degree of chemical alteration in the Awgu group (highlighted in section 4.4.1) is in part due to the more felsic nature of the source rocks for the sediments from the Amansiodo-1 well.

The Eze-Aku unit shows source rock composition varying from (predominantly) mafic to felsic basement rocks owing to a range of Th, Zr, and La concentrations, which are the lowest among the pre-Santonian units (Appendix 2.1b, Fig. 4.4c-d, 4.7a-d).

#### *4.4.2.2 Mamu Formation*

Samples from the pre-Santonian units show a non-uniform Sc concentration as well as variable Th, Zr, and La concentrations. This depicts a (predominant) felsic to intermediate source composition (Fig 4.7b, d, f) hypothesized to be derived from reworked pre-Santonian units as well as (predominantly) silica rich igneous and metamorphic rocks. Evidence for recycling of pre-Santonian units is illustrated by a higher degree of chemical alteration (see section 4.4.1), low index of compositional variability (Edegbai et al., 2019b), a large proportion of the samples having  $Th/Sc > 1$  (characteristic of recycled sedimentary rocks), as well as inferences from  $Th/Sc$  vs.  $Zr/Sc$  and  $Th/Sc$  vs.  $Sc$  (Fig. 4.7f, h) discriminant plots (McLennan and Taylor, 1991; McLennan et al., 1993). In addition, the better textural and mineralogical maturity reported for the post-Santonian units (Hoque, 1977; Amajor, 1987; Odigi, 2007; Igwe, 2017) is attributable to a significant proportion of their provenance originating from reworked pre-Santonian units.

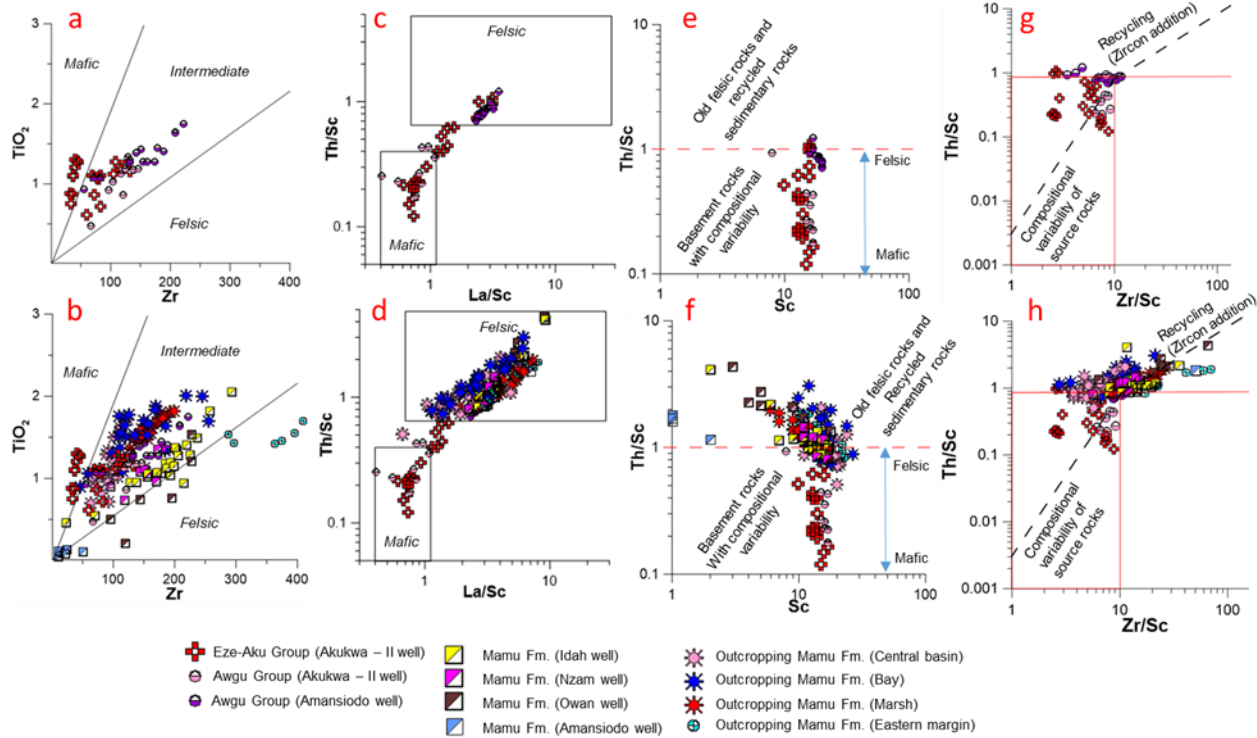


Fig. 4.7.  $TiO_2$  vs.  $Zr$  (a-b) (after Hayashi et al., 1997),  $Th/Sc$  vs.  $La/Sc$  (c-d) (after Cullers, 2000) and binary plots showing source composition of the pre-Santonian units as well as the Mamu Formation.  $Th/Sc$  vs.  $Sc$  (after McLennan and Taylor, 1991) (e-f) and  $Th/Sc$  vs.  $Zr/Sc$  (g-h) (McLennan et al., 1993) binary plots indicate variable basement sources for pre-Santonian strata as well as a combination of felsic basement rocks and recycled pre-Santonian strata sources for the Mamu Formation.

Furthermore,  $Th/Sc < 1$  reported for some samples (Appendix 2.1c), inferences from  $Th/Sc$  vs.  $Zr/Sc$  and  $Th/Sc$  vs.  $Sc$  (Fig. 4.7f, h) discriminant plots (McLennan and Taylor, 1991; McLennan et al., 1993), as well as variability in the degree of chemical alteration (discussed in section 4.4.1) provides evidence for detrital contribution from silica rich igneous and metamorphic rocks. This is further illustrated by the high concentration of W reported for the sediments (especially in the Owan-1, Amansiodo-1 and Idah-1 wells) (see section 4.3.4.2), which are much higher than those recorded for the pre-Santonian units points to detrital contribution from basement rocks, as W is not known to survive several weathering and sedimentation cycles (Imeokparia, 1982a).

#### 4.4.3 Provenance

Leveraging on the reports of geochemical observations of the northcentral and southwestern basement complex, as well as Pb-Zn deposits in southern Benue trough (Imeokparia 1982a, 1982b, 1983; Olade et al., 1979; Olade, 1987; Lapworth et al., 2012), we attempted to work out the dominant source regions in different parts of the Anambra Basin during the late Campanian to early Maastrichtian time.

Three of the factors controlling element associations, which were identified by Lapworth et al (2012), proved to be quite useful in this study. These are:

- a) An iron-oxide/hydroxide and ilmenite factor, which explains the low to moderate positive covariation between Fe and Cu, Cr, Mo, V, Zn, Co, Sn, and Ti. The presence of ilmenite allows for a positive covariance between Fe and Ti or Sn;
- b) A mafic factor, which explains the positive covariation between Fe, Mn, and Mg due to the presence of ferromagnesian minerals such as olivine, pyroxene, hornblende, and biotite;
- c) A coltan factor. Coltan abundance covaries positively with Ta, Nb, Ti, Sn, and W.

##### 4.4.3.1 Mamu Formation:

On the western margin, the outcropping units show a broad Pb-Zn covariation (Fig. 4.8a-c), as well as an enrichment of Pb over Zn ( $Pb/Zn > 1$ ) (Appendix 2.1c). There is a moderate influence from moderate Fe-oxide/hydroxide factor, which is observed only in the more proximal marsh unit as well as a strong to moderate coltan influence for Sn and W as shown by the positive Sn and W covariation with Nb, Ta and Ti (Fig. 4.8a-c). The Sn vs. Pb and W vs. Pb show a broad distribution in the bay unit, whereas a moderate positive covariation is observed in the central basin and marsh units (Fig. 4.8a-c).

On the eastern margin, a weak positive Pb-Zn covariation exists with  $Pb/Zn < 1$ . In addition, there is a strong influence from the mafic factor as well as a minimal influence from the Fe-oxide/hydroxide/ilmenite factor. The absence of Sn and W data prevents a discussion of the coltan factor. However, a moderately positive Pb vs. Nb covariation (Fig. 4.8d) suggests some potential influence by the coltan factor.

There is a coltan source, which exerts a minor influence on the distribution of Ti, Sn, and W in samples from the Owan-1 well (Fig. 4.8e). By contrast, the distributions of Sn and W are strongly controlled by the ilmenite factor as shown by the strong positive covariation of Ti with Sn, Fe and W (Fig. 4.8e). There is also a moderate influence from a mafic source as well as a good Pb-Zn covariation ( $Pb/Zn < 1$ ). In the Amansiodo-1 well, there is a moderate mafic factor influence, a broad Pb-Zn covariation ( $Pb/Zn < 1$ ), as well as a strong Fe-oxide/hydroxide/ilmenite factor (Fig. 4.8e). In contrast to the sediments from the Owan-1 well wherein a moderate positive covariation of Pb vs. Sn is observed, the sediments from the Amansiodo-1 well show a broad Pb vs. Sn covariation as well as a moderate positive coltan influence for Ti and Sn (Fig. 4.9a). Furthermore, in the Owan-1 well there is broad W vs. Pb covariation as well as good W vs. Zn covariation (Fig. 4.8e), whereas the Amansiodo-1 well there is a good positive W vs. Pb covariation as well as a moderate positive W vs. Zn covariation (Fig. 4.9a).

The Pb vs. Zn shows a poor covariation in sediments from the Idah-1 well ( $Pb/Zn > 1$ ), which becomes moderate in the Nzam-1 well ( $Pb/Zn > 1$ ) (Fig. 4.8b-c). The influence of a coltan source for Sn and W improves from being weak in the Idah-1 well samples to moderate in the Nzam-1 well samples (Fig. 4.8b-c). In addition, the influence of the mafic factor as well as the Fe-oxide/hydroxide factor is moderate in samples from these wells (Fig. 4.8b-c).

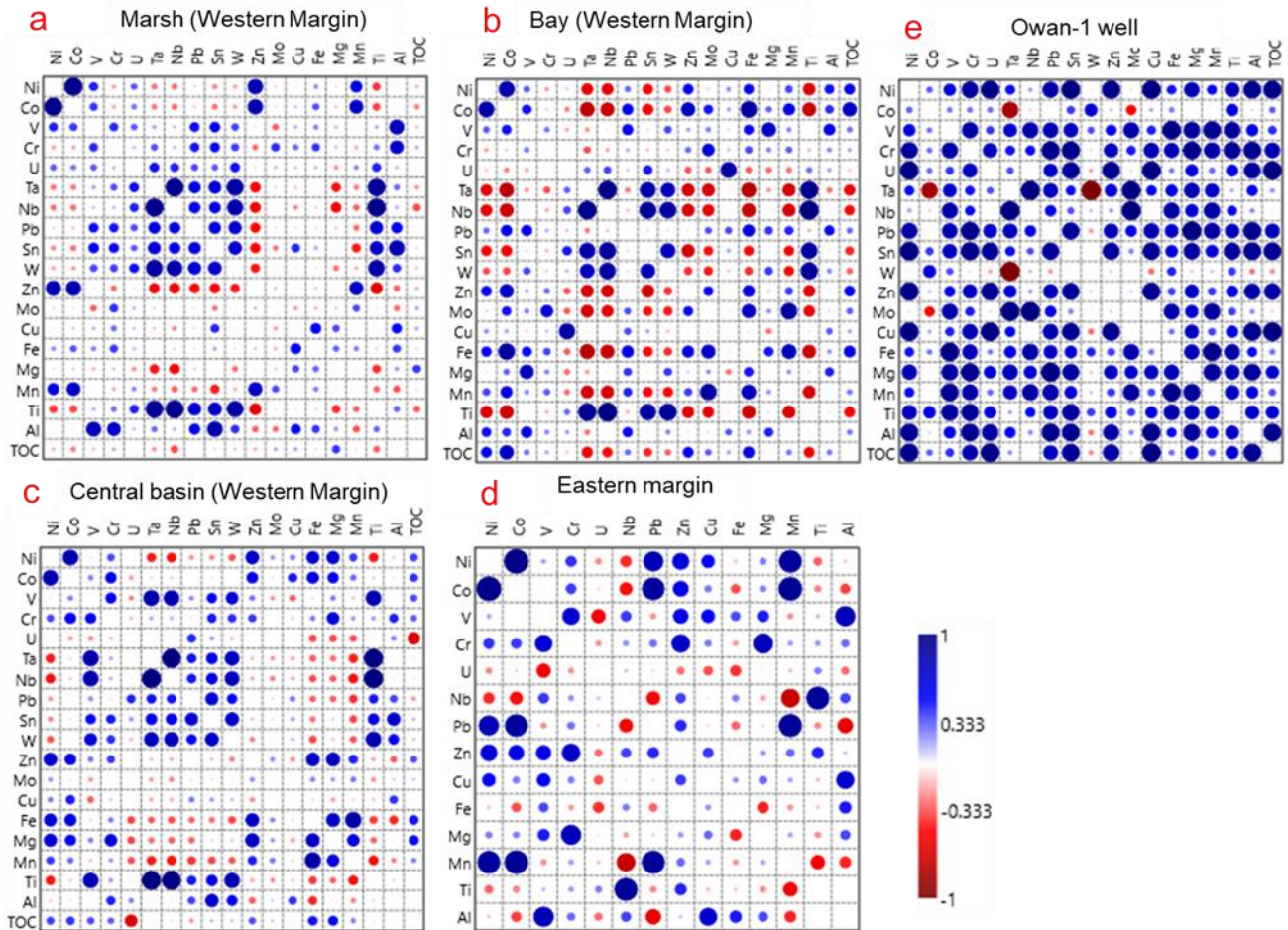


Fig. 4.8. Correlation matrix for major and element abundances as well as TOC in sediments of the Mamu Formation on the western and eastern margins as well as the Owan-1 well

#### 4.4.3.2 Awgu Group

As observed earlier, this unit exhibits strong spatial geochemical variability. In sediments from the Amansiodo-1 well, the Fe-oxide/hydroxide/ilmenite influence is minimal to non-existent (Fig. 4.9d). There is also a strong mafic component as well as good positive Pb-Zn covariation (Fig. 4.9d) (median Pb/Zn = 0.23). Conversely, the sediments from Akukwa-II well show a moderate positive Pb-Zn covariation (median Pb/Zn = 0.17), as well as a fair to strong influence from the mafic and Fe-oxide/hydroxide/ilmenite factors (Fig. 4.9e).



Furthermore, whereas the sediments from the Akukwa-II well show a strong positive covariation of Ta with Sn as well as a strong negative covariation of W with Ta (Fig. 4.9e), the sediments from the Amansiodo-1 well show the opposite. This is illustrated by the moderate covariation of Ta with W as well as a strong negative covariation of Sn with Ta (Fig. 4.9d).

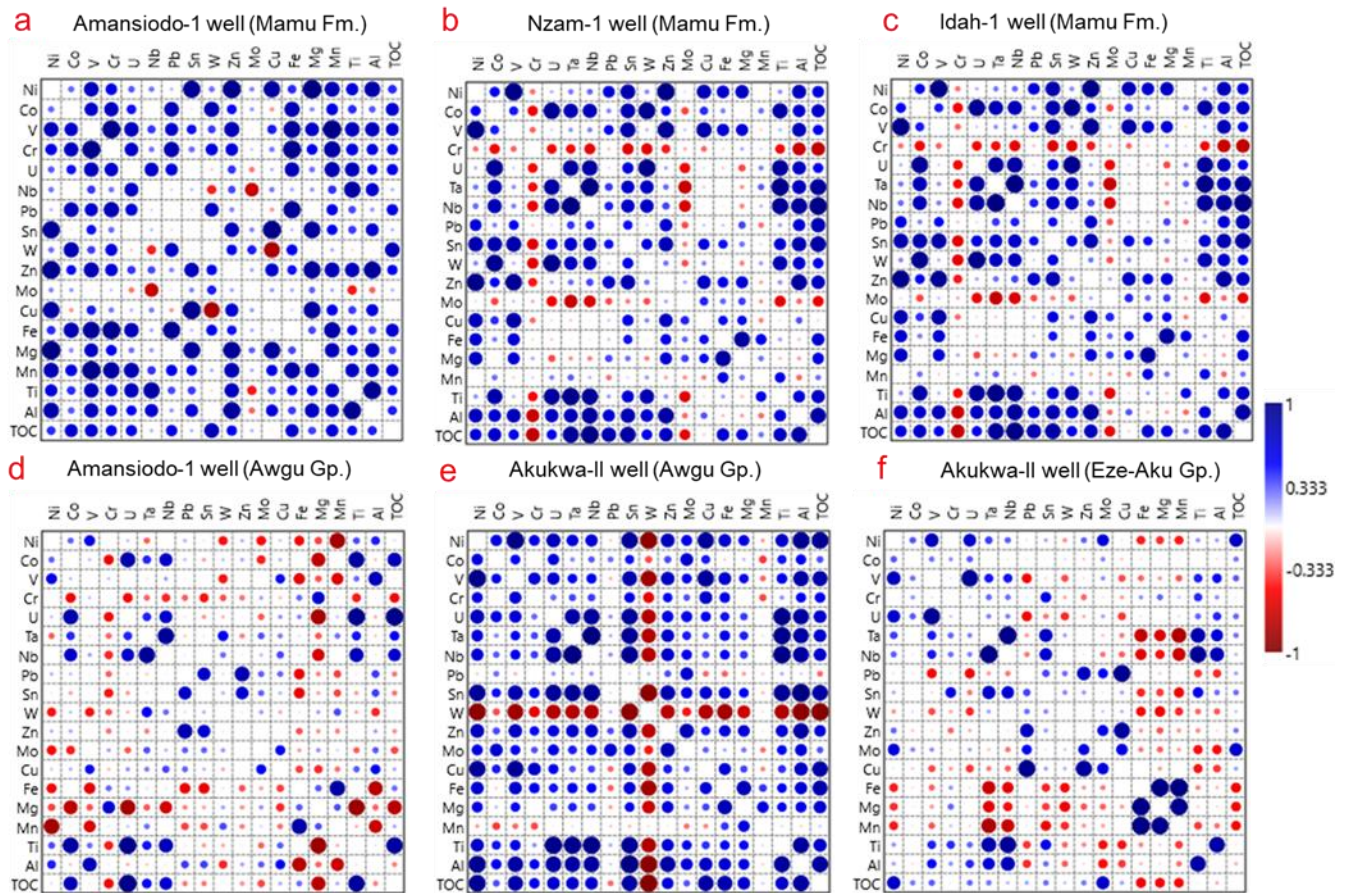


Fig. 4.9. Correlation matrix for major and element abundances as well as TOC in sediments of the Mamu Formation and pre-Santonian units

#### 4.4.3.3 Eze-Aku Group

In the Eze-Aku Group, the influence of the coltan, mafic, as well as the Fe-oxide/hydroxide components are strong (Fig. 4.9f). Sn moderately covaries positively with Nb, Ta, and Ti, whereas W shows a broad to moderately negative covariation with Nb, Ta and Ti (Fig. 4.9f). There is a good positive Pb-Zn covariation (median Pb/ Zn = 0.22).

In general, the pre-Santonian units show a stronger mafic influence as well as a stronger Pb-Zn covariation, which is a function of the composition of the source rocks (section 4.4.2).

#### 4.4.4 *Differentiation of provenance regions*

##### 4.4.4.1 *Pre-Santonian units*

Based on field observations, petrographic studies and paleocurrent measurements, earlier studies favoured the granites, gneisses and metasediments in the eastern highlands and southwestern basement complex of Nigeria (Fig. 4.2) (Hoque, 1977; Odigi, 2007; Igwe, 2017, Edegbai et al., 2019b) as the provenance sources for the pre-Santonian units. The identification of a dominant mafic provenance for the Eze-Aku unit from our data (Fig. 4.7a, c, e), which is strengthened by the strong mafic factor influence as illustrated by the strong positive covariation between Fe vs. Mg, Fe vs. Mn as well as negative covariations of Fe vs. Pb and Fe vs. Sn (Fig. 4.9f) (Lapworth et al., 2012) is quite an interesting find as this has only been advanced for the Asu-River Group (Odigi, 2007).

The basement complex in the eastern highlands have been adduced to be the provenance for the Awgu and Eze-Aku groups in the eastern segment of the Anambra Basin (Odigi, 2007, Dim et al., 2016). However, we hypothesize a significant detrital contribution from the mineralized biotite granites as well the basement complex rocks of northcentral Nigeria (Fig. 4.10a-b) due to the Nb, Ta and W that are above the respective UCC as well as Sn (Appendix 2.1a-b, Fig. 4.4c, 4.5c). A strong detrital contribution from northcentral Nigeria is adduced to be responsible for the distinct geochemical character observed in the sediments from Amansiodo-1 well in comparison to the Akukwa-II well. This is illustrated by the more felsic character of the sediments, higher degree of chemical alteration, higher Th, U, Nb, Ta, Sn (Fig. 4.4c, 4.5c, Appendix 2.1a-b), higher

enrichment of Nb over Ta (Kinnaird, 1984), as well as inference from the Nb/W vs. Nb/Ta bivariate plot (Fig. 4.10a). Conversely, the sediments from Akukwa-II well, which show a higher W (Fig. 4.5c) as well as the strong negative to broad Ta vs. W covariation (Fig. 4.9e-f) strongly suggests a large proportion of detrital contribution from the eastern highlands (Fig. 4.10a-b) whose pegmatites are enriched in W, but barren with respect to Sn, Ta and Nb (Edem et al., 2015, 2016).

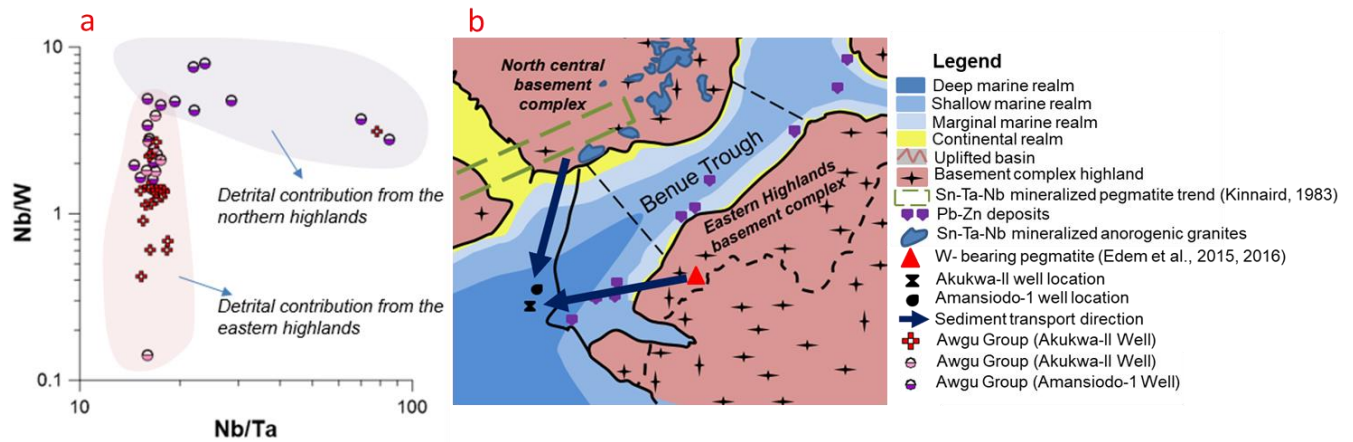


Fig. 4.10. a, Nb/W vs. Nb/Ta binary plot differentiating provenance regions of pre-Santonian units. b, conceptual early Turonian paleogeographic model showing contribution from eastern and northcentral highlands

Furthermore, we hypothesize a spatio-temporal variation in detrital contribution from the various lithostratigraphic units that make up the eastern highlands and northcentral Nigeria. Detrital contribution was more from mafic rocks in the latest Cenomanian to early Turonian, whereas from middle Turonian to Coniacian the detrital contribution was more from felsic sources (Fig 4.7a-f). This is consistent with the findings of Odigi (2007).

#### 4.4.4.2 Mamu Formation

From the geochemical characteristics highlighted above, we hypothesize that the Mamu Formation is sourced from basement complex rocks as well as recycled pre-Santonian strata. In

addition, we can distinguish three broad provenance regions: a Northern provenance, Western provenance, and an Eastern provenance (Fig. 4.11).

#### 4.4.4.2.1 *Western provenance region:*

This region comprises of the southwestern basement complex rocks as well as pre-Santonian units, relics of which exist as inliers within the basement complex rocks (Fig. 4.11). In general, this provenance region is characterized by a strong coltan factor controlling the enrichment of Nb, Ta, Sn, W (and Pb to a certain extent), high levels of Th, U, Ta, Nb, Sn, Pb as well as higher Pb/Zn ( $Pb/Zn > 1$ ) when compared to the eastern province. Leveraging on published data (Lapworth et al., 2012; Nton and Adamolekun, 2016), the main difference between the western provenance terrain from those of the southwestern portion of the northcentral province is the much higher Pb abundance, which is consistent with the findings of Lapworth et al., (2012). There is some variability in the element pattern of the western provenance, as a portion of it is not strongly influenced by the coltan factor as shown by much lower Pb, Sn, Nb, Ta, and Y concentrations, lower Pb/Zn ( $Pb/Zn < 1$ ), as well as much higher W recorded from sediments of the Owan-1 well. The very weak positive covariation for Nb vs. Ti and Nb vs. Sn illustrate further evidence for this (Fig. 4.8e). In addition, the good positive covariation between Ti vs. Sn suggests an alternative source for Ti instead of coltan, which is suspected to be ilmenite (Lapworth et al., 2012) as well as minerals in the ilmenite-geikielite ( $MgTiO_3$ ) and ilmenite-pyrophanite ( $MnTiO_3$ ) solid solution series due to good to moderate positive covariation of Ti vs. Fe, Mn, and Mg (Fig. 4.8e). These Titanium bearing minerals have been documented to occur in the southwestern basement complex rocks (Elueze *in* Mücke and Woakes, 1986; Bafor *in* Mücke and Woakes, 1986; Mücke and Woakes, 1986).

#### 4.4.4.2.2 *Eastern provenance region:*

The eastern provenance region (Fig. 4.8) comprises of the pre-Santonian strata from the Southern Benue Trough as well as the basement complex rocks from the eastern highlands (Fig. 4.11). In general, higher Zn, TTE, Cu, Mo, and major element (excluding Al and Ti) concentrations, much lower Pb/Zn ratios ( $Pb/Zn < 1$ ), a strong W enrichment (Edem et al., 2015, 2016) as well as lower levels of Nb, Ta and Sn in comparison with the northern and western provenance regions characterize the eastern provenance. In addition, there exists a good positive Pb vs. Zn covariation, as well as a less strong coltan influence for Sn, which in contrast with the western provenance region shows a broad or strong negative covariation with W. The much higher major element concentrations characteristic of this provenance region is a function of the strong mafic influence on the sediments.

#### 4.4.4.2.3 *Northern provenance region:*

The anorogenic biotite granites as well as the basement complex rocks in the northcentral provenance region is hypothesized to have contributed detritus for sediments in the northern segment of the basin, sediments close to the western margin, the area around the Amansiodo-1 well, as well as intervals within the Idah-1 well. We came to this conclusion because some intervals in the Idah-1 well have W concentration above 23.2 ppm (Fig. 4.12a), which is the highest W concentration reported for stream sediments draining the southwestern portion of the northcentral basement complex (Lapworth et al., 2012). High levels of W concentration have been reported for the biotite granites in the Afu complex, northcentral Nigeria (Imeokparia, 1982a, 1982b). In addition, these units show high levels of Nb, Y, Th, Zn, Ti, and U, higher enrichment of Nb over Ta (Kinnaird, 1984), as well as low V and Pb/Zn ( $Pb/Zn < 1$ ).

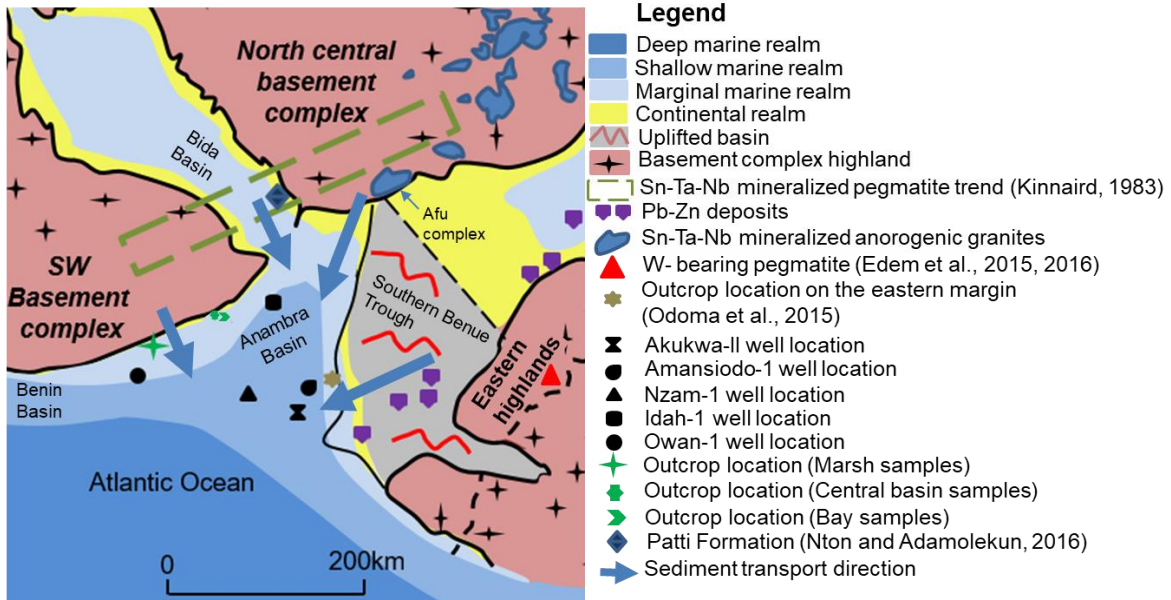


Fig. 4.11. Provenance regions of the Anambra Basin

#### 4.4.4.3 Mixing of provenance regions

Our published data on the outcropping units on the western margin posit that the marsh samples are the most proximal units of the dark mudstone lithofacies (Edegbaei et al., 2019b). This implies that the geochemistry of this unit is the least influenced by mixing from the northern and eastern provenance regions. The bay samples are the most affected by mixing as illustrated by higher median concentrations of HFSE as well as Pb, Sn, and W recorded from the bay samples (Fig. 4.12a-d) when compared with the marsh and central basin samples. This is due to contribution from multiple source regions as depicted by the broad distributions of Pb vs. Sn and W vs. Pb (Fig. 4.8b), the fractionation (concentration gradient) of Pb, Nb, W, and Sn between the outcropping Patti Formation (Bida Basin), sediments from the Idah-1 and Owan-1 wells, as well as the outcropping Mamu Formation on the western margin (Fig. 4.12a-d).

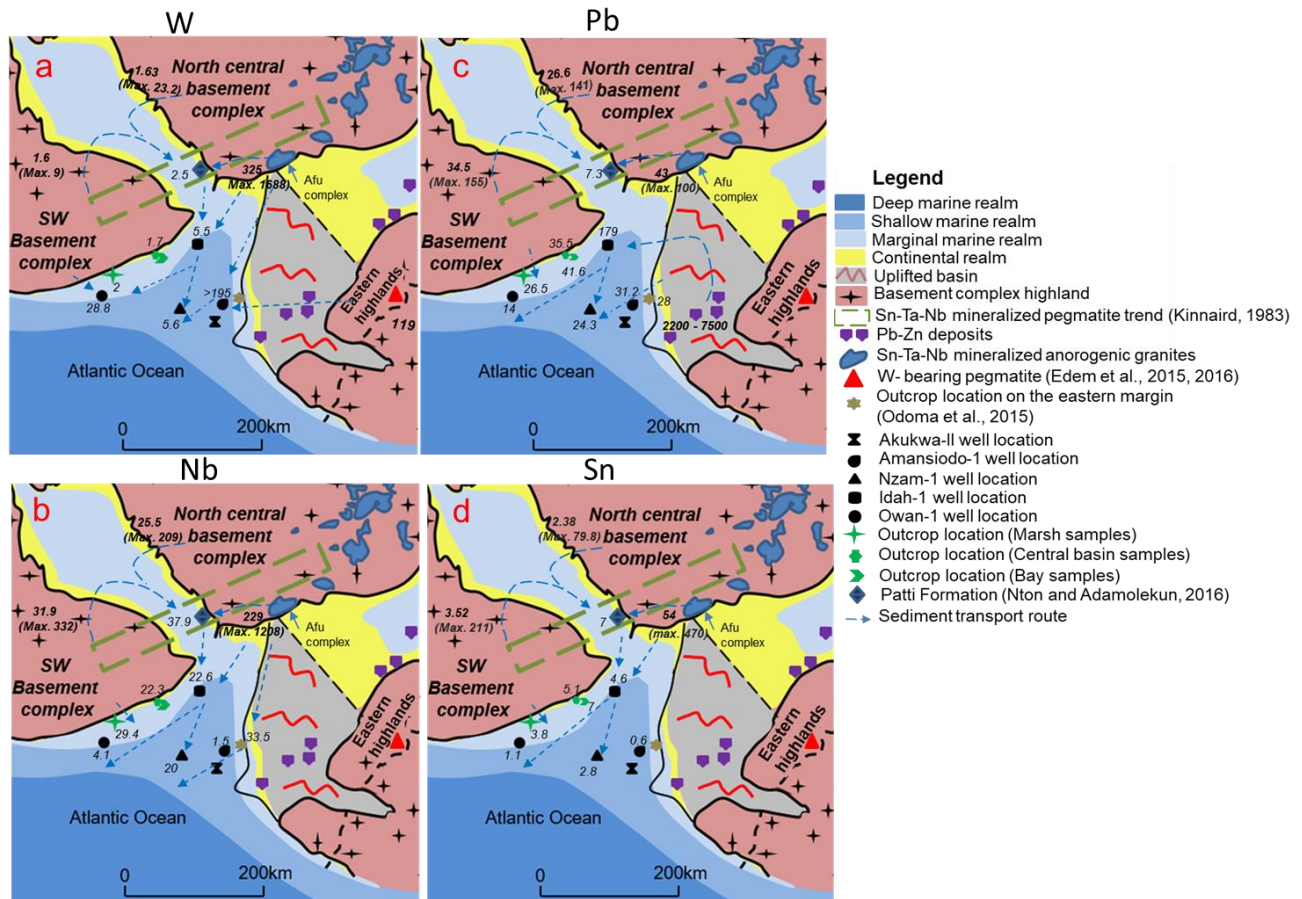


Fig. 4.12. Evidence of mixing of provenance regions deduced from median concentrations of Pb, W, Nb, and Sn from spatial units of the Mamu and Patti formations

The sediments of the more centrally located Idah-1 and Nzam-1 wells also show clear evidence of mixing of source terrains. This is clearly illustrated by the Pb/Nb vs. Pb/Sn as well as the Pb vs. Sn bivariate plots (Fig 4.13a-b). We hypothesize that the high Pb values associated with sediments from the Idah-1 well is due to mixing of detritus from all three-provenance regions, as concentrations well above the lower thresholds for Pb and Zn (100 ppm and 200 ppm respectively) in Pb-Zn mineralized regions of the eastern provenance (Olade et al., 1979; Olade, 1987) abound. In addition, the high levels of W recorded in some intervals in the Idah-1 well as well as the Amansiodo-1 well (Appendix 2.1a) are within the range reported for the Sn-Nb-Ta mineralized

biotite granites of the Afu complex (Imeokparia, 1982a) located in the Northcentral provenance region.

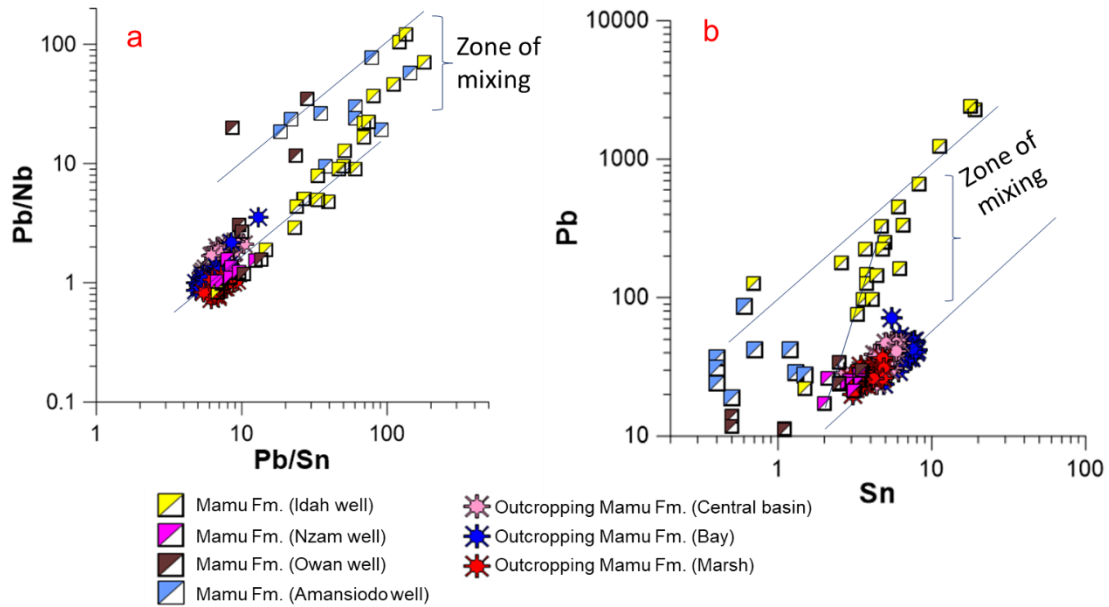


Fig 4.13.  $Pb/Nb$  vs.  $Pb/Sn$  (a) and  $Pb$  vs.  $Sn$  (b) binary plots showing further evidence of mixing of source regions

#### 4.5 Conclusion

This study reports the following findings:

- The pre-Santonian units are sourced from compositionally variable basement complex rocks, ranging from felsic to mafic in composition.
- There is evidence for spatio-temporal variability in the detrital contribution from the basement complex rocks. Detrital contribution was more from mafic rocks in the latest Cenomanian to early Turonian, whereas from middle Turonian to Coniacian the detrital contribution shifted to more felsic sources.
- The provenance of the Mamu Formation is from felsic source rocks comprising of basement complex rocks as well as recycled pre-Santonian rocks. The significant detrital



contribution from basement complex rocks provides clear insight regarding to the origin of large sand volumes in the post-Santonian Anambra basin. These hitherto could not be accounted for, due to the predominance of argillaceous and carbonate rocks in the Southern Benue Trough

- Three provenance regions comprising the northern, western, eastern sectors contributed detritus during the Campano-Maastrichtian with evidence of mixing of provenance sources.
- The Mamu Formation shows evidence of secondary Pb, Sn, and W mineral accumulation.

### **Acknowledgement**

This research received support from University of Benin Research and Publications Committee, the Fulbright Commission (15160892), the Niger Delta Development Commission (NDDC/DEHSS/2015PGFS/EDS/011), and DAAD (ST32 - PKZ: 91559388). Julius Imarhiagbe and Reuben Okoliko assisted with fieldwork and sampling of cuttings and core at the Nigerian Geological Survey Agency respectively. In addition, the first author wishes to acknowledge the motivation, guidance and instruction provided by Prof. W.O. Emofurieta and Mr. Sam Coker during the early phase of this research

**Appendix 2.1a-c: Summary table showing the results of elemental and TOC analysis as well as elemental ratios**

*Appendix 2.1a*

S/N	Lithostratigraphic Unit	Location	Ca	Fe	K	Mg	Mn	Na	Ti	Al	TiO <sub>2</sub>	TOC	Pb	Sn	W	Zn	Mo	Cu
U1 IA	Mamu Formation	Western margin (Marsh subenvironment)	0.021	0.94	0.32	0.07	0.004	0.015	0.91	8.05	1.68	1.4	27.8	3.6	2.1	14	3	7.1
U1 IC			0.014	0.57	0.26	0.05	0.003	0.015	0.83	6.83	1.58	1.3	21.9	3.2	1.7	14	2.6	8.7
U1 2A			0.014	1.19	0.30	0.05	0.003	0.015	0.89	7.89	1.68	1.2	23.4	3.8	2	9	2.2	7.7
U1 2B			0.014	0.72	0.23	0.04	0.003	0.015	0.80	6.46	1.48	1.2	26.5	3	1.7	18	0.9	4.6
U1 2C			0.014	0.57	0.31	0.06	0.003	0.015	0.94	7.89	1.79	1.0	32.4	3.5	1.9	9	2.3	4.2
U1 3A			0.014	1.09	0.32	0.06	0.004	0.015	0.93	7.73	1.75	1.2	25.6	3.7	2.2	15	1.1	6
U1 3B			0.014	0.86	0.38	0.07	0.003	0.022	0.95	9.10	1.81	1.2	28.6	4.3	2.2	15	1.9	5.8
U1 5A			0.021	0.80	0.36	0.07	0.004	0.022	0.90	11.70	1.63	1.2	29.1	4.1	2	15	2.5	6.5
U1 5B			0.021	0.92	0.36	0.07	0.004	0.022	0.85	12.54	1.56	1.8	27.7	4	2	12	2	5.1
U1 6A			0.021	0.87	0.37	0.07	0.003	0.015	0.87	11.75	1.60	1.2	25.6	4.1	2.2	13	1.1	6.6
U1 7A			0.029	1.84	0.25	0.08	0.006	0.022	0.76	10.69	1.47	1.1	23.8	3.2	1.7	211	2.1	27.4
U1 7B			0.014	0.60	0.27	0.07	0.004	0.015	0.87	9.84	1.60	1.0	25.9	3.7	1.9	83	1	11.3
U1 8A			0.014	1.45	0.23	0.07	0.004	0.007	0.78	10.50	1.36	1.1	23.9	3.6	1.5	139	0.8	15.6
U1 8B			0.057	1.27	0.25	0.08	0.008	0.022	0.87	7.62	1.64	1.0	26.2	3.5	2	132	1.4	10.6
U1 8C			0.014	0.49	0.17	0.05	0.008	0.015	0.80	5.72	1.46	1.2	20.1	3.1	1.8	241	3.8	6.8
U1 8D			0.014	0.66	0.22	0.05	0.004	0.022	0.82	8.36	1.55	1.2	27.2	3.7	1.9	155	0.7	6.8
U1 9B			0.014	1.67	0.27	0.05	0.007	0.015	0.93	10.22	1.69	1.0	31.4	3.9	2.2	38	2.5	16.3
U1 9C			0.014	0.83	0.29	0.05	0.005	0.022	0.96	11.06	1.74	1.1	30.9	4.5	2.4	33	1.3	14.2
U1 10			0.014	0.87	0.20	0.04	0.002	0.015	0.96	14.08	1.77	1.2	36.7	4.8	2.4	11	2	14
U1 18			0.014	1.76	0.26	0.04	0.003	0.015	0.97	13.07	1.82	1.1	31	4.9	2.4	10	1.5	31.4
U1 19			0.007	0.73	0.19	0.04	0.003	0.007	0.95	11.61	1.73	0.8	26.1	4.8	1.9	10	1.1	33.1
AU-1a			0.021	1.07	0.70	0.16	0.004	0.022	0.80	10.27	1.51	2.6	27.9	3.9	1.8	21	1.9	36.2
AU 2			0.021	1.55	0.88	0.21	0.003	0.022	0.81	12.13	1.49	1.0	26.2	4.2	1.8	27	1	23.1
Mean			0.02	1.0	0.3	0.07	0.004	0.017	0.9	9.8	1.6	1.2	27.2	3.8	1.9	54	1.8	13.4
Median			0.01	0.9	0.3	0.06	0.004	0.015	0.9	10.2	1.6	1.2	26.5	3.8	2.0	15	1.9	8.7
SD			0.01	0.4	0.2	0.04	0.002	0.005	0.1	2.3	0.1	0.3	3.7	0.5	0.3	70	0.8	9.9
IM 2B	Mamu Formation	Western margin (Central Basin subenvironment)	0.04	2.84	0.99	0.22	0.006	0.02	0.86	14.77	1.59	1.0	39.6	5.6	2.4	43	1.8	25.9
IM 2C			0.03	2.63	1.00	0.23	0.006	0.03	0.97	13.44	1.72	0.9	41.9	5.5	2.5	57	1.5	19.6
IM 2D			0.03	2.90	1.01	0.24	0.006	0.03	0.87	13.44	1.62	1.0	47.2	5.5	2	71	0.6	28.7
IM 2E			0.064	4.57	0.98	0.30	0.016	0.03	0.84	13.60	1.50	1.1	36.7	5.1	2.2	96	1.3	22.7
IM 4A			0.021	4.59	0.71	0.18	0.007	0.03	0.71	10.48	1.24	1.5	32	4.3	1.7	43	1	14.7
IM 11A			0.06	7.20	0.60	0.22	0.008	0.02	0.66	12.60	1.13	1.2	46.2	6.3	1.6	127	1	30.5
IM 11B			0.06	4.02	1.00	0.29	0.010	0.03	0.69	16.62	1.12	1.4	30.7	5.6	1.8	67	1	32.1

IM 11C			0.19	5.01	1.14	0.34	0.014	0.03	0.66	12.54	1.13	0.9	39.5	5.3	1.6	125	0.6	28.1
IM 13A			0.11	7.41	1.00	0.41	0.092	0.03	0.60	13.44	1.05	1.2	26.8	4.7	1.6	106	1.2	31.1
1M 13B			0.043	3.30	1.06	0.30	0.008	0.03	0.76	15.35	1.30	1.3	29.2	5.4	2.2	94	1.1	35.1
IM 14A			0.54	5.32	1.08	0.32	0.021	0.04	0.64	12.60	1.11	1.2	38.8	4.3	1.7	191	2	32.2
IM 16A			0.26	12.52	1.20	0.42	0.253	0.02	0.39	11.86	0.70	1.2	25.9	3.8	1.3	128	2.2	28.9
IM 16B			0.19	7.13	1.36	0.41	0.084	0.03	0.46	13.23	0.82	1.5	31	4	1.6	122	1.7	24.3
1M 16C			0.09	3.97	1.45	0.35	0.021	0.03	0.54	13.92	0.96	1.3	33.7	4.7	1.5	69	1.5	19.2
1M 16D			0.06	2.91	1.35	0.30	0.008	0.03	0.57	13.23	1.02	1.1	23.4	4.4	1.7	38	0.5	17.9
IM 18a			0.79	0.93	1.06	0.13	0.004	0.03	0.42	11.63	0.72	0.3	28.5	2.75	0.9	47	1.1	9.75
IM 18C			0.13	1.41	0.81	0.18	0.004	0.02	0.66	17.78	1.12	0.6	47	5.9	2.1	34	1.5	24.2
IM 19A			0.10	1.96	1.10	0.24	0.004	0.02	0.61	17.25	1.05	0.8	41.9	5.4	1.9	37	2	36.5
IM 19B			0.07	2.34	1.10	0.24	0.003	0.02	0.57	16.99	0.98	0.8	34	5.3	1.7	32	1	43.1
IM 19D			0.05	3.43	0.92	0.19	0.007	0.03	0.61	16.53	1.08	1.0	46.3	5.1	2.2	33	1	209.1
IM 19E			0.04	1.88	1.05	0.22	0.005	0.03	0.71	17.36	1.22	1.2	38.1	5.8	2.3	30	1.9	19.3
IM 2A			0.04	3.18	0.74	0.16	0.004	0.02	0.76	13.50	1.34	1.1	33.7	4.6	1.9	30	1.7	11.3
IM 4B			0.014	4.12	0.48	0.11	0.007	0.01	0.65	7.55	1.10	0.8	29.5	3.5	1.3	32	1.4	22.8
IM 14C			0.24	6.67	1.15	0.39	0.020	0.04	0.52	13.60	0.91	1.1	37.7	4.5	1.5	128	3.3	44
IM 18B			0.16	1.50	0.70	0.15	0.004	0.02	0.64	16.68	1.01	1.3	41.1	5.9	1.7	36	2.2	111.1
IM 19C			0.07	3.81	0.96	0.21	0.004	0.03	0.58	16.20	0.96	1.1	31.1	5	1.7	29	1.3	147.4
Mean			0.13	4.1	1.0	0.3	0.02	0.03	0.7	14.1	1.1	1.1	35.8	4.9	1.8	71.0	1.4	41.1
Median			0.07	3.6	1.0	0.2	0.01	0.03	0.7	13.6	1.1	1.1	35.4	5.1	1.7	52.0	1.4	28.4
SD			0.17	2.5	0.2	0.1	0.05	0.01	0.1	2.4	0.3	0.3	6.9	0.8	0.4	44.2	0.6	45.3
OK 7A	Mamu Formation	Western margin (Bay subenvironment)	0.014	3.28	0.46	0.12	0.004	0.015	0.86	12.01	1.51	2.5	46.6	5.7	2.3	80	3.2	18.3
OK 7B			0.014	2.71	0.23	0.06	0.008	0.015	0.63	6.93	1.09	1.0	23.7	4.9	1.4	174	6.4	13
OK 7C			0.014	6.76	0.46	0.12	0.018	0.030	0.50	15.61	0.90	2.4	71	5.5	1.7	96	7.9	40.7
OK 7D			0.014	5.38	0.42	0.10	0.005	0.022	0.60	15.88	1.06	2.9	52.7	6.2	1.7	118	2.9	38.8
OK 7E			0.014	2.42	0.40	0.08	0.002	0.022	0.94	14.98	1.76	3.0	48.7	6.5	2.8	145	2.5	25.7
OK 7F			0.014	2.02	0.42	0.08	0.005	0.022	0.72	17.04	1.31	2.2	34.6	5.5	2.1	149	1.5	26.7
OK 7G			0.021	1.96	0.47	0.07	0.003	0.030	0.73	11.54	1.34	2.5	35	6.5	2	29	1.8	18
OK 7H			0.014	1.19	0.37	0.07	0.005	0.015	0.83	12.54	1.53	2.6	29.3	6.1	2	30	2.6	15.7
OK 7I			0.021	1.43	0.39	0.07	0.003	0.022	0.87	15.24	1.51	1.8	46.9	7	2.1	37	2.8	30
OK 7J			0.021	1.60	0.44	0.07	0.005	0.022	1.03	13.81	1.88	1.8	47.7	7.5	2.6	31	4.3	29.9
OK 9			0.021	0.80	0.42	0.08	0.002	0.015	0.76	16.88	1.37	0.2	41.1	5.6	2	33	1	19.1
OK 11A			0.014	1.63	0.64	0.12	0.005	0.022	0.99	15.40	1.71	0.7	36.4	7	2.7	31	3.3	17.8
OK 11B			0.021	1.57	0.88	0.16	0.003	0.022	1.05	15.88	1.84	0.4	42.9	7.3	2.9	28	2.1	13.8
OK 13A			0.014	1.29	0.45	0.07	0.004	0.022	0.88	13.07	1.56	0.9	38.4	7.2	2.2	30	3.5	27.1
OK 13B			0.014	1.14	0.50	0.08	0.003	0.022	0.99	15.61	1.74	1.3	49	7.7	2.5	37	1.8	29.9
OK 15			0.021	0.62	0.51	0.05	0.004	0.030	0.94	8.10	1.70	0.4	36.8	7.3	2.3	18	1.5	13.7
OK 17			0.021	0.75	0.47	0.05	0.005	0.022	0.90	11.75	1.64	1.0	34.9	6.4	2.1	23	1.8	36.7
OK 19A			0.014	0.68	0.41	0.06	0.003	0.022	0.93	13.92	1.66	1.2	37.7	7.2	2.2	31	1.1	59.3
OK 19B			0.014	1.04	0.47	0.08	0.003	0.022	1.04	15.72	1.78	0.7	47.5	7.6	2.7	37	1.9	32.7
OK 21A			0.029	1.20	0.60	0.09	0.003	0.022	1.14	10.43	2.00	0.3	41.6	8	2.9	23	1	20.3

OK 21B			0.021	1.55	0.62	0.10	0.003	0.022	1.11	11.91	2.01	0.4	40.7	7.9	2.7	23	1.7	17.8
OK 24A			0.014	0.62	0.42	0.06	0.002	0.022	0.96	13.87	1.65	1.4	42.5	7.5	2.3	30	1.5	63.6
Ok 24B			0.014	0.64	0.41	0.05	0.004	0.022	0.88	10.06	1.53	0.6	43.4	6.2	1.9	19	1.9	26.4
Mean			0.017	1.8	0.5	0.08	0.004	0.022	0.9	13.4	1.6	1.4	42.1	6.7	2.3	54.4	2.6	27.6
Median			0.014	1.5	0.5	0.08	0.004	0.022	0.9	13.9	1.7	1.2	41.6	7	2.2	31.0	1.9	26.4
SD			0.004	1.5	0.1	0.03	0.003	0.004	0.2	2.7	0.3	0.9	9.3	0.7	0.4	47.4	1.7	13.4
Nz-16	Mamu Formation	Nzam-1 Well	0.74	4.35	1.36	0.65	0.07	0.514	0.57	7.74	0.96	-	25.9	2.1	7.5	89	1.6	15
Nz-17			0.51	4.96	1.17	0.58	0.04	0.625	0.65	9.34	1.09	1.91	25	2.9	16.8	126	2.3	18.7
Nz-18			0.47	6.31	1.06	0.81	0.02	0.619	0.54	> 20	0.90	1.73	27.2	3.4	3.7	155	2	27.3
Nz-19			0.17	3.61	2.02	0.39	0.03	0.404	0.81	10.00	1.36	-	24.8	3.4	81.9	119	1.3	22.2
Nz-20			0.32	3.97	0.79	0.46	0.03	0.485	0.44	6.95	0.74	1.11	17	2	2	65	2.5	21.1
Nz-21			0.34	4.29	1.29	0.50	0.05	0.566	0.66	8.60	1.11	-	23.3	2.8	2	94	1.4	17.3
Nz-22			0.34	3.13	1.16	0.32	0.03	0.564	0.61	7.89	1.02	-	23.8	2.5	3.4	64	1.2	13.7
Nz-39			0.36	6.69	1.13	0.65	0.18	0.467	0.81	7.73	1.36	1.77	20.9	3.1	36.6	95	1.6	18.7
Mean			0.4	4.7	1.3	0.6	0.056	0.531	0.6	8.3	1.1	1.6	23.5	2.8	19.2	100.9	1.7	19.3
Median			0.4	4.3	1.2	0.5	0.034	0.539	0.6	7.9	1.1	1.8	24.3	2.9	5.6	94.5	1.6	18.7
SD			0.2	1.3	0.4	0.2	0.051	0.077	0.1	1.1	0.2	0.4	3.22	0.5	27.9	31.1	0.5	4.3
ID-3	Mamu Formation	Idah-1 Well	0.07	0.25	0.02	0.01	0.005	0.014	0.28	0.15	0.46	-	126	0.7	7.9	9	0.3	2.3
ID-4				0.02	1.07	1.59	0.06	0.006	0.074	0.57	4.80	0.94	1.32	22	1.5	103	31	1.6
ID-5			0.23	2.45	0.61	0.37	0.040	0.126	0.33	3.66	0.54	-	179	2.6	3.2	52	0.6	9.8
ID-6			0.37	4.80	1.26	0.80	0.046	0.462	0.81	8.28	1.34	1.27	75.4	3.3	3.2	88	1.4	20.3
ID-7			0.48	5.27	1.34	0.71	0.050	0.469	1.09	6.70	1.82	1.31	148	3.8	4.9	92	1.9	24.2
ID-8			0.43	5.78	1.19	0.84	0.079	0.432	0.71	7.56	1.18	1.91	2290	19.1	23.2	186	1.4	21.4
ID-9			0.48	5.00	1.05	0.71	0.065	0.454	0.63	7.24	1.06	1.65	2400	18	51.6	241	1.6	19.9
ID-10			0.73	6.82	0.80	1.09	0.083	0.314	0.62	4.87	1.04	1.32	325	4.7	25.1	152	1.7	14
ID-11			0.43	4.74	0.83	0.77	0.066	0.402	0.84	5.78	1.40	-	222	3.7	4.8	95	1.3	19.7
ID-12			0.73	7.05	0.93	0.83	0.080	0.280	0.64	6.19	1.07	1.40	450	6.1	57.2	138	1.7	21.8
ID-13			0.58	5.81	1.09	0.55	0.051	0.315	0.77	7.74	1.29	1.66	126	3.8	16.6	187	1.5	20.7
ID-14			0.39	6.47	1.17	0.64	0.051	0.377	0.82	9.23	1.37	-	1250	11.3	13.1	146	1.4	23.4
ID-15			0.40	7.13	1.08	0.66	0.063	0.341	0.77	8.47	1.28	1.95	249	5	3.1	139	1.5	20.8
ID-16			0.25	4.82	1.11	0.48	0.018	0.366	1.23	9.59	2.05	1.41	31.5	4.6	17.1	114	1.1	22.8
ID-17			0.16	4.81	1.02	0.44	0.029	0.229	0.90	10.70	1.49	2.39	163	6.2	76.1	150	1.4	21.4
ID-18			0.35	7.09	1.05	0.53	0.047	0.256	0.71	10.00	1.19	1.76	666	8.3	2.4	136	0.8	24.3
ID-19			0.44	5.97	0.88	0.54	0.031	0.231	0.67	9.47	1.12	2.73	334	6.6	2.9	214	1.3	20.4
ID-20			0.36	5.94	1.07	0.68	0.047	0.334	0.69	9.92	1.15	1.69	222	4.8	2.3	160	1.7	21.7
ID-21			0.69	5.34	1.30	1.06	0.024	0.452	0.57	10.70	0.95	1.14	146	4.4	2.2	208	0.7	25.4
ID-22			0.53	5.27	1.40	1.09	0.031	0.446	0.57	10.80	0.95	0.95	97.1	3.6	2.1	151	0.6	23.5
ID-23			0.71	5.23	1.20	0.98	0.050	0.431	0.63	9.37	1.05	1.18	97.7	4.1	5.5	203	0.9	22.4
Mean			0.4	5.1	1.1	0.7	0.05	0.32	0.7	7.7	1.2	1.6	458.1	6.0	20.4	137.7	1.3	19.5
Median			0.4	5.3	1.1	0.7	0.05	0.34	0.7	8.3	1.2	1.4	179	4.6	5.5	146	1.4	21.4
SD			0.2	1.8	0.3	0.3	0.02	0.13	0.2	2.7	0.4	0.5	683.5	4.7	28.1	60.8	0.4	5.9





Ak-23			12.90	5.60	0.99	0.75	0.102	0.664	0.369	6.56	0.62	1.63	113	4	21.3	383	11.3	177
Ak-24			2.43	5.47	2.04	1.15	0.074	1.430	0.757	10.50	1.26	1.15	38.5	4.4	18.1	135	2.9	30.2
Ak-25			2.11	5.76	1.89	1.12	0.072	1.530	0.771	10.50	1.29	1.58	44.8	4.6	15.5	145	3.8	34.3
Ak-26			2.07	5.77	1.95	1.15	0.080	1.520	0.781	9.98	1.30	1.69	35.6	4.5	18.5	111	3.8	21.9
Ak-27			1.49	5.06	1.52	0.92	0.055	1.230	0.655	8.64	1.09	1.80	39.1	3.9	13.2	100	2.9	31.9
Ak-28			2.14	5.07	1.76	0.94	0.050	1.420	0.724	8.62	1.21	1.28	30.8	4	22.2	88	1.7	20.2
Ak-29			1.49	4.33	1.29	0.81	0.042	1.040	0.524	7.86	0.87	1.43	27.4	3.5	24.2	92	3.1	30.8
Ak-30			2.13	5.01	1.64	0.90	0.045	1.140	0.661	8.67	1.10	1.55	24	4.2	8.1	109	5.1	29.9
Ak-31			3.56	4.13	1.41	0.52	0.043	1.280	0.451	8.18	0.75	1.39	32.4	3.5	36.5	98	3.8	28.3
Ak-32			3.12	4.41	1.48	0.78	0.047	1.210	0.529	8.21	0.88	1.73	32.8	3.5	26.7	131	4.2	25.9
Mean			2.3	5.3	1.5	1.0	0.076	1.054	0.637	9.3	1.1	1.5	31.8	3.7	16.1	141	3.8	35.3
Median			1.6	5.1	1.4	0.9	0.052	1.060	0.661	9.3	1.1	1.5	24.6	3.6	15.3	134	3.1	29.7
SD			2.9	1.8	0.3	0.4	0.092	0.319	0.121	1.4	0.2	0.3	20.0	0.5	7.4	66.0	2.9	32.8

Appendix 2.1b

S/N	Lithostratigraphic Unit	Location	Ni	Co	V	Cr	Sc	Th	U	Ta	Nb	Zr	Y	Hf	La
U1 IA	Mamu Formation	Western margin (Marsh subenvironment)	14.7	3.5	110	108	9	14.8	5	2.1	30.3	173.2	24.4	4.6	50.2
U1 1C			11.3	2.1	90	96	6	11.8	4.3	2	28	157	20.6	4.2	43.9
U1 2A			11.4	2.1	115	100	7	13.1	4.5	2.1	31.8	171.8	22.5	4.4	47.2
U1 2B			8	1.7	102	65	7	11.2	3.8	1.8	26.7	155.8	20.6	3.9	43
U1 2C			10.6	2.2	113	97	9	12.6	4.6	2.1	31.4	176.6	22.7	4.6	47.8
U1 3A			10.3	2.2	110	76	9	12.4	4.6	2.2	33.6	186.1	23.8	5	48.7
U1 3B			16.3	2.9	101	97	10	12.3	4.6	2.5	34.9	193.3	25.8	5.2	49.6
U1 5A			15.1	3.1	159	131	13	14.8	5.1	2.2	30.5	160.7	26.8	4.3	42.8
U1 5B			15.3	2.9	166	128	13	13.4	4.5	2	27.6	149.9	22.6	4.4	35.9
U1 6A			14.3	3.6	166	104	12	13.3	4.4	2.1	29.4	155	20.9	4.7	43.3
U1 7A			50	34.5	148	124	15	16.3	4.5	1.8	24.4	133.1	22	4	47.2
U1 7B			26.2	15	145	66	12	12.6	4.4	1.9	29.1	146	22.5	4	46.1
U1 8A			37.5	23.9	149	85	13	15.1	4.1	1.8	25.5	126.5	19.7	3.6	38.8
U1 8B			31.9	17.9	128	80	13	14.4	4.5	2	28.9	154.9	24	4.1	52.2
U1 8C			31.9	16.5	103	86	10	13.8	4.3	1.8	25.4	142.2	19.6	3.9	42.1
U1 8D			62.2	27.5	172	66	12	11.9	5.4	1.9	28.8	161.5	23.1	4	39.4
U1 9B			37	25.9	157	111	13	15.3	5.5	2.2	32	173.1	22.1	4.4	50.7
U1 9C			31.2	20.4	151	91	13	12.4	5.2	2.4	33.3	178.6	17.3	4.5	40.1
U1 10			22.4	7.4	184	142	12	17.7	4.1	2.3	33.2	182	20.9	4.9	63.5
U1 18			10.6	2	154	128	17	16.7	5.1	2.4	33.2	198.7	20.4	5.8	56.4
U1 19			9.9	1.9	137	93	13	14.6	4.7	2.1	31.4	180.1	19.5	4.7	47.1
AU-1a			15.9	3.5	113	102	13	14.3	4.7	1.8	24.3	138.3	30.6	4	47.2
AU 2			15.6	3.9	127	109	16	13.4	4.1	1.7	25	134	25	3.8	30.1
Mean			22.2	9.9	134.8	99.4	11.6	13.8	4.6	2.1	29.5	162.1	22.5	4.4	45.8
Median			15.6	3.5	137.0	97.0	12.0	13.4	4.5	2.1	29.4	160.7	22.5	4.4	47.1
SD			14.2	10.3	26.9	21.6	2.8	1.7	0.4	0.2	3.2	20.1	2.9	0.5	6.9
IM 2B	Mamu Formation	Western margin (Central Basin subenvironment)	42.7	23	159	103	17	18.1	6.8	2.3	30.6	111.8	20.6	3.4	31.5
IM 2C			32.9	13.2	161	105	16	19.9	7.2	2.4	32.8	123.4	30.5	3.8	40.6
IM 2D			32.1	16.1	150	99	16	20.9	7	2.2	30.7	112.6	26.8	3.4	41.8
IM 2E			46.7	22.5	151	109	16	18.6	5.9	2.1	28.4	102.4	25.9	3.2	42
IM 4A				12	123	75	11	19.5	5.4	1.7	24.4	98.2	19.9	2.8	50.4
IM 11A			53.5	30.7	139	95	15	30.9	9.8	1.8	25	151.4	20.5	4.9	61.3
IM 11B			50.3	21	144	114	21	16.1	7	1.6	24.3	78.2	11.4	2.3	23.6
IM 11C			54.7	31.2	140	125	24	30.3	8.5	1.6	23	111.3	54.8	3.6	87.2
IM 13A			58.8	32	133	131	16	23.8	6.4	1.4	20.3	74.2	21.3	2.3	50
IM 13B			47.7	22.5	146	113	21	18.2	6	1.8	26.6	89.4	14.4	3	28.9



IM 14A			61.9	29.9	131	111	20	23.1	8.3	1.5	21.2	100.5	64.8	2.9	72.1
IM 16A			59.1	26.1	104	104	17	13.4	4.5	0.9	13.1	63.9	30.6	1.9	37.5
IM 16B			60.9	25.1	103	99	18	13.2	4.7	1	15.9	80.8	62.2	2.4	34.8
IM 16C			46.1	15.1	118	101	16	13.3	4.4	1.3	18.2	91.9	31.9	2.8	27.8
IM 16D			39.2	19.2	115	97	17	17.9	4.8	1.3	19.5	108	18.1	3.3	40.2
IM 18a			45.9	3.15	68.5	67.5	19	20.2	12.2	0.9	13.5	93.3	57.6	2.7	89
IM 18C			32.9	6.3	94	94	21	15.3	10.8	1.5	22.5	78.5	14.7	2.3	26.3
IM 19A			28.2	7.6	111	107	20	14.2	8.6	1.5	20.2	98.3	18.3	3.1	27.9
IM 19B			43.2	13.4	109	100	13	13	7.5	1.3	19.9	93	11.9	2.8	20
IM 19D			54.5	36.8	102	105	14	14.2	5.6	1.3	20.6	99.9	13.9	2.7	31.7
IM 19E			26.9	7.4	128	109	20	10.1	5.9	1.7	23.7	114	7.9	3.3	13.3
IM 2A			29.2	9.5	131	101	13	14	6	1.8	27.3	92.9	16.3	2.7	37.2
IM 4B			24.9	11.8	99	68	9	18.6	4.6	1.6	23.6	100.6	19.9	2.9	50.6
IM 14C			75.4	27.5	110	99	19	16.2	7.7	1.2	17.6	70.6	36.7	2	46.8
IM 18B			33.3	8.8	91	89	11	9.6	8.5	1.5	22.1	66.4	10.5	2	11.5
IM 19C			62.6	34.8	98	108	14	16.1	7.7	1.4	18.4	91.8	18.8	2.8	36.1
Mean			45.7	19.5	121.5	101.1	16.7	17.6	7.0	1.6	22.4	96.1	26.2	2.9	40.8
Median			46.1	20.1	120.5	102	16.5	17.5	6.9	1.5	22.3	95.7	20.2	2.8	37.4
SD			13.5	9.8	23.5	14.6	3.6	5.2	2.0	0.4	5.0	19.1	16.3	0.6	19.5
OK 7A	Mamu Formation	Western margin (Bay subenvironment)	33.8	16.2	95	92	13	26.4	7.2	2.5	32.7	120.2	36.9	3.6	62.6
OK 7B			21.6	7.8	69	118	10	24.5	5.6	2	23.5	115.3	32.1	3.8	60
OK 7C			65.7	36.9	114	102	17	19.2	9	1.5	19.9	46.6	39.8	1.3	40.5
OK 7D			57.1	28.8	93	104	17	20.5	11.6	1.8	24	59	43.3	1.9	39.4
OK 7E			43.9	22.9	101	91	16	19.3	8.7	2.9	37.8	110.1	32.7	3.5	42.9
OK 7F			88.4	29.1	98	72	15	11.9	8.5	2.2	28	98.1	14	2.7	16.9
OK 7G			52.5	12.5	105	70	15	26	7.9	2.6	30.4	184.4	21.4	5.8	60
OK 7H			26.4	6.2	67	97	11	20	8.2	2.6	34.1	135.2	12.8	4.3	36.4
OK 7I			26.9	8.9	83	86	14	17.3	12	2.5	34.2	108.5	10.1	3.2	27.1
OK 7J			29.4	6.2	104	119	17	25.7	13.7	3.2	43.3	169.2	17.2	5.2	45.4
OK 9			47.2	6	88	88	14	19.6	10.8	2.5	31.7	111.5	13.2	3.5	35.4
OK 11A			25.3	5.6	103	105	15	14.8	10.3	2.7	37.8	150.7	13.9	4.6	20.1
OK 11B			22.2	5	110	93	15	14.4	8	2.9	39.2	168.1	14.1	5.1	22.6
OK 13A			25.4	5.2	86	99	16	20.5	10.5	2.8	35.1	112	16.7	3.4	40.5
OK 13B			29.2	6.6	96	94	18	13.3	14	3.1	41.2	120.8	13.2	3.7	25.1
OK 15			27.3	3.1	54	56	12	36.4	8.3	3.4	39.1	255.4	24.1	8.1	73.6
OK 17			42.7	4.6	61	84	24	35.1	11.8	3	36.4	185.3	21.3	5.7	64.7
OK 19A			29.8	6.1	76	96	27	23.8	19.5	3.1	38.2	157.2	18.9	5	43.2
OK 19B			35.3	6.5	88	100	18	19.7	12.1	3.1	43.1	125.9	14.6	3.8	34.3
OK 21A			24.1	3.3	94	72	18	35.3	12.4	3.7	45.6	245.8	27.9	7.8	77.7
OK 21B			22.3	4.2	97	90	16	28	10.8	3.5	44.6	219.1	23.1	6.5	71
OK 24A			33.9	5.3	76	86	16	15.9	31.2	3	40	119.4	20.6	3.6	51.9
Ok 24B			25.9	4.2	73	76	15	25.2	11.5	2.9	34.9	156	20.5	5.1	64

Mean			36.4	10.5	88.3	90.9	16.0	22.3	11.5	2.8	35.4	142.3	21.8	4.4	45.9
Median			29.4	6.2	93	92	16	20.5	10.8	2.9	36.4	125.9	20.5	3.8	42.9
SD			16.5	9.6	16.1	15.0	3.7	6.9	5.2	0.5	6.8	52.0	9.4	1.7	18
Nz-16	Mamu Formation	Nzam-1 Well	32.3	14.9	88	100	11	14.4	2.7	1.1	16.8	171	20.9	4.5	39.9
Nz-17			36.3	17.5	120	74	14	16.3	3.1	1.3	20.8	144	21.7	3.8	45.5
Nz-18			50.8	20.2	183	89	17	13.7	2.5	1.1	17.4	95.8	21.5	2.5	39.2
Nz-19			38.5	33.5	126	78	16	18.5	5.9	1.7	25.2	187	26.4	5.2	54.6
Nz-20			26	12.1	89	92	11	13.3	2.4	0.7	12.5	119	16.3	3.2	36.1
Nz-21			33.6	17.7	117	95	13	15.6	3.6	1.4	21.2	152	23	4.1	43
Nz-22			26.1	13	89	89	11	15.9	3	1.3	19.3	156	19.1	4.2	40.1
Nz-39			36.3	25.7	121	86	14	11.8	4.2	1.5	20.6	173	29.1	4.4	42.5
Mean			35	19.3	116.6	87.9	13.4	14.9	3.4	1.26	19.2	149.7	22.25	3.99	42.61
Median			35	17.6	118.5	89	13.5	15	3.05	1.3	19.95	154	21.6	4.15	41.3
SD			7.9	7.2	31.3	8.5	2.3	2.08	1.16	0.30	3.75	30.03	4.01	0.83	5.61
ID-3	Mamu Formation	Idah-1 Well	3.6	4.9	13	19	2	8.2	1.1	0.1	1.8	23.4	5.9	0.3	18.6
ID-4				14	26.4	43	53	6	12.9	3.3	0.5	11.6	215	17	6.4
ID-5			14.5	7.8	53	49	7	7.9	2.1	0.4	8.2	70.7	12.7	2	22.1
ID-6			36	22.4	109	71	14	12.2	6.6	1.8	26	204	28.5	5.5	41
ID-7			35.9	25	103	66	13	13.1	7.8	1.9	31.2	258	35.4	6.6	47.5
ID-8			32.7	21.7	98	78	13	12.5	4.9	1.5	22.1	185	27.2	5.1	40.7
ID-9			33.3	17.4	87	67	12	11.7	4.5	1.4	19.9	179	24.6	5	37.1
ID-10			19.8	16.4	62	54	9	10.5	4.6	1	19.5	194	24.7	5.1	34.4
ID-11			27.6	16.1	76	68	11	11.9	5.4	1.4	24.9	220	27.1	6	38.5
ID-12			29.6	24.1	72	83	11	12.3	4.7	1	20.2	172	27.7	4.6	39.5
ID-13			28.8	21.3	90	76	13	14.4	6.1	1.8	25.6	226	30.5	6.3	45.9
ID-14			34	23.8	103	67	15	15.2	6	1.9	26.9	201	29.6	5.7	45.9
ID-15			33.7	21.9	96	77	14	15.5	5.8	1.8	26.2	206	29.6	5.8	47.6
ID-16			33.5	26.8	121	83	16	17.3	7.1	2.2	38	293	37.2	7.6	58.6
ID-17			36.8	35	92	64	15	19.7	7.2	2.3	32.5	237	30.7	7.3	56.8
ID-18			41	23.4	113	67	16	17.6	7.9	0.6	18.2	194	33.4	5.6	53.1
ID-19			33.6	23.8	84	54	14	18.5	6.3	1.9	26.3	188	27.5	5.6	52.3
ID-20			43.3	29.6	98	62	15	16.6	6.5	1.8	24.6	199	27.6	5.8	47.1
ID-21			45.7	21.5	118	84	16	13.3	4.6	1.4	18.7	128	28.2	3.8	42.8
ID-22			41.3	20.5	113	78	17	17.4	4.8	1.4	19.1	138	27.3	4	47.1
ID-23			43	22.4	113	71	15	13	6.3	1.5	22.6	157	39.2	4.4	47.9
Mean			31.51	21.5	88.43	66.24	12.57	13.89	5.41	1.41	22.1	185.2	27.22	5.17	42.97
Median			33.6	22.4	96	67	14	13.1	5.8	1.5	22.6	194	27.7	5.6	45.9
SD			10.7	6.60	27.39	14.90	3.80	3.19	1.74	0.604	8.09	59.39	7.64	1.67	9.86
OW-10	Mamu Formation	Owan-1 Well	7.3	32.6	37	35	3	13	3	0.5	9.5	196	10.3	6.2	27.2
OW-11				35.9	30.9	50	82	18	24	8.5	< 0.1	1.5	114	40.4	4.5

OW-12			4.6	11.6	10	36	5	13.7	3	< 0.1	0.4	120	14.6	3.6	27.9
OW-13			4.8	23	19	29	4	9	1.9	< 0.1	1	96.1	9.8	2	21.3
OW-14			21	15.4	91	82	11	18.8	4.2	1.3	21.7	228	24.2	6.8	47.8
OW-15			18.7	41.7	71	82	9	18.6	4.4	0.2	7.8	228	27.3	6.1	49.3
OW-16			12.2	29.4	43	38	5	10.6	3.2	0.1	4.1	144	12.4	4.1	29.1
Mean			14.93	26.4	45.86	54.86	7.86	15.38	4.03	0.53	6.57	160.9	19.86	4.76	38.43
Median			12.2	29.4	43	38	5	13.7	3.2	0.35	4.1	144	14.6	4.5	29.1
SD			11.29	10.4	28.22	25.54	5.30	5.30	2.14	0.54	7.53	55.67	11.34	1.71	16.36
Am-3	Mamu Formation	Amansiodo-1 Well	4.5	35.9	12	11	1	1.8	0.6	< 0.1	1.2	11.5	4	0.4	6.8
Am-4			5.3	35.7	14	16	1	1.6	0.6	< 0.1	1.5	11.5	4.6	0.3	7.1
Am-5			6.4	51.3	22	21	2	2.3	0.8	< 0.1	1.6	24.6	4.9	0.7	7.9
Am-6			2.5	35.1	10	10	1	1.8	0.8	< 0.1	2	50.5	3.3	0.6	5.8
Am-7			3	45.5	10	11	1	1.6	0.6	< 0.1	1.4	13.3	3.4	0.3	5.6
Am-8			2.4	39.2	10	13	1	1.7	0.7	< 0.1	1.9	13.3	3.4	0.3	5.7
Am-9			2.1	40.6	9	12	< 1	1.3	0.5	< 0.1	1	22.8	2.8	0.5	4.6
Am-10			1.9	40.4	6	10	< 1	1.1	0.5	< 0.1	0.4	11	2.2	0.3	3.6
Am-11			3.5	50.2	21	24	2	2.3	0.9	< 0.1	1.5	10.7	3.8	0.3	7.2
Mean			3.51	41.54	12.67	14.22	1.29	1.72	0.67	-	1.39	18.8	3.6	0.41	6.03
Median			3	40.4	10	12	1	1.7	0.6	-	1.5	13.3	3.4	0.3	5.8
SD			1.57	6.13	5.45	5.09	0.49	0.40	0.14	-	0.48	12.98	0.84	0.15	1.36
Enu 1.1	Mamu Formation	Eastern margin (Odoma et al., 2015)	42	34	119	100	22	21	6	-	31	296	-	9	-
Enu 1.2			22	16	95	88	12	22	6	-	33	717	-	21	-
Enu 1.3			19	14	103	90	10	19	8	-	34	700	-	18	-
Enu 1.4			31	23	101	81	23	19	6	-	31	395	-	17	-
Enu 1.5			35	28	103	86	17	18	7	-	31	375	-	8	-
Enu 2.2			20	6	120	86	16	18	5	-	34	363	-	14	-
Enu2.3			18	5	101	83	10	17	8	-	38	409	-	10	-
Enu2.4			21	9	120	92	14	21	6	-	34	287	-	6	-
Enu2.5			27	17	125	96	22	23	6	-	43	491	-	14	-
mean			26.11	16.89	109.67	89.11	16.22	19.78	6.44	-	34.33	448.1	-	13.0	-
median			22	16	103	88	16	19	6	-	34	395	-	14	-
SD			8.31	9.91	11.12	6.11	5.17	2.05	1.01	-	3.94	159.5	-	5.07	-
	Mamu Formation average		25.45	18.85	99.5	88	13.75	14.35	5.15	1.5	22.45	149	20.5	4.28	41.3
	Pre-Santonian Units														
Am-23	Awgu Group	Amansiodo-1 Well	42.8	29.4	140	81	19	16.6	7.6	1.8	28.6	222	59.4	5.1	60.5
Am-24			46.6	28	154	87	20	15.6	5.4	1.7	27.1	208	37.5	4.8	52.1
Am-25			46.7	28.7	145	83	19	16.5	5.9	1.7	27.4	208	35.4	4.7	53.6

Am-26			45.1	29.5	172	101	20	14.5	4.2	1.5	25	179	32.2	4.1	47.4
Am-27			47.3	25.3	162	113	20	14.1	3.5	1	22	174	27.8	4.2	46.3
Am-28			45.8	23.9	165	102	19	15.7	4.3	0.7	19.9	189	30.8	4.3	51.1
Am-29			45.9	24	151	93	19	16.1	4.1	0.2	14	155	30.7	3.8	52.6
Am-30			46.4	24.5	150	93	18	15.9	4	0.2	17	161	34.7	4.5	48.7
Am-31			46.2	21.9	171	120	19	15.9	3.7	0.8	19	132	28.8	3.4	49.2
Am-32			46.1	23.4	174	121	19	15.6	4.1	1.4	24.5	151	32.3	3.6	49.9
Am-33			45.3	22.3	174	118	19	15.8	4	1.2	23.1	143	29.3	3.6	51.5
Am-34			45.5	21.4	173	120	20	15.9	3.7	0.9	19.7	133	25.3	3.2	48.5
Am-35			42.3	21.7	145	89	17	20.7	2.9	1.6	23.3	82.2	25.7	2.4	60.1
Am-36			42.9	19	119	152	16	15.1	2.4	0.9	14.9	55.6	59.9	1.5	51.6
Am-37			43.8	19.9	142	77	17	17.1	2.8	1.3	19.7	71.7	23.6	2	51.4
Mean			45.25	24.2	155.8	103.3	18.73	16.07	4.17	1.13	21.68	151	34.23	3.68	51.63
Median			45.8	23.9	154	101	19	15.9	4	1.2	22	155	30.8	3.8	51.4
SD			1.56	3.38	16.17	20.43	1.22	1.49	1.31	0.51	4.46	50.20	-	1.05	4.05
Ak-3	Awgu Group	Akukwa-II Well	48.1	16.5	168	89	15	6.6	2.3	1	16.1	121	21.6	2.9	14.6
Ak-4			56.6	22.3	193	110	16	4.1	2.9	0.9	15.4	97.3	21.7	2.4	6.5
Ak-5			50.6	20	159	109	17	7.3	2.9	1.3	22	146	28.9	3.5	14.5
Ak-6			53.5	22.7	171	60	16	3.7	2.6	1	16.5	104	24.5	2.5	8.8
Ak-7			47.2	21.8	137	53	15	4	3	1.1	18.6	137	25.5	3.3	12.2
Ak-8			55.6	25.3	182	66	17	3	3.2	1.1	19.3	124	24	3	13
Ak-9			47.9	19.8	160	65	16	5.7	2.8	1.1	17.5	117	24.8	2.9	17.4
Ak-10			20.9	17.8	87	42	8	7.4	1.6	0.6	9.6	66.8	12.4	1.6	23.5
Ak-11			46.6	19.8	157	69	17	3.8	3.4	1.3	21.7	129	24.5	3.2	14.7
Mean			47.44	20.7	157.1	73.67	15.22	5.07	2.74	1.04	17.41	115.8	23.1	2.81	13.91
Median			48.1	20	160	66	16	4.1	2.9	1.1	17.5	121	24.5	2.9	14.5
SD			10.62	2.67	30.72	23.92	2.82	1.7	0.53	0.21	3.74	23.75	4.55	0.58	4.88
Ak-12	Eze-Aku Group	Akukwa-II Well	53.7	22	165	62	17	2.8	3.3	1.2	20.3	129	25.3	3.1	12.2
Ak-13				46.6	20.6	167	64	16	2.4	3.1	1.1	19.3	117	27.8	2.8
Ak-14			29.1	20.1	107	81	16	11.7	2.6	0.1	7.8	82.8	17.7	2.2	37.7
Ak-15			43.9	17.1	161	58	15	1.8	2.8	1.2	21.4	132	25.1	3.2	11.1
Ak-16			39.8	17.7	157	63	14	2.7	2.6	1.1	18.4	105	24.2	2.6	10.3
Ak-17			45.1	22.1	179	101	16	9.7	3.5	1.3	21.2	108	23.1	2.8	21.8
Ak-18			40.2	17.6	132	65	14	3.2	2.5	1.1	18.6	79.7	20.8	2.1	10.8
Ak-19			66.5	28.5	226	77	13	5.7	4.2	1	16	73.2	21.6	1.9	17.7
Ak-20			45.2	20.3	168	67	14	4.2	2.6	1.1	18.7	69.4	20.9	1.8	13.1
Ak-21			44.1	22	145	65	13	5.2	2.7	1.1	19.2	83.3	20.8	2.2	14.9
Ak-22			39.1	17.5	157	81	13	8	2.9	1.2	18.9	77	20.7	2	20
Ak-23			43.9	19	96	65	10	5.2	1.8	0.7	12.8	59.9	23.9	1.3	12.2
Ak-24			43.9	27.3	149	102	16	15.9	2.6	1.3	22	45.6	22.3	1.2	39.2
Ak-25			43.7	20.7	141	101	16	17.1	2.6	1.4	21.2	43.7	21	1.2	50.2

Ak-26			43.5	22.2	142	102	16	15.4	2.6	1.3	21.2	41.1	21.6	1.1	50.2
Ak-27			43.2	19.8	119	80	14	3.2	2.3	1	17.9	37.4	19.6	1.1	11.3
Ak-28			41.7	21.8	138	81	14	5.6	2.6	1.3	20.1	41	18.5	1.1	17.8
Ak-29			37.3	30.5	118	67	13	2.7	2.3	0.9	16.5	35.7	19.8	1	9.5
Ak-30			48.9	16.9	134	89	14	3	2.5	1.1	17.8	36.7	20.3	1	8.5
Ak-31			37.7	17	115	68	13	3	2.4	1	15.3	33.2	18.1	0.9	9.9
Ak-32			44.6	23.4	128	67	13	2.9	2.5	1	16.2	32.3	19	0.9	9.6
Mean			43.89	21.1	145	76.48	14.29	6.26	2.71	1.07	18.13	69.67	21.53	1.79	18.99
Median			43.9	20.6	142	68	14	4.2	2.6	1.1	18.7	69.4	20.9	1.8	12.2
SD			7.08	3.78	28.72	14.77	1.65	4.84	0.49	0.27	3.32	33.08	2.60	0.78	13.35

Appendix 2.1c

S/N	Lithostratigraphic Unit	Location	Th/Sc	Zr/Sc	La/Sc	Pb/Zn	K/Al	Mg/K	Mg/Ti	Pb/Nb	Pb/Sn	Na/Al	Na/K	Nb/Ta	Nb/W
U1 IA	Mamu Formation	Western margin (Marsh subenvironment)	1.64	19.24	5.58	1.99	0.04	0.21	0.07	0.92	7.72	0.002	0.05	14.4	14.4
U1 1C			1.97	26.17	7.32	1.56	0.04	0.21	0.07	0.78	6.84	0.002	0.06	14.0	16.5
U1 2A			1.87	24.54	6.74	2.6	0.04	0.18	0.06	0.74	6.16	0.002	0.05	15.1	15.9
U1 2B			1.60	22.26	6.14	1.47	0.04	0.18	0.05	0.99	8.83	0.002	0.06	14.8	15.7
U1 2C			1.40	19.62	5.31	3.6	0.04	0.2	0.06	1.03	9.26	0.002	0.05	15.0	16.5
U1 3A			1.38	20.68	5.41	1.71	0.04	0.19	0.07	0.76	6.92	0.002	0.05	15.3	15.3
U1 3B			1.23	19.33	4.96	1.91	0.04	0.19	0.08	0.82	6.65	0.002	0.06	14.0	15.9
U1 5A			1.14	12.36	3.29	1.94	0.03	0.2	0.08	0.95	7.1	0.002	0.06	13.9	15.3
U1 5B			1.03	11.53	2.76	2.31	0.03	0.2	0.09	1.0	6.93	0.002	0.06	13.8	13.8
U1 6A			1.11	12.92	3.61	1.97	0.03	0.2	0.08	0.87	6.24	0.001	0.04	14.0	13.4
U1 7A			1.09	8.87	3.15	0.11	0.02	0.32	0.1	0.98	7.44	0.002	0.09	13.6	14.4
U1 7B			1.05	12.17	3.84	0.31	0.03	0.24	0.08	0.89	7.00	0.002	0.05	15.3	15.3
U1 8A			1.16	9.73	2.99	0.17	0.02	0.29	0.09	0.94	6.64	0.001	0.03	14.2	17.0
U1 8B			1.11	11.92	4.02	0.2	0.03	0.32	0.09	0.91	7.49	0.003	0.09	14.5	14.5
U1 8C			1.38	14.22	4.21	0.08	0.03	0.31	0.07	0.79	6.48	0.003	0.09	14.1	14.1
U1 8D			0.99	13.46	3.28	0.18	0.03	0.22	0.06	0.94	7.35	0.003	0.10	15.2	15.2
U1 9B			1.18	13.32	3.90	0.83	0.03	0.18	0.05	0.98	8.05	0.001	0.05	14.5	14.5
U1 9C			0.95	13.74	3.09	0.94	0.03	0.19	0.06	0.93	6.87	0.002	0.08	13.9	13.9
U1 10			1.48	15.17	5.29	3.34	0.01	0.21	0.04	1.11	7.65	0.001	0.07	14.4	13.8
U1 18			0.98	11.69	3.32	3.10	0.02	0.16	0.04	0.93	6.33	0.001	0.06	13.8	13.8
U1 19			1.12	13.85	3.62	2.61	0.02	0.19	0.04	0.83	5.44	0.001	0.04	15.0	16.5
AU-1a			1.1	10.64	3.63	1.33	0.07	0.23	0.2	1.15	7.15	0.002	0.03	13.5	13.5
AU 2			0.84	8.38	1.88	0.97	0.07	0.23	0.25	1.05	6.24	0.002	0.03	14.7	13.9
Mean			1.25	15.03	4.23	1.53	0.03	0.22	0.08	0.93	7.08	0.002	0.06	14.4	14.9
Median			1.14	13.46	3.84	1.56	0.03	0.2	0.07	0.93	6.93	0.002	0.06	14.4	14.5
SD			0.29	4.99	1.37	1.09	0.01	0.05	0.05	0.11	0.86	0.001	0.02	0.6	1.1
IM 2B	Mamu Formation	Western margin (Central Basin subenvironment)	1.07	6.58	1.85	0.92	0.07	0.22	0.25	1.29	7.07	0.002	0.02	13.3	12.8
IM 2C			1.24	7.71	2.54	0.74	0.08	0.23	0.24	1.28	7.62	0.002	0.03	13.7	13.1
IM 2D			1.31	7.04	2.61	0.67	0.08	0.24	0.28	1.54	8.58	0.002	0.03	14.0	15.4
IM 2E			1.16	6.40	2.63	0.38	0.07	0.31	0.36	1.29	7.20	0.002	0.03	13.5	12.9
IM 4A			1.77	8.93	4.58	0.74	0.07	0.25	0.25	1.31	7.44	0.003	0.04	14.4	14.4
IM 11A			2.06	10.09	4.09	0.36	0.05	0.37	0.34	1.85	7.33	0.002	0.04	13.9	15.6
IM 11B			0.77	3.72	1.12	0.46	0.06	0.29	0.42	1.26	5.48	0.002	0.03	15.2	13.5
IM 11C			1.26	4.64	3.63	0.32	0.09	0.30	0.51	1.72	7.45	0.002	0.03	14.4	14.4
IM 13A			1.49	4.64	3.13	0.25	0.07	0.41	0.68	1.32	5.70	0.002	0.03	14.5	12.7
IM 13B			0.87	4.26	1.38	0.31	0.07	0.28	0.39	1.10	5.41	0.002	0.03	14.8	12.1

IM 14A			1.16	5.03	3.61	0.20	0.09	0.30	0.50	1.83	9.02	0.003	0.03	14.1	12.5
IM 16A			0.79	3.76	2.21	0.20	0.10	0.35	1.08	1.98	6.82	0.002	0.02	14.6	10.1
IM 16B			0.73	4.49	1.93	0.25	0.10	0.30	0.89	1.95	7.75	0.002	0.02	15.9	9.9
IM 16C			0.83	5.74	1.74	0.49	0.10	0.24	0.65	1.85	7.17	0.002	0.02	14.0	12.1
IM 16D			1.05	6.35	2.37	0.62	0.10	0.22	0.53	1.20	5.32	0.002	0.02	15.0	11.5
IM 18a			1.06	4.91	4.68	0.61	0.09	0.12	0.30	2.11	10.36	0.003	0.03	15.0	15.0
IM 18C			0.73	3.74	1.25	1.38	0.05	0.22	0.27	2.09	7.97	0.001	0.03	15.0	10.7
IM 19A			0.71	4.92	1.40	1.13	0.06	0.22	0.39	2.07	7.76	0.001	0.02	13.5	10.6
IM 19B			1.00	7.15	1.54	1.06	0.07	0.22	0.41	1.71	6.42	0.001	0.02	15.3	11.7
IM 19D			1.01	7.14	2.26	1.40	0.06	0.21	0.32	2.25	9.08	0.002	0.03	15.8	9.4
IM 19E			0.51	5.70	0.67	1.27	0.06	0.21	0.31	1.61	6.57	0.002	0.03	13.9	10.3
IM 2A			1.08	7.15	2.86	1.12	0.06	0.22	0.22	1.23	7.33	0.002	0.03	15.2	14.4
IM 4B			2.07	11.18	5.62	0.92	0.06	0.23	0.17	1.25	8.43	0.002	0.03	14.8	18.2
IM 14C			0.85	3.72	2.46	0.30	0.09	0.33	0.74	2.14	8.38	0.003	0.03	14.7	11.7
IM 18B			0.87	6.04	1.05	1.14	0.04	0.21	0.23	1.86	6.97	0.001	0.02	14.7	13.0
IM 19C			1.15	6.56	2.58	1.07	0.06	0.21	0.35	1.69	6.22	0.002	0.03	13.1	10.8
Mean			1.10	6.06	2.53	0.71	0.07	0.26	0.43	1.65	7.34	0.002	0.03	14.5	12.6
Median			1.06	5.89	2.41	0.64	0.07	0.23	0.36	1.70	7.33	0.002	0.03	14.5	12.6
SD			0.39	1.94	1.24	0.40	0.02	0.06	0.22	0.36	1.21	0.001	0.01	0.7	2.1
OK 7A	Mamu Formation	Western margin (Bay subenvironment)	2.03	9.25	4.82	0.58	0.04	0.26	0.14	1.43	8.18	0.001	0.03	13.1	14.2
OK 7B			2.45	11.53	6.0	0.14	0.03	0.26	0.10	1.01	4.84	0.002	0.06	11.8	16.8
OK 7C			1.13	2.74	2.38	0.74	0.03	0.25	0.23	3.57	12.91	0.002	0.07	13.3	11.7
OK 7D			1.21	3.47	2.32	0.45	0.03	0.23	0.16	2.20	8.50	0.001	0.05	13.3	14.1
OK 7E			1.21	6.88	2.68	0.34	0.03	0.20	0.08	1.29	7.49	0.001	0.06	13.0	13.5
OK 7F			0.79	6.54	1.13	0.23	0.02	0.20	0.12	1.24	6.29	0.001	0.05	12.7	13.3
OK 7G			1.73	12.29	4.0	1.21	0.04	0.14	0.09	1.15	5.39	0.003	0.06	11.7	15.2
OK 7H			1.82	12.29	3.31	0.98	0.03	0.18	0.08	0.86	4.80	0.001	0.04	13.1	17.1
OK 7I			1.24	7.75	1.94	1.27	0.03	0.19	0.08	1.37	6.70	0.001	0.06	13.7	16.3
OK 7J			1.51	9.95	2.67	1.54	0.03	0.16	0.07	1.10	6.36	0.002	0.05	13.5	16.7
OK 9			1.40	7.96	2.53	1.25	0.03	0.19	0.10	1.30	7.34	0.001	0.04	12.7	15.9
OK 11A			0.99	10.05	1.34	1.17	0.04	0.18	0.12	0.96	5.20	0.001	0.04	14.0	14.0
OK 11B			0.96	11.21	1.51	1.53	0.06	0.18	0.15	1.09	5.88	0.001	0.03	13.5	13.5
OK 13A			1.28	7.0	2.53	1.28	0.03	0.16	0.08	1.09	5.33	0.002	0.05	12.5	16.0
OK 13B			0.74	6.71	1.39	1.32	0.03	0.16	0.08	1.19	6.36	0.001	0.05	13.3	16.5
OK 15			3.03	21.28	6.13	2.04	0.06	0.11	0.06	0.94	5.04	0.004	0.06	11.5	17.0
OK 17			1.46	7.72	2.70	1.52	0.04	0.10	0.05	0.96	5.45	0.002	0.05	12.1	17.3
OK 19A			0.88	5.82	1.60	1.22	0.03	0.15	0.07	0.99	5.24	0.002	0.06	12.3	17.4
OK 19B			1.09	6.99	1.91	1.28	0.03	0.17	0.08	1.10	6.25	0.001	0.05	13.9	16.0
OK 21A			1.96	13.66	4.32	1.81	0.06	0.15	0.08	0.91	5.20	0.002	0.04	12.3	15.7
OK 21B			1.75	13.69	4.44	1.77	0.05	0.17	0.09	0.91	5.15	0.002	0.04	12.7	16.5
OK 24A			0.99	7.46	3.24	1.42	0.03	0.14	0.06	1.06	5.67	0.002	0.05	13.3	17.4
Ok 24B			1.68	10.4	4.27	2.28	0.04	0.12	0.06	1.24	7.00	0.002	0.06	12.0	18.4

Mean			1.45	9.25	3.01	1.19	0.04	0.18	0.10	1.26	6.37	0.002	0.05	12.8	15.7	
Median			1.26	7.86	2.60	1.26	0.03	0.17	0.08	1.10	5.77	0.002	0.05	13.1	16.0	
SD			0.56	3.93	1.44	0.57	0.01	0.04	0.04	0.57	1.77	0.001	0.01	0.7	1.7	
Nz-16	Mamu Formation	Nzam-1 Well	1.31	15.55	3.63	0.29	0.18	0.48	1.13	1.54	12.33	0.066	0.38	15.27	2.24	
Nz-17			1.16	10.29	3.25	0.20	0.13	0.50	0.89	1.20	8.62	0.067	0.53	16.0	1.24	
Nz-18			0.81	5.64	2.31	0.18	-	0.76	1.49	1.56	8.0	-	0.58	15.82	4.70	
Nz-19			1.16	11.69	3.41	0.21	0.20	0.19	0.48	0.98	7.29	0.040	0.20	14.82	0.31	
Nz-20			1.21	10.82	3.28	0.26	0.11	0.58	1.04	1.36	8.50	0.070	0.61	17.86	6.25	
Nz-21			1.20	11.69	3.31	0.25	0.15	0.39	0.75	1.10	8.32	0.066	0.44	15.14	10.60	
Nz-22			1.45	14.18	3.65	0.37	0.15	0.28	0.53	1.23	9.52	0.071	0.49	14.85	5.68	
Nz-39			0.84	12.36	3.04	0.22	0.15	0.58	0.80	1.02	6.74	0.060	0.41	13.73	0.56	
Mean			1.14	11.53	3.23	0.25	0.15	0.47	0.89	1.25	8.67	0.063	0.46	15.44	3.95	
Median			1.18	11.69	3.30	0.23	0.15	0.49	0.85	1.22	8.41	0.066	0.46	15.21	3.47	
SD			0.22	2.95	0.43	0.06	0.03	0.18	0.33	0.22	1.71	0.011	0.13	1.20	3.55	
ID-3	Mamu Formation	Idah-1 Well	4.10	11.70	9.30	14.00	0.13	0.50	0.04	70.0	180	0.093	0.70	18.0	0.23	
ID-4			2.15	35.83	6.33	0.71	0.33	0.04	0.11	1.90	14.67	0.015	0.05	23.20	0.11	
ID-5			1.13	10.10	3.16	3.44	0.17	0.61	1.14	21.83	68.85	0.034	0.21	20.50	2.56	
ID-6			0.87	14.57	2.93	0.86	0.15	0.64	0.99	2.90	22.85	0.056	0.37	14.44	8.13	
ID-7			1.01	19.85	3.65	1.61	0.20	0.53	0.65	4.74	38.95	0.070	0.35	16.42	6.37	
ID-8			0.96	14.23	3.13	12.31	0.16	0.71	1.19	103.6	119.9	0.057	0.36	14.73	0.95	
ID-9			0.98	14.92	3.09	9.96	0.15	0.68	1.12	120.6	133.3	0.063	0.43	14.21	0.39	
ID-10			1.17	21.56	3.82	2.14	0.16	1.36	1.76	16.67	69.15	0.064	0.39	19.50	0.78	
ID-11			1.08	20.00	3.50	2.34	0.14	0.93	0.92	8.92	60	0.070	0.48	17.79	5.19	
ID-12			1.12	15.64	3.59	3.26	0.15	0.89	1.29	22.28	73.77	0.045	0.30	20.20	0.35	
ID-13			1.11	17.39	3.53	0.67	0.14	0.51	0.71	4.92	33.16	0.041	0.29	14.22	1.54	
ID-14			1.01	13.40	3.06	8.56	0.13	0.55	0.78	46.47	110.6	0.041	0.32	14.16	2.05	
ID-15			1.11	14.71	3.40	1.79	0.13	0.61	0.86	9.50	49.8	0.040	0.32	14.56	8.45	
ID-16			1.08	18.31	3.66	0.28	0.12	0.43	0.39	0.83	6.85	0.038	0.33	17.27	2.22	
ID-17			1.31	15.80	3.79	1.09	0.10	0.43	0.49	5.02	26.29	0.021	0.23	14.13	0.43	
ID-18			1.10	12.13	3.32	4.90	0.11	0.51	0.74	36.59	80.24	0.026	0.24	30.33	7.58	
ID-19			1.32	13.43	3.74	1.56	0.09	0.61	0.80	12.70	50.61	0.024	0.26	13.84	9.07	
ID-20			1.11	13.27	3.14	1.39	0.11	0.64	0.99	9.02	46.25	0.034	0.31	13.67	10.70	
ID-21			0.83	8.00	2.68	0.70	0.12	0.82	1.87	7.81	33.18	0.042	0.35	13.36	8.50	
ID-22			1.02	8.12	2.77	0.64	0.13	0.78	1.92	5.08	26.97	0.041	0.32	13.64	9.10	
ID-23			0.87	10.47	3.19	0.48	0.13	0.82	1.56	4.32	23.83	0.046	0.36	15.07	4.11	
Mean				1.26	15.40	3.75	3.46	0.14	0.65	0.97	24.56	60.44	0.05	0.33	16.82	4.23
Median				1.10	14.57	3.40	1.61	0.13	0.61	0.92	9.02	49.80	0.04	0.32	14.73	2.56
SD			0.70	5.95	1.47	4.12	0.05	0.25	0.52	33.81	44.01	0.02	0.12	4.15	3.71	
OW-10	Mamu Formation	Owan-1 Well	4.33	65.33	9.07	0.38	0.02	0.67	0.04	1.19	10.27	0.006	0.33	19		
OW-11			1.33	6.33	3.69	0.30	0.03	0.19	0.08	20.13	8.63	0.002	0.06	-	0.52	



OW-12			2.74	24.0	5.58	0.54	0.02	0.29	0.16	35.0	28.0	0.003	0.14	-	0.09
OW-13			2.25	24.03	5.33	0.66	0.02	0.29	0.07	11.80	23.60	0.003	0.13	-	0.06
OW-14			1.71	20.73	4.35	0.52	0.03	0.42	0.11	1.57	13.64	0.002	0.06	16.69	0.52
OW-15			2.07	25.33	5.48	0.60	0.03	0.24	0.05	3.08	9.60	0.002	0.08	39.0	0.05
OW-16			2.12	28.80	5.82	0.22	0.04	0.20	0.05	2.71	10.09	0.003	0.08	41.0	0.02
Mean			2.37	27.79	5.62	0.46	0.03	0.33	0.08	10.78	14.83	0.003	0.13	28.92	0.21
Median			2.12	24.03	5.48	0.52	0.03	0.29	0.07	3.08	10.27	0.003	0.08	29.00	0.08
SD			0.97	18.05	1.70	0.16	0.01	0.17	0.04	12.76	7.76	0.002	0.10	12.85	0.24
Am-3	Mamu Formation	Amansiodo-1 Well	1.80	11.50	6.80	0.47	0.06	1.75	1.23	23.75	21.92	0.037	0.60	-	-
Am-4			1.60	11.50	7.10	0.36	0.04	3.0	1.43	18.47	18.47	0.031	0.733	-	-
Am-5			1.15	12.30	3.95	0.38	0.06	2.40	1.48	26.38	35.17	0.057	1.0	-	-
Am-6			1.80	50.50	5.80	0.51	0.06	1.0	0.48	9.50	38.0	0.028	0.50	-	0.01
Am-7			1.60	13.30	5.60	0.72	0.07	0.50	0.31	30.14	60.29	0.023	0.35	-	-
Am-8			1.70	13.30	5.70	0.66	0.06	0.50	0.29	19.16	91.0	0.021	0.35	-	0.01
Am-9			-	-	-	0.71	0.06	0.67	0.42	24.10	60.25	0.020	0.333	-	-
Am-10			-	-	-	1.01	0.08	1.0	0.71	78.0	78.0	0.027	0.35	-	0.002
Am-11			1.15	5.35	3.60	1.49	0.05	1.33	0.58	57.67	144.20	0.018	0.37	-	0.008
Mean			1.54	16.82	5.51	0.70	0.06	1.35	0.77	31.91	60.81	0.029	0.51	-	0.007
Median			1.60	12.30	5.70	0.66	0.06	1.00	0.58	24.10	60.25	0.027	0.37	-	0.009
SD			0.24	13.16	1.14	0.32	0.01	0.79	0.43	19.62	35.55	0.011	0.21	-	0.003
Enu 1.1	Mamu Formation	Eastern margin (Odoma et al., 2015)	0.95	-	3.27	0.29	0.09	0.38	0.42	1.13	-	0.02	0.16	-	-
Enu 1.2			1.83	-	6.50	0.57	0.14	0.25	0.29	0.91	-	0.03	0.22	-	-
Enu 1.3			1.90	-	8.20	0.55	0.14	0.25	0.30	0.85	-	0.03	0.22	-	-
Enu 1.4			0.83	-	2.91	0.46	0.12	0.21	0.24	1.03	-	0.03	0.22	-	-
Enu 1.5			1.06	-	3.65	0.37	0.11	0.27	0.32	0.94	-	0.02	0.18	-	-
Enu 2.2			1.13	-	3.38	0.49	0.08	0.30	0.30	0.74	-	0.01	0.15	-	-
Enu2.3			1.70	-	7.60	0.62	0.08	0.28	0.24	0.63	-	0.01	0.16	-	-
Enu2.4			1.50	-	5.36	0.45	0.13	0.25	0.40	0.68	-	0.01	0.11	-	-
Enu2.5			1.05	-	3.60	0.18	0.09	0.28	0.22	0.63	-	0.02	0.18	-	-
mean			1.33	-	4.94	0.44	0.11	0.28	0.30	0.84	-	0.02	0.18	-	-
median			1.13	-	3.65	0.46	0.11	0.27	0.30	0.85	-	0.02	0.18	-	-
SD			0.41	-	2.03	0.14	0.02	0.05	0.07	0.18	-	0.01	0.04	-	-
	Mamu Formation average			1.04	10.84	3.00	0.18	0.15	0.63	1.36	1.32	6.83	0.11	0.74	14.97
	Pre-Santonian Units														
Am-23	Awgu Group	Amansiodo-1 Well	0.87	11.68	3.18	0.23	0.12	0.66	0.74	0.86	6.45	0.044	0.38	15.89	4.85
Am-24			0.78	10.40	2.61	0.22	0.16	0.42	0.84	1.03	6.95	0.044	0.27	15.94	3.39
Am-25			0.87	10.95	2.82	0.25	0.14	0.46	0.75	0.99	6.80	0.045	0.33	16.12	2.82

Am-26			0.73	8.95	2.37	0.22	0.20	0.46	1.19	1.02	6.92	0.054	0.27	16.67	2.02
Am-27			0.71	8.70	2.32	0.23	0.16	0.60	1.51	1.31	7.18	0.054	0.34	22.0	4.15
Am-28			0.83	9.95	2.69	0.23	0.13	0.63	1.13	1.29	6.74	0.051	0.39	28.43	4.74
Am-29			0.85	8.16	2.77	0.25	0.12	0.68	1.32	1.94	6.95	0.051	0.43	70.0	3.68
Am-30			0.88	8.94	2.71	0.16	0.11	0.78	1.30	1.81	7.00	0.057	0.51	85.0	2.79
Am-31			0.84	6.95	2.59	0.19	0.11	0.73	1.37	1.34	6.35	0.055	0.49	23.75	7.92
Am-32			0.82	7.95	2.63	0.24	0.11	0.70	1.18	1.01	6.20	0.056	0.50	17.50	4.45
Am-33			0.83	7.53	2.71	0.25	0.14	0.57	1.21	1.12	6.48	0.050	0.37	19.25	4.71
Am-34			0.80	6.65	2.43	0.30	0.13	0.62	1.37	1.35	6.82	0.057	0.42	21.89	7.58
Am-35			1.22	4.84	3.54	0.20	0.30	0.29	1.67	1.40	7.41	0.045	0.15	14.56	1.94
Am-36			0.94	3.48	3.23	0.27	0.12	1.35	2.79	1.57	6.50	0.077	0.64	16.56	1.60
Am-37			1.01	4.22	3.02	0.27	0.15	0.73	1.87	1.19	5.57	0.070	0.46	15.15	1.64
Mean			0.86	7.96	2.77	0.23	0.15	0.65	1.35	1.28	6.69	0.054	0.4	26.58	3.89
Median			0.84	8.16	2.71	0.23	0.13	0.63	1.30	1.29	6.80	0.054	0.39	17.50	3.68
SD			0.12	2.42	0.34	0.03	0.05	0.24	0.51	0.31	0.45	0.009	0.12	21.21	1.94
Ak-3	Awgu Group	Akukwa-II Well	0.44	8.07	0.97	0.15	0.11	1.04	2.32	1.39	7.19	0.073	0.65	16.10	2.73
Ak-4			0.26	6.08	0.41	0.19	0.12	0.59	1.34	1.62	7.55	0.067	0.59	17.11	2.26
Ak-5			0.43	8.59	0.85	0.17	0.09	0.70	1.07	1.27	7.37	0.062	0.67	16.92	3.86
Ak-6			0.23	6.50	0.55	0.17	0.10	0.83	1.50	1.31	6.55	0.066	0.65	16.50	1.41
Ak-7			0.27	9.13	0.81	0.21	0.09	1.18	1.58	1.37	7.97	0.073	0.82	16.91	1.79
Ak-8			0.18	7.29	0.77	0.16	0.11	0.80	1.45	1.48	7.94	0.070	0.63	17.55	2.10
Ak-9			0.36	7.31	1.09	0.17	0.11	0.90	1.69	1.53	8.12	0.062	0.55	15.91	1.80
Ak-10			0.93	8.35	2.94	0.32	0.13	0.51	1.57	2.75	15.53	0.203	1.56	16.00	0.14
Ak-11			0.22	7.59	0.87	0.19	0.13	0.55	0.99	1.12	6.78	0.063	0.48	16.69	2.47
Mean			0.37	7.66	1.03	0.19	0.11	0.79	1.50	1.54	8.33	0.082	0.73	16.63	2.06
Median			0.27	7.59	0.85	0.17	0.11	0.80	1.50	1.39	7.55	0.067	0.65	16.69	2.10
SD			0.23	0.99	0.75	0.05	0.02	0.23	0.39	0.48	2.75	0.046	0.32	0.55	1.01
Ak-12	Eze-Aku Group	Akukwa-II Well	0.17	7.59	0.72	0.11	0.10	0.69	1.10	1.19	6.72	0.061	0.59	16.92	2.67
Ak-13				0.15	7.31	0.68	0.14	0.11	0.74	1.31	0.98	5.73	0.065	0.59	17.55
Ak-14			0.73	5.18	2.36	0.44	0.17	1.98	5.87	3.13	10.61	0.056	0.34	78.00	3.12
Ak-15			0.12	8.80	0.74	0.17	0.17	0.49	1.24	1.09	6.47	0.064	0.37	17.83	1.39
Ak-16			0.19	7.50	0.74	0.15	0.13	0.73	1.40	1.21	6.73	0.079	0.59	16.73	1.35
Ak-17			0.61	6.75	1.36	0.22	0.10	0.82	1.27	1.38	7.49	0.071	0.7	16.31	2.26
Ak-18			0.23	5.69	0.77	0.11	0.14	0.63	1.37	1.15	5.92	0.106	0.77	16.91	1.39
Ak-19			0.44	5.63	1.36	0.13	0.16	0.69	1.64	1.23	6.32	0.117	0.75	16.00	1.45
Ak-20			0.30	4.96	0.94	0.12	0.16	0.65	1.46	0.90	4.67	0.113	0.73	17.00	1.33
Ak-21			0.40	6.41	1.15	0.16	0.16	0.62	1.34	1.28	6.83	0.114	0.72	17.45	1.39
Ak-22			0.62	5.92	1.54	0.20	0.16	0.50	1.10	1.27	7.06	0.155	1.0	15.75	1.13
Ak-23			0.52	5.99	1.22	0.30	0.15	0.76	2.03	8.83	28.25	0.101	0.67	18.29	0.60
Ak-24			0.99	2.85	2.45	0.29	0.19	0.56	1.52	1.75	8.75	0.136	0.70	16.92	1.22
Ak-25			1.07	2.73	3.14	0.31	0.18	0.59	1.45	2.11	9.74	0.146	0.81	15.14	1.37

Ak-26			0.96	2.57	3.14	0.32	0.20	0.59	1.47	1.68	7.91	0.152	0.78	16.31	1.15
Ak-27			0.23	2.67	0.81	0.39	0.18	0.61	1.41	2.18	10.03	0.142	0.81	17.90	1.36
Ak-28			0.40	2.93	1.27	0.35	0.20	0.53	1.30	1.53	7.70	0.165	0.81	15.46	0.91
Ak-29			0.21	2.75	0.73	0.30	0.16	0.63	1.55	1.66	7.83	0.132	0.81	18.33	0.68
Ak-30			0.21	2.62	0.61	0.22	0.19	0.55	1.36	1.35	5.71	0.131	0.7	16.18	2.20
Ak-31			0.23	2.55	0.76	0.33	0.17	0.37	1.15	2.12	9.26	0.156	0.91	15.30	0.42
Ak-32			0.22	2.49	0.74	0.25	0.18	0.53	1.47	2.03	9.37	0.147	0.82	16.20	0.61
Mean			0.43	4.85	1.30	0.24	0.16	0.68	1.61	1.91	8.53	0.115	0.71	19.64	1.39
Median			0.30	5.18	0.94	0.22	0.16	0.62	1.40	1.38	7.49	0.117	0.73	16.91	1.35
SD			0.30	2.10	0.80	0.10	0.03	0.32	1.00	1.67	4.79	0.036	0.16	13.40	0.68

## Chapter 5

### 5.0 Conclusion and Outlook

#### 5.1 Conclusion

At the beginning of this study, we set out to identify and characterize the lithofacies of the Mamu Formation in the western section of the Anambra Basin using complementary multidisciplinary techniques. This was done to provide answers to the research questions raised earlier that border on Campano-Maastrichtian paleoenvironment, palaeoceanography, paleoclimate, and provenance regions. In addition, this study was undertaken with materials from four outcrop sections on the western section of the Anambra Basin, as well as ditch cuttings/core from five wells from western, central and eastern parts of the Anambra Basin, two of which penetrated pre-Santonian units were investigated during the course of this study. The key findings are listed below.

➤ *Campano-Maastrichtian Paleoenvironment:*

This study on the outcropping units in the western section has documented the occurrence of seven lithofacies, which were combined into central basin, marsh, bay, barrier, beach, and washover fan facies association, as well as meandering fluvial-tidal channel facies association. These facies associations are hypothesized to indicate a tidally influenced wave dominated estuarine paleoenvironment in this part of the basin during the Campano-Maastrichtian age.

➤ *Campano-Maastrichtian paleoceanographic conditions*

Investigations conducted on the dark mudstone lithofacies reveal that the Trans-Saharan seaway was brackish (low salinity), with spatially variable organic facies preserved in the sediments. The more proximal dark mudstone units were deposited under higher energy shallow water conditions

characterized by terrestrial organic matter dilution (organic facies C and CD), whereas the more distal unit with less terrestrial organic matter dilution (organic facies BC and C) was deposited under lower energy at deeper water depth. Oxidic paleoredox bottom waters predominated. However, our findings suggest that anoxic conditions prevailed in the bottom water close to the sediment water interface as well as in pore waters a few centimetres below the sediment water interface. Furthermore, we hypothesize that conditions such as the presence of more reactive organic matter (marine palynomorphs), higher salinity (more sulphate), mineralogy (higher clay content), and slower rate of sedimentation (microfabric with thinner lamination and lower degree of bioturbation), which catalyse pyrite and preservation were more favourable in the more distal central basin than in the proximal units.

➤ *Campano-Maastrichtian paleoclimate and provenance characteristics*

This study has shown that the source areas of Mamu Formation experienced a high degree of chemical alteration, which contrasts the lower degree of chemical alteration observed for provenance areas of the pre-Santonian strata. This implies that a hot and humid paleoclimate prevailed at this time. In addition, subtle spatial variation in the extent of chemical alteration experienced by the Mamu Formation was observed. Sediments from the western section (outcropping units and samples from the Owan-1 well) show higher degrees of chemical alteration in comparison to the units from the central parts (Nzam-1 and Idah -1 wells) as well as from the eastern section (Amansiodo-1 well) of the Anambra Basin. This variability in the extent of chemical alteration is a consequence of salinity and the nature of detrital source.

Furthermore, this study has shown that during the Campano-Maastrichtian age, silica enriched detritus was contributed from Precambrian basement rocks, Jurassic granites as well as recycled pre-Santonian strata from three provenance regions with clear evidence of mixing, which

are the eastern, western and northern provenance regions. The eastern provenance region is characterized by low concentrations of Nb, Ta, Sn, Ti, high levels of W, Pb, Zn with enrichment of Pb over Zn, whereas the northern and western provenance regions are characterized by lower levels of Pb and Zn, as well as high levels of Nb, Ta, Sn and Ti. In addition, the northern provenance region is distinct from its western counterpart by the high levels of W, high enrichment of Nb relative to Ta as well as lower Zn concentration relative to Pb.

## 5.2 *Outlook*

The scope of the paleoceanographic study was limited to the western section of the Anambra Basin. It will be interesting to study the variability in organic facies, paleoredox and paleosalinity conditions across the Anambra, Bida, Benin and Sokoto basins during the Campano-Maastrichtian age. This will provide a regional insight on the nature of the Maastrichtian Trans-Saharan seaway. In addition, since data exists, it will be worthwhile to investigate the entire lithic fill of the Anambra Basin as well as the Paleogene sediments of the Niger Delta Basin. The following studies are herewith proposed:

- Investigation of Campano-Maastrichtian organic facies and paleoredox conditions across the Anambra Basin;
- Investigation of the spatio-temporal evolution of detrital contribution from provenance regions during late upper Cretaceous (Anambra Basin) to Paleogene (Niger Delta Basin);
- Investigation of late Cenomanian to Thanetian (late Paleocene) evolution of organic facies and paleoceanographic conditions of southern Nigeria with emphasis on understanding the nature and sea-surface temperatures of the Maastrichtian and Turonian Trans-Saharan seaways, as well as the Paleocene transgressive event.

- Investigation of hydrocarbon generation and mineral resource potentials of pre-Santonian (Benue Trough), post-Santonian (Anambra Basin) and Paleocene units (Niger Delta). This study will be complemented by geochemical evaluation of oils and coals from southern Nigeria. The oil samples have already been collected and preliminarily characterized by molecular geochemistry.

Furthermore, the Akukwa-II well penetrated the Cenomanian-Turonian boundary, which coincides with the OAE-2. Studies on this material as well as complementary materials from outcrops and other wells in the Benue Trough will provide a good insight on the regional expression and the driving mechanism(s) of this event in Benue Trough.

## References

- Abimbola, A.F., 1997. Petrographic and paragenetic studies of the Agbaja Ironstone Formation, Nupe Basin, Nigeria. *Journal of African Earth Sciences* 25 (2), 169-181.
- Abubakar, M.B., 2014. Petroleum Potentials of the Nigerian Benue Trough and Anambra Basin: A Regional Synthesis. *Natural Resources* 5, 25-58.
- Adebayo, O. F., Akinyemi, S. A. and Ojo, A. O. 2015. Paleoenvironmental studies of Odagbo coal mine sequence, northern Anambra basin, Nigeria: Insight from Palynomorph and geochemical analyses. *International Journal of Current Research*, 7 (9), 20274- 20286
- Adedosu, T. A., Sonibare, O. O., Ekundayo, O., and Tuo, J., 2010. Hydrocarbon-generative potential of coal and interbedded shale of Mamu formation, Benue Trough, Nigeria. *J. Pet. Sci. Technol.* 28, 412–427.
- Adedosu, T. A., Sonibare, O. O., Tuo, J., and Ekundayo, O., 2014. The Occurrence of Lacustrine Depositional Setting in the Mamu Formation, Anambra Basin, Nigeria, *Energy Sources, Part A: Recovery, Utilization, and Environmental Effects* 36 (4), 374-382. <https://doi.org/10.1080/15567036.2010.538801>
- Adegoke, A.K., Abdullah, W.H., Hakimi, M.H., Sarki Yandoka, B.M., 2014. Geochemical characterisation of Fika Formation in the Chad (Bornu) Basin, Northeastern Nigeria: Implications for depositional environment and tectonic setting. *Applied Geochemistry* 43, 1–12.
- Adelana, S.M.A., Olasehinde, P.I., Bale, R.B., Vrbka, P., Edet, A.E., Goni, I.B., 2008. An overview of the geology and hydrogeology of Nigeria. In: Adelana, S.M.A., MacDonald, A.M. (Eds.) *Applied Groundwater Studies in Africa. IAH Selected Papers in Hydrogeology* 13, pp. 171-197.
- Adeleye, D.R., 1973. Origin of ironstones, an example from the Middle Niger Valley, Nigeria *Journ. Sed. Petrology* 43, 709-727.
- Adeleye, D.R., 1974. Sedimentology of the fluvial Bida Sandstones (Cretaceous) Nigeria. *Sedimentary Geology* 12, 1-24.
- Adeleye, D. R., 1975. Nigerian Late Cretaceous stratigraphy and palaeogeography. *American Association of Petroleum Geologists Bulletin* 59, 2302–2313.
- Adekoya, J.A., Ola, P.S., Olabode, S.O., 2014. Possible Bornu Basin Hydrocarbon Habitat—A Review. *International Journal of Geosciences* 5, 983-996.



- Adepoju, S.A., Ojo, O.J., 2013. Petrophysical and Geochemical Studies of the Gongila Formation at Ashaka, Gongola Basin, Nigeria. *NAPE Bulletin* 25 (1), 43-51.
- Adetunji, J. R., Kogbe, C. A., 1986. The Maastrichtian marine environment in the southeastern flank of the Iullemeden Basin of West Africa. *Journal of African Earth Sciences* 5, 635–639.
- Agagu, O.K., Adighije C.I. 1983. Tectonic and sedimentation framework of the lower Benue Trough, Southeastern Nigeria. *Journal of African Earth Sciences* 1, 267–274
- Aganbi, E.G. 2010. Geochemical and Source rock evaluation of Campano-Maastrichtian rocks, in the Anambra Basin Southeastern Nigeria. Unpublished M.Sc. thesis, University of Benin, 88p.
- Agumanu, A.E., Enu, E.I., 1990. Late Cretaceous clay distribution in the Lower Benue Trough; its palaeoenvironmental and tectonic implication. *Journal of African Earth Sciences* 10 (3), 465-470.
- Agyingi, C. M., 1993. Palynological evidence for a Late Cretaceous age for the Patti Formation, eastern Bida basin, Nigeria. *Journal of African Earth Sciences* 17(4), 513-523.
- Ajayi, T.R., Isklander, F.Y., Asubiojo, O.I., and Klein, D.E., 1989. Geochemistry of Upper Cretaceous clastic sediments of Ifon area Southwestern Nigeria. *Journal of Mining and Geology* 25, 11-24.
- Akaegbobi, I.M., Nwachukwu, J.I., and Schmitt, M., 2000. Aromatic hydrocarbon distribution and calculation of oil and gas volumes in post-Santonian shale and coal, Anambra basin, Nigeria. In: Mello, M.R. and Katz, B.J. (Eds.), *Petroleum Systems of South Atlantic margins*. AAPG memoir 73, 233-245.
- Akande, S.O., Mücke, A., 1993. Tectonic and sedimentation framework of the Lower Benue Trough, Southeastern Nigeria. *Journal of African Earth Sciences* 17 (4), 445-456.
- Akande, S.O., Ojo, O.J., Erdtmann, B.D., Hetenyi, M., 1998. Palaeoenvironments, source rock potential and thermal maturity of the Upper Benue rift basins, Nigeria: implications for hydrocarbon exploration. *Organic Geochemistry* 29, 531-542.
- Akande, S.O., Erdtmann, B.D., 1998. Burial metamorphism (thermal maturation) in Cretaceous Sediments of the southern Benue Trough and the Anambra Basin, Nigeria. *AAPG Bulletin* 82, 1191–1206.
- Akande, S.O., Ojo, O.J., Erdtmann, B.D., Hetenyi, M., 2005. Palaeoenvironments, organic

- petrology and Rock-Eval studies on source rock facies of the Lower Maastrichtian Patti Formation, southern Bida Basin, Nigeria. *Journal of African Earth Science* 41, 394–406.
- Akande, S.O., Ogunmoyero, I.B., Petersen, H.I., Nytoft, H.P., 2007. Source rock evaluation of Coals from the lower Maastrichtian Mamu Formation, SE Nigeria. *Journal of Petroleum Geology* 30 (4), 303–324
- Akande, S.O., Egenhoff, S.O., Obaje, N.G., Ojo, O.J., Adekeye, O.A., Erdtmann, B.D., 2012. Hydrocarbon potential of Cretaceous sediments in the Lower and Middle Benue Trough, Nigeria: Insights from new source rock facies evaluation. *Journal of African Earth Science* 64, 34-47.
- Akinyemi, S.A., Adebayo, O. F., Ojo, O. A., Fadipe, O. A., Gitari, W. M. 2013. Mineralogy and Geochemical Appraisal of Paleo-Redox Indicators in Maastrichtian Outcrop Shales of Mamu Formation, Anambra Basin, Nigeria. *Journal of Natural Sciences Research* 3 (10), 2224-3186
- Akujieze, C.N., Coker, S.J., Oteze, G.E., 2003. Groundwater in Nigeria-a millennium experience-distribution, practice, problems and solutions. *Hydrogeol. J.* 11 (2), 259–274.
- Alafara, A., Adekola, F.A., Folashade, A.O., 2005. Quantitative leaching of a Nigerian iron ore in hydrochloric acid. *J. Appl. Sci. Environ. Mgt.* 9 (3), 15–20.
- Alalade, B., Tyson, R.V., 2013. Influence of igneous intrusions on thermal maturity of Late Cretaceous Shales in the Tuma-1 well, Chad Basin, NE Nigeria. *Journal of African Earth Science* 77, 59-66.
- Allix, P., Popoff, M., 1983. Le Crétacé inférieur de la partie nord-orientale du fossé de la Bénoué (Nigeria); un exemple de relation étroite entre tectonique et sédimentation. *Bulletin des Centres des Recherches Exploration–Production Elf-Aquitaine* 7 (1), 349 - 359.
- Ali, S., Statterger, K., Garbe-Schönberg, D., Frank, M., Kraft, S., Kuhnt, W., 2014. The provenance of Cretaceous to Quaternary sediments in the Tarfaya Basin, SW Morocco: evidence from trace element geochemistry and radiogenic Nd-Sr isotopes. *Journal of African Earth Sciences*, 90, 64-76
- Aliyu, A.H., Mamman, Y.D., Abubakar, M.B., Sarki Yandoka, M.B., Jitong, J.S., Shettima, B., 2017. Paleodepositional environment and age of Kanawa Member of Pindiga Formation, Gongola Sub-basin, Northern Benue Trough, NE Nigeria: Sedimentological and palynological approach. *Journal of African Earth Sciences* 134, 345 – 351.

- Amajor, L.C., 1987a. Major and trace element geochemistry of Albian and Turonian shales from the Southern Benue trough, Nigeria. *Journal of African Earth Sciences*, 6 (5), 633-641
- Amajor, L.C., 1987b. Paleocurrent, Petrography and Provenance analyses of the Ajali Sandstone (Upper Cretaceous), Southeastern Benue trough, Nigeria. *Sedimentary Geology*, 54, 47-60.
- Amedjoe, C.G., Gawu, S.K.Y., Ali, B., Aseidu, D.K., Nude, P.M., 2018. Geochemical composition of Neoproterozoic to lower Paleozoic (?) shales and siltstones in the Volta Basin (Ghana): Constraints on provenance and tectonic setting. *Sedimentary Geology*, 368, 114-131
- Amobi, J.O., Okogbue, C.O., Mode, A.W., Ofoma, A.E., Dim, C.I.P., Okwara, I.C., 2019. Regional 1D hydrocarbon maturation modelling of the Cenomanian–Turonian Lokpanta Shale, southern Benue Trough, Nigeria: Implications for the origin of Niger Delta deep sea oils. *J. Earth Syst. Sci.* 128:174 <https://doi.org/10.1007/s12040-019-1192-8>
- Anderson, D.H., Hawkes, H.E., 1958. Relative mobility of the common elements in weathering of some schist and granite areas. *Geochim. Cosmo.* 14, 204 – 210.
- Andrade, G.R.P., Azevedo, A.C., Cuadros, J., Furquim, S.A.C., Souza Junior, V.S., Kiyohara, P.K., Vidal-Torrado, P., 2014. Transformation of kaolinite into smectite and Fe-illite in Brazilian mangrove soils. *Soil Science Society of America Journal.* 78, 655–672.
- Arthur, M.A., Dean, W.E., Claypool, G.E., 1985. Anomalous <sup>13</sup>C-enrichment in modern marine organic matter, *Nature*, 315, 216-218,
- Asadu, A. N., and Ibe, K. A., 2017. Petroleum Geology of Outcropping Sediments along Imiegba Road in Etsako East Local Government Area of Edo State, Southern Anambra Basin Flank, Nigeria: Inference from Sedimentology and Organic Geochemistry. *Journal of Geography, Environment and Earth Science International* 10(3), 1-10
- Ayinla, H.A., Abdullah, W.H., Makeen, Y.M., Abubakar, M.B., Jauro, A., Sarki Yandoka, B.M., Mustapha, K.A., Zainal Abidin, N.S., 2017. Source rock characteristics, depositional setting and hydrocarbon generation potential of Cretaceous coals and organic rich mudstones from Gombe Formation, Gongola Sub-basin, Northern Benue Trough, NE Nigeria. *International Journal of Coal Geology* 173, 212–226.
- Ayoola, E.O., 1981. Paleocurrent and sedimentological studies in the Benue Trough, Nigeria. *Sedimentary Geology*, 28, 153-162.

- Bata, T., Parnell, J., Samaila, N.K., Abubakar, M.B., Maigari, A.S., 2015. Geochemical evidence for a Cretaceous oil sand (Bima oil sand) in the Chad Basin, Nigeria. *Journal of African Earth Sciences* 111, 148 – 155.
- Babatunde, O.L., 2010. The main oil source formations of the Anambra Basin, Southeastern Nigeria. AAPG Search and Discovery Article #90108©2010 AAPG International Convention and Exhibition, September 12-15, 2010 Calgary, Alberta, Canada.
- Banerjee, I., 1981. Storm lag and related facies of the bioclastic limestones of the Eze-Aku Formation (Turonian), Nigeria. *Sed. Geo.* 30, 133-147
- Basu, A., Bickford, M.E., Deasy, R., 2016. Inferring tectonic provenance of siliciclastic rocks from their chemical compositions: a dissent. *Sedimentary Geology* 336, 26-35
- Bauersachs, T., Schouten, S., Schwark, L., 2014. Characterization of the sedimentary organic matter preserved in Messel oil shale by bulk geochemistry and stable isotopes. *Palaeo., Palaeo.*, *Palaeo.* 410, 390–400.
- Behre Dolbear and Company, 2006. Nigerian Coal Resource development feasibility study report. Project 04-084. 236p.
- Benkhelil, J., 1982. Benue Trough and Benue Chain. *Geol. Mag.* 119, 155-168.
- Benkhelil, J., 1986. Caractéristiques structurales et évolution géodynamique du bassin intracontinental de la Bénoué (Nigéria). Thèse d'état, Nice, p. 275.
- Benkhelil, J., 1989. The origin and evolution of the Cretaceous Benue Trough, Nigeria. *Journal of African Earth Science* 8, 251–282.
- Benkhelil, J., Robineau, B., 1983. Le fossé de la Bénoué est-il un rift? In: Popoff, M., Tiercelin, J.J. (Eds.). *Rifts et fossés anciens. Bulletin des Centres des Recherches Exploration–Production Elf-Aquitaine* 7, 315-32.
- Berner, R.A., 1984. Sedimentary pyrite formation: An update\*. *Geochimica et Cosmochimica Acta* 48, 605-615
- Best, M. G. 2003. *Igneous and Metamorphic Petrology*: 2nd ed. Oxford Blackwell Science xxi + 729p.
- Bhatia, M.R., Crook, K.A.W., 1986, Trace element characteristics of greywackes and tectonic setting discrimination of sedimentary basins: *Contributions to Mineralogy and Petrology*, 92, 181–193. <https://doi.org/10.1007/BF00375292>
- Binks, R.M., Fairhead, J.D., 1992. A plate tectonic setting for Mesozoic rifts of West and Central

- Africa. In: Ziegler P.A. (Ed.), *Geodynamics of Rifting, Volume II. Case History Studies on Rifts: North and South America and Africa*. *Tectonophysics* 213, 141-151.
- Boboye, O.A., Abimbola, A.F., 2009. Hydrocarbon potential of the lithostratigraphic units in Late Cenomanian-Early Paleocene shale, Southwestern Chad Basin. *World Appl. Sci. J.* 7 (5), p. 567-573.
- Bodin, S., Meissner, P., Janssen, N.M., Steuber, T., Mutterlose, J., 2015. Large igneous provinces and Organic carbon burial: controls on global temperature and continental weathering during the Early Cretaceous. *Glob. Planet. Chang.* 133, 238-253.
- Bonne, K. P. M., 2014. Reconstruction of the evolution of the Niger River and implications for sediment supply to the Equatorial Atlantic margin of Africa during the Cretaceous and the Cenozoic. *Geological Society, London, Special Publications* 386, 327-349. <https://doi.org/10.1144/SP386.20>
- Boyd, R., Dalrymple, R.W., Zaitlin, B.A., 2006. Estuarine and incised valley facies models. In: Posamentier, H.W., Walker, R.G. (Eds.), *Facies Models Revisited*. *SEPM Special Publication*, 84, 171–235.
- Brownfield, M.E., Charpentier, R.R., 2006. Geology and total petroleum systems of the Gulf of Guinea Province of West Africa. *U.S Geological Survey Bulletin* 2207-C, 1-32.
- Burke, K.C., Dewey J.F., 1974. Two plates in Africa during the Cretaceous? *Nature* 249, 313-316.
- Burke, K.C., Whiteman, A.J., 1973. Uplift, Rifting and the Break Up of Africa. In: Tarling, D.H. and Runcorn, S.K (Eds.), *Implications on Continental Drift to Earth Sciences*, Academic Press, London, pp. 735-755.
- Burke, K.C., Dessauvage, T.F.J., Whiteman, A.J., 1970. Geological history of the Benue Valley and adjacent areas. In: Dessauvage, T.F.J., Whiteman, A.J. (Eds.), *African Geology*, University of Ibadan Press, Nigeria, pp. 187-205.
- Busby, C.J., Ingersoll, R.V., Editors, 1995. *Tectonics of Sedimentary Basins*. Blackwell Science, Cambridge, Massachusetts, p. 579.
- Chiaghanam, O.I., Chiadikobi, K.C., Ikegwuonu, O.N., Omoboriowo, A.O., Onyemesili, O.C., Acra E.J., 2013. Palynofacies and Kerogen Analysis of Upper Cretaceous (Early Campanian to Maastrichtian) Enugu Shale and Mamu Formation in Anambra Basin, South-Eastern Nigeria: *International Journal of Scientific & Technology Research* 2 (8), 87-97
- Coker, S.J.L., Ejedawe, J.E., 1987. Petroleum prospects of the Benin basin. *Nigerian journal of*

- Mining and Geology 23, 27-43.
- Courville, P., Lang, J., Thierry, J., 1998. Ammonite faunal exchanges between south Tethyan Platforms and south Atlantic during the Uppermost Cenomanian-Lower-most Middle Turonian in the Benue trough (Nigeria). *Geobios* 31, (2), 187-214.
- Cox, R., Lowe, D.R., Cullers, R.L., 1995. The influence of sediment recycling and basement composition on evolution of mudrock chemistry in the southwestern United States. *Geochimica et Cosmochimica Acta* 59 (14), 2919-2940.
- Cuadros, J., Andrade, G., Ferreira, T.O., Partiti, C.S.M., Cohen, R., Vidal-Torrado, P., 2017. The Mangrove reactor: fast clay transformation and potassium sink. *Applied Clay Science* 140, 50–58
- Cratchley, C.R., Jones, J.P., 1965. An interpretation of the geology and gravity anomalies of the Benue Valley, Nigeria. *Overseas Geol Surv. Geophys. Paper* 9, 1-28.
- Cullers, R.L., Stone, J., 1991. Chemical and mineralogical comparison of the Pennsylvanian Fountain Formation, Colorado, U.S.A. (an uplifted continental block) to sedimentary rocks from other tectonic environments. *Lithos* 27, 115–131.
- Cullers, R.L., 1995. The controls on the major- and trace-element evolution of shales, siltstones and sandstones of Ordovician to Tertiary age in the Wet Mountains region, Colorado, U.S.A. *Chemical Geology* 123, 107-131.
- Cullers, R.L., 2000. The geochemistry of shales, siltstones and sandstones of Pennsylvanian-Permian age, Colorado, U.S.A.: implications for provenance and metamorphic studies. *Lithos* 51, 181–203.
- d’Almeida, G.A.F., Kaki, C., Adeoye, J.A., 2016. Benin and Western Nigeria offshore basins: a stratigraphic nomenclature comparison. *International Journal of Geosciences*, 7, 177-188.
- Dalrymple, R.W., Zaitlin, B.A., Boyd, R., 1992. Estuarine facies models: conceptual basis and stratigraphic implications. *Journal of Sedimentary Petrology* 62, 1130-1146.
- Dim, C.I.P., Okwara, I.C., Mode, A.W., Onuoha, K.M., 2016. Lithofacies and environments of deposition within the Middle–Upper Cretaceous successions of Southeastern Nigeria. *Arabian Journal Geoscience* 9, 1-17.
- Dim, C.I.P., Onuoha, K.M., Anyiam, O.A., Okwara, I.C., Oha, I.A., Okonkwo, I.A., Okeugo, C.G., Nkitam, E.E., Ozumba, B.M., 2018. Analysis of petroleum system for exploration

- and risk reduction in the south-eastern inland basins of Nigeria. *Pet. Coal* vol. 60 (2), 305-320.
- Dim, C.I.P., Onuoha, K.M., Okwara, I.C., Okonkwo, I.A., Ibemesi, P.O., 2019. Facies analysis and depositional environment of the Campano – Maastrichtian coal bearing Mamu Formation in the Anambra Basin, Nigeria. *Journal of African Earth Sciences*, 152, 69 -83. DOI: <https://doi.org/10.1016/j.jafrearsci.2019.01.011>
- Edegbai, A.J., Emofurieta, W.O., 2015. Preliminary assessment of source rock potential and palynofacies analysis of Maastrichtian Dark Shale, SW Anambra basin. *Ife J. Sci.* 17(1), 131-139.
- Edegbai, A.J., Schwark, L., Oboh-Ikuenobe, F.E., 2019a. A review of the latest Cenomanian to Maastrichtian geological evolution of Nigeria and its stratigraphic and paleogeographic implications. *Journal of African Earth Sciences*, 150, 823-837 <https://doi.org/10.1016/j.jafrearsci.2018.10.007>
- Edegbai, A.J., Schwark, L., Oboh-Ikuenobe, F.E., 2019b. Campano-Maastrichtian paleoenvironment, paleotectonics and sediment provenance of Western Anambra Basin, Nigeria: Multi-proxy evidences from the Mamu Formation. <https://doi.org/10.1016/j.jafrearsci.2019.04.001>
- Edem, G.O., Ekwueme, B.N., Ephraim, B.E., 2015. Geochemical signatures and mineralization potentials of precambrian pegmatites of southern Obudu, Bamenda Massif, southeastern Nigeria. *International Journal of Geophysics and Geochemistry* 2(3), 53-67.
- Edem, G.O., Ekwueme, B.N., Ephraim, B.E., Igonor, E.E., 2016. Preliminary investigation of pegmatites in Obudu area, southeastern Nigeria, using stream sediments geochemistry. *Global journal of pure and applied sciences* 22, 167-175.
- Edet, J.J., Nyong, E.E., 1993. Depositional environments, sea-level history and paleobiogeography of the late Campanian-Maastrichtian on the Calabar flank, SE Nigeria. *Palaeogeography, Palaeoclimatology, Palaeoecology*, 102, 1161-175.
- Ejeh, O.I. 2016. The Maastrichtian sedimentary successions of the Anambra Basin recently exposed around Okpekpe and Imiegba: Part of the Mamu or Ajali Formation. *Nigerian Journal of Science and Environment*, 14 (1), 38-48
- Ehinola, O.A., Ekweozor, C.M., Oros, D.R., Simoneit, B.R.T., 2002. Geology, geochemistry and biomarker evaluation of Lafia-Obi coal, Benue Trough, Nigeria. *Fuel* 81, 219–233.

- Ehinola, O.A., Sonibare, O.O. Falode, O.A., Awofala, B.O., 2005. Hydrocarbon potential and thermal maturity of Nkporo Shale from Lower Benue Trough, Nigeria. *Journal of Applied Sciences* 5(4), 689-695.
- Elewa, A.T.M., 2017. Ostracod provincialism and migration as a response to movements of Earth's plates: Cretaceous-Paleogene ostracods of West Africa, North Africa and the Middle East. *Journal of African Earth Sciences* 134, 92-105. <https://doi.org/10.1016/j.jafrearsci.2017.06.022>.
- Enu, E.I., 1985. Textural characteristics of the Nigerian tar sands. *Sedimentary Geology* 44, 65-81
- El Hassan, W. M., Farwa, A.G., Awad, M.Z., 2017. Inversion tectonics in Central Africa Rift System: evidence from the Heglig Field. *Marine and Petroleum Geology* 80, 293-306.
- Fairhead. J.D., 1988. Mesozoic plate tectonic reconstructions of the central South Atlantic Ocean: the role of the West and Central African rift system. In: Scotese, C.R., Sager, W.W. (Eds.), *Mesozoic and Cenozoic Plate Reconstructions*. *Tectonophysics* 155, 181-191.
- Fairhead, J.D., Green, C.M., 1989. Controls on rifting in Africa and the regional tectonic model for the Nigerian and East Niger rift basins. *Journal of African Earth Sciences* 8 (2-4), 231-249.
- Fairhead, J.D, Binks, R.M., 1991. Differential opening of the Central and South Atlantic Oceans and the opening of the West African Rift System. *Tectonophysics*, 187, 191-203.
- Fairhead, J.D., Green, C.M., Masterton, S.M., Guiraud, R., 2013. The role that plate tectonics, inferred stress changes and stratigraphic unconformities have on the evolution of the West and Central African Rift System and the Atlantic continental margins. *Tectonophysics* 594, 118–127.
- Feng, R., Kerrich, R., 1990. Geochemistry of fine grained clastic sediments in the Archaean Abitibi greenstone belt, Canada: implication for provenance and tectonic setting. *Geochimica et Cosmochimica Acta* 54, 1061–1081.
- Folk, R.L. 1974. *Petrology of Sedimentary Rocks*: Hemphill Publishing Co., Austin, 170 p.
- Gebhardt, H., 1997. Cenomanian to Turonian foraminifera from Ashaka (NE Nigeria): quantitative analysis and palaeoenvironmental interpretation. *Cretaceous Research* 18, 17–36.
- Gebhardt, H., 1998. Benthic foraminifera from the Maastrichtian lower Mamu Formation near Leru (southern Nigeria): paleoecology and paleogeographic significance. *Journal of Foraminiferal Research* 28, 76–89.



- Gebhardt, H., 1999. Cenomanian to Coniacian ostracods from the Nkalagu area (SE Nigeria): biostratigraphy and palaeoecology. *Paläontologische Zeitschrift* 73, 77-98
- Gebhardt, H., 2001. Calcareous nannofossils from the Nkalagu Formation type locality (middle Turonian to Coniacian, southern Nigeria): biostratigraphy and palaeoceanic implications. *Journal of African Earth Sciences*, 32 (3), 391-402.
- Gebhardt, H., 2004. Planktonic foraminifera of the Nkalagu Formation type locality (southern Nigeria, Cenomanian to Coniacian): biostratigraphy and palaeoenvironmental interpretation. *Cretaceous Research* 25, 191-209.
- Guiraud, M., 1990. Tectono-sedimentary framework of the Early Cretaceous continental Bima Formation (Upper Benue Trough, NE Nigeria). *Journal of African Earth Sciences* 10, 341–353.
- Guiraud, R., Bosworth, W., 1997. Senonian basin inversion and rejuvenation of rifting in Africa and Arabia. Synthesis and implications to plate-scale tectonics. *Tectonophysics* 282, 39-82.
- Genik, G.J., 1992. Regional framework, structural and petroleum aspects of rift basins in Niger, Chad and the Central African Republic (C.A.R.). In: Ziegler, P.A. (Ed.), *Geodynamics of Rifting, Volume II. Case History Studies on Rifts: North and South America and Africa*. *Tectonophysics* 213, 169-185.
- Hamza, H., Obaje, N.G., Moumouni, A., 2011. Benthonic foraminiferal assemblages from the Bornu Basin, Northeastern Nigeria. *Journal of Mining and Geology* 48 (2), 91–115.
- Hassan, A.M., 2017. Mineral composition and geochemistry of the Upper Cretaceous siliciclastics (Nubia Group), Aswan District, south Egypt: Implications for provenance and weathering. *Journal of African Earth Sciences* 135, 82-95
- Hay, W.W., Floegel, S., 2012. New thoughts about the Cretaceous climate and oceans. *Earth-Science Reviews*, 115, 262-272
- Hoque, M., 1977. Petrographic differentiation of tectonically controlled Cretaceous sedimentary cycles, southeastern Nigeria. *Sedimentary Geology* 17: 235—245
- Idowu, J.O., Enu, E.I., 1992. Petroleum geochemistry of some Late Cretaceous shales from the Lokoja Sandstone of Middle Niger Basin, Nigeria. *Journal of African Earth Sciences* 14 (3), 443-455.
- Igbinigie, N.S., Ogbamikhumi, A., Komlan-Dodoh, N.O., 2017. Palynological Evaluation of

- Potential Source Rocks at Imiegba, Benin Flank of the Anambra Basin, Nigeria. *Indo-Iranian Journal of Scientific Research* 1, 88-94.
- Igwe, E.O., Okoro, A.U., 2016. Field and lithostratigraphic studies of the Eze-Aku Group in the Afikpo Synclinorium, southern Benue Trough, Nigeria. *Journal of African Earth Sciences* 119, 38-51.
- Igwe, E.O., 2017. Composition, provenance and tectonic setting of Eze-Aku Sandstone facies in the Afikpo Synclinorium, Southern Benue Trough, Nigeria. *Environmental Earth Sciences* 76, 1-12. <https://doi.org/10.1007/s12665-017-6750-2>
- Imarhiagbe, J.O., 2017. Geochemistry and rare earth element characterization of syenite intrusions and associated rocks in Igarra, South West Nigeria. Unpublished M.Sc. Dissertation, University of Benin.
- Imeokparia, E.G., 1982a. Abundance and distribution of tungsten in the Afu Younger Granite complex, central Nigeria. *J. of Geochem. Expl.* 17, 93--108
- Imeokparia, E.G., 1982b. Tin content of biotites from the Afu Younger Granite complex, central Nigeria. *Econ. Geology* 77, 1710-1724
- Imeokparia, E. G., and Onyeobi, T. U., 2007. Geochemistry and Depositional Characteristics Of Maastrichtian Shales in parts of southwestern Nigeria. *Journal of Mining and Geology* 43 (2), 167-174.
- Jauro, A., Obaje, N.G., Agho, M.O., Abubakar, M.B., Tukur, A., 2007. Organic geochemistry of Cretaceous Lamza and Chikila coals, Upper Benue trough, Nigeria. *Fuel* 86, 520–532.
- Jenkyns, H. C., 2010. Geochemistry of oceanic anoxic events. *Geochem. Geophys. Geosyst.*, 11 (3), 1-30.
- Kaki, C., d'Almeida, G.A.F., Yalo, N., Amelina, S., 2013. Geology and Petroleum Systems of the Offshore Benin Basin. *Oil and Gas Science and Technology-Rev. IFP Energies nouvelles*, 68 (2), 363-381.
- King, L.C., 1950. Speculations upon the outline and mode of disruption of Gondwanaland: *Geol. Mag.* 87, 353-359.
- Klein, G.D., 1995. Intracratonic basins. In: Busby, C.J., Ingersoll, R.V. (Eds.). *Tectonics of Sedimentary Basins*. Blackwell Science Inc., Cambridge, Massachusetts, pp. 459–478.
- Kinnaird, J.A., 1984. Contrasting styles of Sn-Nb-Ta-Zn mineralization in Nigeria. *J. Afr. Earth Sci.* 2 (2), 81-90

- Kogbe, C.A. 1976. Outline of the geology of the Iullemeden Basin in Northwestern Nigeria. In: Kogbe, C.A. (Ed.), *Geology of Nigeria*, Elizabethan Publishing Co., Lagos, pp. 331-338.
- Kogbe, C. A. 1980. The Transsaharan seaway during the Cretaceous. In: Salem, M.J., Busrewil, M.T. (Eds.), *Geology of Libya, Volume 1*. Academic Press, London, pp. 91–96.
- Kogbe, C.A., 1981. Cretaceous and Tertiary of the Iullemeden Basin of Nigeria (West Africa). *Cretaceous Research* 2, 129–186.
- Kogbe, C.A., Ajakaiye, D.E., Matheis, G., 1983. Confirmation of rift structure along the Mid-Niger Valley, Nigeria: *Journal of African Earth Sciences* 1, 127–131.
- Kuhnt, W., Herbin, J.P., Thurow, J., Wiedmann, J., 1990. Distribution of Cenomanian-Turonian Organic Facies in the Western Mediterranean and Along the Adjacent Atlantic Margin In: Huc, A. Y. (Ed.): *Deposition of Organic Facies*. American Association of Petroleum Geologists, *Studies in Geology* 30, 133-160. DOI: <https://doi.org/10.1306/St30517>
- Ladipo, K.O., 1986. Tidal shelf depositional model for the Ajali Sandstone, Anambra Basin, southern Nigeria. *J. African Earth Sci.* 5, 177-185
- Ladipo, K.O., 1988. Paleogeography, sedimentation and tectonics of the Upper Cretaceous Anambra Basin, Southeastern Nigeria. *Journal of African Earth Sciences* 7, 865- 871.
- Lamb, A.L., Wilson, G.P., Leng, M.J., 2006. A review of coastal palaeoclimate and relative sea-level reconstructions using  $\delta^{13}\text{C}$  and C/N ratios in organic material. *Earth-Sci. Rev.* 75, 29-57
- Lapworth, D.J., Knights, K.V., Key, R.M., Johnson, C.C., Ayoade, E., Adekanmi, M.A., Arisekola, T.M., Okunlola, O.A., Backman, B., Eklund, M., Everett, P.A., Lister, R.T., Ridgway, J., Watts, M.J., Kemp, S.J., Pitfield, P.E.J., 2012. Geochemical mapping using stream sediments in west-central Nigeria: implications for environmental studies and mineral exploration in West Africa. *Applied Geochemistry* 27, 1035–1052.
- Lazar, O.R., Bohacs, K.M., Macquaker, J.H.S., Schieber, J., Demko, T.M., 2015. Capturing key attributes of fine-grained sedimentary rocks in outcrops, cores, and thin sections: nomenclature and description guidelines *Journal of Sedimentary Research* 85 (3), 230-246
- Lingham-Soliar, T., 1998. A new mosasaur *Pluridens walker* from the Upper Cretaceous Maastrichtian of the Iullemeden basin, Southwest Niger. *J. Vertebr. Paleontol.* 18(4), 709–717.
- Luger, P., 2003. Palaeobiogeography of late early cretaceous to early Paleocene marine ostracoda

- in Arabia and North to equatorial Africa. *Palaeogeogr. Palaeoclim. Palaeoecol.* 196, 319-342.
- Markwick, P.J., 2018. Palaeogeography in exploration. *Geological Magazine*, 1-42.  
<https://doi.org/10.1017/S0016756818000468>
- McLennan, S.M., Taylor, S.R., 1991. Sedimentary rocks and crustal evolution: tectonic setting and secular trends. *J. of Geology* 99, 1-21
- McLennan, S. M., Hemming, S., McDaniel, D. K., and Hanson, G. N., 1993. Geochemical approaches to sedimentation, provenance, and tectonics, In: Johnsson, M. J., and Basu, A., (Eds.), *Processes Controlling the Composition of Clastic Sediments*: Boulder, Colorado. Geological Society of America Special Paper 284, 21–40.
- McLennan, S. M., 2001. Relationships between the trace element composition of sedimentary Rocks and upper continental crust, *Geochemistry Geophysics and Geosystems* 2, <https://doi.org/10.1029/2000GC000109>.
- Meyers, P.A., 1994. Preservation of elemental and isotopic source identification of sedimentary organic matter. *Chemical Geology* 114, 289–302.
- Meyers, P.A., 1997. Organic geochemical proxies of paleoceanographic, paleolimnologic, and paleoclimatic processes. *Organic Geochemistry* 27, 213– 250.
- Moody, R.T.J., Sutcliffe, P.J.C., 1991 The Cretaceous deposits of the Iullemeden Basin of Niger, Central West Africa. *Cretaceous Research* 12, 137-157.
- Moulin, M., Aslanian, D., Unternehr, P., 2010. A new starting point for the South and Equatorial Atlantic Ocean. *Earth-Science Reviews* 98, 1–37.
- Mücke, A., Woakes, M., 1986. Pyrophanite: a typical mineral in the Pan-African Province of Western and Central Nigeria. *J. Afr. Earth Sci.* 5(6), 675-689
- Mücke, A., Badejoko, T.A., Akande, S.O., 1999. Petrographic – microchemical studies and origin of the Agbaja Phanerozoic Ironstone Formation, Nupe Basin, Nigeria: a product of a ferruginized ooidal kaolin precursor not identical to the Minette-type. *Mineralium Deposita* 34, 284-296.
- Mücke, A., 2000. Environmental conditions in the Late Cretaceous African Tethys: conclusions from a microscopic-microchemical study of ooidal ironstones from Egypt, Sudan and Nigeria. *Journal of African Earth Sciences* 30, 25-46
- Müller P. J., 1977. CN ratios in Pacific deep-sea sediments: Effect of inorganic ammonium and

- organic nitrogen compounds sorbed by clays. *Geochim. Cosmochim. Acta* 41(6), 765–776.
- Murat, R.C., 1972. Stratigraphy and paleogeography of the Cretaceous and Lower Tertiary in Southern Nigeria. In: Dessauvage, T.F.J., Whiteman, A.J. (Eds.), *African Geology*, University of Ibadan Press, Nigeria, pp. 251-266.
- Nesbitt, H.W., Young, G.M., 1982. Early Proterozoic climates and plate motions inferred from major element chemistry of lutites: *Nature* 299, 715–717
- Nigerian Geological Survey Agency (NGSA), 2006. Geological and mineral resources map of Edo State
- Nton, M. E., Awarun, A. O., 2011. Organic geochemical characterization and hydrocarbon potential of subsurface sediments from Anambra basin, SE Nigeria: *Mineral Wealth* 162, 23–42
- Nton, M.E., Okunade, A., 2013. Aspects of hydrocarbon potential and clay mineralogy of the Patti Formation, southern Bida Basin, Nigeria. *NAPE Bulletin* 25 (1), 15-28.
- Nton, M.E., Adamolekun, O.J., 2016. Sedimentological and geochemical characteristics of outcrop sediments of Southern Bida Basin, central Nigeria: implications for provenance, paleoenvironment and tectonic history. *Ife Journal of Science* 18 (2), 345-369.
- Nwajide, C.S., 1988. Convergent mud drapes on some planar cross-beds in the fluvial Turonian Sandstones of the Makurdi formation, Benue Trough, Nigeria. *Journal of African Earth Sciences* 7(1), 113-120.
- Nwajide, C.S., 2013. *Geology of Nigeria's Sedimentary Basins*. CSS Bookshop Ltd., Lagos, p. 565.
- Obaje, N.G., Ligouis, B., Abaa, S.I., 1994. Petrographic composition and depositional environments of Cretaceous coals and coal measures in the Middle Benue Trough of Nigeria. *International Journal of Coal Geology* 26, 233-260.
- Obaje, N.G., Ligouis, B., 1996. Petrographic evaluation of the depositional environments of the Cretaceous Obi/Lafia coal deposits in the Benue trough of Nigeria. *Journal of African Earth Sciences* 22(2), 159-171.
- Obaje, N.G., Wehner, H., Scheeder, G., Abubakar, M.B., Jauro, A., 2004. Hydrocarbon prospectivity of Nigeria's inland basins: from the viewpoint of organic geochemistry and organic petrology. *AAPG Bulletin*, 88 (3), 325–353.
- Obaje, N.G., Attah, D.O., Opeloye, S.A., Moumouni, A., 2006. Geochemical evaluation of the

- hydrocarbon prospects of sedimentary basins in Northern Nigeria. *Geochemical Journal* 40, 227 -243.
- Obaje, N.G., 2009. *Geology and Mineral Resources of Nigeria*. Springer-Verlag Berlin Heidelberg, p. 221.
- Obi, G.C., 1998. Upper Cretaceous Gongila Formation in the Hawal Basin, Northeast Benue Trough: a storm and wave dominated regressive shoreline complex. *Journal of African Earth Sciences* 26 (4), 619-632.
- Obi, G.C. and Okogbue, C.O., 2004. Sedimentary response to tectonism in the Campanian–Maastrichtian succession, Anambra Basin, Southeastern Nigeria: *J. Afr. Earth Sci.* 38, p.99–108.
- O'Brien, N. R., and Slatt, R. M., 1990. *Argillaceous rock atlas*: Springer-Verlag, 141 p.
- Odedede, O., 2013. Palaeopalynology and sequence stratigraphy of the Mamu Formation around Orhua, Southwestern Nigeria. *Nigerian Journal of Science and Environment* 12, 128-134
- Odeyemi, I. B., 1988. Lithostratigraphic and structural relationships of the upper Precambrian Metasediments in Igarra area, Western Nigeria. *In*: Oluyide, P. O., Mbonu, W. O., Ogezi, A. E. O., Egbuniwe, I. G., Ajibade, A. C., and Umeji, A. O. (eds.), *Precambrian Geology of Nigeria*. Geological survey of Nigeria publication, Kaduna, 111-123.
- Odigi, M.I., Amajor, L.C., 2010. Organic geochemical evaluation of the oil/gas-generative potential of organic matter in Cretaceous strata from the Lower Benue Trough, Nigeria: *Chin. J. Geochem.* 29, 233-241. <https://doi.org/10.1007/s11631-010-0451-9>
- Odigi, M.I., 2007. Facies architecture and sequence stratigraphy of Cretaceous formations, southeastern Benue Trough, Nigeria. Unpublished Ph.D thesis, University of Port Harcourt, Nigeria, 288p.
- Odoma, A.N., Obaje, N.G., Omada, J.I., Idakwo, S.O., Erbacher, J., 2015. Mineralogical, chemical composition and distribution of rare earth elements in clay-rich sediments from Southeastern Nigeria. *Journal of African Earth Sciences* 102, 50-60.
- Odunze, S.O., Obi, G.C., Yuan, W., and Min, L., 2013. Sedimentology and sequence stratigraphy of the Nkporo Group (Campanian-Maastrichtian), Anambra Basin, Nigeria. *Journal of Palaeogeography* 2(2), 192-208.
- Offodile, M.E., 1984. The geology and tectonics of Awe brine field. *Journal of African Earth Sciences* 2(3), 191- 202.

- Ogungbesan, G.O., Akaegbobi, I.M., 2011. Petrography and geochemistry of Turonian Eze-Aku sandstone ridges, lower Benue Trough, Nigeria: implication for provenance and tectonic setting. *Ife Journal of Science* 13, 263–277.
- Ogala, J. E., 2011. Hydrocarbon potentials of The Upper Cretaceous coal and shale units in the Anambra Basin, Southeastern Nigeria: *Petroleum and Coal*, 53(1), 35 – 44
- Ogbamikhumi, A., Igbini, N.S., 2017. Palynological and Organic Geochemical Studies for source rock characterisation and evaluation of Mamu Formation in the Benin Flank of the Anambra Basin. *The International of Engineering and Science* 6, 55 – 60.
- Ojo, O.J., Akande, S.O., 2004. Palynological and paleoenvironmental studies of Gombe Formation, Gongola basin, Nigeria. *Journal of Mining and Geology* 40, 143-149.
- Ojo, O.J., Akande, S.O., 2009. Sedimentology and depositional environments of the Maastrichtian Patti Formation, SE Bida Basin, Nigeria. *Cretaceous Research*, 30, 1415–1425.
- Ojo, O.J., Akande, O.S., 2012. Sedimentary facies relationships and depositional environments of the Maastrichtian Enagi Formation, Northern Bida Basin, Nigeria. *Journal of Geography and Geology* 4, 136-147.
- Ojo, O.J., Babatunde, F.R., Adepoju, S.A., Akande, S. O., Momoh, A., 2016. Provenance and weathering history of the Maastrichtian shale member of the Patti Formation, southern Bida Basin, Nigeria. *J. Geol. Soc. India* 88, 471-480.
- Okereke, C.S., Ofoegbu, C.O., 1990. Gravity and magnetic data over the Yola Arm of the Upper Benue Trough. In: Ofoegbu, C.O. (Ed.), *The Benue Trough: Structure and Evolution*. Friedr. Vieweg & Sohn, Wiesbaden. Pp. 161-169
- Okoro, A.U., Igwe, E.O., 2018a. Sequence stratigraphy and controls on sedimentation of the Upper Cretaceous in the Afikpo Sub-basin, southeastern Nigeria. *Arabian Journal of Geosciences* 11: 125. <https://doi.org/10.1007/s12517-018-3468-8>
- Okoro, A.U., Igwe, E.O., 2018b. Lithostratigraphic characterization of the Upper Campanian – Maastrichtian succession in the Afikpo Sub-basin, southern Anambra Basin, Nigeria. *J. Afr. Earth Sci.*, 147, 178–189.
- Ola-Buraimo, A.O., Oluwajana, O.A., Ehinola, O.A. and Ogundana, O., 2014. Biostratigraphy of the Campano-Maastrichtian Uzeeba Shale deposit, Dahomey Basin Southwestern Nigeria. *Elixir Geoscience* 69, 22812-22818
- Olade, M.A., 1975. Evolution of Nigeria's Benue Trough (Aulacogen): a tectonic model. *Geol.*

- Mag. 112, 575-581.
- Olade, M. A., Van de Kraats, A. H., and Ukpong, E. E., 1978. Effects of environmental parameters on metal dispersion patterns in stream sediments from the lead-zinc belt. Benue Trough, Nigeria. *Geologie en Mijnb.*, 58, 341-351.
- Olade, M.A., 1987. Dispersion of Cadmium, Lead and Zinc in Soils and Sediments of a Humid Tropical Ecosystem in Nigeria in T. C. Hutchinson and K. M. Meema (Eds.) *Lead, Mercury, Cadmium and Arsenic in the Environment*. John Wiley & Sons Ltd, New York, Scope 31, 303-313
- Olawoki, O.A., Coker, S.J.L., Rahaman, M.A., Fadiya, S.L., Bale, R.B., 2018. Studies assess Central Nigeria's Bida basin potential. *Oil and Gas Journal* 116 (16), 39-43. <https://www.ogj.com/articles/print/volume-116/issue-6/exploration-development/studies-assess-central-nigeria-s-bida-basin-potential.html>.
- Olaniyan, O., Olobaniyi, S.B., 1996. Facies analysis of the Bida Sandstone Formation around Kajita, Nupe basin, Nigeria. *Journal of African Earth Sciences* 23 (2), 253-256.
- Omatsola, M.E., Adegoke, O.S., 1981. Tectonic evolution and Cretaceous stratigraphy of the Dahomey Basin. *Journal of Mining and Geology* 18, 130–137.
- Onuigbo, E. N., Okoro A. U., Etu-Efeotor, J. O., Akpunonu, E. O. and Okeke, H. C., 2015. Paleocology of Enugu and Mamu formations in Anambra Basin, Southeastern Nigeria. *Advances in Applied Science Research*, 6(4), 23-39
- Osokpor, J., Okiti, J., 2013. Sedimentological and paleodepositional studies of outcropping sediments in parts of southern Middle Niger Basin. *International Journal of Science and Technology* 2 (12), 839-846.
- Oteze, G.E., 1981. Water resources in Nigeria. *Environ Geol.* 3, 177–184.
- Petters, S.W., 1978. Mid-Cretaceous paleoenvironments and biostratigraphy of the Benue Trough, Nigeria. *Geological Society of America Bulletin* 89, 151-154.
- Petters, S.W., 1982. Central West African Cretaceous-Tertiary benthic foraminifera and stratigraphy. *Palaeontographica Abteilung A* 179, 1–104.
- Petters, S.W., Ekweozor, C.M., 1982. Origin of Mid-Cretaceous black shales in the Benue trough, Nigeria. *Palaeogeography, Palaeoclimatology, Palaeoecology*, 40, 311-319.
- Popoff, M., Wiedmann, J., de Klasz, I., 1986. The Upper Cretaceous Gongila and Pindiga



- formations, Northern Nigeria: subdivisions, age, stratigraphic correlations and paleogeographic Implications. *Eclogue Geologicae Helvetiae*, 79, 343–363.
- Potter, P.E., Maynard, J.B., Depetris, P.J., 2005. *Mud and Mudstones: Introduction and Overview*. Springer-Verlag, 297p.
- Raiswell, R., Berner, R.A., 1985. Pyrite formation in euxinic and semi-euxinic sediments. *Amer. J. Sci.* 285, 710-724.
- Reinson, G.E., 1992. Transgressive Barrier Island and estuarine systems: *In* Walker, R.G., James, N.P. (Eds.), *Facies Models: Response to Sea Level Change*. Geological Association of Canada, 179-194.
- Reyment, R.A., 1965. Aspect of the Geology of Nigeria. Ibadan University Press, Nigeria, p. 145.
- Reyment, R.A., 1980. Biogeography of the Saharan Cretaceous and Paleocene epicontinental transgressions. *Cretaceous Research* 1, 299-327.
- Reyment, R.A., Dingle, R.V., 1987. Palaeogeography of Africa during the Cretaceous Period. *Palaeogeography, Palaeoclimatology, Palaeoecology* 59, 93–116.
- Rimstidt, J.D., Chermak, J.A., Schreiber, M.E., 2017. Processes that control mineral and element abundances in shales. *Earth Science Reviews* 171, 383–399
- Roser, B.P., Korsch, R.J., 1986. Determination of tectonic setting of sandstone mudstone suites using SiO<sub>2</sub> content and K<sub>2</sub>O/Na<sub>2</sub>O ratio. *The Journal of Geology* 94 (5), 635–650.
- Ruebsam, W., Müller, T., Kovács, J., Pálffy, J., Schwark, L., 2018. Environmental response to the early Toarcian carbon cycle and climate perturbations in the northeastern part of the West Tethys shelf. *Gondwana Research* 59, 144–158
- Salami, M.B., 1986. Palynomorph taxa from the "Lower Coal Measures" deposits (? Campanian-Maastrichtian) of Anambra Trough, Southeastern Nigeria. *Journal of African Earth Sciences* 11(1-2), 135-150.
- Santos, A.S, Helenes, J, Carvalho, M.A. 2013. Palynofacies evidence of dysoxia and upwelling in the Turonian of the Sergipe Basin, Brazil. *Cretaceous Research* 46, 151–165
- Sarki Yandoka, B.M., Abubakar, M.B., Abdullah, W.H., Amir Hassan, M.H., Adamu, B.U., Jitong, J.S., Aliyu, A.H., Adegoke, A.K., 2014. Facies analysis, palaeoenvironmental reconstruction and stratigraphic development of the Early Cretaceous sediments (Lower Bima Member) in the Yola Sub-basin, Northern Benue Trough, NE Nigeria . *Journal of African Earth Sciences* 96, 168-179.

- Sarki Yandoka, B.M., Abdullah, W.H., Abubakar, M.B., Hakimi, M.H., Jauro, A., Mustapha, K.A., Adegoke, A.K., 2015. Organic geochemical characteristics of Cretaceous Lamja Formation from Yola Sub-basin, Northern Benue Trough, NE Nigeria. Implication for hydrocarbon generating Potential and paleodepositional setting. *Arab. J. Geosci.* 8 (9), 7371–7386.
- Sarki Yandoka, B.M., Abdullah, W.H., Abubakar, M.B., Hakimi, M.H., Jauro, A., Adegoke, A.K., 2016. Organic geochemical characterization of shallow marine Cretaceous formations from Yola sub-basin, Northern Benue Trough, NE Nigeria. *Journal of African Earth Sciences* 117, 235-251
- Sarki Yandoka, B.M., Abdullah, W.H., Abubakar, M.B., Adegoke, A.K., Maigari, A.S., Haruna, A.I., Yaro, U.Y., 2017. Hydrocarbon potential of Early Cretaceous lacustrine sediments from Bima Formation, Yola Sub-basin, Northern Benue Trough, NE Nigeria: insight from organic geochemistry and petrology. *Journal of African Earth Sciences* 129, 153-164.
- Schlanger, S.O., Jenkyns, H.C., 1976. Cretaceous anoxic events: causes and consequences. *Geol. Mijnb.*, 55, 179–184.
- Scotese, C.R., 2014. Atlas of Late Cretaceous Maps, PALEOMAP Atlas for ArcGIS, volume 2, The Cretaceous, Maps 16-22, Mollweide Projection, PALEOMAP Project, Evanston, IL.
- Shettima, B., Abubakar, M.B., Kuku, A., Haruna, A.I., 2018. Facies analysis, depositional Environments and paleoclimate of the Cretaceous Bima Formation in the Gongola Sub – Basin, Northern Benue Trough, NE Nigeria. *Journal of African Earth Sciences* 137, 193-207.
- Simpson, A., 1954. The Nigerian Coal Field: The geology of parts of Onitsha, Owerri and Benue Provinces. *GSN Bull.* 24, p. 67.
- Singer, A., 1984. The paleoclimatic interpretation of clay minerals in sediments - a review. *Earth-Science Reviews* 21, 251-293
- Skelton, P.W., Spicer, R.A., Kelley, S.P., Gilmour, L., 2003. *The Cretaceous World*. Cambridge University Press, Cambridge, pp. 360.
- Stoneley, I.L., 1966. The Niger delta region in the light of the theory of the continental drift. *Geol. Mag.* 103, 385-266.
- Suleiman, A. A., Magee, C., Jackson, C.A.L., Fraser, A.J., 2017. Igneous activity in the Bornu Basin, onshore NE Nigeria; implications for opening of the south Atlantic. *Journal of the*

- Geological Society 174, 667-678.
- Szczepanik, P., Gize, A., Sawlowicz, C., 2017. Pyritization of dinoflagellate cysts: A case study from the Polish Middle Jurassic (Bathonian). *Review of Palaeobotany and Palynology* 247, 1-12
- Teme, S.C., 1991. Geotechnical characteristics of some clays from south—western Nigeria: Implications for industrial utilization. [Engineering Geology 30 \(3–4\)](#), 305-324
- Tijani, M. N., Nton, M. E. and Kitagawa, R. 2010. Textural and geochemical characteristics of the Ajali Sandstone, Anambra basin, SE Nigeria: Implication for its provenance. *Comptes Rendus Geoscience*, vol. 342, 136–150
- Total, 1984. Some geochemical data in the Anambra basin. Unpublished report 05NG006-0142, 1-15.
- Total, 1988. OPL 447 – Anambra River Field evaluation quicklook du gisement. Unpublished report 05NG006-0192, 1-70.
- Traverse, A., 2007. *Paleopalynology 2<sup>nd</sup> ed.*, Topics in Geobiology 28. Springer 813p.
- Tribouvillard, N., Algeo, T.J., Lyons, T.W., Riboulleau, A., 2006. Trace metals as paleoredox and paleoproductivity proxies: an update. *Chemical Geology* 232, 12–32
- Tyson, R.V., 1995. *Sedimentary Organic Matter Organic facies and palynofacies*. Chapman & Hall, London, 615p.
- Umeji, O.P., 1984. Ammonite palaeoecology of the Eze-Aku Formation, southeastern Nigeria. *Nigerian Journal of Mining and Geology*, 21, 55-59
- Umeji, A.C., 2000. Evolution of the Abakaliki and the Anambra sedimentary basins, Southeastern Nigeria. A report submitted to the Shell Petroleum Development Company Nigeria Ltd., 155p with enclosures.
- Umeji, O.P., Nwajide, C.S., 2007. Age control and designation of the Standard stratotype of Nsukka Formation of Anambra Basin, Southeastern Nigeria. *Journal of Mining and Geology* 43 (2), 147-166.
- Umeorah, E.M., 1987. Depositional environment and facies relationships of the Cretaceous ironstone of the Agbaja Plateau, Nigeria. *Journal of African Earth Sciences* 6, 385-390.
- Unomah, G.I., 1991. Organic geochemical characteristics of the pre-uplift Awgu Shale at Okpa River: implication for the petroleum potential of the Anambra Basin, Nigeria. *Journal of African Earth Sciences* 13 (3-4), 377-385.

- Uzoegbu, U.M., Ekeleme, I.A., and Uchebo, U.A., 2014. Oil Generation Capacity of Maastrichtian Coals from the Anambra Basin, SE Nigeria. *The International Journal of Engineering and Science* 3, 33-46
- Uzoegbu, M.U., and Okon, O.S., 2017. Sedimentology and Geochemical Evaluation of Campano-Maastrichtian Sediments, Anambra Basin, Nigeria. *International Journal Geology and Mining* 3(2), 110-127
- Wang, W., Zeng, M., Zhou, M., Zhao, J., Zheng, J., Lan, Z., 2018. Age, provenance and tectonic Setting of Neoproterozoic to early Paleozoic sequences in southeastern South China Block: Constraints on its linkage to western Australia-East Antarctica. *Precambrian Research*, 309, 290–308.
- Wedepohl, K.H., 1971. Environmental influences on the chemical composition of shales and clays. In: Ahrens, L.H., Press, F., Runcorn, S.K., Urey, H.C. (Eds.), *Physics and Chemistry of the Earth*. Pergamon, Oxford, 8, 307–333.
- Wedepohl, K.H., 1991. The composition of the upper earth's crust and the natural cycles of selected metals. *Metals in natural raw materials. Natural Resources*. In: Merian, E. (Ed.), *Metals and Their Compounds in the Environment*. VCH, Weinheim, 3 – 17.
- Westrich, J.T., Berner, R.A., 1984. The role of sedimentary organic matter in bacterial sulfate reduction: The G model tested. *Limnology and Oceanography* 29(2), 236-249
- Withjack, M.O., Schlische, R.W., Olsen, P.E., 2002. Rift-Basin structure and its influence on sedimentary systems: sedimentation in continental rifts. *SEPM Special Publ.* 73, 57-81.
- Wozny, E., Kogbe, C.A., 1983. Further evidence of marine Cenomanian, lower Turonian and Maastrichtian in the Upper Benue basin of Nigeria (West Africa). *Cretaceous Research* 4(1), 95-99.
- Woakes, M. Ajibade C.A., Rahaman, M.A., 1987: Some metallogenic features of the Nigerian Basement, *Journal of African Earth Science* 5, 655-664.
- Wright, J.B., Hastings, D.A., Williams, H.R., 1985. *Geology and mineral resources of West Africa*. George Allen & Unwin, London, p. 187.
- Wronkiewicz, D.J and Condie, K.C., 1990. Geochemistry and mineralogy of sediments from the Ventersdorp and Transvaal Supergroups, South Africa: Cratonic evolution during the early Proterozoic. *Geochimica et Cosmochimica Acta* 54, 343-354
- Zaborski, P.M.P., 1983. Campano-Maastrichtian ammonites, correlation and palaeogeography in

- Nigeria. *Journal of African Earth Sciences* 1, 59-63.
- Zaborski, P.M.P., Ugoduluwa, F., Idornigie, A., Nnabo, P., Ibe, K., 1997. Stratigraphy and structure of the Cretaceous Gongola Basin, Northeastern Nigeria. *Bulletin des Centres des Recherches Exploration–Production Elf-Aquitaine* 21, 153–185.
- Zaborski, P.M.P., Morris, N.J., 1999. The Late Cretaceous ammonite genus *Libycoceras* in the Iullemeden Basin (West Africa) and its palaeogeographical significance. *Cretaceous Research* 20, 63–79.
- Zaid, S.M., Geochemistry of sandstones from the Pliocene Gabir Formation, north of Marsa Alam, Red Sea, Egypt: Implication for provenance, weathering and tectonic setting. *Journal of African Earth Sciences* 102, 1–17.

